

Landslides, stratigraphy, and surficial geology of the Hydraulic map sheet (NTS 93A/12),
British Columbia, Canada

by

Ahren Johannes Bichler
B.Sc., University of Victoria, 2000

A thesis submitted in partial fulfillment of the requirements for the degree of

MASTERS OF SCIENCE

in the Department of Earth and Ocean Sciences

© Ahren Johannes Bichler, 2003
University of Victoria

All rights reserved. This thesis may not be reproduced in whole or in part, by
photocopying or other means, without the permission of the author.

Supervisor: Dr. Peter Bobrowsky

ABSTRACT

The landslides, stratigraphy, and surficial geology of the Hydraulic map sheet (NTS 93A/12), located in the interior of British Columbia, were examined. The research centred on landslide processes within the upper Quesnel River valley. It consists of three major components, each conducted at a different scale.

At the smallest scale, surficial geological mapping was conducted at a scale of 1:50 000. Three hundred and twenty eight terrain polygons were identified, of which 32% were verified by fieldwork. Polygons containing morainal sediment as its primary surficial material make up 86% of the surficial area. Glaciofluvial and colluvial sediments, confined to the major valleys, are also important units. Glaciolacustrine sediment was rarely identified as the primary sediment but underlies all glaciofluvial terraces within the valleys. Bi-directional ice flow indicators show a strong northwest-southeast orientation while limited uni-directional data indicate flow to the northwest.

The medium scale part of the project was a stratigraphic assessment of sediment within the Quesnel and Cariboo River valleys and the description of landslide processes. Twenty four natural exposures were investigated, including nine landslides. Nine stratigraphic units were identified, of which only three are actively involved in modern landslide processes. Advance-phase glaciolacustrine sediment, of the Fraser Glaciation, hosts two styles of failure: 1) long-lived, flow dominated failures that occur as a series of smaller events and 2) short-lived, rapid, slide dominated failures. A third style of landsliding was recognized within an upper clay unit and Fraser till. These landslides are short-lived, rapid events that are the most fluid-like failures found within the region.

The largest scale research was a detailed site investigation of a landslide using a variety of geophysical methods. Ground penetrating radar techniques offered detailed information on the upper 20 m of surficial material including the internal structure of individual units as well as the ability to image the surface of rupture and the surface of

separation. Direct current electrical resistivity and seismic surveys yielded data on the geometries of the stratigraphic units to depths of 40 m and 80 m respectively. Direct current electrical resistivity was further able to image the surfaces of rupture and separation based on the juxtaposition of stratigraphic units. Through the integration of geophysical data with stratigraphy and digital terrain models a three-dimensional structural model of the landslide was created.

TABLE OF CONTENTS

Section		Page
	Title Page	i
	Abstract	ii
	Table of Contents	iv
	List of Tables	vi
	List of Figures	vii
	Acknowledgements	x
	Dedication	xii
1	Introduction	1
2	Stratigraphy and landslide processes in the Quesnel and Cariboo River valleys, British Columbia	3
2.1	Abstract	3
2.2	Introduction	3
2.3	Study Area	4
2.4	Previous Work	8
2.5	Methods	9
2.6	Results	12
2.6.1	Stratigraphy	12
2.6.2	Landslides	22
2.7	Inferred Quaternary History	31
2.8	Discussion	37
2.8.1	Landslides and Stratigraphy	37
2.8.2	Landslide Triggers	40
2.9	Conclusions	47
3	Three-dimensional mapping of a landslide using a multi-geophysical approach: the Quesnel Forks Landslide	49
3.1	Abstract	49
3.2	Introduction	49
3.3	Study Area and the Quesnel Forks Landslide	50
3.4	Methods	55
3.5	Site Characteristics	57
3.5.1	Stratigraphy	58
3.5.2	Surficial Characteristics	60
3.6	Digital Terrain Models	63
3.7	Geophysical Results	65
3.7.1	Ground Penetrating Radar	65
3.7.2	Direct Current Resistivity	69
3.7.3	Seismic Reflection and Refraction	71
3.8	Geophysical Interpretation	71
3.9	Discussion	79
3.10	Conclusions	81
4	Summary	83
5	References	85

Appendices

A	Surficial Geology Map	96
B	Stratigraphic Data	97
C	Digital Terrain Models	135
D	Geophysical Data	138
D1	Ground Penetrating Radar	140
D2	Direct Current Resistivity	157
D3	Seismic Reflection and Refraction	185

LIST OF TABLES

Table		Page
2.1	List of aerial photographs available for the study area.	11
2.2	Selective geochemistry run by ICP-MS for diamicton samples interpreted as till. Elemental averages calculated for till (Fraser Glaciation) and from the penultimate glaciation are also given.	16
2.3	Correlation between stratigraphic units described from this and other research in the interior of British Columbia.	34
3.1	Examples of geophysical surveys conducted for landslides using geophysical techniques similar to those used at the Quesnel Forks Landslide.	51
3.2	Geophysical parameters of various substrates used during the interpretation of geophysical data.	74

LIST OF FIGURES

Figure		Page
2.1	The study area and location of stratigraphic sections along the Quesnel and Cariboo Rivers. Sections conducted at landslides are denoted with an "L" while other natural exposures with an "S".	5
2.2	View northwest, towards the Quesnel River valley, of typical gently rolling topography found on the plateau.	6
2.3	View southwest down the Cariboo River valley, looking into the Quesnel River valley.	7
2.4	The generalized stratigraphy of the Quesnel and Cariboo River valleys and the Bullion Pit. Units are denoted A through I, from oldest to youngest, as referred to throughout the text (Bullion Pit stratigraphic column modified from Clague <i>et al.</i> 1990 and Clague 1991).	13
2.5	Bullion Pit exposure described by Clague <i>et al.</i> (1990) and Clague (1991). The lower stratified drift is correlated with units A and B, the Olympic Non-glacial with unit C, the upper stratified drift with units D to F and the till with unit G.	14
2.6	Exposure adjacent to Quesnel Forks consisting of till (unit A) overlain by ice-contact sediments (unit B). The exposure is approximately 25 metres high (section AJB02-S12).	15
2.7	Typical Fraser advance-phase glaciolacustrine sediment found throughout the Quesnel River valley (section AJB01-L6). The exposure is approximately 60 metres high and consists entirely of interbedded silt, clay and sand (unit D). Note person standing at base of exposure for scale, just left of centre.	18
2.8	An exposure of Fraser, advance-phase, glaciolacustrine sediment in the Cariboo River valley (unit D). Sediment is coarser than in the Quesnel River valley. The top of the section is capped by rhythmically bedded silt containing dropstones (unit F). The exposure is approximately 140 metres high (section AJB01-S2).	20
2.9	Fraser Glaciation till (unit G) exposed in the headscarp of a landslide (section AJB01-L5).	21
2.10	Typical Holocene gravel sediments (unit I) found throughout the valley that form the surface of lower terraces. Here, gravel overlies rhythmically bedded clay (unit D).	23
2.11	Figure 2.11. Digital elevation model, looking upstream, showing the location of the nine major landslides along the Quesnel River and their characteristics. Age ranges are determined from sequential airphoto analysis whereas activity, type of failure, surficial area and volume were assessed by fieldwork and chrono-sequential airphoto analysis.	24
2.12	Landslide exhibiting predominately flow-type failure (section AJB01-L9). Note the levees formed where an intact bluff composed of unit D diverted flow material. The primary failed material is till (unit G) and the upper, fine-grained glaciolacustrine sediment (unit F).	26

Figure		Page
2.13	Gully formed in unit D that periodically delivers debris to the Quesnel River (section AJB01-L5). Note person for scale.	27
2.14	Typical landslide involving interbedded glaciolacustrine sediment (AJB01-L1). Failure is primarily by flow though some intact blocks are found near the head scarp.	28
2.15	Landslide located at Quesnel Forks that failed primarily by sliding and consists of two rotated blocks (section AJB01-L4). The primary material involved is interbedded glaciolacustrine sediment. The terrace is approximately 75 metres high.	29
2.16	Proposed sequence of events for the Quesnel and Cariboo River valleys, spanning the Quaternary: 16.1) Tertiary sediment at the beginning of the Quaternary; 16.2) penultimate glaciation and deposition of till; 16.3) deposition of recessional, ice-contact sediments; 16.4) formation of large recessional lake and the deposition of glaciolacustrine sediments; 16.5) middle Wisconsin valley incision; 16.6) formation of Fraser, advance-phase glacial lake and deposition of coarsening upwards glaciolacustrine sediments; 16.7) relative deepening of glacial lake; 16.8) occupation by Fraser Glacial ice and deposition of till; 16.9) recessional glaciofluvial deposition; and 16.10) Holocene valley incision.	32
2.17	River discharge for 1976 for the upper and lower Quesnel River and the Cariboo River as well as the combined data for the upper Quesnel and lower Cariboo rivers. Data was collected at Environment Canada stations 08KH001, 08KH006 and 08KH003, respectively.	41
2.18	River discharge for 1996 for the upper and lower Quesnel River Data was collected at Environment Canada stations 08KH001 and 08KH006, respectively.	42
2.19	Yearly, cumulative departure from the mean for 3 factors influencing regional landslide activity. Landslide ages are indicated as either a year (dashed line) or an age range (shaded box). Data was collected from Environment Canada stations as follows: discharge, 08KH006; snow pack, 1C24; precipitation at Likely, 1094616; precipitation at Horsefly, 1093600.	44
2.20	Summed cumulative departure from the mean for three factors influencing regional landslide activity. Landslide ages are indicated as either a year (dashed line) or an age range (shaded box).	46
3.1	Location map showing the National Topographic System (NTS) map sheet and orthophoto of Quesnel Forks. The Quesnel Forks Landslide is the eastern most landslide of nine landslides investigated. The white dashed line on the photo is the boundary of the head scarp.	52
3.2	a) Pre-failure photograph of Quesnel Forks. View is to the northeast, showing large amounts of silt being introduced into the Quesnel River. Dotted line shows the approximate location of the head scarp (photograph courtesy of Marie Elliot); b) View to the southeast of the Quesnel Forks Landslide, taken from the Quesnel Forks town site.	54

Figure		Page
3.3	Composite stratigraphic column for Quesnel Forks Landslide.	59
3.4	a) Photograph of the upper rotational block and head scarp where the original forest floor remains intact. Note the person standing on the headscarp for scale; b) View to east along the top of the lower rotational block on which the person is standing. Most of the primary vegetation has been removed during failure.	61
3.5	Close-up of weathered clay blocks that create the hummocky surface on a portion of the foot. The power bar in the foreground is 25 cm in length.	62
3.6	Digital terrain models of the Quesnel Forks Landslide and surrounding area: a) pre-failure shaded relief map; b) pre-failure 3D oblique view to southeast; c) post-failure shaded relief map with morphological division of foot (see section 6.2); and d) post-failure 3D oblique view to southeast.	64
3.7	3D oblique change of elevation map created from DTMs. View is to the southeast. Brown shades indicate an increase in elevation from the 1986 to the 2002 airphoto. Green, blue and red shades represent a decrease in elevation.	66
3.8	DTMs with geophysical survey lines superimposed onto its surface: a) GPR; b) DC resistivity; and c) seismic reflection and refraction. Profiles obtained from corresponding survey lines are annotated as in sections 6.1, 6.2, and 6.3.	67
3.9	GPR profiles, corresponding with profiles in Fig. 8: a) perpendicular to head scarp on terrace and upper block; and b) perpendicular to head scarp on foot. Uninterpreted profiles are given on the left. Correlation of facies with other geophysical and stratigraphic data is given in Fig. 3.12.	68
3.10	DC resistivity profiles, corresponding with profiles in Fig. 8: a) perpendicular to head scarp; b) parallel to head scarp; and c) 3d fence diagram of all resistivity data. Uninterpreted profiles are given on the left. Correlation of units with other geophysical and stratigraphic data is given in Fig. 3.12.	70
3.11	Seismic profiles, corresponding with profiles in Fig. 8: a) parallel to headscarp on the terrace (P-wave reflection); b) parallel to headscarp on the foot (S-wave reflection). Uninterpreted profiles are given on the left. Correlation of units with other geophysical and stratigraphic data is given in Fig. 3.12.	72
3.12	An oblique 3D cross-section of the Quesnel Forks landslide based on geophysical data. Geophysical units are correlated with each other and stratigraphic units in the accompanying matrix. Elevation is given in metres above sea level and distance in metres.	73

ACKNOWLEDGEMENTS

The success of this thesis is largely attributed to the support, collaboration, and guidance the author received from a diverse group of individuals, organizations, and agencies. I would like to begin by thanking the members of the supervising committee who throughout the course of the research remained the foundation for advice and scientific inspiration. Their range in expertise and willingness to share their knowledge provided the basis for the interdisciplinary tone of this thesis. A special gratitude is owed to Dr. P. Bobrowsky whom over the many years has been my mentor and guide in all aspects of my education, career, and professional development. Dr. E. Van der Flier-Keller gave me some of my first insight to the field of earth sciences during my undergraduate program and has managed to capture my attention ever since. Dr. M. Best stimulated my interests for geophysics and has been my strongest supporter for bridging the gap between geology and physics for non-physicists. A subject I knew nothing of before becoming acquainted with him. Mr. D. VanDine has introduced me to the world of landslides and geohazards. My collaboration with him has had a tremendous effect on my knowledge, scientific thought, and confidence.

The primary financial and technical support was provided by the Geological Survey of Canada, Terrain Sciences Division and the British Columbia Ministry of Energy and Mines, Geosciences, Research and Development Branch. The Geological Survey of Canada sponsored the geophysical portion of the research, supplying access to the instrumentation used but more importantly to the specialists and their wealth of knowledge. The BC Ministry of Energy and Mines sponsored the surficial mapping and stratigraphy component of the thesis as well as the logistical support. The BC Ministry of Transportation also graciously supplied access to the ground penetrating radar unit. The University of Victoria, School of Earth and Ocean Sciences kindly provided a seismic instrument. Barker Minerals provided much appreciated support during fieldwork. The author benefited greatly from collaboration and assistance from Dr. J. Hunter, Dr. T. Calvert, Mr. M. Douma and Mr. R. Burns who helped design and carry out the geophysical surveys. In addition, Dr. J. Hunter, Dr. T. Calvert, and Mr. R. Burns were

responsible for processing the raw geophysical data for the seismic and direct current resistivity methods.

The author would also like to recognize the hard work of the many people who gave invaluable assistance during fieldwork, including Adrian Hickin, Roger Paulen, Katie Dexter, Nicole Vinette, Paul Grant, Hart Bichler and Mr. M. Geertsema. Additional scientific and technical support was received from Dr. V. Levson, Mr. B. Grant, Dr. L. Pyle, Dr. G. Bichler-Robertson, Travis Ferbey, Derek Uddenberg and Mr. P. LePine.

The camaraderie I have experienced while attending the School of Earth and Ocean Sciences, during my employment at the BC Ministry of Energy and Mines, and through my dealings with the Geological Survey of Canada has had a profound effect on me. I have learned so much over the years from countless people whether during an impromptu conversation over a beer, in a lecture, at a conference, or hanging from a rope off the side of a cliff. These years will not be forgotten.

DEDICATION

I would like to dedicate these writings to Katja Strauss, my friend, partner, and wife. It is the strength, confidence, and pride that she instils within me that made this thesis possible.

In addition, I would like to dedicate the thesis to my family whose support and advice were often required beyond reasonable expectation but was always offered without hesitation or expectations. In particular I would like to thank my father who is an exemplary role model that taught me the value of hard work, forethought, and perseverance and who gave me my passion for earth sciences.

CHAPTER 1

INTRODUCTION

Landslides are the movement of rock, debris, or earth down slope and the resulting geomorphic features (Cruden 1991). Landslides occur both naturally and by consequence of anthropogenic activities. They occur in a wide variety of materials and within many different landscapes. The characteristics, triggers, and media of landslides located along the upper Quesnel River, British Columbia were studied.

There are many reasons for studying landslides. The most obvious are the loss of life and economic impacts. During the 20th century, tens of thousands of people were killed throughout the world by landslides and between Japan, the United States, Italy, and India, approximately \$6 billion (US) is lost annually (Schuster 1996). Landslides are Canada's most destructive natural hazard (Evans 2003), with over 600 deaths and billions of dollars in damage and economic loss since the mid 19th century (Evans 2000; Evans *et al.* 2002). Within British Columbia, landslides cause damage to housing, utility corridors, transportation routes, as well as forestry, fisheries, mining, and port resources and facilities (Evans and Clague 1988). Landslides within the study area have impacted placer mining operations, fisheries, pulp mills, and important historical sites. Furthermore, landslide activity is expected to increase globally during the 21st century based on three factors: 1) increased urbanization and development in landslide-prone areas; 2) continued deforestation; and 3) increased regional precipitation caused by changing climate patterns (Schuster 1996). Given the serious nature of the impacts of landslides and the potential increase in their occurrence, landslide research is of paramount importance.

There were three main objectives in this study with the combined purpose being to document landslide processes and the setting in which they occur. The three objectives pertain to three scales of investigation, each comprising a separate component of the study. Each component is presented herein as chapters and an appendix, which were written as independent publications.

The first part of the study involved the characterization of surficial geology and geomorphic processes. Its purpose was to provide a regional context for landslide processes as well as to update previous surficial geology maps to new terrain mapping standards for British Columbia. Mapping was carried out at a scale of 1:50 000 for the Hydraulic map sheet (NTS 93A/12). The map is presented as Appendix A and is published elsewhere as Bichler and Bobrowsky (2003).

A stratigraphy and landslide study was carried out as the second part of the thesis. The purpose was to describe the style of landslides and to correlate them with stratigraphic units prone to failure. The stratigraphy of 24 naturally exposed sections within the Quesnel and Cariboo River valleys was examined, including 9 landslides. Information on the mode of failure, dimensions, and ages of the landslides was collected, as well as climate and river discharge data for the region. This work is presented as Chapter 2.

The third part of the research was a detailed site investigation of a landslide. The purpose of the site investigation was to map the internal structure of a landslide using a suite of geophysical techniques and digital terrain models. Ground penetrating radar, direct current resistivity, and seismic reflection and refraction surveys were carried out over the Quesnel Forks Landslide. This work is presented herein as Chapter 3 and is published elsewhere as Bichler *et al.* (in press).

Conclusions for the thesis are presented in Chapter 4. The remaining appendices contain supplementary material and data. Appendix B contains the stratigraphic logs for the field stations. Appendix C consists of two topographic maps of the Quesnel Forks Landslide for pre and post-failure conditions and appendix D is a compilation of the geophysical data collected.

CHAPTER 2

STRATIGRAPHY AND LANDSLIDE PROCESSES IN THE QUESNEL AND CARIBOO RIVER VALLEYS, BRITISH COLUMBIA, CANADA

2.1 Abstract

The stratigraphy of the Quesnel and Cariboo River valleys, in central British Columbia, Canada are studied in order to gain a better understanding of local landslide processes. In total, 24 natural exposures were examined including nine landslides. Nine lithostratigraphic units are identified. Three of the stratigraphic units are actively involved in landsliding. Advance-phase glaciolacustrine sediment is the most common unit that fails. Slope failure is most likely to occur where this sediment is found on the outer erosive bend of a river meander. Terraces are prone to failure by sliding whereas valley slopes are more likely to fail by flow. Both riverbank erosion and precipitation are important environmental factors that trigger landslides. Other landslides studied involve till overlying clay. They are predominately flow-type failures that occur where the sediments are found high on valley slopes. Precipitation is the primary triggering factor, as riverbank erosion is not linked to these flow-type failures.

2.2 Introduction

Landslides are a product of specific geological and the environmental factors. The regional characterization of landslides thus requires knowledge of stratigraphy, geomorphic, and geological processes. Landslides within unconsolidated sediments, especially glaciolacustrine and till deposits, are common in British Columbia and often have costly consequences (Evans 1982). Nine active or recently active landslides, two of which blocked the river, were identified along the upper Quesnel River in the interior of British Columbia. Major valleys of the region are known to contain glacial sediment prone to failure and yet landslide studies in this area have been limited.

This paper focuses on the stratigraphy of the Quesnel and Cariboo River valleys in relation to landslide processes. Landslides are characterized according to the styles of

failure and their associated sediments. An attempt is also made to relate selected environmental factors to the timing of landslides. The information collected can be used to help determine where landslides are more likely to occur in the future.

2.3 Study Area

The study area is located approximately 50 km southeast of Quesnel, near the township of Likely, British Columbia, within the Hydraulic map sheet (NTS 93A/12). Stratigraphic and landslide studies were confined to the upper Quesnel and lower Cariboo River valleys (Fig. 2.1). All landslides studied occurred within the Quesnel River valley whereas stratigraphic descriptions were carried out for exposures from both valleys.

The study area lies on the eastern edge of the Interior Plateau at the boundary of the Quesnel Highlands and the Fraser Plateau (Holland 1976). Local topography is characterized by a gently rolling plateau with an average elevation of 940 m asl (Fig. 2.2). Two major valleys trending east-west dissect the plateau and contain the Quesnel and Cariboo rivers. Both valleys average 280 m in depth and 1.5 km in width (Fig. 2.3).

The Quesnel River has a drainage area of approximately 11 500 km² (Pedersen 1998). Flow is to the west, with the river dropping approximately 90 m over a distance of 32 km. Its largest tributary is the Cariboo River.

Sub-boreal spruce zone occupies the majority of the region up to an elevation of 1300 m asl above which the Engelmann spruce-subalpine fir zone occurs (Meidinger and Pojar 1991). Seasonal extremes typify the climate with a temperature range between -39 °C and 35 °C. The area experiences a moderate annual precipitation, on average 690 mm per year with approximately 70% as rain.

The majority of the study area is underlain by volcanic arc rocks of the Quesnel Terrane (upper Triassic to lower Jurassic) including andesite, dacite, rhyolite, shale and siltstone (Bailey 1989). Subordinate amounts of Kootenay and Cache Creek terranes are

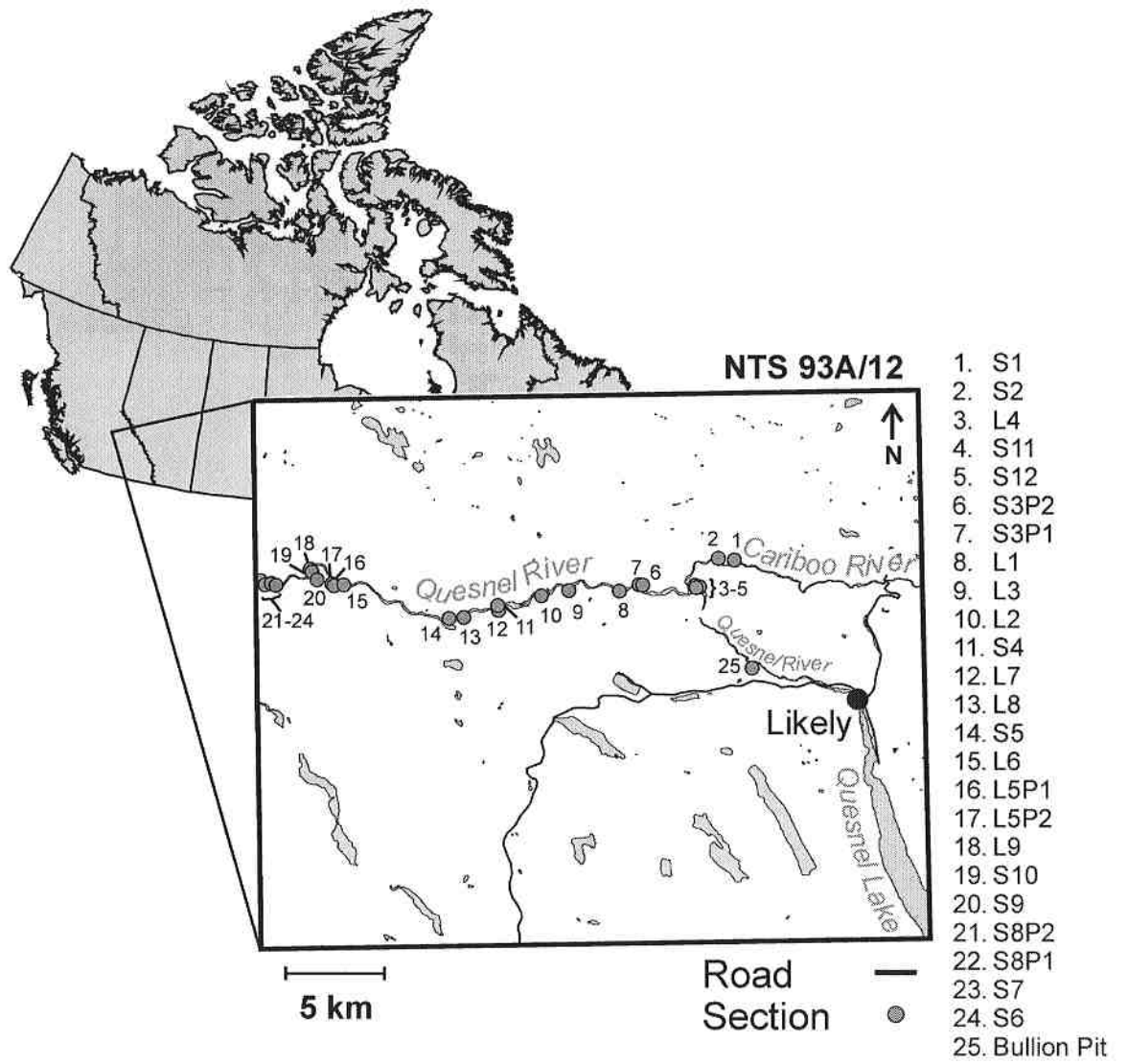


Figure 2.1. The study area and location of stratigraphic sections along the Quesnel and Cariboo Rivers. Sections conducted at landslides are denoted with an “L” while other natural exposures with an “S”.



Figure 2.2. View northwest, towards the Quesnel River valley, of typical gently rolling topography found on the plateau.



Figure 2.3. View southwest down the Cariboo River valley, looking into the Quesnel River valley.

also present, which are Precambrian to Paleozoic pericratonic, marine clastic, and volcanic rocks and upper Paleozoic to lower Jurassic oceanic rocks, respectively.

The Quesnel River watershed contains important social, economic and biological resources that are affected by or affect landslide processes. The forestry industry comprises as much as 31% of the employment in the area (British Columbia Forest Service 2001). Though logging on the plateau is common, only a limited amount of land (approximately 1.5%) in the Quesnel River valley has been harvested (Rowland and MacDonald 1996). The watershed is also a major salmon spawning route and rearing habitat for chinook (*Oncorhynchus tshawytscha*), sockeye (*O. nerka*), kokanee (*O. nerka*), coho (*O. kisutch*) and pink salmon (*O. gorbuscha*) (Pedersen 1998). It also contains important recreational, tourism, cultural, and archaeological resources (Horsefly Sub-regional Plan Interagency Planning Team 2001) such as the abandoned, historical town site of Quesnel Forks.

2.4 Previous Work

Literature concerning landslide processes and related Quaternary stratigraphy within the study area is limited. Only four studies specifically focused on landslides are known. A site investigation (Thurber Consultants Ltd. 1976a) following a large slope failure prompted an airphoto investigation of the Quesnel River valley by Thurber Consultants Ltd. to address the surficial geology, areas of past and present instability, and assess future instability using a qualitative approach (Thurber Consultants Ltd. 1976b). Two additional reports concerning another large failure were conducted by Klohn-Crippen (1996) and Gottesfeld and Poirier (1999). Both landslides blocked the Quesnel River for a short period of time. A fifth study was conducted in association with the project described herein on the latter landslide (Bichler *et al.* in press).

Surficial geology was mapped by Lord (1980) at a scale of 1:50 000 and has since been updated by Bichler and Bobrowsky (2003) (Appendix A). The stratigraphy of sediment within a buried valley and the Quesnel River valley were described by Clague *et al.* (1990) and Clague (1991), respectively. In addition, Levson and Giles (1993) discuss the

importance of sediment to placer mining in the Cariboo region. These studies describe sediment deposited during at least two glacial cycles. Typical sediments include interbedded glaciolacustrine sand, silt, and clay, glaciofluvial gravel, till, and colluvium. Clague (1987), Broster and Clague (1987), Eyles and Clague (1987), Clague (1988), and Eyles and Clague (1991) describe genetically related sediment from locations in the lower Quesnel and upper Fraser River valleys, west of the study area.

2.5 Methods

This study consisted of two aspects of investigation: stratigraphy and landslide processes. At sites consisting of landslides, both stratigraphic and landslide information was collected. Primary fieldwork was carried out during the summer and fall of 2001.

All stratigraphic sections studied were naturally exposed sections located along slopes adjacent to the Quesnel or Cariboo rivers. Access to these sites was gained through the use of a four-wheel drive vehicle and by boat. Large vertical sections required rappelling gear. Sections were measured relative to the river using a combination of measuring tape, inclinometer, and digital range finder. Elevations above sea level were then determined by integrating these data with a geographical information system (GIS) and 1:20 000 provincial Terrain Resource Information Mapping (TRIM) data. Sedimentological characteristics such as colour, grain-size, angularity, compaction, structure, lateral continuity and contacts were described for individual units within the sections. Samples were collected for select units. Those interpreted as till were submitted to Acme Labs for elemental geochemical analysis using induced coupled plasma mass spectrometry (ICP-MS) techniques.

Stratigraphic units identified during fieldwork were correlated between sections based on lithological characteristics and interpreted depositional environments. In addition, results from this study were correlated to a section at the Bullion Pit (Fig. 2.1), described by Clague *et al.* (1990) and Clague (1991).

Landslide information was collected from fieldwork and airphoto interpretation. Standard measurements and nomenclature outlined by the UNESCO Working Party on World Landslide Inventory (1991, 1993a, 1993b) and the IAEG Commission on Landslides (1990) were applied. Landslide classification followed the system proposed by Varnes (1978) and revised by Cruden and Varnes (1996).

To characterize the landslides, geomorphologic, dimensional, and age data were collected. Geomorphic features such as surficial material, ponded water, tension cracks, and vegetation cover were noted. Volume estimates of total disturbed material were made using simple geometries and an estimation of depth of displaced material and depth of rupture surface. Surficial area of disturbed material was reported where volume estimates were not possible and were measured using a combination of field measurements and airphotos. Landslides were dated from historical records or through chronosequential airphoto analysis, reported as a range in years. The range was determined by the year when the first appearance of the landslide was evident and the last year when the landslide was not evident. Table 2.1 summarizes the airphotos used for the study. Some sets cover only a portion of the region.

Climate, snow pack, and river discharge data were collected from Environment Canada at several stations. Climate data, including precipitation and temperature, are available for stations at Likely and at Horsefly (approximately 40 km southeast of Likely). The sites are at 724 m and 777 m asl, respectively. Snow pack data were collected for a station on Yank's Peak, approximately 30 km northeast of Likely at 1710 m asl. River discharge data are available at three sites: 1) at the headwaters of the Quesnel River, near Likely; 2) directly upstream of Quesnel Forks on the Cariboo River; and 3) close to the mouth of the Quesnel River, near the city of Quesnel. These data are available from approximately 1975 to 2001, though some years are absent from some data sets.

Year	Airphoto Series	Scale
1955	BC1981, BC1987, BC2140	1:15 000
1957	BC2379	1:15 000
1970	BC7260	1:15 000
1974	BC7604	1:15 000
1978	BCB78099	1:40 000
1985	BCC353	1:15 000
1986	BCC485	1:10 000
1987	BCC598	1:15 000
1989	BCC1001, BCC1008	1:15 000
1991	BCC91104	1:15 000
1992	BCB92009	1:20 000
1996	BCC96153	1:15 000
1998	BCB98021	1:40 000
2000	BCC00090	1:15 000

BCB - black and white

BCC - colour

Table 2.1. List of aerial photographs available for the study area.

2.6 Results

In total, 24 stratigraphic sections were described, nine of which are landslides. The results of stratigraphic and landslide fieldwork are discussed separately. The relation between stratigraphy and slope stability is discussed in section 2.8.1.

2.6.1 Stratigraphy

The stratigraphy of the Quesnel River valley is illustrated in simplified columns (Fig. 2.4). The most complete succession is found at the Bullion Pit and was described by Clague *et al.* (1990) and Clague (1991). Herein, nine lithostratigraphic units were assigned labels *A* through *I*. These units span from the Early Wisconsin to Recent and are grouped below accordingly.

Early Wisconsin

The oldest unit is a diamicton that was interpreted by Clague *et al.* (1990) as till from a glacial event that pre-dates the Fraser Glaciation. Thus far, it is found at only two sites within the study area, the Bullion Pit (Fig. 2.5) and Quesnel Forks, section AJB02-S12 (Fig. 2.6). At the Bullion Pit, *unit A* is a compact, cemented, massive diamicton (up to 5 m thick) containing striated clasts that directly overlies bedrock at the base of the pit walls (Clague *et al.* 1990). Similar till was found overlying bedrock at Quesnel Forks, where it has a clast content between 25% and 35% with a clayey, silt matrix.

Geochemical analysis shows that till from both sites is enriched in silver, arsenic, calcium, copper, mercury, selenium and strontium when compared to till found high on valley sides and assumed to be deposited during the Fraser Glaciation (Table 2.2). In addition, the till shows a relative depletion of lanthanum. Based on the similar lithology, topographic and stratigraphic position and geochemical similarities, these tills are correlative.

Unit B is sand and gravel deposited in close association with ice. Like *unit A*, it was identified only at the Bullion Pit and at Quesnel Forks. It is poorly sorted, stratified and irregularly bedded gravel and sand, with minor amounts of fine-grained sediment. Large and small scale folding is evident. At Quesnel Forks, the contact between *unit B* and *unit*

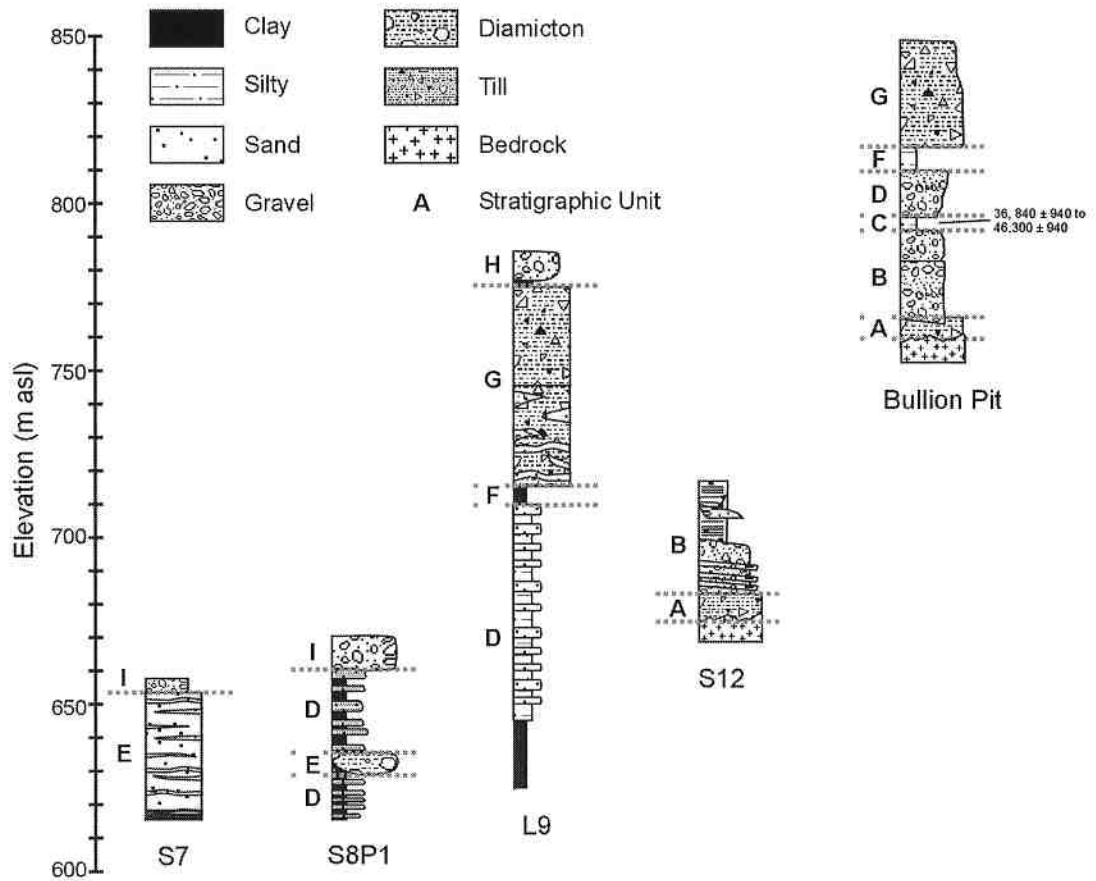


Figure 2.4. The generalized stratigraphy of the Quesnel and Cariboo River valleys and the Bullion Pit. Units are denoted A through I, from oldest to youngest, as referred to throughout the text (Bullion Pit stratigraphic column modified from Clague *et al.* 1990 and Clague 1991).

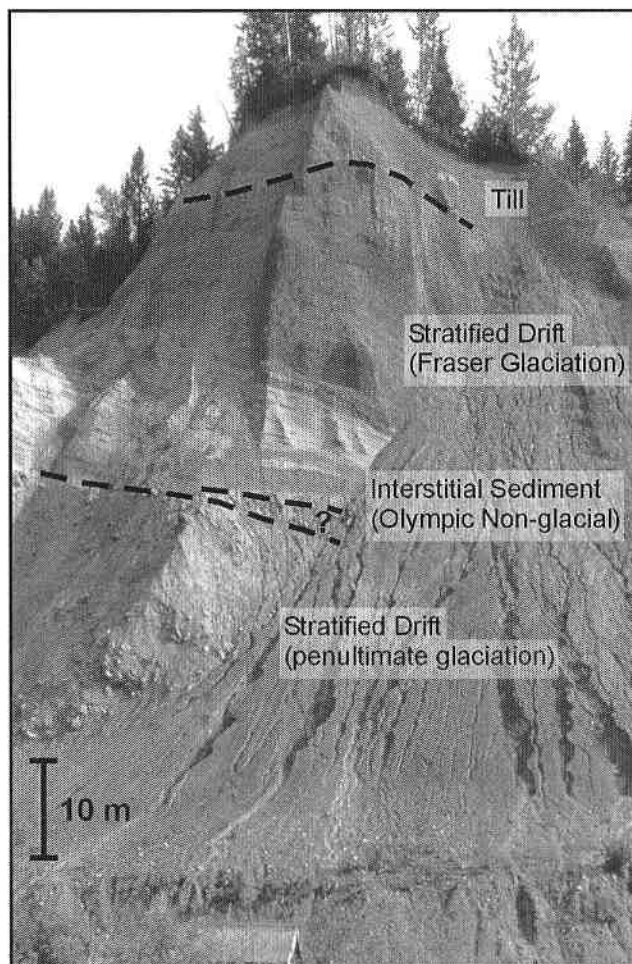


Figure 2.5. Bullion Pit exposure described by Clague *et al.* (1990) and Clague (1991). The lower stratified drift is correlated with units A and B, the Olympic Non-glacial with unit C, the upper stratified drift with units D to F and the till with unit G.

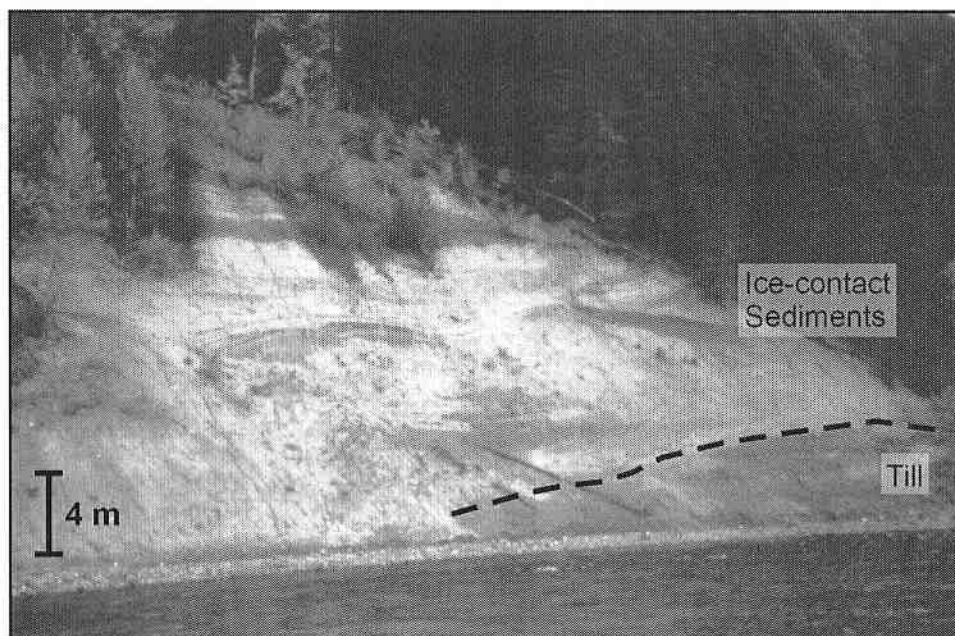


Figure 2.6. Exposure adjacent to Quesnel Forks consisting of till (unit A) overlain by ice-contact sediments (unit B). The exposure is approximately 25 metres high (section AJB02-S12).

Sample	Interpretation	Element							
		ppb Ag	ppm As	% Ca	ppm Cu	ppb Hg	ppm La	ppm Se	ppm Sr
AJB01 L2P3-01	Fraser Till	85	10.4	1.1	63.6	80	21.5	< .1	66.9
AJB01 S10P1-01	Fraser Till	97	12.1	0.2	65.4	8	22.9	0.3	11.2
AJB01 S1P1-01	Fraser Till	74	10.4	0.2	42.9	14	20.0	0.1	10.1
AJB01 L5P1-01	Fraser Till	107	9.6	2.0	98.1	59	14.4	0.1	92.1
AJB01 L9P1-01	Fraser Till	117	8.1	1.8	65.5	59	13.8	< .1	86.6
AJB02 S12-01	Penultimate Till	342	51.5	3.9	147.5	291	7.9	2.6	135.1
AJB02 S12-02	Penultimate Till	305	52.5	3.9	119.3	263	7.7	3.7	136.5
Bullion Pit 1	Penultimate Till	215	32.4	3.0	102.9	130	9.3	1.6	122.7
Bullion Pit 2	Penultimate Till	136	25.5	2.7	73.6	101	8.4	0.9	111.5

Average

Fraser Till	96.0	10.1	1.0	67.1	44.0	18.5	0.2	53.4
Penultimate Till	249.5	40.5	3.3	110.8	196.3	8.3	2.2	126.5

Table 2.2. Selective geochemistry run by ICP-MS for diamicton samples interpreted as till. Elemental averages calculated for till (Fraser Glaciation) and from the penultimate glaciation are also given.

A is gradational over several metres where poorly sorted gravel is crudely stratified with diamicton. Gravel beds are up to a metre thick and show weak imbrication. Diamicton beds are up to 20 cm thick and are similar to *unit A* but are less compact. Beds strike 210° and have an apparent dip 10° to the northwest. The top of the unit consists of laminated sand with contorted, intertonguing lenses of gravel and laminated clay and silt. Lenses are several metres thick and up to 7 m wide.

Olympia Interstade

The only unit that belongs to the Olympia Interstade are organic bearing sediments found at the Bullion Pit (Fig. 2.4, *unit C*). They are interbedded peat and organic-rich silt, sand, and gravel (2.5 m thick) described by Clague *et al.* (1990). Radiocarbon dates ranging from $46\,300 \pm 1740$ to $36\,840 \pm 430$ years BP were obtained from wood debris found within the beds (Clague *et al.* 1990). The unit is a localized record of deposition adjacent to bedrock during an ice-free time (Clague 1991). This unit is no longer exposed as it has been buried by slumping of the valley sides.

Late Wisconsin

Glaciolacustrine sediment overlies inter-glacial sediment at the Bullion Pit in addition to forming the base of most sections (Fig. 2.4, *unit D*). It is commonly found up to 120 m above the current river level (Fig. 2.7). *Unit D* is a coarsening upward succession of interbedded sediment. Towards its base, it typically consists of sub-horizontal, rhythmically bedded sand, silt, and clay. Some small-scale folding and fracturing is evident towards its base. Both grain size and bedding thickness increase up-section. Clay and silt laminae grade into clay or silt interbeds up to decimetres in thickness and sand beds on the metre-scale. Climbing ripples and scour and fill structures are common within sand beds while soft-sediment deformation, such as ball and pillow or flame structures, are common at bed interfaces. Interbeds of sand and pebble gravel are found where the upper facies of the unit is preserved. Here, the beds become steeply dipping (up to 20°) and are interpreted as foreset beds. Occasionally, gravel top-set beds cap the unit. Laterally, the unit becomes coarser in an up-valley (east) direction and particularly



Figure 2.7. Typical Fraser advance-phase glaciolacustrine sediment found throughout the Quesnel River valley (section AJB01-L6). The exposure is approximately 60 metres high and consists entirely of interbedded silt, clay and sand (unit D). Note person standing at base of exposure for scale, just left of centre.

within the Cariboo River valley (Fig. 2.8). There, interbeds are sand, pebble gravel, and cobble gravel and comprise a coarsening upward package that becomes steeply dipping.

Unit E is also glaciolacustrine sediment, which cuts through or is contained within *unit D*. It consists of massive sand (up to 20 m thick) intertonguing with cobble, pebble gravel beds that are on the metre-scale and are laterally discontinuous. Clasts within the gravel are up to 2.5 m in diameter. Both small and large-scale folds are common. At section AJB01-S8P1 (Fig. 2.4), the unit has a channel structure with an erosional basal contact and a semi-gradational upper contact. It is clast supported, very poorly sorted gravel with angular clasts of local phyllitic bedrock. These sediments are interpreted as subaqueous sediment-gravity flow deposits.

Unit F is more glaciolacustrine sediment found at several sections overlying *unit D*. It is a thick package (approximately 10 m) of fine-grained glaciolacustrine sediments composed of laminated and massive clay or silt (Fig. 2.8). Laminations are up to a centimetre thick and are predominant at the base of the unit. The top of the unit is characterized by massive, fissile clay containing dropstones. The basal contact is sharp and drapes underlying sediment. Like *unit D*, sediment from *unit F* found in the Cariboo River valley and at the Bullion Pit are coarser.

The youngest till (*unit G*) is found high on valley slopes as well as covering most of the plateau. It is a well-compacted, silty clay diamicton that has a matrix that becomes clay-rich towards the base of the unit where it overlies *unit F*. It exhibits moderate fissility and jointing (Fig. 2.9). Clast content is approximately 30%. Faceted and striated clasts are abundant. At most sites, *unit G* is approximately 10 m thick though it may be substantially thicker (e.g. Fig. 2.4, section AJB01-S9).

Glaciofluvial sediment (*unit H*) is found overlying till at several sites. It is moderately to poorly sorted gravel that is moderately to crudely stratified, generally clast-supported, and has interbeds of medium to coarse sand. The base of the unit is marked by sand or

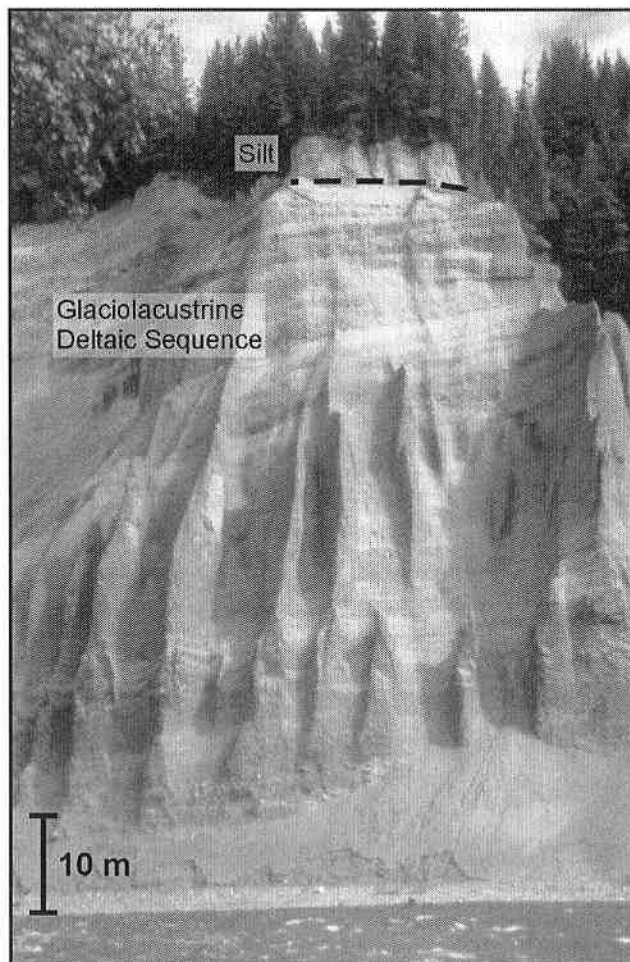


Figure 2.8. An exposure of Fraser, advance-phase, glaciolacustrine sediment in the Cariboo River valley (unit D). Sediment is coarser than in the Quesnel River valley. The top of the section is capped by rhythmically bedded silt containing dropstones (unit F). The exposure is approximately 140 metres high (section AJB01-S2).



Figure 2.9. Fraser Glaciation till (unit G) exposed in the headscarp of a landslide (section AJB01-L5).

silty clay beds (approximately 10 to 20 cm thick). Gravel beds dip strongly (up to 30°) in a general down-valley (west) direction.

Holocene

Glaciofluvial and fluvial gravel (*unit I*) are found at varying levels throughout the valleys and comprise the surface of terraces. They are moderately to poorly sorted cobble gravels with a sand matrix (Fig. 2.10). The highest terraces (approximately 70 m) contain clasts up to several metres in diameter and are typically more poorly sorted than lower terraces that have smaller clasts. Imbrication indicates a westward flow. This unit forms erosional contacts with all of the older sediments discussed.

2.6.2 Landslides

The characteristics of the nine landslides investigated are reported in terms of their classification, dimensions and state of activity. A summary of this information and the location of the landslides discussed is illustrated in Figure 2.11.

Landslide Classification

Landslides were classified based on the system proposed by Cruden and Varnes (1996). Seven of the nine landslides investigated showed signs of failure from the preceding spring or were failing during fieldwork and are classified as active. Of these, five are further classified as reactivated since part or all of a pre-existing landslide failed. The remaining two landslides are classified as dormant since they showed no signs of instability for several years.

Retrogressive failure is the most common landslide process. Such failures are characterized by a rupture surface that extends beyond the pre-existing headscarp, opposite to the direction of movement (Cruden and Varnes 1996). Five retrogressive failures are identified. An additional three failures were confined to within the body of the original landslide, and are classified as diminishing (e.g. AJB01-L2, L3, and L7, Fig. 2.11).

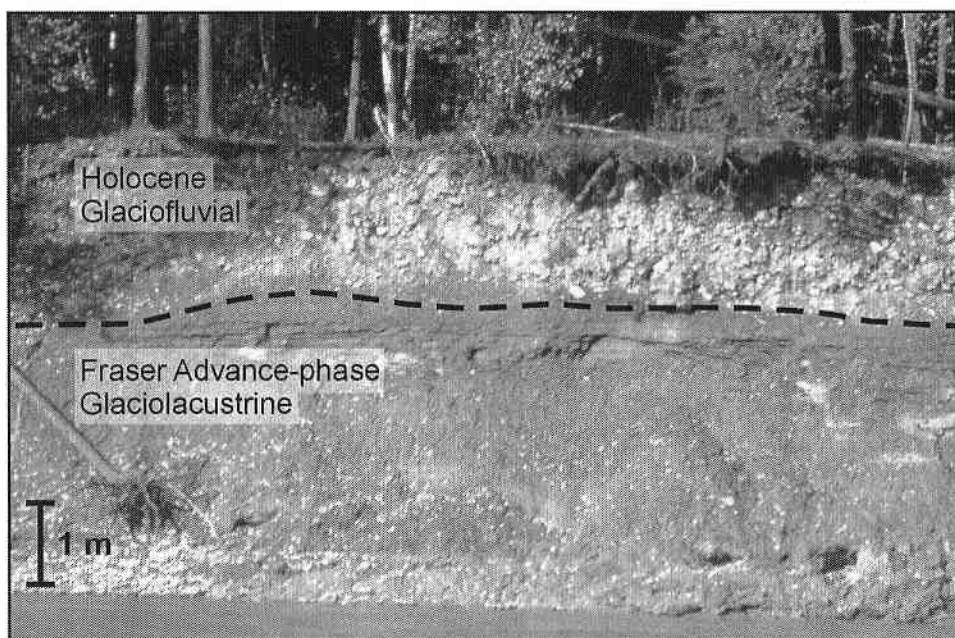
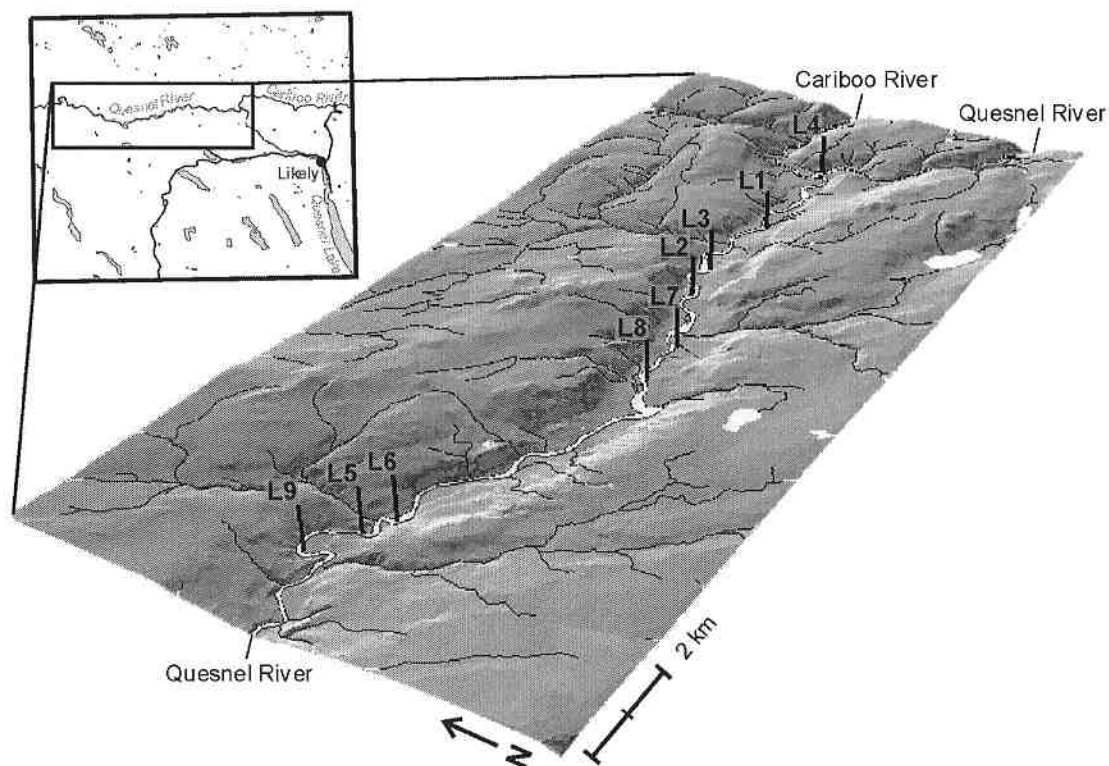


Figure 2.10. Typical Holocene gravel sediments (unit I) found throughout the valley that form the surface of lower terraces. Here, gravel overlies rhythmically bedded clay (unit D).



Station	Age Range	Activity	Type of Failure	Surface Area ($m^2 \times 10^3$)	Volume ($m^3 \times 10^3$)
AJB01-L1	1978 - 1985	Active	Retrogressive, wet, earth slide-earth flow	32	108
AJB01-L2	1996 - 1998 (<1955*)	Reactivated	Diminishing, wet, earth slide-earth flow	11 (59*)	-
AJB01-L3	1978 - 1985 (1970 - 1978*)	Reactivated	Diminishing, wet, earth slide-earth flow	49 (207*)	-
AJB01-L4	28-Apr-96	Dormant	Retrogressive, very rapid, dry, earth slide-debris flow	104	924
AJB01-L5	Spring, 2001	Reactivated	Retrogressive, complex, wet earth flow-debris fall	40 (96*)	169
AJB01-L6	1996 - 1998 (<1957*)	Reactivated	Retrogressive, very wet, earth flow	32 (139*)	76
AJB01-L7	1996 - 1998 (07-May-1976*)	Reactivated	Diminishing, complex, earth slide-earth topple (Retrogressive, rapid, wet earth slide-earth flow*)	16 (357*)	58 (> 1 000*)
AJB01-L8	1978 - 1986	Active	Complex, earth slide-earth topple	11	42
AJB01-L9	1992 - 1996	Dormant	Retrogressive, wet, earth slide-debris flow	164	-

* Data for pre-existing landslide

Figure 2.11. Digital elevation model, looking upstream, showing the location of the nine major landslides along the Quesnel River and their characteristics. Age ranges are determined from sequential airphoto analysis whereas activity, type of failure, surficial area and volume were assessed by fieldwork and chrono-sequential airphoto analysis.

All landslides investigated are earth landslides because they occurred in unconsolidated sediment, primarily consisting of fine-grained material. At sites AJB01-L4, AJB01-L5, and AJB01-L9 there is enough coarse material in the displaced mass to include a debris descriptor.

The most common type of failure is flow. The main bodies of the displaced material show abundant flow features. Levees are common where flow was diverted around large obstacles or stable bluffs (Fig. 2.12). Extremely fluidized flow is evident adjacent to AJB01-L5 where a gully periodically delivers sediment and debris to the Quesnel River (Fig. 2.13). Some flows have slide components although typically of limited extent (Fig. 2.14). Rotated or translated blocks are sometimes present near headscarps but are rarely found lower in the foot of the landslide. At several sites, the initial failure was by sliding (Fig. 2.15), where an intact block was mobilized along a plane of shear. Remoulded material then developed into a flow. An alternative explanation is that sufficiently saturated material failed by flow, removing lateral support for more competent material, which then failed by sliding. Other landslides are classified as having a topple or fall component. These failures are very localized events and were found adjacent to riverbanks where compact fine-grained sediment was undercut by river erosion.

Landslides are denoted as complex when more than one type of motion was experienced by the same mass. As an example, at site AJB01-L5, the rupture surface was located high above the river where it daylighted in a steep bluff face. Flow initially delivered material to the bluff where it continued by fall. At other sites (AJB01-L7 and AJB01-L8), sliding material is delivered to the banks of the Quesnel River, where undercutting caused topple and fall of coherent, jointed clay.

Landslide Dimensions

Landslides vary in size from very small to large (*cf.* Fell 1994). The aerial extent of disturbed material for all landslides ranges from $11 \times 10^3 \text{ m}^2$ to $357 \times 10^3 \text{ m}^2$ (Fig. 2.11). In addition, for some landslides a volume was calculated based on simplified geometric

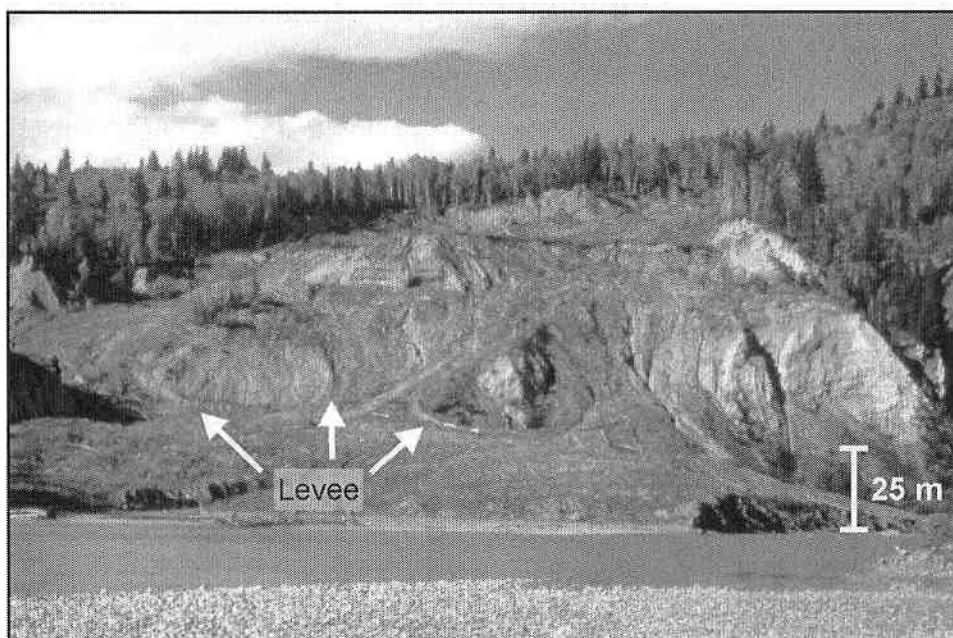


Figure 2.12. Landslide exhibiting predominately flow-type failure (section AJB01-L9). Note the levees formed where an intact bluff composed of unit D diverted flow material. The primary failed material is till (unit G) and the upper, fine-grained glaciolacustrine sediment (unit F).



Figure 2.13. Gully formed in unit D that periodically delivers debris to the Quesnel River (section AJB01-L5). Note person for scale.

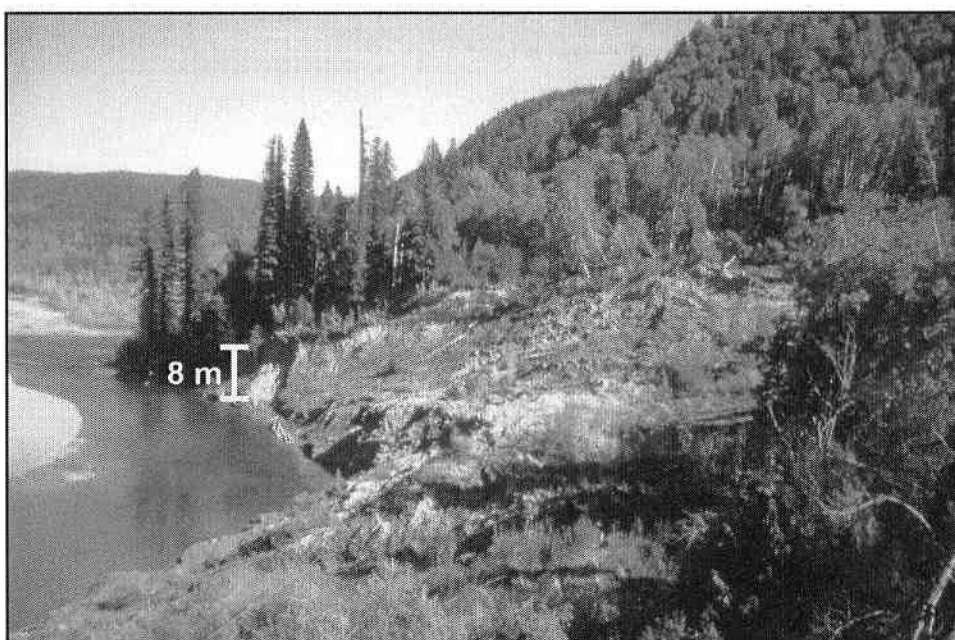


Figure 2.14. Typical landslide involving interbedded glaciolacustrine sediment (AJB01-L1). Failure is primarily by flow though some intact blocks are found near the head scarp.

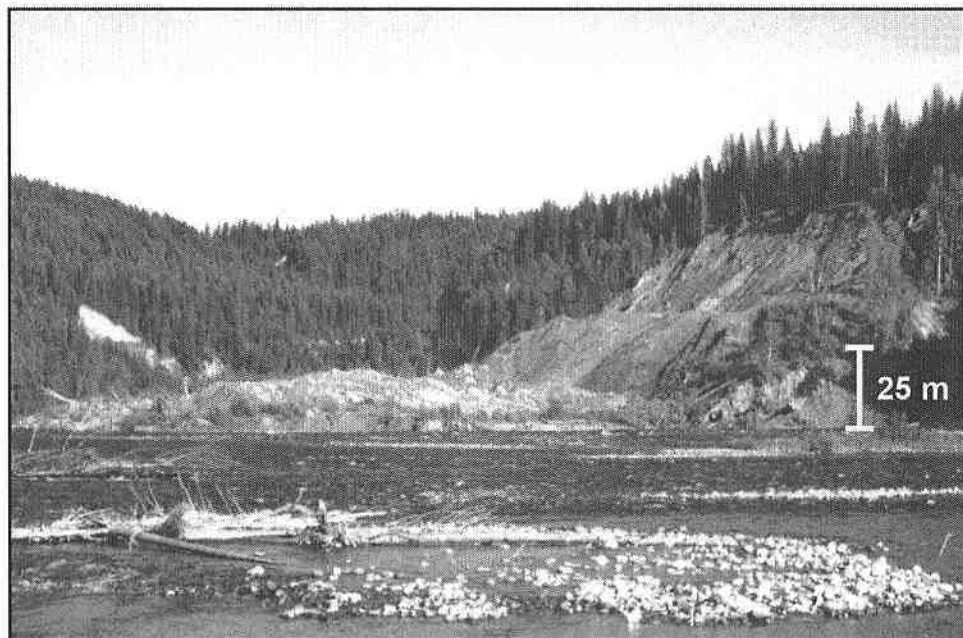


Figure 2.15. Landslide located at Quesnel Forks that failed primarily by sliding and consists of two rotated blocks (section AJB01-L4). The primary material involved is interbedded glaciolacustrine sediment. The terrace is approximately 75 metres high.

models and ranged from $42 \times 10^3 \text{ m}^3$ to $924 \times 10^3 \text{ m}^3$. Landslide AJB01-L7 is the largest in both surface area and volume. It is thought to be in excess of $1 \times 10^6 \text{ m}^3$.

The largest landslide is approximately 925 m in length (AJB01-L7), measured along the axis perpendicular to the head scarp, whereas the smallest is 87 m in length (AJB01-L8). The average length is 380 m. Widths were measured along the axis parallel to the head scarp and range from 165 (AJB01-L2) to 470 m (AJB01-L7) with an average of 260 m. The maximum crown elevation observed is 180 m above the current river level (AJB01-L9) and the lowest is 22 m (AJB01-L1). Height-length ratios range from 0.10 to 0.39 with an average of 0.24. Landslides described as rotational have a ratio of depth of rupture surface to length of rupture surface equal to approximately 0.17. This value is consistent with values reported by Skempton and Hutchinson (1969), who noted that rotational earth slides generally have a value between 0.15 and 0.33.

Landslide Activity

Of the nine landslides investigated, the timing of only two events is definitively known. Landslide AJB01-L7 occurred on May 7, 1976 as reported by a resident of the area whose excavator became buried beneath the foot of the landslide (Thurber Consultants Ltd. 1976a). This is the largest landslide in the area with its head scarp nearly a kilometre away from the river. Pre-failure airphotos show only limited slumping that occurred prior to failure and was localized directly adjacent to the river. Since the occurrence of the landslide, its surface has become stabilized and re-vegetated except for the toe that has remained active. The second event is AJB01-L4, which occurred on April 28, 1996 and was witnessed by recreational campers who were awoken in the early morning by a loud rumbling (Giesbrecht 2000). Historical documentation describes a previous landslide that occurred in roughly the same location in 1898 (Elliot 1996). This is supported by the airphotos from 1955 that show the remnants of a foot of a landslide at this location, though the slope was heavily vegetated.

For all other landslides, failure is estimated to have occurred within a time range (Fig. 2.11). The time frame reported is for the initial failure as many of the sites are still

experiencing movement. At locations AJB01-L1, L2, L3, L6 and L9, evidence of landslides preceding the earliest airphotos are identified. With the exception of AJB01-L2 and L9, the sites were heavily vegetated indicating the landslides were either inactive or possibly even relict. The other two sites showed signs of recent failure. Eventually each site experienced another major failure. In contrast, landslides AJB01-L5 and L8 occurred where no previous landslides were identified.

In general, all landslides investigated show signs of failure within the past 10 years, most being currently active or reactivated. Excluding evidence of failures that occurred prior to the availability of airphotos, initiation of five of the nine landslides occurred since the mid 1990s. The other four events were initiated in the mid 1970s to early 1980s.

2.7 Inferred Quaternary History

The stratigraphic record of the Quesnel and Cariboo River valleys is primarily the product of the Fraser Glaciation and associated depositional environments. The following section describes the sequence of events that have lead to the emplacement of sediment within the valleys, which are involved in landslide processes. These events are illustrated in Figure 2.16. In addition, the stratigraphic units are correlated to similar units identified elsewhere in central British Columbia (Table 2.3).

Pre-late Wisconsin

Sediments deposited prior to the Late Wisconsin (*ca.* 23 ka BP) are only known at two locations within the study area. Only limited inferences can be made and are based on the work of others. Preceding the Early Wisconsin, non-glacial Tertiary gravels were deposited by an ancestral Quesnel River (Fig. 2.16.1) and are found throughout the Cariboo region (Rouse *et al.* 1990; Levson and Giles 1993). Before 59 ka BP, the climate deteriorated and a glacial event ensued (Clague 1992). Davis and Mathews (1944) and Fulton (1991) describe the general model for the inception of the Cordilleran Ice Sheet. Glacial ice covered the study area, scouring and eroding previous valley fill and plateau sediments (Fig. 2.16.2). A blanket of till (*unit A*) was deposited during this event.

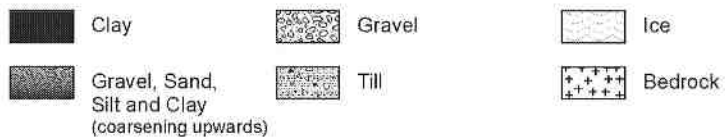
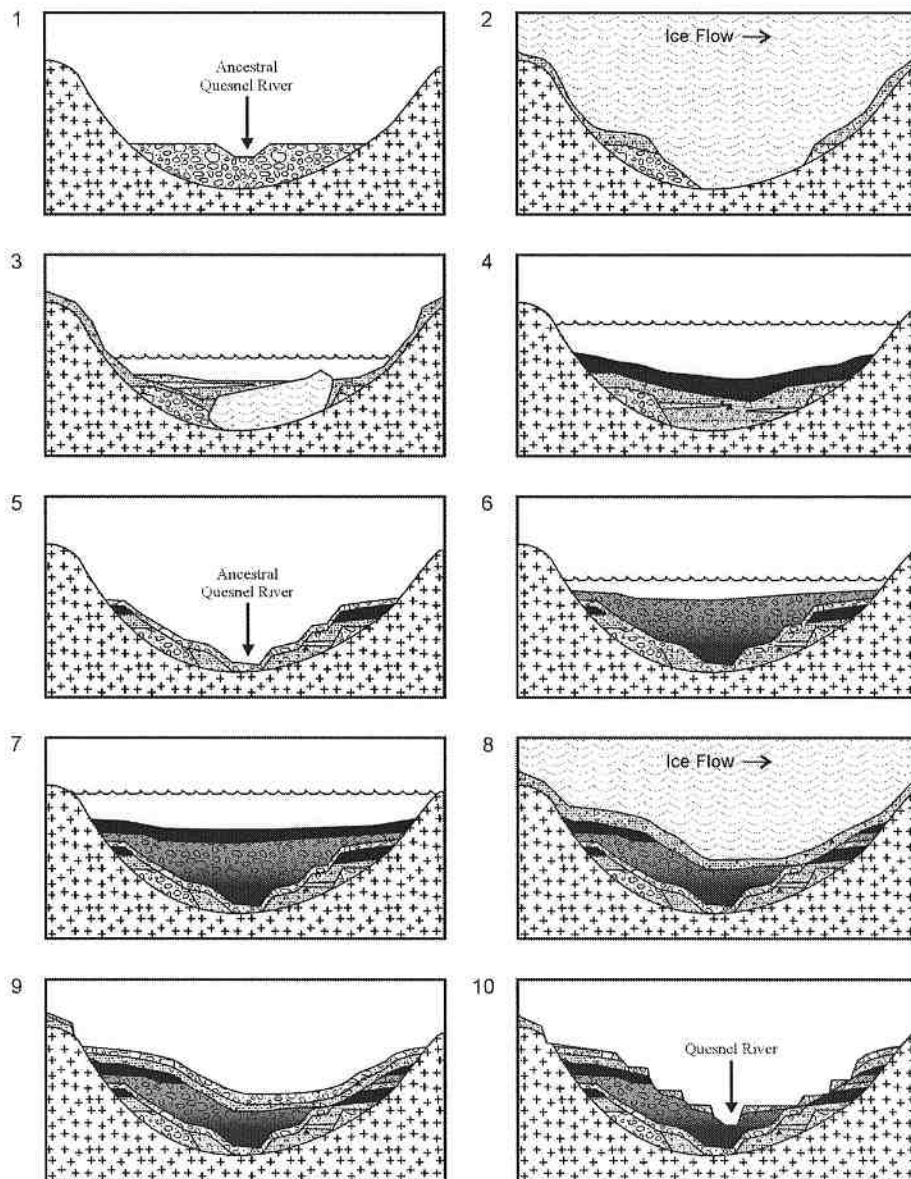


Figure 2.16. Proposed sequence of events for the Quesnel and Cariboo River valleys, spanning the Quaternary: 16.1) Tertiary sediment at the beginning of the Quaternary; 16.2) penultimate glaciation and deposition of till; 16.3) deposition of recessional, ice-contact sediments; 16.4) formation of large recessional lake and the deposition of glaciolacustrine sediments; 16.5) middle Wisconsin valley incision; 16.6) formation of Fraser, advance-phase glacial lake and deposition of coarsening upwards glaciolacustrine sediments; 16.7) relative deepening of glacial lake; 16.8) occupation by Fraser Glacial ice and deposition of till; 16.9) recessional glaciofluvial deposition; and 16.10) Holocene valley incision.

Time	Geologic Event	Quesnel and Cariboo River Valleys (this paper)	Central B.C.	Quesnel and Cariboo River Valleys	Bullion Pit and Mexican Hill	Quesnel	Williams Lake	South-central B.C.
Holocene	Non-glacial	I	Eyles and Clague 1991	Clague 1991	Clague et al. 1990	Clague 1988	Clague 1987	Fulton and Smith 1978
		H	E	h		13	9, 10	Postglacial sediments
		G	Late Wisconsin till	g	Late Wisconsin till	12	7, 8	upper stratified
		D - F	C, D	f	stratified drift	11	6	unstratified
Olympic Interstade	Non-glacial	C		d, e	organic bearing sediments	9?, 10	3?, 4, 5	lower stratified
		B	B1, B2	c	older drift unit			Besette sediments
Early Wisconsin	Penultimate Glaciation	A	A?	a	older drift unit	1 - 8?	2	Okanagan Centre Drift
							1?	
Pre-Wisconsin	Non-glacial							Westwold sediments

Table 2.3. Correlation between stratigraphic units described from this and other research in the interior of British Columbia.

At the onset of deglaciation, topographic highs became ice-free causing the isolation of ice lobes. Glaciers continued to retreat towards the thickest accumulations of ice that were found in the valleys (Fulton 1991). Drainage became blocked by either ice or outwash sediment and formed large lakes. Eyles *et al.* (1987) describe similar late-glacial lakes as supraglacial since they contained large amounts of stagnating ice. At this time, the ice-contact sediments (*unit B*) were deposited in close association with till (Fig. 2.16.3). The sediments show deformation, likely both syn and post-depositional, caused by the melting of ice and subsequent loss of support (Broster and Clague 1987).

Clague (1991) describes thick accumulations (up to 80 m) of massive and stratified silt, sand, gravel, and minor diamicton that make up the majority of the stratigraphy within the Quesnel and Cariboo River valleys (*unit D*). The sediments were interpreted as being deposited in a late-glacial lake that occupied the valleys during the penultimate deglaciation (Fig. 2.16.4). Though such sediments may exist, an alternative explanation is that *unit D* is younger and was instead deposited during the advance-phase of the Fraser Glaciation. The initial interpretation by Clague (1991) was founded on the presence of an unconformity between the glaciolacustrine unit and an overlying fluvial/glaciofluvial gravel unit that represent incision during a non-glacial interval. Based on the present study, the gravel package conformably overlies the glaciolacustrine sediments and is interpreted as part of the deltaic succession. Similar pre-Fraser stratigraphic units are described elsewhere in central British Columbia (e.g. Fulton and Smith 1978; Clague 1987; Clague 1988; Clague *et al.* 1990; Eyles and Clague 1991).

Unit C is representative of the Olympia Interstade (*ca.* 25 – 59 ka BP) and of at least several thousand years during which the climate within the study area was substantially warmer, though drier and cooler than that of today (Clague *et al.* 1990). Interstades are periods of denudation and during this time the ancestral Quesnel River incised the valley to depths greater than what is seen today since the unconformity that represents this period lies below the current river level in most places (Fig. 2.16.5).

Late Wisconsin

Between 29 and 25 ka BP the climate deteriorated and the Fraser Glaciation began (Ryder and Clague 1989). By 19 ka BP the mountain ice sheet phase of Davis and Mathews (1944) was established in south-central British Columbia (Fulton and Smith 1978). Ryder *et al.* (1991) suggest that the southern extent of glaciation was reached between 14 ka BP to 14.5 ka BP.

The first evidence of Fraser glacial sediment is a thick glaciolacustrine package (*unit D*) that filled the Quesnel and Cariboo River valleys (Fig. 2.16.6). The unit represents advance-phase sediments similar to deposits described within the Fraser Valley (Clague 1987; Clague 1988; Eyles and Clague 1991). During the deposition of *unit D*, inundated valley slopes became unstable and sediment was deposited by subaqueous gravity flows (*unit E*). Such deposits are common within advance-phase glaciolacustrine sediment (Clague 1988). As glaciers advanced, sediment became coarser and a delta prograded into the lake. The unit coarsens up valley (east) indicating the presence of glaciers expanding from the Cariboo Mountains. The minimum elevation of the lake was 730 m asl, based on upper elevations of *unit D*. This is comparable to advance-phase glacial lake levels reported over a wide area (Clague 1988; Huntley and Broster 1994) and suggests that a large lake system may have developed in response to disrupted drainage. Huntley and Broster (1994) proposed a combination of glaciofluvial aggradation and ice damming within the Fraser Valley responsible for the creation of a large lake called "Glacial Lake Camelsfoot". Alternatively, a more complex system of independent lakes may have existed.

Sometime prior to the lake being overridden by advancing glaciers, the lake deepened, depositing *unit F* (Fig. 2.16.7). Though this unit is evident throughout the Quesnel and Cariboo river valleys, it has not been reported elsewhere in central British Columbia. As such, this may be a local event restricted to the study area. It may record the advance of an ice tongue down the Fraser Valley, blocking the mouth of the Quesnel River valley.

Ice eventually overrode the area, eroding older sediments and depositing till (*unit G*) (Fig. 2.16.8). The weight of ice caused underlying sediment to become over-consolidated. Deglaciation was well advanced by 11.5 ka BP (Ryder *et al.* 1991) though a minor re-advance from the Cariboo Mountains occurred (Tipper 1971a,b). Drumlins, flutings, crag and tails, and striations record the pattern of ice flow at this time. Ice flowed from the Cariboo Mountains northwest (Bichler and Bobrowsky 2003). The preservation of advance-phase and older sediments is likely the product of glacial flow being oblique to the orientation of major valleys.

No evidence exists for major recessional glacial lakes and instead glaciofluvial gravel (*unit H*) overlies till. It is, however, marked at the base by a thin unit of fine-grained sediment. If regional ponding occurred, it did not persist for long before drainage was re-established (Fig. 2.16.9). Flow within the valley was to the west, like that of the modern Quesnel and Cariboo rivers.

Holocene

Once glaciers had completely receded, the modern Quesnel and Cariboo Rivers became established and continued to incise the valleys (Fig. 2.12.10). During this process, terraces were created and are underlain by coarse gravel (*unit I*). This is the youngest unit deposited and involved in the modern landslide processes.

2.8 Discussion

The landslides within the Quesnel and Cariboo river valleys are the product of a sequence of events that began with the deposition of sediment. Subsequently, environmental factors affected sediments and triggered the events. The relation between stratigraphy and landslides is first discussed, followed by some possible triggering mechanisms.

2.8.1 Landslides and Stratigraphy

The stratigraphy of the Quesnel River valley is largely responsible for the distribution and abundance of landslides. The primary units involved in landsliding are advance-phase glaciolacustrine sediments (*units D and F*) and till (*unit G*). Glaciofluvial/fluvial

material (*units H and I*) often overlies other sediment but plays primarily a passive role in slope stability. The thickest exposures of these units occurs on the south side of the valley, for reasons described in section 2.7, where all but one landslide are found.

The most common unit involved in landslides is the interbedded glaciolacustrine sediment (*unit D*). This is partially because it is the most extensive unit and it is currently being exposed at river level. Within it, the rupture surface is located where fine-grained, rhythmically bedded sediment is dominant (i.e. towards the base of the unit). The rupture surface typically daylight at or near the river level. The upper several metres of most scarps generally consist of coarser material overlying fine-grained material, in a transition zone between sand dominated facies and clay or silt facies.

The clay and silt beds create perched and multiple-confined water tables that are evident where water seeps from above clay layers, out of overlying sand. The presence of water increases pore water pressure, which decreases material strength, and increases shear stresses due to artificial loading (Cruden and Varnes 1996). Such failures are typically intermittently active with localized movements that are a reflection of changes in pore-water pressure (Skempton and Hutchinson 1969). No landslides occurred where *unit D* is composed of coarser, better-drained sediment (i.e. in the Cariboo River valley).

Two groups of failures are observed to take place within *unit D*. Landslides AJB01-L1, L2, L3, and L7 are dominantly flow-type failures with minor slide components (Fig. 2.14). Intact blocks that have rotated or translated near the head scarp are sometimes found. Surface water is only present in small quantities though the displaced material remained moist during the dry season and is susceptible to saturation by rainfall. Evidence of fluidized flow is common with minor flow events occurring during moderate rainfall. These landslides occurred on valley slopes of approximately 15°. Chrono-sequential airphotos reveal that the landslides have occurred as a series of failures spanning many years except AJB01-L7, which occurred primarily as a single event, though parts of the slide remain active nearly 30 years later.

Landslides AJB01-L4 and L8 are the second group of failures occurring primarily in *unit D*. They are dominantly slide-type failures with minor flow components (Fig. 2.15). Large blocks consisting of intact stratigraphic units make up the majority of the displaced material. No surface water is evident and surficial sediments are dry. Both landslides contain unusually thick units of clay and occurred in a terrace, capped by coarse-grained glaciofluvial sediment (*unit I*). It is known that landslide AJB01-L4 occurred as a singular event as perhaps did AJB01-L8.

The remaining landslides involve the failure of the clay unit (*F*) deposited during the over-deepening of the pro-glacial lake and till (*unit G*). The units are found high on valley slopes overlying *unit D*. The rupture surface extends through overlying glaciofluvial sediment (*unit H*) or till, cuts through these units, and shallows within the interbedded glaciolacustrine sediments. The rupture surface daylights high above the river. The failures are primarily isolated events, though multiple failures are possible, and have occurred over short periods of time.

The presence of the clay unit at landslides of this type likely acts as an aquitard and creates a perched water table. In addition, lodgement till (i.e. *unit G*) consists of up to 80% of material derived from local bedrock (Bell 1993). Within the study area, the bedrock consists primarily of siltstone, shale, slate, phyllite and mafic volcanics. Such rocks generally produce plastic, clay-rich tills with slightly higher moisture contents than tills derived from other bedrock sources (Bell 1993). The observed fissility and jointing would further enhance water infiltration.

Landslides AJB01-05, AJB01-06 and AJB01-09 involve *units F* and *G*. The landslides are the most fluid-like failures investigated (Fig. 2.12). They contain abundant flow features such as levees and evidence of liquefaction (e.g. debris enshrouded by liquefied sand). At these sites, *unit D* remained intact and displaced material flowed overtop, partially eroding its surface. The displaced material is moist and easily becomes saturated during light rainfall. Valley slopes are approximately 18° where the landslides occurred.

The style of large failures within the different stratigraphic units is unique. Smaller failures and other modes of mass movement were present within many of the units described in section 2.6.1 but were not studied.

2.8.2 Landslide Triggers

The temporal occurrence of landslides is primarily related to the environmental factors that act upon the observed stratigraphy. As noted above, some units have inherent properties that make them prone to failure. Even so, an external source of energy is required to initiate failure; the trigger. Environmental factors that are associated with triggering mechanisms and that are discussed herein are: river discharge, precipitation, and snow pack. They are discussed in terms of short and long-term effects.

Short-term factors are defined here as those that vary within a daily time-scale and are associated with isolated events such as rainstorms. River discharge and precipitation are the most important short-term factors. River discharge can be used as relative representation of the energy available for erosion. Bank erosion leads to the removal of lateral support and an increase in internal shear stress (Cruden and Varnes 1996). Its importance as a triggering factor is evident since all landslides occurred on the outer, erosive edge of a meander. Precipitation has also been linked to slope instability (e.g. Crozier 1999). It may act to decrease material strength or load strata, increasing shear stress (Cruden and Varnes 1996).

The discharge of the Quesnel and Cariboo Rivers at three stations around the time of the 1976 failure of landslide AJB01-L7 is illustrated in Figure 2.17. Failure occurred at the beginning of the spring run-off during a distinct surge when flow was $467 \text{ m}^3/\text{s}$. This flow was well above the daily mean discharge for that year ($306 \text{ m}^3/\text{s}$) and was nearly four times higher than the average flow for the nine months preceding the failure ($136 \text{ m}^3/\text{s}$). A similar situation exists for the 1996 failure at AJB01-L4 (Fig. 2.18). Flow was $292 \text{ m}^3/\text{s}$ compared to the daily mean of $261 \text{ m}^3/\text{s}$ for that year and was more than double the average flow during the preceding nine months ($139 \text{ m}^3/\text{s}$).

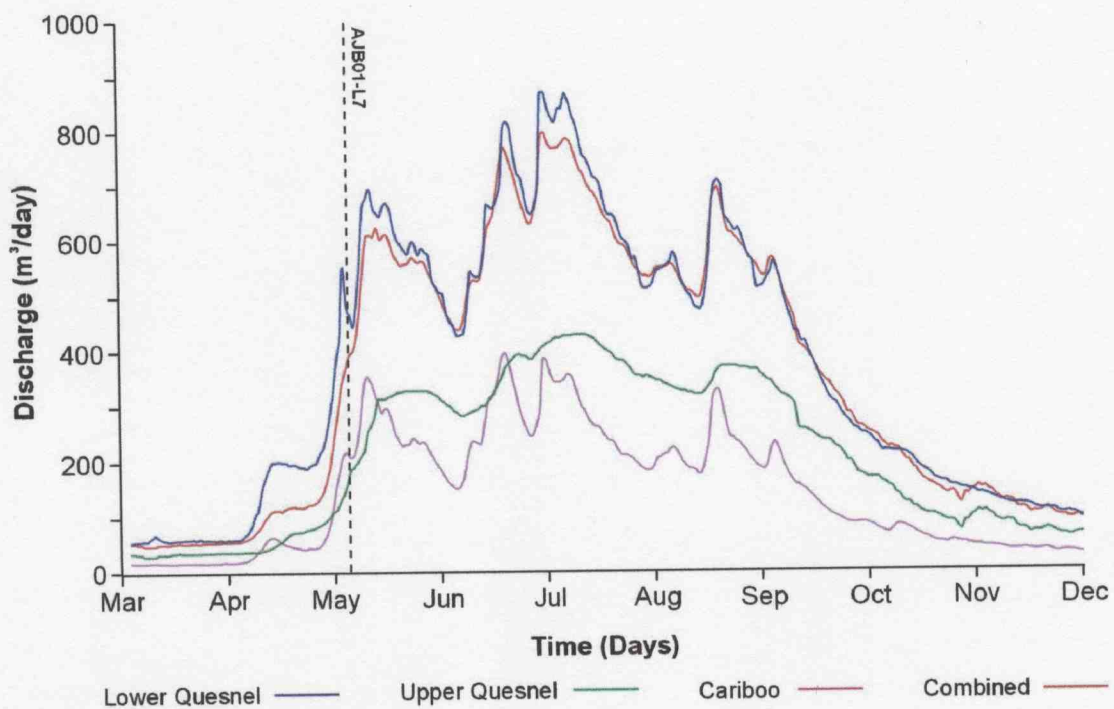


Figure 2.17. River discharge for 1976 for the upper and lower Quesnel River and the Cariboo River as well as the combined data for the upper Quesnel and lower Cariboo rivers. Data was collected at Environment Canada stations 08KH001, 08KH006 and 08KH003, respectively.

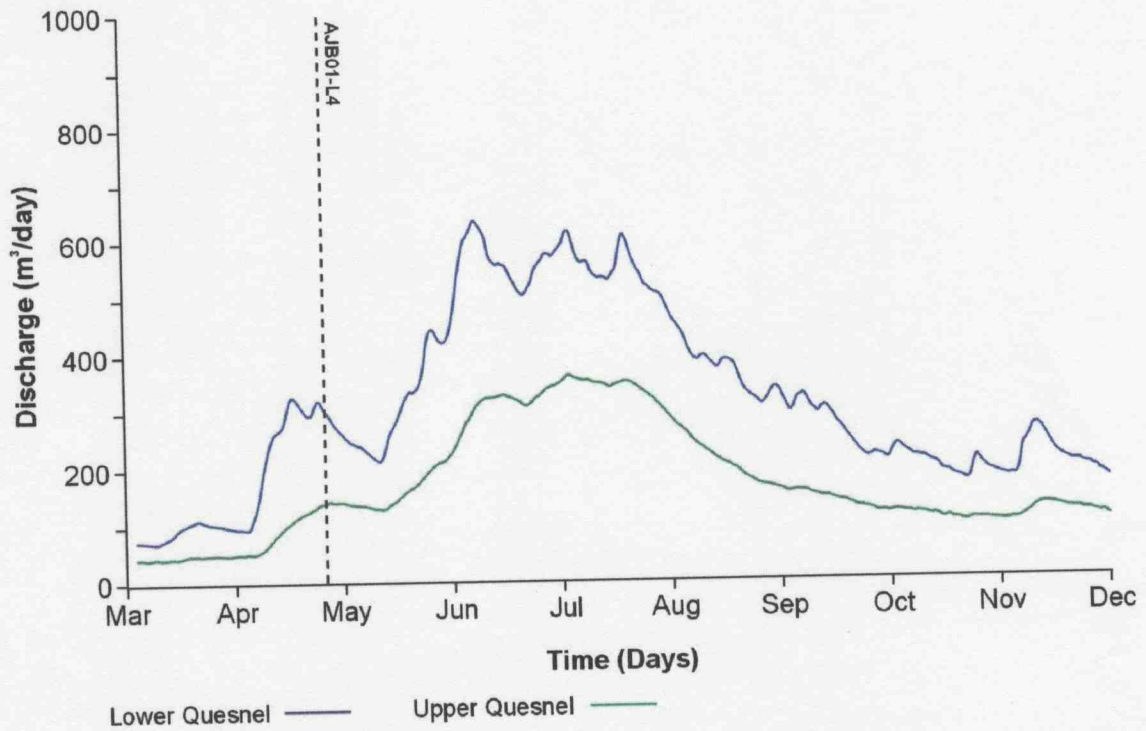


Figure 2.18. River discharge for 1996 for the upper and lower Quesnel River Data was collected at Environment Canada stations 08KH001 and 08KH006, respectively.

Both events occurred at the beginning of spring flood, prior to the highest discharge rates. It is proposed that unconsolidated material accumulates at the base of slopes during low water and once spring flood begins, water levels rapidly rise and quickly erode the material. The banks are thereby over-steepened and lateral support is decreased, which may lead to failure.

Precipitation records preceding both landslides show no substantial rainfall preceding the event. The only significant rain was recorded approximately two weeks prior to the failure of AJB01-L7. It was the fifth highest amount of rainfall in a 24-hour period between 1974 and 1993.

Though precipitation is likely not the final trigger, it is a significant factor in reducing material strength and exploiting lithological and stratigraphic weaknesses. Precipitation becomes even more important within previously disturbed material that remains moist over large portions of the landslides throughout the spring and summer months. With only minor amounts of rainfall, surficial material was noted as becoming saturated, liquefying in many areas with small slumps and flows constantly occurring during fieldwork.

Long-term factors are defined here as environmental trends acting over multiple years that affect the stability of slopes. The long-term factors examined are the annual averages for river discharge, precipitation and snow pack. The cumulative departure from the mean for these variables is illustrated in Figure 2.19. It was calculated based on yearly totals using the equation $\Sigma\{x_i/x_{\text{mean}}-1\} \times 100$ as described by Barrett (1979) and Bovis and Jones (1992), where x_i is the total for year 'i' and x_{mean} is the average over the entire sampling period. When the slope is positive it represents two or more years that the factor is recorded as being above average whereas a negative slope denotes consecutive years that the factor is below average, and a slope of zero means the factor was average during that year. The difference in value from one year to the next is the percent above or below the mean.

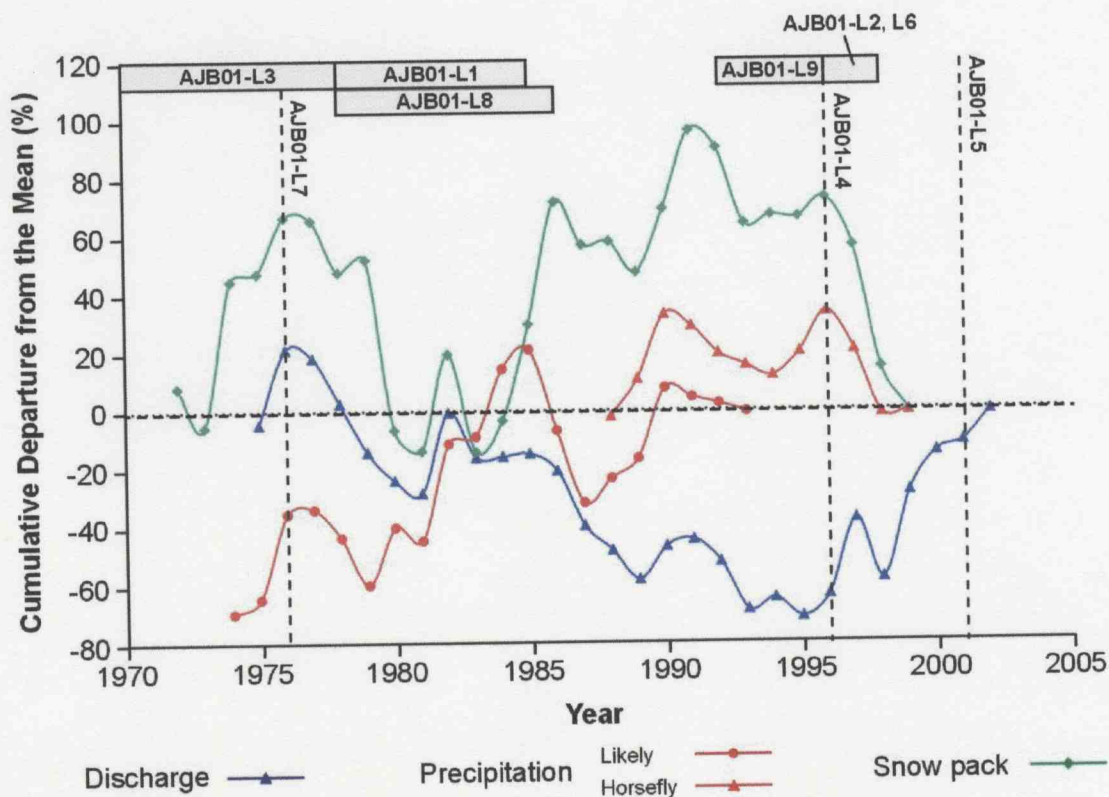


Figure 2.19. Yearly, cumulative departure from the mean for 3 factors influencing regional landslide activity. Landslide ages are indicated as either a year (dashed line) or an age range (shaded box). Data was collected from Environment Canada stations as follows: discharge, 08KH006; snow pack, 1C24; precipitation at Likely, 1094616; precipitation at Horsefly, 1093600.

Consecutive years having high river discharge may aid short-term factors in triggering a landslide as less material is deposited at the base of slopes along the riverbanks and more erosion of in situ material takes place during spring flood. River discharge was progressively below average between 1976 and 1995, after which it remained mostly above average until the present. This latter period corresponds to the initiation of 5 of the 9 landslides and to continuing movements at many of the sites. The only landslide that occurred prior to 1995 that has a definitive date is AJB01-L7. It also occurred during consecutive years of high discharge.

During consecutive years of abnormally high precipitation, surficial material may stay wetter longer and high ground water tables may persist. This would promote the reduction of material strength and increase internal shear stress. The trend in precipitation is more variable than for discharge data. Even so, periods having consecutively above average precipitation are identified and correspond to ranges in time of failure for most landslides. Two exceptions are landslides AJB01-L2 and L6, which occurred during consecutive years of below average precipitation.

The third factor considered is snow pack as it is directly related to both discharge and precipitation. The Quesnel and Cariboo Rivers are primarily controlled by snowmelt (Pederson 1998) and thus years with larger snow packs have a higher potential for large spring floods and increased pore water pressures. Except for the period between 1983 and 1986 discharge and snow pack have similar trends. As such, the relation between landslide events and snow pack follows the relation with discharge.

General correlations between the three variables can be drawn. Landslides AJB01-L4 and L7 occurred in years where discharge, precipitation, and snow pack were above average. In 1976, the annual flow was 17% above the annual mean while precipitation and snow pack was 30% and 20% above average, respectively. Similarly, in 1996, they were 8%, 15% and 7% higher, respectively. Based on this positive relationship, adding the departures from the mean for these three factors produces a simple bar graph that can be used to predict in which years the landslides are most likely to have occurred (Fig. 2.20).

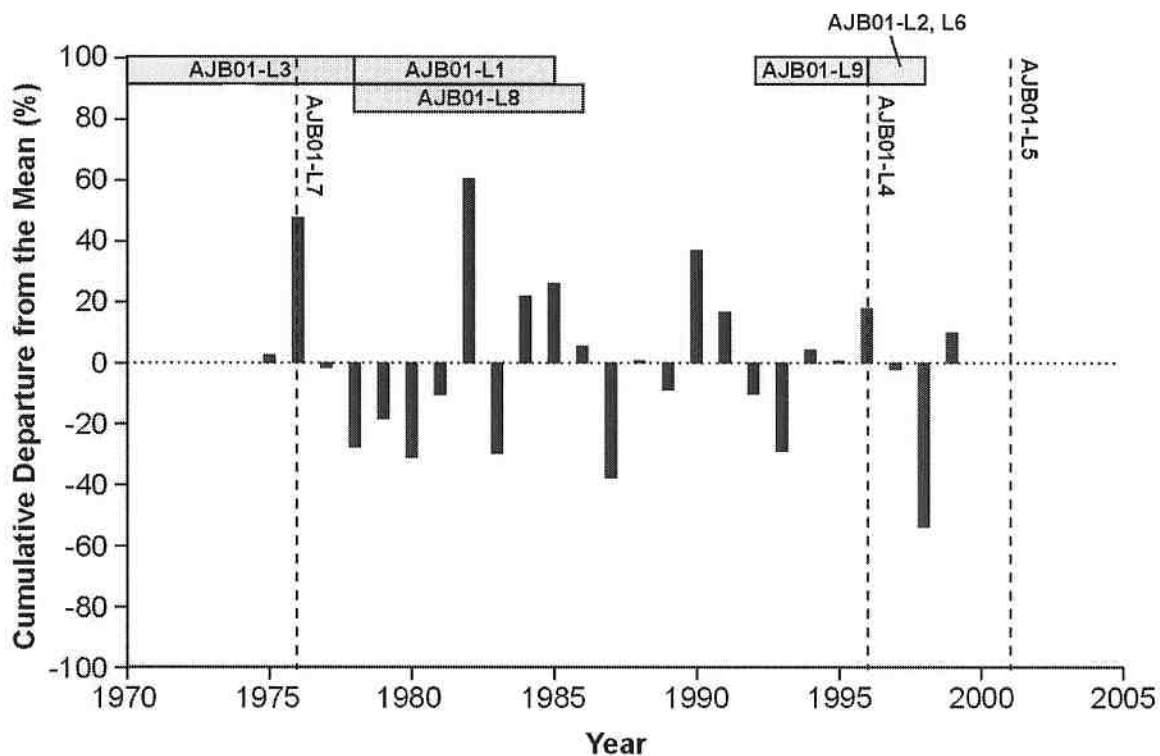


Figure 2.20. Summed cumulative departure from the mean for three factors influencing regional landslide activity. Landslide ages are indicated as either a year (dashed line) or an age range (shaded box). Precipitation data for the years 1988 – 1993 were averaged for the Horsefly and Likely stations.

Landslides are more likely to have occurred during years, within the ranges determined by airphoto analysis, that have high positive departures from the mean. As an example, landslides AJB01-L1 and L8 likely occurred in 1982.

2.9 Conclusions

Landslide processes within the Quesnel River valley were characterized in the course of a regional investigation of stratigraphy and landslides. The stratigraphic units described during fieldwork complement previous studies within central British Columbia and help to explain the distribution of landslides within the study area. Of particular importance is the identification of a previously unrecognized unit of clay that occurs regionally at a stratigraphically high position. Three styles of failure were identified based on the relation between stratigraphic units and landslide characteristics:

- 1) The most common style of failure occurs within advance-phase glaciolacustrine sediment comprised of interbedded clay, silt, and sand. These landslides are found on valley slopes. Failure is dominated by flow with minor slide components. Such landslides are typically long-lived and occur as a series of smaller failures.
- 2) The second style of failures also occurs within advance-phase glaciolacustrine sediment but is associated with abnormally thick beds of clay and occurs within terrace landforms. Failure is dominated by slide with minor flow components. These landslides are single, rapid events.
- 3) The final group of landslides occurs within clay and till found high on valley slopes. Underlying units are not involved in failure. These landslides have the strongest flow component and are short-lived, rapid events.

No landslides were identified involving pre-Fraser sediment since the occurrence of these units at surface is rare. Over time, river incision will expose older sediment and they too will be subject to landsliding.

Slope undercutting due to riverbank erosion is the most important process for triggering the first two styles of failure, which occur in the advance-phase glaciolacustrine

sediment. As such, these styles of landslides can be expected to occur where thick accumulations of fine-grained glaciolacustrine sediment occurs on the outer bend of a meander. Precipitation is also an important factor but likely plays a subordinate role. The third style of failure is unlikely attributed to riverbank erosion as its rupture surfaces are located high above the river. Instead, precipitation and snowmelt are the most important environmental factor discussed. This style of failure can occur anywhere the stratigraphic units are present. Both short and long-term factors influence failure and no conclusion on which is more important is offered. It is however proposed that consecutive years having high river discharge, precipitation, and snow packs are more conducive for failure.

CHAPTER 3

THREE-DIMENSIONAL MAPPING OF A LANDSLIDE USING A MULTI-GEOPHYSICAL APPROACH: THE QUESNEL FORKS LANDSLIDE

3.1 Abstract

A landslide located on the Quesnel River in British Columbia, Canada is used as a case study to demonstrate the utility of a multi-geophysical approach to subsurface mapping of unstable slopes. Ground penetrating radar (GPR), direct current (DC) resistivity and seismic reflection and refraction surveys were conducted over the landslide and adjacent terrain. Geophysical data were interpreted based on stratigraphic and geomorphologic observations, including the use of digital terrain models (DTMs), and then integrated into a 3-dimensional model. GPR surveys yielded high-resolution data that were correlated with stratigraphic units to a maximum depth of 25 m. DC electrical resistivity offered limited data on specific units but was effective for resolving stratigraphic relationships between units to a maximum depth of 40 m. Seismic surveys were primarily used to obtain unit boundaries up to a depth of > 80 m. Surfaces of rupture and separation were successfully identified by GPR and DC electrical resistivity techniques.

3.2 Introduction

The complex nature of many landslides necessitates the need for investigating their characteristics in as detailed a manner as possible (Bogoslovsky and Ogilvy 1977). To this end, it becomes important that the internal structure of the landslide and its surrounding environment be determined in order to facilitate reliable stability analyses and mitigation (Johnston and Ambos 1994; Bruno and Marillier 2000).

Models of landslide structure have traditionally been constructed based on geomorphic observations and when possible with the aid of limited subsurface data obtained by boreholes or excavations. Such direct methods (Hunt 1984) are more common but require labour intensive, and often costly, field work (Sharma 1997). During the past 20 years, advancements in computer processing and geophysical instrumentation have provided

other means of collecting proxy data. Geophysical methods are considered indirect methods and provide non-destructive, portable techniques that can be used to cover large areas at relatively low costs (McGuffey *et al.* 1996). Still, geophysical surveys are rarely utilized to their full potential (Hack 2000). A comprehensive review of direct and indirect techniques is presented by Hunt (1984), Hutchinson (1984) and McGuffey *et al.* (1996) whereas Ogil'vi (1974), Bogoslovsky and Ogilvy (1977), Goryainov *et al.* (1988), McCann and Forster (1990) and Hack (2000) describe geophysical techniques as applied to landslides. Table 3.1 lists several examples of geophysical techniques applied to other landslides that are relevant to the research discussed herein.

The purpose of this chapter is to present the results of a multi-parameter geophysical survey carried out on a landslide with the intention of mapping its internal structure. In addition it is shown that such integrated geophysical studies are effective in subsurface landslide investigation. The primary geophysical method used was direct current (DC) electrical resistivity, applied over a substantial portion of the landslide and adjacent terrain. Ground penetrating radar (GPR) and seismic surveys were also conducted, but over smaller areas. Geophysical data were calibrated against stratigraphic and surficial mapping and digital terrain models. The end result was the construction of an interpreted 3-dimensional structural model of the landslide.

3.3 Study Area and the Quesnel Forks Landslide

The landslide under investigation is located near the confluence of the Quesnel and Cariboo rivers (52° 40' N, 121° 40' W), near the eastern boundary of the Interior Plateau of British Columbia, Canada (Fig. 3.1). Local topography is characterized by a gently rolling plateau with an average elevation of 940 m asl near the landslide. East-west trending river valleys averaging 280 m in depth and 1.5 km in length incise the plateau. Climate data collected from Environment Canada stations for the period 1975 to 1993 show an annual temperature range between -39 °C and 35 °C and an average precipitation of 688 mm per year where approximately 480 mm is rain.

GPR	Resistivity	Seismic
Nichol <i>et al.</i> 2003	Godio and Bottino 2001	Bruno and Marillier 2000
Barnhardt and Kayen 2000	Havenith <i>et al.</i> 2000	Havenith <i>et al.</i> 2000
Bruno and Marillier 2000	Schmutz <i>et al.</i> 2000	Fraseri <i>et al.</i> 1998
Brooks and Pilon 1995	Fraseri <i>et al.</i> 1998	Gowda <i>et al.</i> 1998
	Gowda <i>et al.</i> 1998	Allen 1997
	Allen 1997	Pant <i>et al.</i> 1997
	Pant 1997	Cummings and Clark 1988
	Cummings and Clark 1988	Palmer and Weisgarber 1988
	Palmer and Weisgarber 1988	

Table 3.1. Examples of geophysical surveys conducted for landslides using geophysical techniques similar to those used at the Quesnel Forks Landslide.

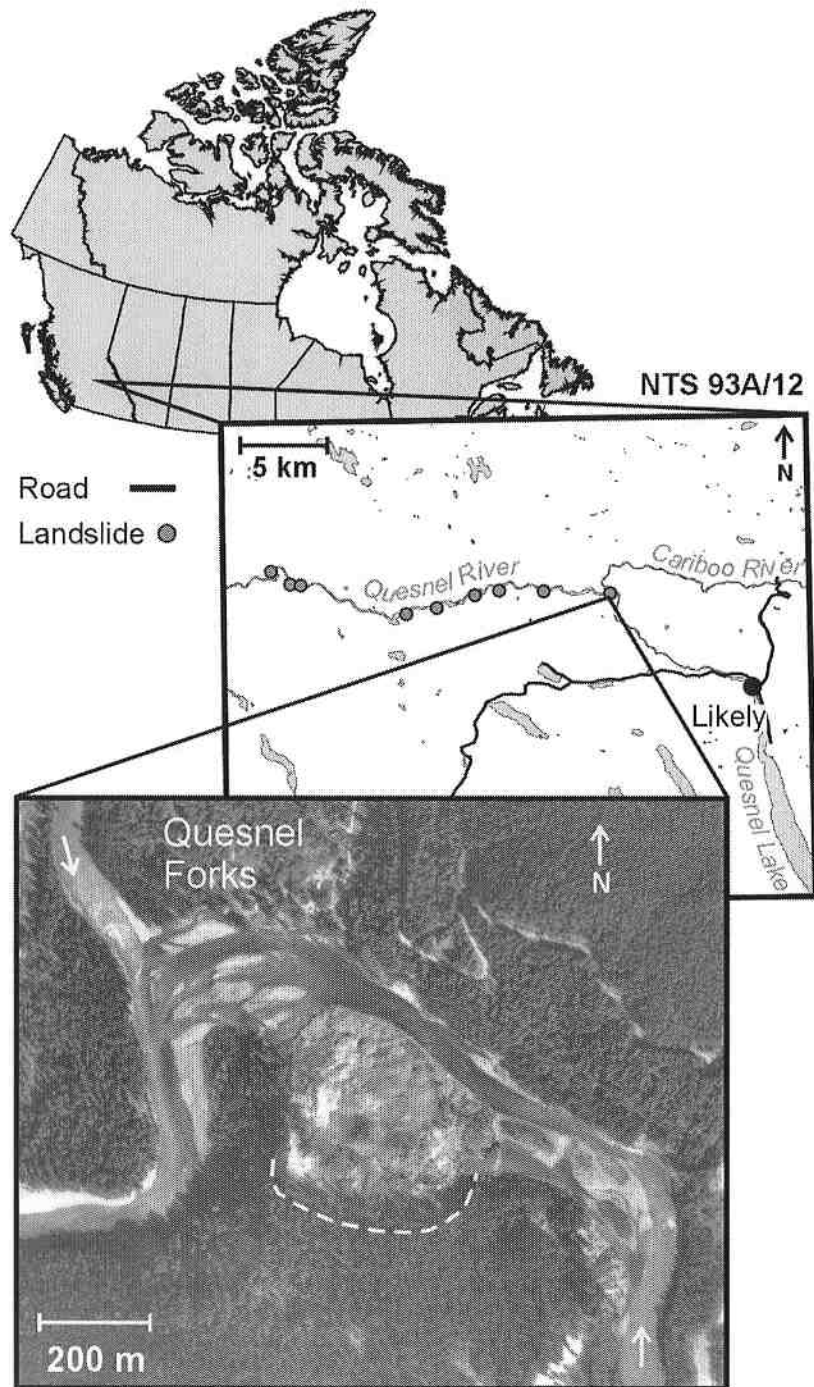


Figure 3.1. Location map showing the National Topographic System (NTS) map sheet and orthophoto of Quesnel Forks. The Quesnel Forks Landslide is the eastern most landslide of nine landslides investigated. The white dashed line on the photo is the boundary of the head scarp.

The Quesnel Forks Landslide occurred on April 28th, 1996 in the early morning and was witnessed by recreational campers at Quesnel Forks who reported hearing a loud rumble (Giesbrecht 2000). It occurred in a terrace opposite to the historical town site of Quesnel Forks (Fig. 3.2a). The terrace is 75 m high (Fig. 3.2b) and is bound to the north, east and west by the Quesnel River (Fig. 3.1). To the south, the terrace gives way to a steep bedrock-cored knob some 240 m high above the river. The terrace is primarily composed of sediment deposited during the last glaciation (*cf.* Chapter 2) and is underlain by bedrock of the Quesnel Terrane, related to a volcanic arc system (Bailey 1989). Phyllitic bedrock outcrops on the north side of the river and is assumed to underlie the terrace as well, though its depth is unknown.

The Quesnel River had a daily average discharge of 132 m³/s for the period 1975 to 2002, measured at a gauge station 10 km upstream of the landslide and maintained by Environment Canada. There are no major tributaries between the gauge station and the landslide. At the time of failure, during the onset of the spring flood, flow was 292 m³/s, which is more than double the daily average flow for the preceding nine months. Precipitation data are not available for the site at this time, though a station approximately 40 km to the southeast recorded no substantial rainfall preceding the event.

According to the classification of Cruden and Varnes (1996), the landslide was a retrogressive, dry earth slide-debris flow. The foot of the landslide temporarily dammed the river, after which the river breached the dam, partially eroding the foot and the riverbank adjacent to the town. The duration of river damming is unknown but was less than a few hours. River levels on the upstream side of the landslide remained 1 to 2 m higher at least several days after blockage (Klohn-Crippen Consultants Ltd. 1996).

Evidence for prior instability of the terrace is known. In 1898 a landslide occurred upstream of a bridge formerly located at the base of the western edge of the terrace (Elliot 1996). By 1903 the road leading to the bridge required multiple relocations and by that time, approximately \$10 000 (Canadian) had been spent in mitigation (Elliot 1996). Fear

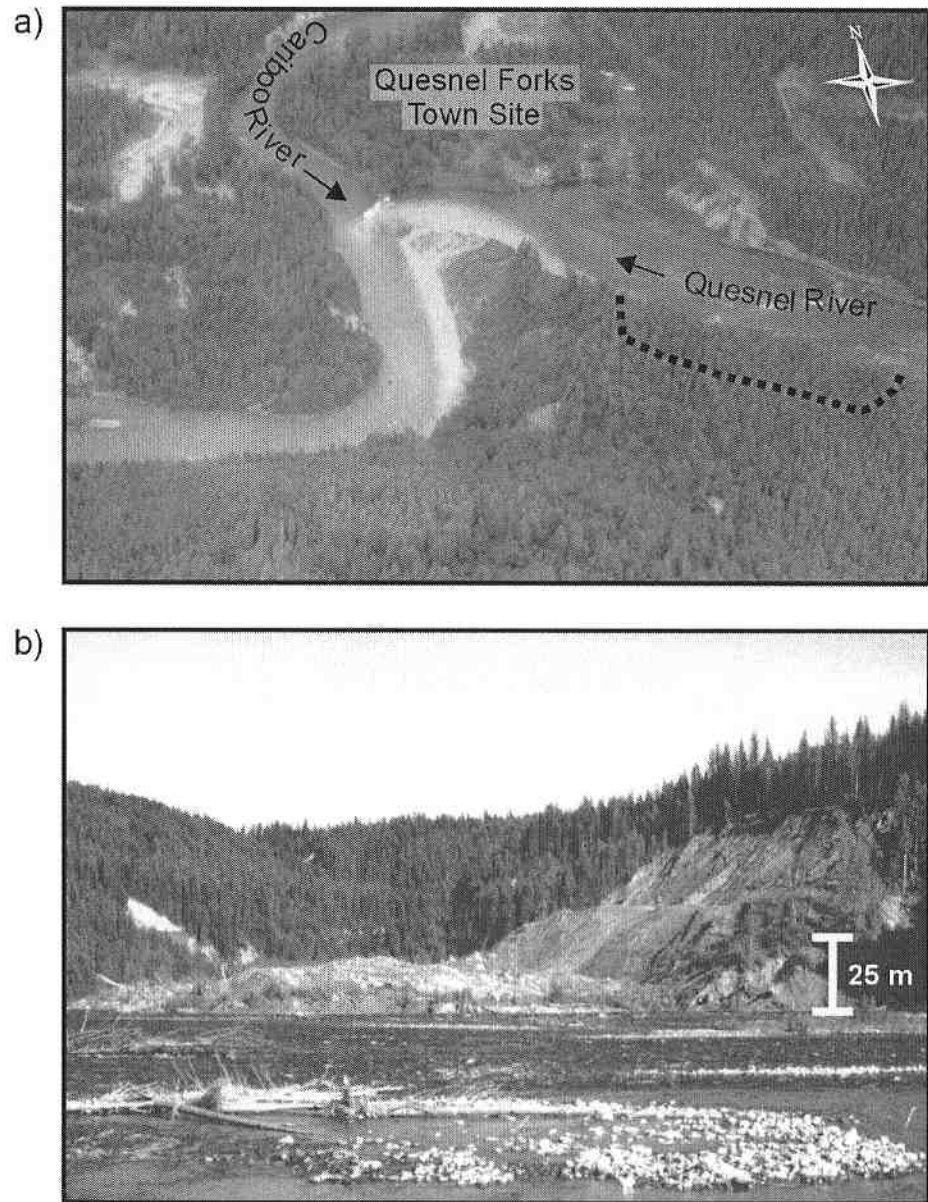


Figure 3.2. a) Pre-failure photograph of Quesnel Forks taken the year prior to failure (1995). View is from an airplane to the northeast, showing large amounts of silt being introduced into the Quesnel River. Dotted line shows the approximate location of the head scarp (photograph courtesy of Marie Elliot); b) View to the southeast of the Quesnel Forks Landslide, taken from the Quesnel Forks town site in 2001.

mounted that a major landslide could occur opposite Quesnel Forks endangering the town via a shift in river position (Wright 1987). The earliest airphotos examined of the site from 1955 shows a partially eroded foot of a relict landslide that protected the face of the terrace from fluvial erosion. This may be the remnant of the 1898 event. As evident from airphotos, by 1970, the sediment was removed and erosion of the toe had started.

Previous investigations of the landslide are limited to two site investigations focused on bank erosion caused by the landslide (Klohn-Crippen Consultants Ltd. 1996; Gottesfeld and Poirier 1999). Only brief descriptions of the landslide were included in these reports.

3.4 Methods

The investigation of the landslide involved several techniques including surficial mapping, stratigraphic and sedimentological studies, the creation of digital terrain models (DTMs) and geophysical surveys.

Initial efforts were directed towards the sedimentological and stratigraphic description of the landslide and terrace. Stratigraphic units were characterized using basic mapping methods from exposures along the escarpments of the terrace and the landslide. In addition, the contacts between units and other important topographical and structural features were surveyed for position and elevation using a laser theodolite station.

DTMs for both pre and post-failure conditions were constructed from vertical aerial photographs taken in 1986 and 2002. The information was digitized at a scale of 1:1 000. Topographic and cartographic data were then used to construct the surface of the DTMs and elevation change maps.

The geophysical methods applied at the site were GPR, DC electrical resistivity and seismic reflection and refraction. The methods were chosen based on the expected characteristics of the landslide following reconnaissance geological mapping. All surveys were conducted during the late summer or early fall of 2002, which corresponds to the

dry-season. This minimized the variability of geophysical results due to moisture differences (Bogoslovsky and Ogilvy 1977).

The GPR system used was the PulseEkko IV system from Sensors and Software. A 50 MHz antenna and receiver was chosen as a compromise between resolution and penetration depth. Ten metres of penetration is typical at this frequency (Annan and Cosway 1992) but depends strongly on the subsurface sediment characteristics. Resolution can be approximated by a fraction of the electromagnetic wave length, $\lambda/4$ to $\lambda/2$ (Sheriff 1984), and was calculated to be between 0.5 m and 1 m assuming an average velocity of 0.1 m/ns for the electromagnetic wave. Two types of GPR surveys were conducted: reflection profiling to obtain pseudosections and expanding spreads or common mid-point for velocity analysis. All reflection surveys were carried out with a constant offset of 2 m between the transmitter and receiver. The measurement point is considered to be the mid-point between the transmitter and receiver. For this study a constant spacing of 0.5 m was used between measurement points. Velocity data were collected by expanding the separation between the transmitter and receiver about a central point in 1 m steps. The antenna and receiver were oriented perpendicular to the survey line for both types of surveys. Data processing was limited to topographic corrections based on surveyed elevations.

An IRIS Instruments SYSCAL R1-Plus Switch 48 DC electrical resistivity system was used for resistivity profiling. It is a 48 electrode system with the ability to select array types and collect multiple spreads. For survey lines longer than one spread of electrodes (48), the first 24 electrodes were moved to the end of the 48 electrode spread leaving electrodes 25-48 in their former positions for data collection in the new electrode array. This leapfrog approach was continued until the total line was covered. Electrode spacing was 5 m and the data were collected using a Wenner array configuration. Measurements were taken at a -spacings of 5, 10, 15, 25, 35, 45, 55, 65, and 75 m. Topographic corrections and 2-dimensional model inversions were performed using Res2Dinv v3.4 software from GEOTOMO Software, which applies a least-squares method for determining the optimum inversion model (*cf.* Loke and Barker 1996).

Seismic surveys were conducted using a Geometrics SmartSeis R-48 seismograph. The system was a 48-channel instrument, although only 36 channels were used during the survey. Four types of surveys were carried out: 1) P-wave reflection, 2) P-wave refraction, 3) S-wave reflection, and 4) S-wave refraction. Geophones were spaced at 3 m intervals. P-wave surveys used 100 Hz vertical geophones whereas S-wave surveys used 8 Hz horizontal geophones mounted perpendicular to the survey line. A hammer seismic source was used for all surveys. A 16-pound hammer and 0.3 m section of I-beam was used for P-wave surveys whereas both the 16-pound hammer and I-beam and a 1.5-pound hammer and simple cylindrical rod were used for S-wave surveys. The direction of the S-wave source was also perpendicular to the line direction producing horizontally polarized (SH) shear wave energy. P-wave energy was minimized by reversing the S-wave source direction while simultaneously reversing the polarity of the received signal in the S-wave geophones. Reflection surveys were conducted using a 3 m spacing between shots. Refraction surveys had shot locations at both ends of the spread and in the centre. Data processing involved a combination of static and normal move-out corrections and the application of time domain and frequency domain filters.

The interpretation of geophysical units was based on internal characteristics, the orientation, depths, and geometries of contacts, stratigraphic descriptions, and knowledge of Quaternary and landslide processes. Depths of correlated units were then translated into a 3-dimensional model of the landslide and terrace.

3.5 Site Characteristics

The following description of sediment and surficial material of the terrace and landslide is the result of reconnaissance mapping and provides the framework in which geophysical surveys were conducted. This information was then used to interpret the geophysical data in section 3.7.

3.5.1 Stratigraphy

The stratigraphy of the terrace is well exposed. The terrace consists primarily of sediment deposited during the Fraser Glaciation and is illustrated in a simplified column (Fig. 3.3). All stratigraphic units, except unit G, were deposited in association with advance outwash sediment and a pro-glacial lake that formed when drainage of the Quesnel River valley became obstructed. Younger sediments were deposited but were subsequently removed by a combination of glacial and fluvial erosion.

The oldest stratigraphic unit is well-compacted, horizontally interbedded, silty sand and clay (unit A). Bedding ranges from laminae to beds on the centimetre-scale. The unit is not exposed at the landslide but was described from an outcrop located across the river where a 3 m thick outcrop is present. The basal and upper contacts are not evident. Its presence is inferred based on pre-failure photographs.

The lowest units visible at the landslide consist of well-compacted, laminated sand that overlies crudely stratified pebble gravel (units C and B respectively). Beds within both units dip 18° to 20° to the southwest. Unit B is at least 2.5 m thick whereas unit C is approximately 12 m thick. The basal contact of unit B is not exposed but a gradational contact separates units C and B.

Clay with inclusions of fine sandy clay is the next oldest unit (unit D). It is moist and plastic. The unit is up to 22 m thick and has a sharp, gently undulating basal contact.

Overlying the clay are sand and gravel units. Unit E is moderately compact, laminated sand. Laminae are locally discontinuous and are horizontal. The unit is approximately 10 m thick and thins to the west. It has a sharp, erosional, and undulating basal contact. Unit F consists of well-bedded, well-sorted, pebble gravel that grades to coarse, immature sand to the west and disappears to the east. The pebble gravel is highly cemented, has an open framework, and is clast-supported. Beds dip 22° to the northeast. The unit is lenticular and up to 7 m thick. The lower contact is sharp and erosional.

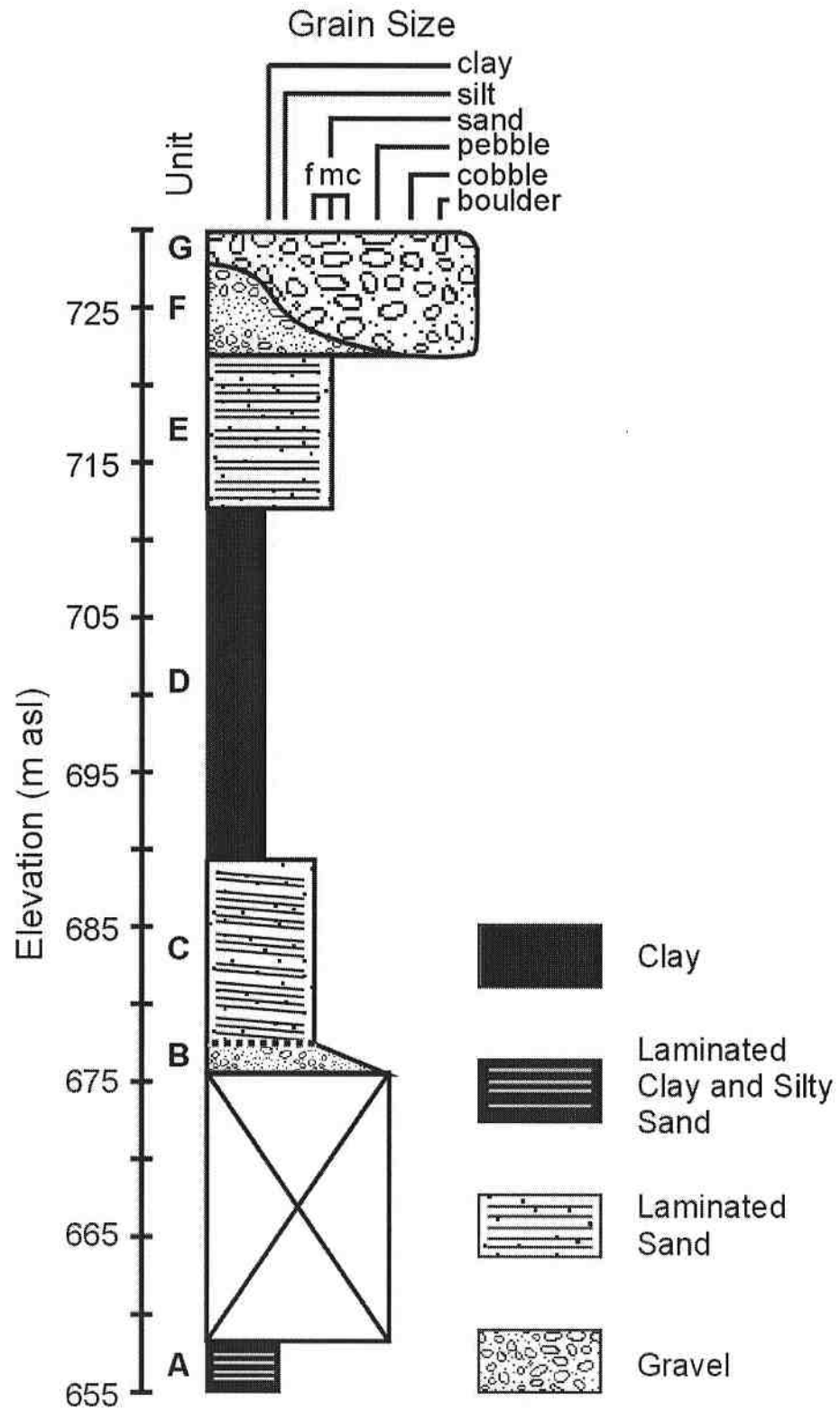


Figure 3.3. Composite stratigraphic column for Quesnel Forks Landslide.

Unit G is the uppermost unit that forms the surface of the terrace and consists of a cobble, boulder gravel with a pebble and sand matrix. Clasts are up to 3 m in diameter. It is thickest, approximately 7 m, in the east part of the terrace. The lower contact is undulating and erosional. The formation of the terrace's surface is attributed to the deposition of unit G during the recession of glaciers during the early Holocene. Subsequent incision by the river created the landform and exposed the stratigraphy.

3.5.2 Surficial Characteristics

The distribution of surficial material is a product of the sediment comprising the terrace and the landslide. The ground conditions and surficial material are important because they affect the operation and effectiveness of geophysical surveys.

The terrace is heavily forested. The ground surface is flat and consists of a well-developed soil horizon that forms the forest floor. The southwest corner of the terrace is swampy. A poor road crosses the terrace from east to west.

The distribution of material over the landslide is complex. The upper translated block remains heavily forested (Fig. 3.4a). The forest floor remained intact during failure and is flat, including the surface of the road that shows no deformation. This is in contrast to the lower block that is largely bare of vegetation with a severely disturbed surface (Fig 3.4b). Surficial material on this block consists of sand and gravel from units F and G, including intact cemented blocks composed of pebble gravel (unit F). The surface of the lower block is undulating.

The escarpment separating the upper and lower blocks is stripped of vegetation. Its slope is approximately 40°. Primary stratigraphy is observed where the slope is steepest. A thick blanket of colluvium covers the surface where the slope is less steep. The surface of the escarpment separating the lower block from the foot of the landslide closely resembles the upper escarpment, though its slope is generally less steep, approximately 30°.

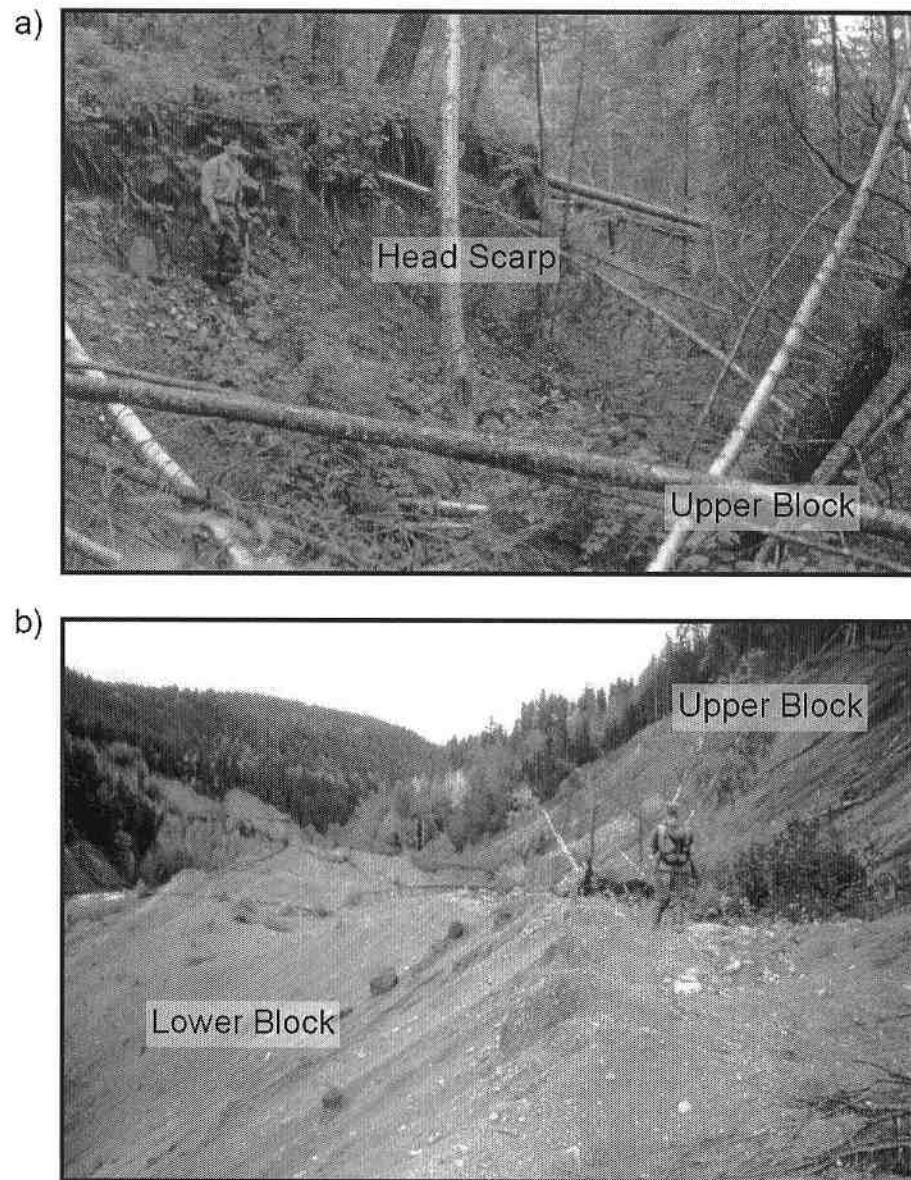


Figure 3.4. a) Photograph of the upper rotational block and head scarp where the original forest floor has been partially disturbed, evident by the jack-strawed tress though it remains largely intact. Note the person standing on the headscarp for scale; b) View to east along the top of the lower rotational block on which the person is standing. Most of the primary vegetation was removed during failure.



Figure 3.5. Close-up of weathered clay blocks that create the hummocky surface on a portion of the foot. The power bar in the foreground is 25 cm in length.

The foot of the landslide displays a variety of surficial materials and morphology. The most prevalent consists of hummocky clay or hummocky sand and gravel that can have local relief of more than 2 m (Fig. 3.5; see also Fig. 3.6c). Near the centre of the foot, a splayed pattern consisting of pebble sand is present. The surface of the upstream (east) edge of the foot consists of well-sorted cobbles. The downstream (west) edge consists of fine-grained sand.

The volume of displaced material was estimated during surficial mapping, based on the geometry of the landslide. Assuming that the landslide has a typical spoon-shaped failure, the volume can be approximated by that of a half ellipsoid (Cruden and Varnes 1996) and was calculated to be $9.24 \times 10^5 \text{ m}^3$.

In general, surficial conditions were well suited for carrying out geophysical surveys. In heavily forested areas, GPR and seismic surveys were conducted along roads to help facilitate data collection. The firm ground underlying the road offered better coupling for the GPR antenna and receiver as well as for the seismic energy source. Furthermore, dry loose sand covered much of the slopes and is a poor electrical conductor, making it difficult to release sufficient energy into the ground during the resistivity survey. This also impeded the transfer of seismic energy into the ground and from the ground to the geophones, which is a common problem for seismic surveys conducted over landslides (Bruno and Marillier 2000). Lastly, the steep irregular landscape caused concern for collecting and interpreting the geophysical data because coupling between the geophysical transducers and the ground was difficult and complex corrections were required.

3.6 Digital Terrain Models

The DTMs record the pre and post-failure geomorphology of the terrace and landslide (Fig. 3.6a, b, c and d). Along the northern edge of the terrace in the pre-failure DTM (Fig. 3.6a) a break in slope is evident and marks the future position of the head scarp (Fig. 3.6c). The face of the terrace was steep, especially at river level. The post-failure DTM shows the general morphology of the landslide, shift in river position, and erosion of the northern bank of the Quesnel River affecting the town site.

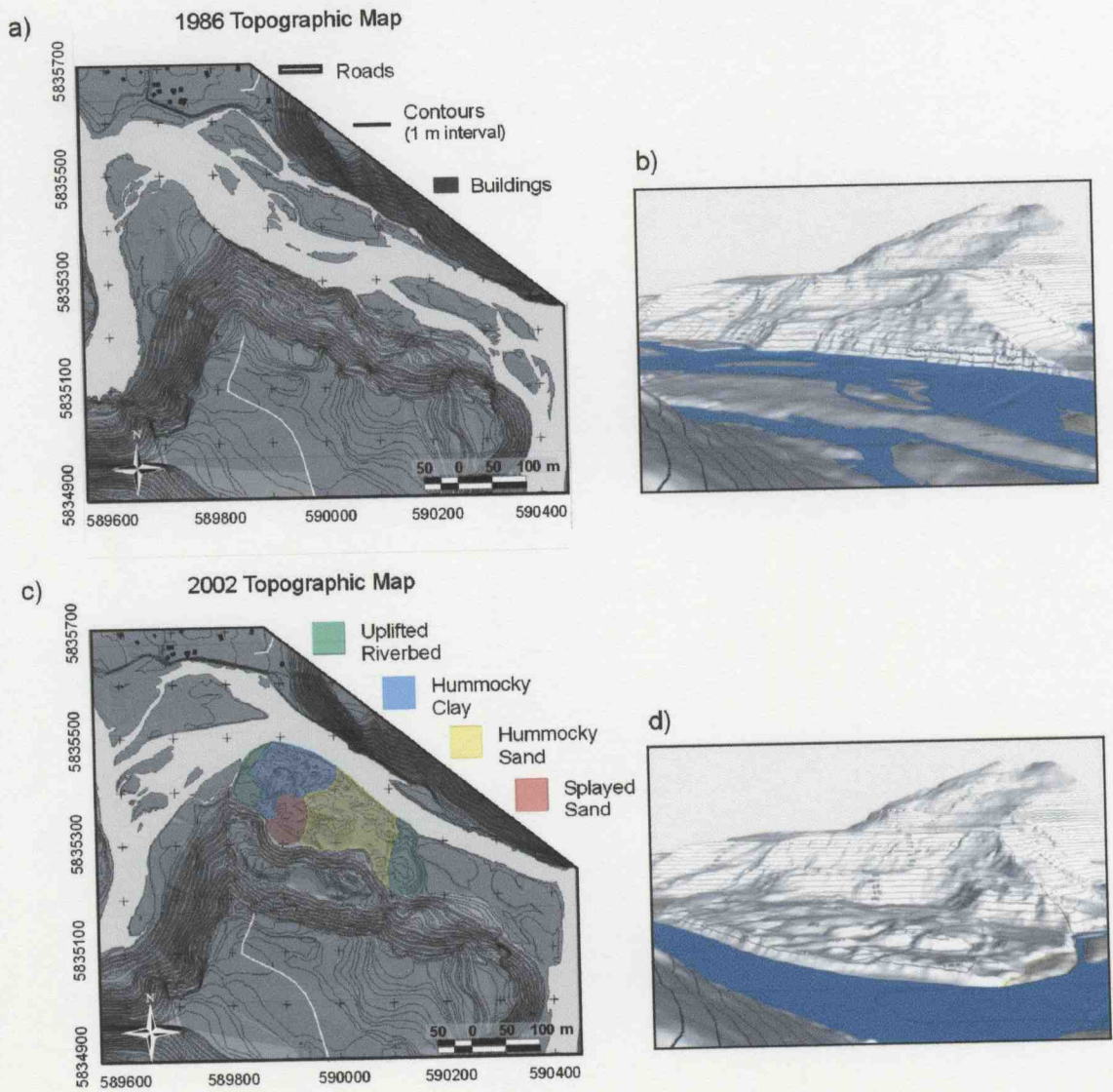


Figure 3.6. Digital terrain models of the Quesnel Forks Landslide and surrounding area: a) pre-failure shaded relief map; b) pre-failure 3D oblique view to southeast; c) post-failure shaded relief map with morphological division of foot (see section 3.6.2); and d) post-failure 3D oblique view to southeast.

An elevation change map was created based on these models (Fig. 3.7). Vertical displacements for the upper and lower blocks are 6 m and 50 m respectively. The DTMs were also used to calculate the net volume change. The area defined by a decrease in volume is the depletion and has a loss equal to approximately $5.3 \times 10^5 \text{ m}^3$. Conversely, the area with a net gain in volume is the accumulation and is approximately $3.6 \times 10^5 \text{ m}^3$.

3.7 Geophysical Results

Using the three geophysical methods described in section 3.4, 28 profiles were generated: 7 GPR, 12 DC electrical resistivity, and 9 seismic (Fig. 3.8). Several profiles that characterize the most important features of each method have been selected for discussion. The interpretation and relation of geophysical data to stratigraphic data are then presented in the following section (section 3.9).

3.7.1 Ground Penetrating Radar

A total of 340 m of GPR reflection profiles were acquired. Two profiles are presented, A-A' and B-B', which have a maximum penetration depth of approximately 25 m (Fig. 3.9a and b respectively). Both are perpendicular to the head scarp and run north-south (Fig. 3.8a). Profile A-A' was conducted along the road on the terrace and ends at the edge of the upper block. No data were collected from 52 to 62 m due to the steep face of the head scarp. Profile B-B' begins at the escarpment of the lower block and extends away from the head scarp. Depths for profiles were calculated assuming a constant velocity of 0.1 m/ns, as determined from velocity analysis.

A total of seven radar facies are identified. Dipping or hummocky reflectors characterize the upper two facies in both profiles and form the upper 8 to 12 m (facies 1, 2, 5 and 6). Individual reflectors are up to 1.5 m thick. Beneath are subhorizontal, coherent, and laterally extensive reflectors (facies 3 and 7). In profile A-A', facies 3 is approximately 14 m thick. The thickness of facies 7 in profile B-B' is indeterminate. A fourth facies (facies 4) in profile A-A' is identified by a weak, continuous horizontal reflector that marks its upper contact.

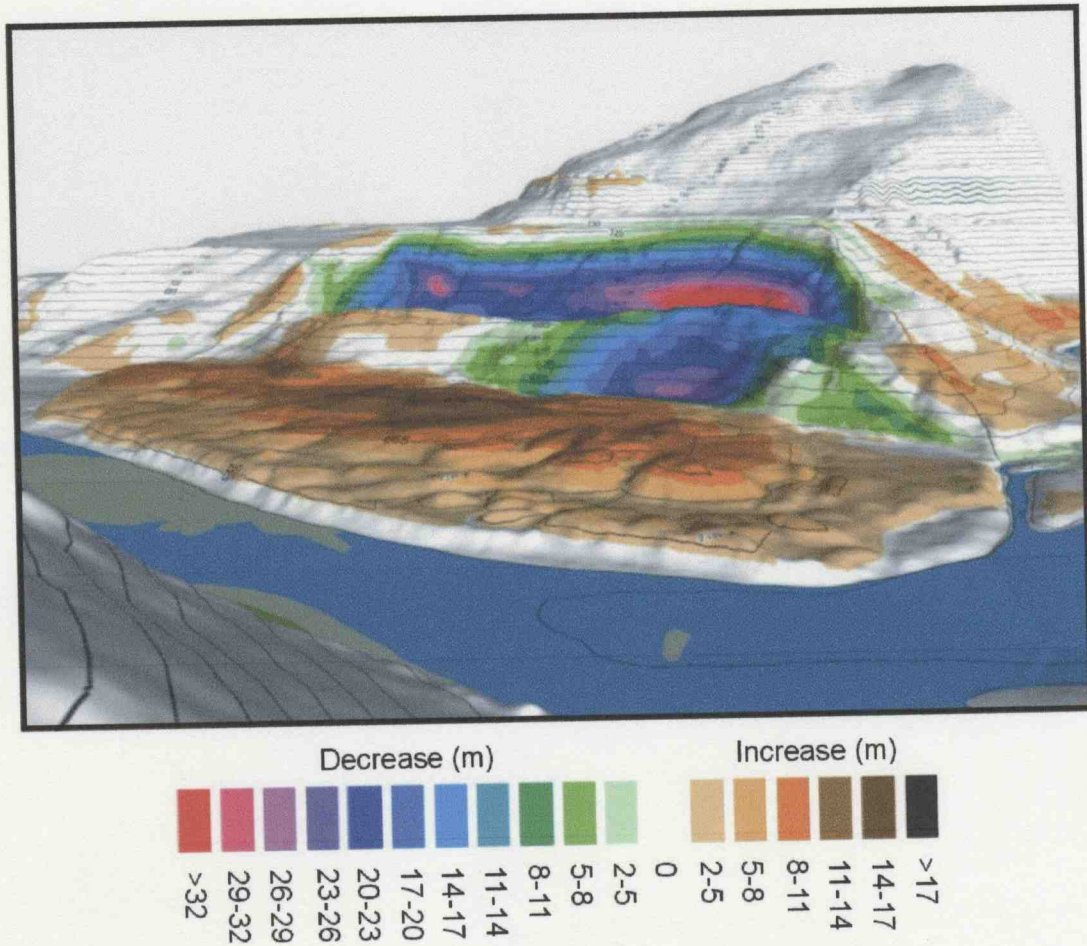


Figure 3.7. 3D oblique change of elevation map created from DTMs. Brown shades indicate an increase in elevation from the 1986 to the 2002 airphoto. Green, blue and red shades represent a decrease in elevation. View is to the southeast.

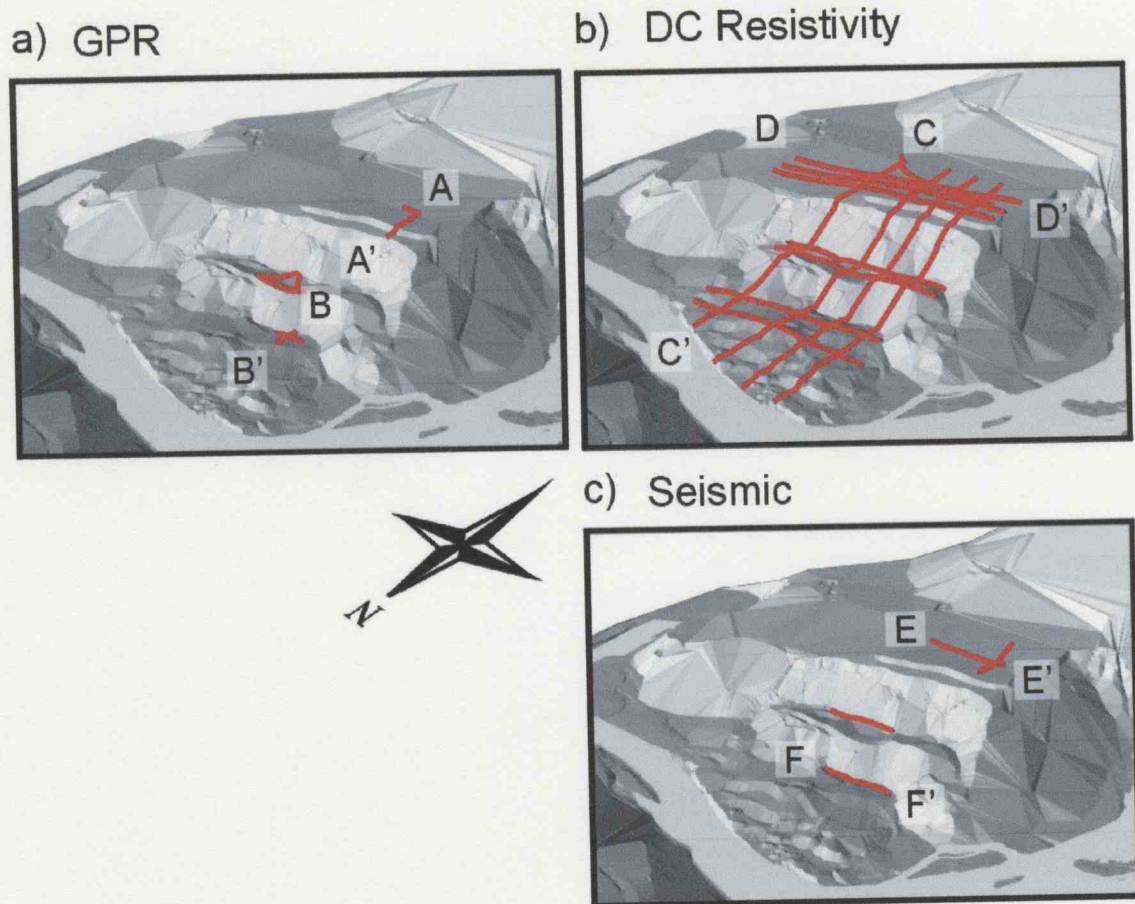


Figure 3.8. DTMs with geophysical survey lines superimposed onto its surface: a) GPR; b) DC electrical resistivity; and c) seismic reflection and refraction. Profiles obtained from corresponding survey lines are discussed in sections 3.6.1, 3.6.2, and 3.6.3 of the text.

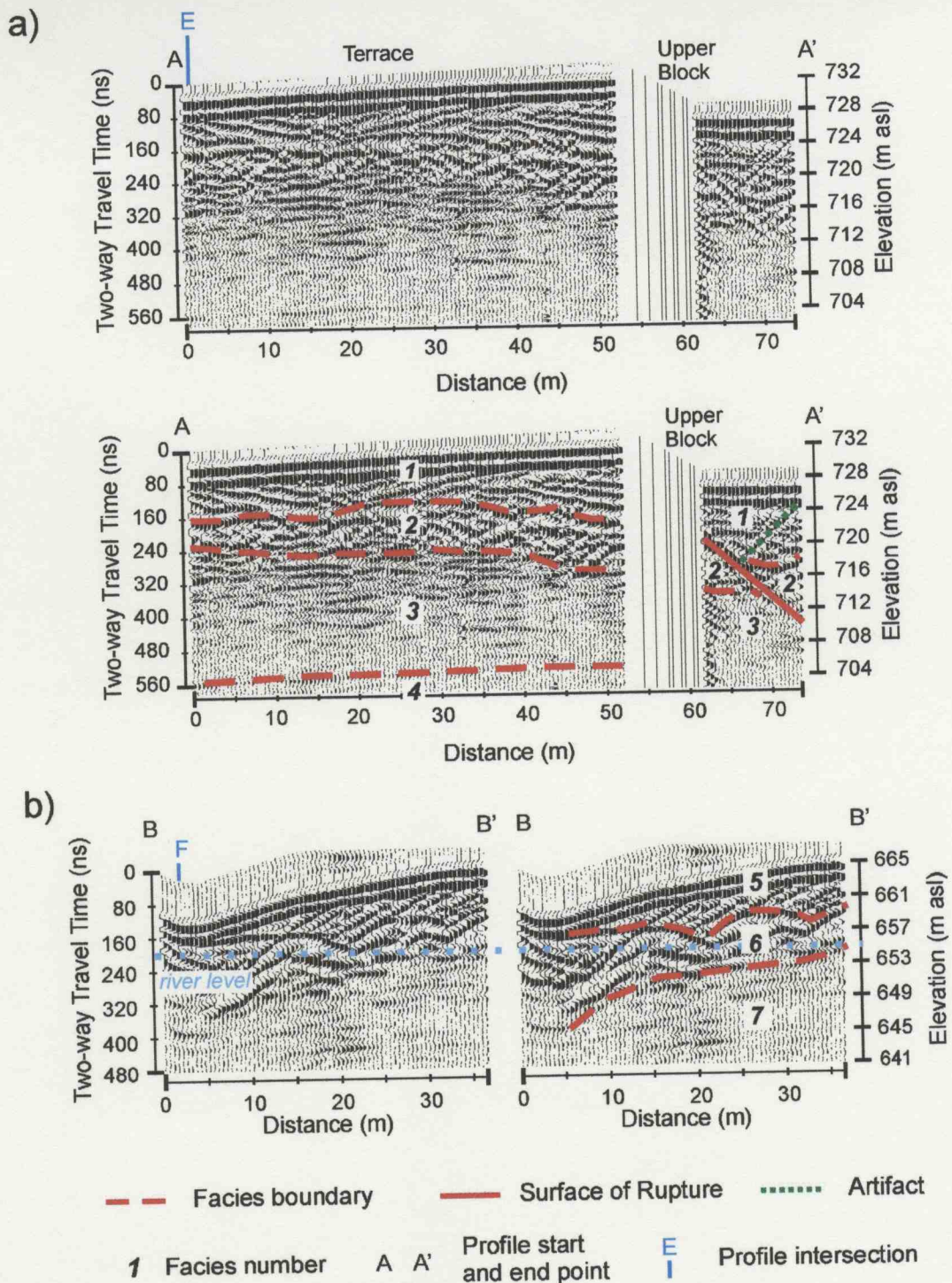


Figure 9. GPR profiles (both interpreted and uninterpreted), corresponding with profiles in Fig. 3.8: a) perpendicular to head scarp on terrace and upper block (A-A'); and b) perpendicular to head scarp on foot (B-B'). Correlation of facies with other geophysical and stratigraphic data is given in Fig. 3.12.

Two steeply dipping reflectors are recognized within the upper block that cross cut radar facies and that do not define facies boundaries (Fig. 3.9a). The first event has an apparent dip of 40° to the north (solid red line). It offsets facies boundaries and reflectors. The second event has an apparent dip of 45° to the south (dashed green line) with no evidence of offset.

3.7.2 Direct Current Electrical Resistivity

A total of 4100 m of profiles were collected during the resistivity survey. Two profiles are presented, C-C' and D-D' (Fig. 3.10a and 3.10b respectively). The mean depth of investigation for the DC resistivity surveying technique is primarily a function of the largest spacing between electrodes and is calculated to be 39 m using Edwards (1977). Profile C-C' is perpendicular to the head scarp and extends from the terrace to the tip of the foot whereas profile D-D' is parallel to the head scarp on the terrace (Fig. 3.8b). In addition, all the resistivity data collected are illustrated in a 3-dimensional fence diagram (Fig. 3.10c).

Six resistivity units are identified from the data, each with its own range of resistivities. Some resistivity values within a given unit are outside the ranges of the unit, a result of processing or high topographic relief. Units 1 and 2 have high resistivity values ≥ 960 ohm·m and 240 to 960 ohm·m, respectively. They are found near-surface and are thickest under the east side of the terrace, approximately 35 m. Both disappear toward the southwest. The units are comparably thin and discontinuous over the landslide. A third highly resistive unit (unit 6) is found below the foot and has a resistivity range between 640 to 1280 ohm·m. Its upper contact dips 20° toward the valley centre (south) with no basal contact evident.

The least resistive unit (unit 3 with resistivity values < 120 ohm·m) is found both beneath the terrace and landslide. Within the terrace it is up to 30 m thick. The unit underlies units 1 and 2, except in the southwest where it comes to surface. Under the landslide it is up to 40 m thick and is thickest below the lower block.

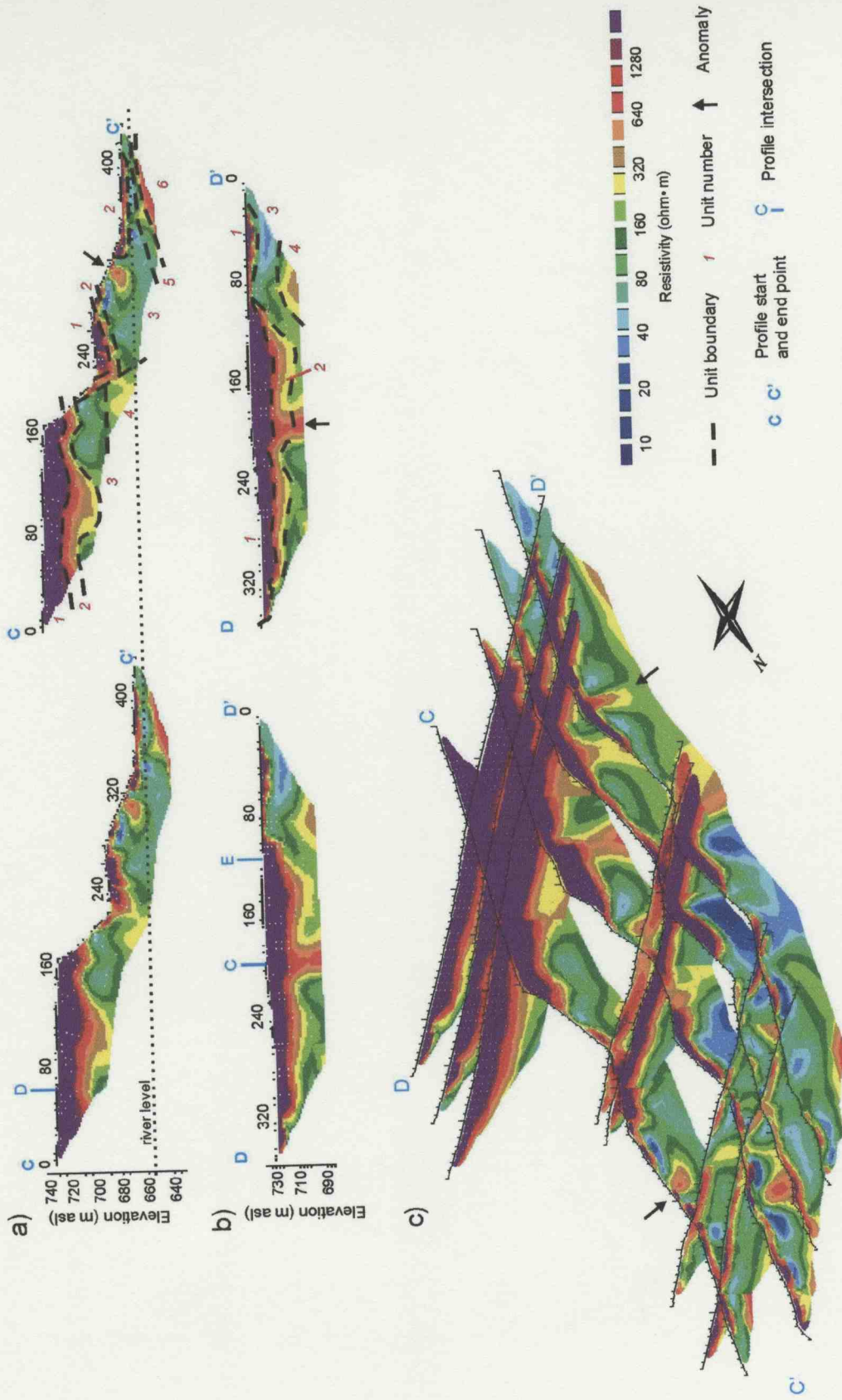


Figure 3.10. DC electrical resistivity profiles (both interpreted and uninterpreted), corresponding with profiles in Fig. 3.8: a) perpendicular to head scarp (C-C'); b) parallel to head scarp (D-D'); and c) 3D fence diagram of all resistivity data. Correlation of units with other geophysical and stratigraphic data is given in Fig. 3.12.

Units 4 and 5 have considerable overlap in their resistivity values, 120 to 640 ohm·m and 60 to 320 ohm·m respectively. Unit 4 is > 20 m thick and is found beneath the terrace whereas unit 5 ranges from 5 to 10 m thick and is found below the foot (Fig. 3.10a).

3.7.3 Seismic Reflection and Refraction

A total of 852 m of profiles were collected using seismic methods. Reflection profiles E-E' and F-F' (Fig. 3.11a and b respectively) are both parallel to the head scarp (Fig. 3.8c). Profile E-E' is a P-wave reflection profile collected along the road on the terrace. The deepest reflector identified is roughly 80 m below surface whereas the shallowest is 15 m. Profile F-F' is an S-wave reflection profile collected on the foot of the landslide. The deepest reflector from this profile is 30 m deep and the shallowest 20 m deep.

Eight seismic units were identified. Seven units are present in the terrace on Profile E-E' with units 6, 7 and an additional unit (unit 8) in the foot of the landslide on Profile F-F'. In profile E-E', reflectors are roughly parallel with the upper three units thickening to the east. The thickest unit bounded by an upper and lower reflector is unit 6, thickening from 20 to 30 m to the west. The second thickest is unit 3, which thickens from 7 to 20 m to the east. An estimated P-wave velocity of 1450 m/s was chosen for calculating the depth scale based on velocity analysis. Unit 6 is the only unit bound by two reflectors and is approximately 8 m thick for profile F-F'. If unit 8 extends to surface, it is 22 m thick. The depth scale for this profile was calculated using an estimated S-wave velocity of 250 m/s, also based on velocity analysis.

3.8 Geophysical Interpretation

Surficial and stratigraphic mapping is combined with geophysical data to create a 3-dimensional cut-away model of the Quesnel Forks Landslide (Fig. 3.12). Typical ranges of geophysical parameters (resistivity, P and S-wave velocities, dielectric constant or radar velocity) for material similar to those described in section 3.6 are given in Table 3.2 and are used in the interpretations. The characteristics of the terrace are addressed first

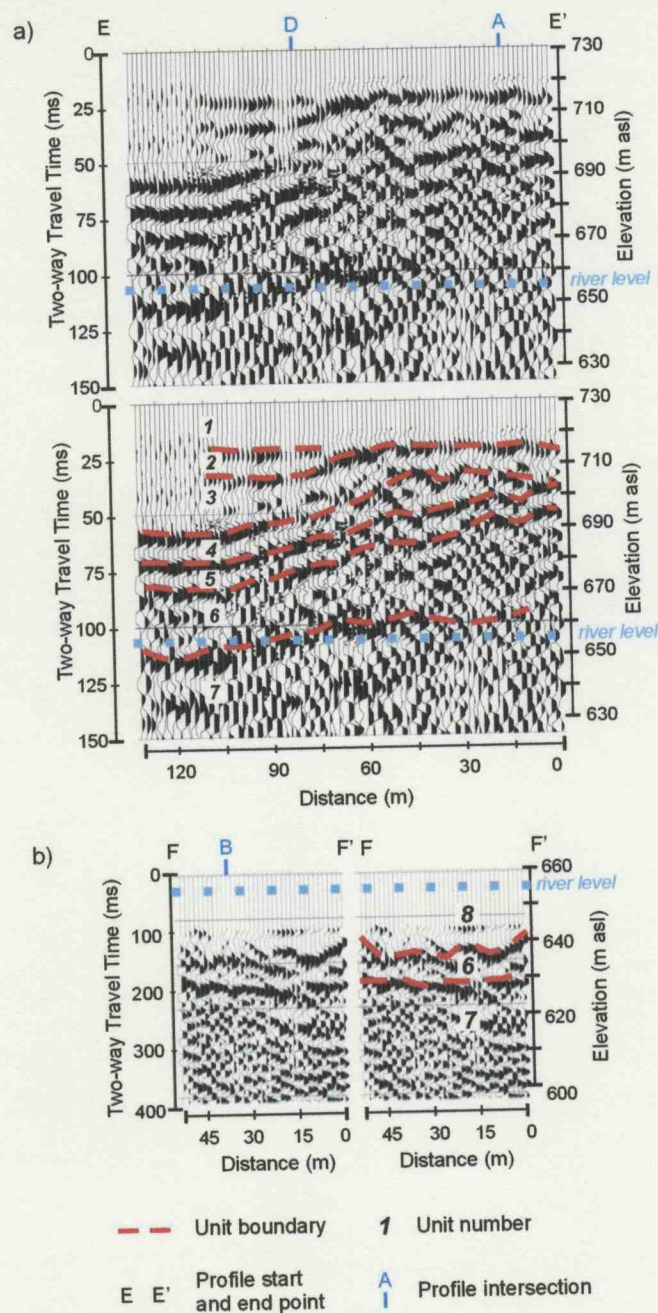
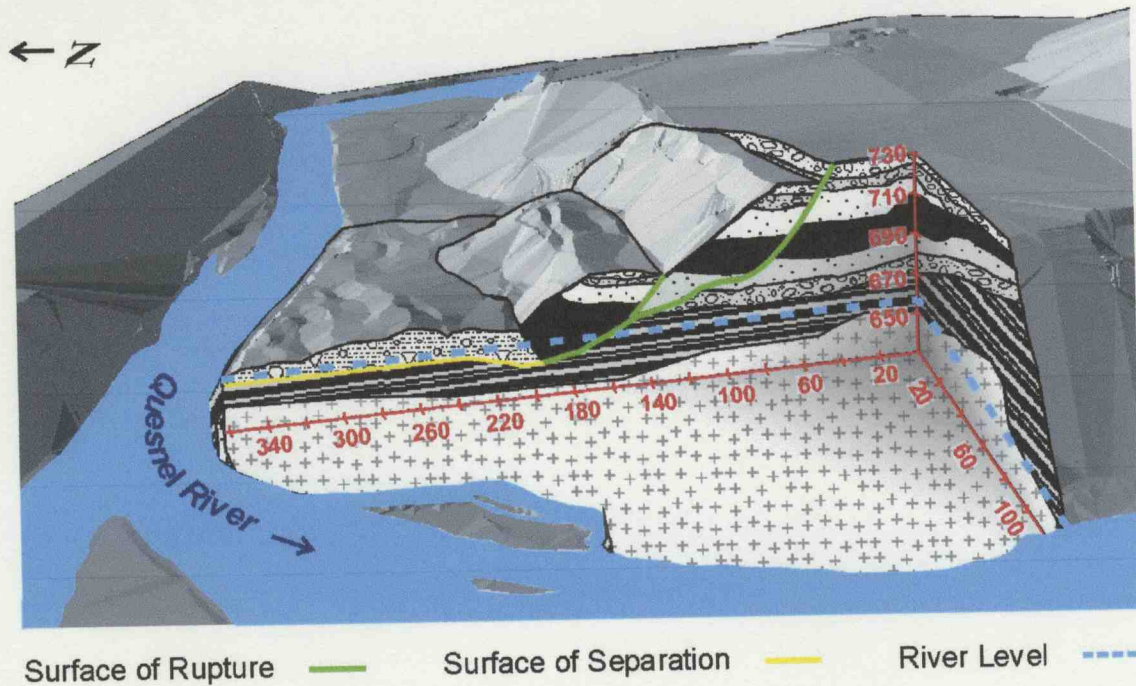


Figure 3.11. Seismic profiles (both interpreted and uninterpreted), corresponding with profiles in Fig. 3.8: a) parallel to headscarp on the terrace (P-wave reflection) (E-E'); b) parallel to headscarp on the foot (S-wave reflection) (F-F'). Correlation of units with other geophysical and stratigraphic data is given in Fig. 3.12.



	Bedrock	Interbedded, Silty Sand and Clay	Gravel	Sand	Clay	Debris
Stratigraphy	—	A	B F G	C E	D	—
GPR	—	7	— 2 1	4 —	3	5,6
Resistivity	6	5	4 1 1	4 2	3	3
Seismic	7	6	5 1 1	4 2	3	8

Figure 3.12. An oblique 3D cut-away cross-section of the Quesnel Forks landslide based on geophysical data. Geophysical units are correlated with each other and stratigraphic units in the accompanying matrix. Elevation is given in metres above sea level and distance in metres.

Substrate	Seismic Vp (m/s) (Lankston 1990; Sharma 1997)	Seismic Vs (m/s) (Lankston 1990)	Resistivity (Ω m) (Ward 1990; Sharma 1997)	GPR V (m/ns) (Davis and Annan 1989; Sharma 1997)
Air	330			0.30
Water (fresh)	1400-1500		4-100	0.03
Alluvium, sand (dry)	300-1000		1-1000	0.15
Sand and Gravel	1050	520	800-10000	0.09-0.15
Sand	500-1300	300-570	800 - 5000	
Sand (water saturated)	1200-2200	540		0.06
Silt				0.07
Clay	730-2500	390-410	1-120	0.05-0.17
Glacial moraine	1500-2600		8-4000	

Table 3.2. Geophysical parameters of various substrates used during the interpretation of geophysical data.

and are representative of the pre-failure state of the material involved in the landslide (*cf.* McCann and Forster 1990). Interpretations of the displaced material follow.

The terrace is composed of eight geophysical units or layers that are nearly horizontal. Seven of the layers are correlated to stratigraphic units described in section 3.4.1. The upper gravel units (G and F) are correlated to radar facies 1 and 2 respectively, and seismic and resistivity unit 1 (Fig. 3.12). GPR data show that the terrace gravels (unit G) consists of channel structures whereas the cemented gravels (unit F) consist of hummocky beds. The high resistivity values and the P-wave velocity obtained by refraction surveys (501 m/s) are indicative of dry sand and gravel (Table 3.2).

The upper laminated sand (unit E) is interpreted as resistivity and seismic unit 2. It is absent from the GPR profile A-A' because it disappears towards the west as shown in profiles D-D' and E-E' (Fig. 3.10b and 3.11a). Resistivity values are slightly less than for the overlying gravel, which is reasonable especially if the sand has greater moisture content.

The appearance of laminated sand corresponds to an abrupt thickening of coarse-grained units in the east part of the terrace (Fig. 3.10b). This may reflect the preference of the ancestral Quesnel River to erode less consolidated sand and gravel rather than more competent units. The laminated sand and gravel units comprise a succession of porous sediment that are likely permeable (*cf.* Fetter 2001).

Clay (unit D) is interpreted as radar facies 3, which shows substantial internal structure contrary to stratigraphic descriptions. This suggests that the pockets of sand contained within unit D have a more coherent structure than previously recognized. This unit is also correlated with resistivity and seismic unit 3 (Fig. 12). Resistivity values are low and are typical of clay (Table 2). A refraction survey yielded a P-wave velocity of 1502 m/s and is also suggestive of fine-grained, water-saturated sediment. Resistivity profiles show that the unit comes to surface to the southwest (Fig. 10c) and because clay is relatively impermeable, this explains the presence of surface water.

Though the penetration of GPR signals is normally rapidly attenuated in clay, a weak reflection from the base of the clay unit is evident and marks the contact with the lower laminated sand unit (C). The sand is thus correlated with radar, resistivity, and seismic unit 4 (Fig. 3.12). Like the upper laminated sand unit, resistivity values are less than the gravel units but greater than those of clay.

The lower gravel unit (unit B) is correlated with seismic unit 5 (Fig. 3.12). An equivalent radar facies is absent because the unit lies below the effective penetration depth of the GPR system. It is also absent from resistivity data. Two possible reasons exist: it may not differ sufficiently in electrical properties from the overlying sand or it is too thin to be detected as a separate unit at this depth. In either case, it is incorporated into resistivity unit 4.

The interbedded, silty sand and clay (unit A) is assumed to underlie the lower gravel unit (B) and is correlated with seismic unit 6 (Fig. 3.12). This in turn overlies bedrock (seismic unit 7) which is the deepest reflector observed in the terrace. Both units lie below the effective penetration depths for GPR and resistivity methods.

Geophysical data within the displaced blocks of the landslide resemble those of the terrace with a few exceptions. The upper coarse-grained units are thinner and show signs of deformation, particularly in the western half of the lower block where the units have partially slid off the block (Fig. 3.10c). Measurements of the orientation of unit boundaries in the east half of the lower block indicate that units underwent approximately 12° of back rotation (Fig. 3.10a). A third difference is that resistive unit 3 is thicker and is not underlain by resistive units seen in the terrace. As such, the lower sand and gravel units (B and C) are thought to be absent below the block. These units were likely remobilized during failure and are incorporated into the foot of the landslide. It is believed that the unusual thickness of unit 3 is due the loss of resolution at depth that leads to the electrical indifference between displaced clay (unit D) and adjacent

interbedded, silty sand and clay (unit A).

Separating the blocks from the terrace is the rupture surface, which is imaged with both GPR and resistivity surveys. The northward dipping reflector in profile A-A' represents the rupture surface for the upper block (Fig. 3.9a, solid red line). Displacement is approximately 5.5 m in the vertical direction, measured from the upper contact of the cemented gravel unit (facies 2). This agrees with measurements based on the DTMs, that is approximately 6 m. In addition, beds along this surface show deformation indicative of a downward motion of the upper block. The second dipping surface is interpreted as an artifact created by the reflection of a surface wave from the edge of the block at the sediment-air interface (Fig. 3.9a, dashed green line).

The rupture surface below the lower block is seen in resistivity profiles where displacements lead to the juxtaposition of electrically contrasting units. This is illustrated in profile C-C' (Fig. 3.10a) where gravel, sand and clay (units 1, 2, and 3) are found adjacent to laminated sand (unit 4). The rupture surface dips approximately 60° to the north and lessens to 45° to the west. Total vertical displacement is 40 m as measured from the offset of the upper contact of the clay unit, though this is about 10 m less than observations from the DTMs.

Two radar facies (5 and 6), two resistivity units (2 and 3) and one seismic unit (8) make up the displaced material within the foot (Fig. 3.12). The upper facies in GPR profile B-B' masks underlying topography and is composed of a series of reflectors that dip into the head scarp (Fig. 3.9b, facies 5). This unit corresponds to pebbly sand identified during surficial mapping as being splayed over the foot. The parent material is interpreted to be the cemented pebble gravel (unit F) though the origin of the internal structure is unknown. The sediment was likely deposited when a block disintegrated on impact with the foot of the landslide.

Much of the foot consists of radar facies 6, which is correlated with resistivity unit 3 (Fig. 3.12). It is composed of hummocky beds of low resistivity typical of clay (Table 3.2) but

has layers of contrasting material that generate the strong reflectors seen in the GPR data. The unit is composed of material mobilized by flow. As such, resistivity unit 3 is correlated to two separate lithological units: the clay found within the terrace and blocks and the material within the foot (Fig. 3.12).

Radar facies 7, resistivity unit 5 and seismic unit 6 are correlated with the interbedded, silty sand and clay (unit A) (Fig. 3.12). Radar data indicate that the unit has sub-horizontal bedding consistent with stratigraphic descriptions. Resistivity values for the unit are slightly greater than for clay or disturbed material from within the foot. Even so, it remains conductive, which is evident by the strong attenuation of the GPR signal. Because the unit is not deformed, the upper contact is interpreted as the surface of separation and is correlated to the contact between resistivity units 3 and 6 and seismic units 8 and 6 (Fig. 3.12). This surface displays undulations perpendicular to flow, is deepest nearest the toe of the lower block, approximately 20 m, and shallows away from the head scarp.

The area consisting of cobble gravel along the eastern edge of the foot (Fig 3.6c) is known to directly overlie an undisturbed stratum (resistivity unit 5). The sediment bears a strong resemblance to lateral bars found in the river near the landslide and is interpreted as a displaced part of the riverbed. The fine-grained, relatively flat area along the western edge of the foot may also be a part of the river or was deposited as a back channel when the river began to erode the foot of the landslide.

Using the surfaces of rupture and separation to define the boundary of displaced material, an estimation of the volume was made. Through this method, approximately $1.7 \times 10^6 \text{ m}^3$ of material was displaced.

Resistive unit 6 is interpreted as bedrock. This is supported by the presence of bedrock on the north side of the river, adjacent to the foot. As such, seismic unit 7 also represents bedrock and can be seen beneath the terrace as well as the foot (Fig. 3.11). The data show that bedrock dips towards a central point located under the landslide.

3.9 Discussion

From this study it was found that the most useful data for mapping the terrace and landslide in three dimensions was that obtained using resistivity mapping. This was primarily the result of the higher density of data collection. Seismic and GPR data could not so easily be collected on the slopes as resistivity data mainly because of coupling problems. Bogoslovsky and Ogilvy (1977) suggest that at least three profiles along the axis of the landslide and several perpendicular be conducted and should extend beyond the limits of the landslide. Additionally, the resistivity survey offered a compromise between shallow high-resolution (GPR) and deep low-resolution (seismic) techniques. These other geophysical methods proved useful for extending interpretations beyond the limits of the resistivity data.

The excellent exposure of stratigraphy at surface and along escarpments provided the basis for interpreting geophysical data. Survey lines conducted directly over these exposures yielded data that correlate well with geophysical parameters and stratigraphic units. Furthermore, good correlation exists between data from different geophysical techniques where survey lines crossed or were coincident. An example is the intersection of resistivity line D-D' and seismic line E-E' where the upper contact of the clay unit (resistivity and seismic unit 3) is determined to be approximately 20 m and 22 m below surface respectively (Fig. 3.10b and 3.11a). Elsewhere, GPR line A-A' crosses seismic line E-E' where the same contact has depths of approximately 10 m and 12 m respectively (Fig. 3.9a and 3.11a). A high degree of correlation also exists for survey lines conducted by the same method. An exception is the variance seen in resistivity data, though this variation occurs primarily within the respective range of a unit and therefore contact boundaries are unaffected. Note that resistivity values have the largest range of any geophysical parameter and logarithmic variations are common within a given resistivity unit.

The rupture surface for the upper block is best imaged by the GPR method. The reflection of the GPR signal by this surface suggests that material has contrasting geophysical properties (i.e. dielectric constant), likely brought about by shearing. It is possible that

this boundary is also evident in the resistivity data but the presence of resistivity variations attributed to the inversion process impedes a reliable conclusion (Fig. 3.10c). In contrast, the rupture surface of the lower block is best imaged by the resistivity method and is visible because of contrasting resistivity values of lithological units brought about by emplacement during failure. The surface itself has no uniquely identifiable electrical properties at the resolution of the survey conducted. Like the rupture surface, the surface of separation is also identifiable by the geophysical methods due to its contrasting geophysical properties across the boundary but has no unique properties itself.

The volume of the landslide was calculated by three different methods. Calculations based on DTMs are not representative of the total volume of displaced mass. Instead they are an estimate of displaced material relative the original ground surface. It estimated the lowest volume: more than three times lower than the volume calculated using the geophysical data. A problem inherent to volumes based on DTMs is that no account is taken of the depth of water, in this case the amount of material deposited into the river channel. This is partially responsible for the discrepancy between the volume of the depletion and accumulation. An additional factor is the erosion of material from the foot by the river that is common to calculations based on geophysical data as well. The volume obtained by field observations and a simplified geometry of the landslide estimates the total volume of displaced mass and represents the second highest volume. It is still half of the volume estimated using the geophysical data. The volume calculated using the geophysical data is considered to be the best approximation and thus further emphasizes the importance of these methods in landslide mapping.

The 3-dimensional model of the terrace and landslide constructed from the geophysical data aids in the understanding of landslide processes. Though no slope stability analysis was attempted, some general statements can be made based on the results of this investigation. 1) The presence of a thick succession of coarse-grained sediment overlying clay may have led to the formation of a perched water table that would have increased pore water pressure within underlying clay unit and therefore decreased the effective strength of that unit. The perched water table may have also increased shear stresses

within the terrace. These sediments thicken towards the east and would have concentrated groundwater in this region. 2) The rupture surfaces penetrate all stratigraphic units except the interbedded, silty sand and clay (unit A). Within this unit the surface shallows. 3) The role of bedrock is negligible as it is found at a substantial depth beneath the boundaries confining the landslide.

3.10 Conclusions

The suite of geophysical techniques employed over the Quesnel Forks Landslide has proved to be a valuable tool for subsurface investigations of unstable slopes. The multi-geophysical survey approach resulted in a more detailed and less ambiguous interpretation of the 3-dimensional structure of the landslide and terrace than if any one geophysical method were used in isolation. The variance of scales of resolution and penetration and geophysical parameters was important since no one method was ideal for characterizing the environment.

The choice of DC electrical resistivity as the primary method for mapping was appropriate given the electrical contrasts and geometry of strata and the target depths. Penetration to approximately 40 m was achieved. Ground penetrating radar helped resolve near-surface structures (up to approximately 25 m depth) whereas seismic methods provided structural information for greater depths (approximately 80 m).

Geophysical data collected show a close correlation with units identified by each of the perspective methods as well as to the observed stratigraphy. This allowed the construction of a reliable 3-dimensional model. It shows sub-horizontal units of unconsolidated sediment overlying bedrock within the terrace. Two displaced blocks of sediment are identified and consist of a succession of similar units. These sediments have undergone relatively little deformation and maintain the integrity of their original characteristics. The material comprising the foot has undergone extensive deformation and no longer resembles the primary stratigraphy. The boundaries separating the displaced material from undisturbed strata were also identified.

From this model, it is suggested that increased pore water pressures in the clay unit and artificial loading of terrace due to a perched water table played a role in the instability of the terrace but was not necessarily the trigger. It is much more likely that fluvial erosion of the terrace face was responsible for the loss of shear strength and subsequent collapse of the terrace. Similar to the landslide that occurred in 1898, the foot of the Quesnel Forks Landslide protects the terrace from erosion and will likely do so for many years.

CHAPTER 4

SUMMARY

The research compiled within this thesis represents three investigative scales of landslide processes and the environment and sediments within which they occur. Each component contributes to our understanding of landslide processes and surficial geology within the study area in a different way. As a whole, the research provides a framework for comparable studies in the region.

The surficial geology of the study area was updated using current terrain mapping standards for British Columbia. Terrain mapping provides the spatial distribution of Quaternary sediment as well as geomorphic processes, including landslides. The surficial geology of the region is primarily linked to the Fraser Glaciation, the majority of which is till. Within the major valleys, terraces composed of recessional glaciofluvial sediment overlying advance-phase glaciolacustrine sediment are dominant. Modern landslide processes are confined to these valleys.

Several major contributions come from the stratigraphy and landslide study. The stratigraphy of the Quesnel and Cariboo River valleys was refined. Sediment previously attributed to the penultimate glaciation was reassigned to the onset of the Fraser Glaciation and correlates with sediment described elsewhere in the interior of British Columbia. In addition, a previously unrecognized unit of glaciolacustrine sediment was described that records a sudden deepening of the advance-phase glacial lake. It was observed that both of these units, in addition to till, are the primary stratigraphic units involved in landsliding within the Quesnel River valley. Three styles of landslides were documented that occur within particular stratigraphic successions. Flow and slide dominated failures occur in advance-phase glaciolacustrine sediment whereas primarily flow-type failures occur where till overlies clay. Triggering factors were only briefly addressed with riverbank erosion recognized as being the most active. The degradation of

material strength due to the presence of ground water and the increase of shear stresses due to artificial loading is also suspected.

The detailed site investigation of the Quesnel Forks Landslide provided an account of the subsurface characteristics for one style of landslide found within the study area. This case study demonstrated the utility of a multi-geophysical approach. The value of using three methods that exploit three different geophysical parameters, at three different scales of resolution, was shown by successfully imaging the internal geometry of the landslide and surrounding terrain and correlating the data between the methods.

Future work related to landslides within the study area should be focused on improving knowledge of the distribution of stratigraphic units known to be involved in landslide processes. Landforms that contain those characteristics deemed prone to failure should be mapped. This includes terrain and terrain stability mapping at larger scales and further site investigations. The multi-geophysical approach taken for subsurface mapping should be employed at other sites, in particular to the other two styles of landslides identified, to further evaluate their effectiveness for subsurface mapping of landslides.

CHAPTER 5

REFERENCES

- Allen, C.K. 1997. Analysis of Lawyer's Point Drive Landslide, Anderson Township, Cincinnati, Ohio. M.Sc. thesis, Graduate College of Bowling Green State University, Bowling Green, 131 pp.
- Annan, A.P. and Cosway, S.W., 1992. Ground Penetrating Radar Survey Design, Sensors and Software.
- Bailey, D.G. 1989. Geology of the Hydraulic Map Area, NTS 93A/12. British Columbia Ministry of Energy, Mines and Petroleum Resources, Victoria, Preliminary Map Number 67.
- Barnhardt, W.A. and Kayen, R.E. 2000. Radar structure of earthquake-induced, coastal landslides in Anchorage, Alaska. *Environmental Geosciences*, 7(1): 38-45.
- Barrett, G. 1979. Changes in the discharge of selected rivers in British Columbia during the period of instrumental records. B.Sc. thesis, University of British Columbia, Vancouver.
- Bell, F.G. 1993. *Engineering Geology*. Blackwell Scientific Publications, London, 359 pp.
- Bichler, A., Bobrowsky, P., Best, M., Douma, M., Hunter, J., Calvert, T. and Burns, R. in press. Three-dimensional mapping of a landslide using a multi-geophysical approach: the Quesnel Forks Landslide. *Landslides*.

Bichler, A.J. and Bobrowsky, P.T. 2003. Quaternary geology of the Hyrdaulic map sheet (NTS map sheet 93A/12). British Columbia Geosciences, Research and Development Branch, Victoria, 1:50 000 scale, Open File 2003-7.

Bogoslovsky, V.A. and Ogilvy, A.A. 1977. Geophysical methods for the investigation of landslides. *Geophysics*, **42**: 562-571.

Bovis, M.J. and Jones, P. 1992. Holocene history of earthflow mass movements in south-central British Columbia: the influence of hydroclimatic changes. *Canadian Journal of Earth Sciences*, **29**: 1746-1755.

British Columbia Forest Service, 2001. Williams Lake Timber Supply Area, Public Discussion Paper, British Columbia Ministry of Forests, Victoria.

Brooks, G.R. and Pilon, J.A. 1995. Ground penetrating radar survey of the Katz Slide, southwestern British Columbia. *Current Research, Geological Survey of Canada, Cordillera and Pacific margin, Part A*, pp. 33-40.

Broster, B.E. and Clague, J.J. 1987. Advance and retreat glacial deformation at Williams Lake, British Columbia. *Canadian Journal of Earth Sciences*, **24**: 1421-1430.

Bruno, F. and Marillier, F. 2000. Test of high-resolution seismic reflection and other geophysical techniques on the Boup Landslide in the Swiss Alps. *Surveys in Geophysics*, **21**: 333-348.

Clague, J.J. 1987. Quaternary stratigraphy and history, Williams Lake, British Columbia. *Canadian Journal of Earth Sciences*, **24**: 147-158.

Clague, J.J. 1988. Quaternary stratigraphy and history, Quesnel, British Columbia. *Geographie physique et Quaternaire*, **42**(3): 279-288.

Clague, J.J. 1991. Quaternary stratigraphy and history of Quesnel and Cariboo river valleys, British Columbia: implications for placer gold exploration. Current Research, Part A, Geological Survey of Canada, Paper 91-1A, pp. 1-5.

Clague, J.J. 1992. Chapter 12: Quaternary glaciation and sedimentation. *In* The geology of North America. *Edited by* H. Gabrielse and C.J. Yorath. Geological Survey of Canada, Ottawa, G-2, pp. 421-434.

Clague, J.J., Hebda, R.J. and Mathewes, R.W. 1990. Stratigraphy and paleoecology of Pleistocene interstadial sediments, central British Columbia. *Quaternary Research*, **34**: 208-226.

Crozier, M.J. 1999. Prediction of rainfall-triggered landslides: a test of the Antecedent Water Status model. *Earth Surface Processes and Landforms*, **24**: 825-833.

Cruden, D.M. 1991. A simple definition of a landslide. *Bulletin of the International Association of Engineering Geology*, **43**: 27-29.

Cruden, D.M. and Varnes, D.J. 1996. Landslide types and processes. *In* Landslides: Investigation and Mitigation. *Edited by* A.K. Turner and R.L. Schuster. Transportation Research Board, Washington, Special Report 247, pp. 36-75.

Cummings, D. and Clark, B.R. 1988. Use of seismic refraction and electrical resistivity surveys in landslide investigation. *Bulletin of the Association of Engineering Geologists*, **25**(4): 459-464.

Davis, J.L. and Annan, A.P. 1989. Ground-penetrating radar for high-resolution mapping of soil and rock stratigraphy. *Geophysical Prospecting*, **37**: 531-551.

Davis, N.F.G. and Mathews, W.H. 1944. Four phases of glaciation with illustrations from southwestern British Columbia. *Journal of Geology*, **52**: 403-413.

- Edwards, L.S. 1977. A modified pseudosection for resistivity and induced-polarization. *Geophysics*, **42**: 1020-1036.
- Elliot, M. 1996. Quesnel Forks: slides 1898 and 1996. *British Columbia Historical News*, **29(4)**: 2-3.
- Evans, S.G. 1982. Landslides and surficial deposits in urban areas of British Columbia: a review. *Canadian Geotechnical Journal*, **19(3)**: 269-288.
- Evans, S.G. 2000. The record of disastrous landslides and geotechnical failures in Canada 1840-1999: implications for risk management. *Proceedings of the 53rd Canadian Workshop on Geotechnique and Natural Hazards: An IDNDR Perspective*, Montreal, Quebec, pp. 21-28.
- Evans, S.G. 2003. Characterising landslide risk in Canada. *3rd Canadian Conference on Geotechnique and Natural Hazards*, Edmonton, Alberta, pp. 35-57.
- Evans, S.G. and Clague, J.J., 1988. Destructive landslides in the Canadian Cordillera; 1950-1987, Geological Survey of Canada, Ottawa, Paper 84-19.
- Evans, S.G., Raymond, E.L. and Couture, R. 2002. Landslide hazard assessment using historical data: the case of the southeastern Cordillera. *28th Annual Meeting of the Canadian Geophysical Union*, Banff, Alberta, Canada, Programs with Abstracts, May 18 – 21.
- Eyles, N. and Clague, J.J. 1987. Landsliding caused by Pleistocene lake ponding- an example from central British Columbia. *Canadian Geotechnical Journal*, **24**: 656-663.

- Eyles, N. and Clague, J.J. 1991. Glaciolacustrine sedimentation during the advance and retreat of the Cordilleran Ice Sheet in central British Columbia. *Geographie physique et Quaternaire*, **45**(3): 317-331.
- Eyles, N., Clark, B.M. and Clague, J.J. 1987. Coarse-grained sediment gravity flow facies in a large supraglacial lake. *Sedimentary Geology*, **34**: 193-216.
- Fell, R. 1994. Landslide risk assessment and acceptable risk. *Canadian Geotechnical Journal*, **31**: 261-272.
- Fetter, C.W. 2001. *Applied Hydrogeology*. Prentice Hall, Upper Saddle River, 592 pp.
- Fraseri, A., Kapllani, L. and Dhima, F. 1998. Geophysical landslide investigation and prediction in the hydrotechnical works. *Journal of the Balkan Geophysical Society*, **1**(3): 38-43.
- Fulton, R.J. 1991. A conceptual model for growth and decay of the Cordilleran Ice Sheet. *Geographie physique et Quaternaire*, **45**(3): 281-286.
- Fulton, R.J. and Smith, G.W. 1978. Late Pleistocene stratigraphy of south-central British Columbia. *Canadian Journal of Earth Sciences*, **15**: 971-980.
- Giesbrecht, B.D., 2000. Quesnel Forks Restoration Project, Restoration Project Committee of the Likely and District Chamber of Commerce, Likely, 26 pp.
- Godio, A. and Bottino, G. 2001. Electrical and electromagnetic investigation for landslide characterisation. *Physical, Chemical and Earth Sciences, Part C*, **26**(9): 705-710.
- Goryainov, N.N., Matveev, V.S. and Varlarnov, N.M. 1988. Use of geophysical methods for landslide and mudflow investigations. *In Landslides and Mudflows. Edited by Y.A. Kozlovskii*. UNESCO, Moscow, 1, pp. 134-145.

Gottesfeld, A.S. and Poirier, R.W., 1999. Quesnel Forks Historic Townsite: Erosion Protection Project, Quesnel River Enhancement Society, 12 pp.

Gowda, B.M.R., Ghosh, N., Wadhwa, R.S., Akut, P.V. and Vaidya, S.D. 1998. Seismic refraction and electrical resistivity methods in landslide investigation in the Himalayan foothills. *Environmental and Engineering Geoscience*, **4**(1): 130-135.

Griffiths, D.H. and King, R.F. 1981. *Applied geophysics for engineers and geologists*. Pergamon Press, London, 242 pp.

Hack, R. 2000. Geophysics for slope stability. *Surveys in Geophysics*, **21**: 423-338.

Havenith, H., Jongmans, D., Abdrakhmatov, K., Trefois, P., Delvaux, D. and Torgoev, I. 2000. Geophysics investigations of seismically induced surface effects: case study of a landslide in the Suusamyr Valley, Kyrgyzstan. *Surveys in Geophysics*, **21**: 349-369.

Holland, S. 1976. Landforms of British Columbia, a physiographic outline. Bulletin 48. B.C. Ministry of Energy, Mines and Petroleum Resources, 138 pp.

Horsefly Sub-regional Plan Interagency Planning Team, 2001. Horsefly Sub-Regional Plan, British Columbia Ministry of Forests, Williams Lake.

Hunt, R.E. 1984. *Geotechnical Engineering Investigation Manual*. McGraw-Hill, New York, 983 pp.

Huntley, D.H. and Broster, B.E. 1994. Glacial Lake Camelsfoot: a Late Wisconsinan advance stage proglacial lake in the Fraser River valley, Gang Ranch area, British Columbia. *Canadian Journal of Earth Sciences*, **31**: 798-807.

Hutchinson, J.N. 1984. Methods of locating slip surfaces in landslides. *Bulletin of the Association of Engineering Geologists*, **20**(3): 235-252.

International Association of Engineering Geology Commission on Landslides. 1990. Suggested nomenclature for landslides. *Bulletin of the Association of Engineering Geologists*, **41**: 13-16.

Johnston, J.J. and Ambos, E.L. 1994. Three-dimensional landslide structure for seismic refraction data analysis: a case study from Blind Canyon, northern Santa Ana Mountains, California. *Society of Exploration Geophysicists Annual Meeting, Tulsa*, vol. **64**, pp. 799-801.

Klohn-Crippen Consultants Ltd. 1996. Quesnel Forks erosion assessment, R.F. Rodman, Richmond, May 10, 1996.

Lankston, R.W. 1990. High-resolution refraction seismic data acquisition and interpretation. *In Geotechnical and Environmental Geophysics. Edited by S.H. Ward. Review and Tutorial. Society of Exploration Geophysicists, Tulsa*, 1, pp. 45-73.

Levson, V.M. and Giles, T.R. 1993. Geology of Tertiary and Quaternary gold-bearing placers in the Cariboo region, British Columbia (93A, B, G, H), British Columbia Ministry of Energy and Mines, Victoria, Bulletin 89, 206 pp.

Loke, M.H. and Barker, R.D. 1996. Rapid least-squares inversion of apparent resistivity pseudosections by a quasi-Newton method. *Geophysical Prospecting*, **44**: 131-152.

Lord, T. 1980. Soils and landforms of the Hyrdraulic map sheet (NTS map sheet 93A/12). British Columbia Ministry of Environment, Victoria.

McCann, D.M. and Forster, A. 1990. Reconnaissance geophysical methods in landslide investigations. *Engineering Geology*, **29**: 59-78.

McGuffey, V.C., Modeer, V.A. and Turner, A.K. 1996. Subsurface exploration. *In* Landslides: Investigation and Mitigation. *Edited by* A.K. Turner and R.L. Schuster. Transportation Research Board, Special Report 247, pp. 231-277.

Meidinger, D. and Pojar, J., 1991. Ecosystems of British Columbia. no. 6, B.C. Ministry of Forests.

Nichol, D., Lenham, J.W. and Reynolds, J.M. 2003. Application of ground-penetrating radar to investigate the effects of badger setts on slope stability at St Asaph Bypass, North Wales. *Quarterly Journal of Engineering Geology and Hydrogeology*, **36**(2): 143-154.

Ogil'vi, A.A. 1974. Current trends in the use of geophysical methods in the study of landslide phenomena. *Moscow University Geology Bulletin*, **29**(4): 48-50.

Palmer, D.F. and Weisgarber, S.L. 1988. Geophysical survey of the Stumpy Basin Landslide, Ohio. *Bulletin of the Association of Engineering Geologists*, **25**(3): 363-370.

Pant, S.R. 1997. Use of pole-pole and Schlumberger electrode arrangement of electrical resistivity measurement for landslide investigation: a case study. *Journal of Nepal Geological Society, Abstract Volume: Second Nepal Geological Congress*, **16**: 95-97.

Pant, S.R., Li, T., Yi, F.W. and Jiaman, C. 1997. High resolution seismic refraction data interpretation: an example from Xiakou Landslide, Yaan City area, People's Republic of China. *Journal of Nepal Geological Society, Abstract Volume: Second Nepal Geological Congress* **16**: 98.

Pedersen, R., 1998. Overview Report: Quesnel River Study Area Fish Habitat Assessment Procedure, Carmanah Research Ltd., Victoria.

- Rouse, G.E., Lesack, K.A. and Hughes, B.L. 1990. Palynological dating of sediments associated with placer gold deposits in the Barkerville-Quesnel-Prince George region, south-central British Columbia. *In Geological Fieldwork 1989*. British Columbia Ministry of Energy, Mines and Petroleum Resources, Paper 1990-1, Victoria, pp. 531-532.
- Rowland, D.E. and MacDonald, L.B., 1996. Salmon Watershed Planning Profiles for the Fraser River Basin within the Cariboo-Chilcotin Land Use Plan (CCLUP) area, Department of Fisheries and Oceans, Vancouver.
- Ryder, J.M. and Clague, J.J. 1989. British Columbia (Quaternary stratigraphy and history, Cordilleran Ice Sheet. *In Quaternary Geology of Canada and Greenland. Edited by R.J. Fulton*. Geological Survey of Canada, Ottawa, pp. 48-58.
- Ryder, J.M., Fulton, R.J. and Clague, J.J. 1991. The Cordilleran Ice Sheet and the glacial geomorphology of southern and central British Columbia. *Geographie physique et Quaternaire*, **45**(3): 365-377.
- Schmutz, M., Albouy, Y., Guerin, R., Maquaire, O., Vassal, J., Schott, J. and Descloitres, M. 2000. Joint electrical and time domain electromagnetism (TDEM) data inversion applied to the Super Sauze earthflow (France). *Surveys in Geophysics*, **21**: 371-390.
- Schuster, R.L. 1996. Socioeconomic significance of landslides. *In Landslides: Investigation and Mitigation. Edited by A.K. Turner and R.L. Schuster*. Transportation Research Board, Special Report 247, pp. 12-35.
- Sharma, P.V. 1997. Environmental and engineering geophysics. Cambridge University Press, New York, 475 pp.
- Sheriff, R.E. 1984. Encyclopedic Dictionary of Exploration Geophysics. Society of Exploration Geophysicists, Tulsa, 266 pp.

Skempton, A.W. and Hutchinson, J.N. 1969. Stability of natural slopes and embankment foundations. Proceedings of the 7th International Conference on Soil Mechanics and Foundation Engineering, Mexico City, vol. pp. 291-340.

Thurber Consultants Ltd. 1976a. Report on a site examination of a large landslide on the Quesnel River near Morehead Creek, on May 13th, 1976, D.A. MacLean, Victoria, 26 pp.

Thurber Consultants Ltd. 1976b. Stability assessment: Quesnel and Cariboo rivers, D.F. VanDine, Victoria, 14 pp.

Tipper, H.W. 1971a. Multiple glaciation in central British Columbia. Canadian Journal of Earth Sciences, **8**: 743-752.

Tipper, H.W. 1971b. Glacial geomorphology and Pleistocene history of central British Columbia. Bulletin 196. Geological Survey of Canada, Ottawa, 89 pp.

UNESCO Working Party on World Landslide Inventory. 1991. A suggested method for a landslide summary. Bulletin of the International Association of Engineering Geology, **43**: 101-110.

UNESCO Working Party on World Landslide Inventory. 1993. Multilingual landslide glossary. BiTech Publishers Ltd., Richmond.

UNESCO Working Party on World Landslide Inventory. 1993a. A suggested method for describing the activity of a landslide. Bulletin of the International Association of Engineering Geology, **47**: 53-57.

UNESCO Working Party on World Landslide Inventory. 1993b. Multilingual landslide glossary. BiTech Publishers Ltd., Richmond.

Varnes, D.J. 1978. Slope movement types and processes. *In* Landslides, Analysis and Control. *Edited by* R.L. Schuster and R.J. Krizek. Special Report 176. National Academy of Sciences, National Research Council, Washington, D.C., pp. 11-33.

Ward, S.H. 1990. Resistivity and induced polarization methods. *In* Geotechnical and Environmental Geophysics. *Edited by* S.H. Ward. Review and Tutorial. Society of Exploration Geophysicists, Tulsa, 1, pp. 147-189.

Wright, R.T., 1987. Quesnelle Forks: a goldrush town in historical perspective, Friends of Barkerville Historical Society, Barkerville.

Appendix A

Surficial Geology Map

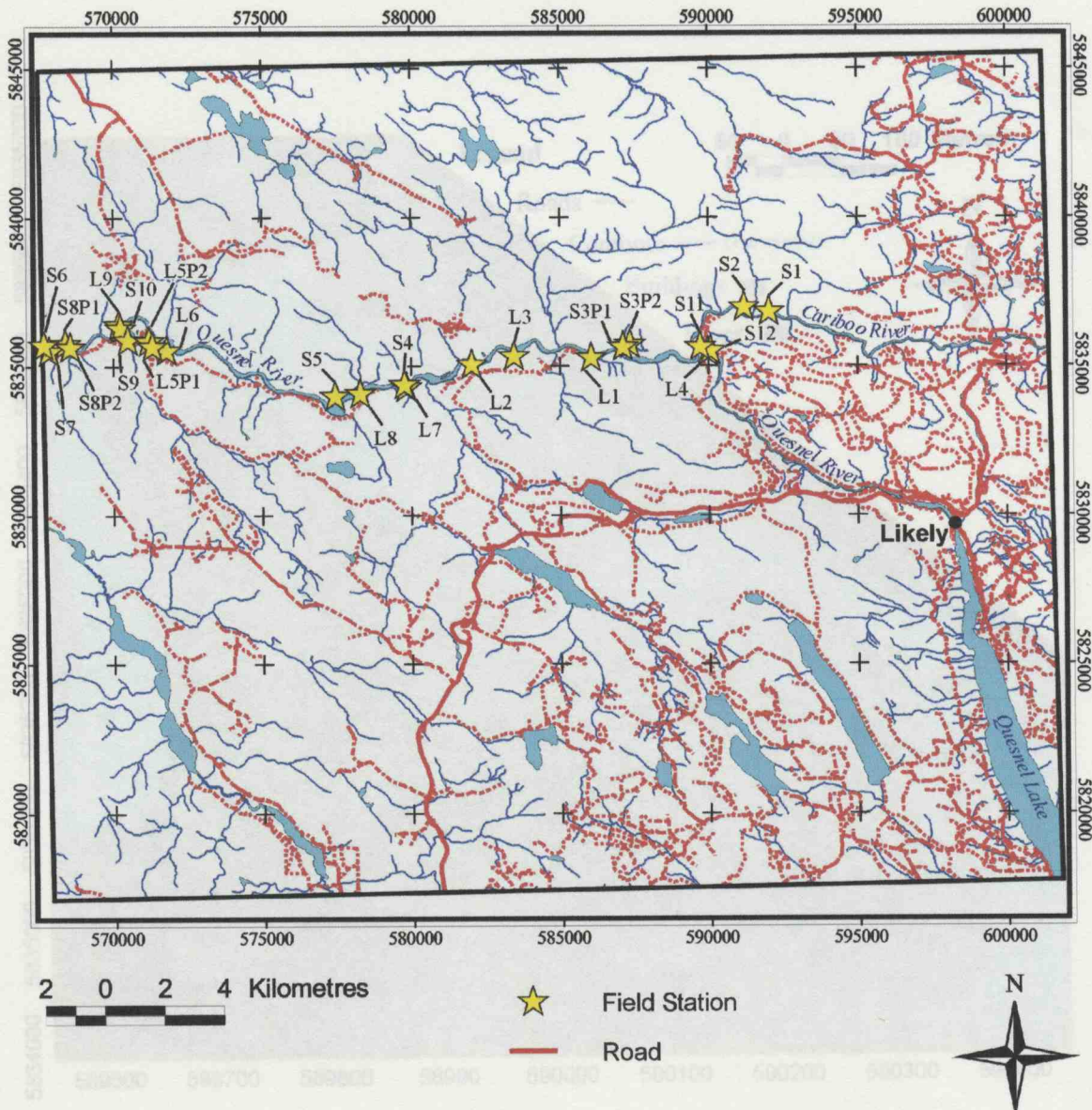
Contained within this appendix is the surficial geology map for the National Topographic System 1:50 000 map sheet 93A/12 (Hydraulic). The map is published by the Geosciences, Research and Development Branch, Ministry of Energy and Mines as Open File 2003-7 (Bichler and Bobrowsky 2003).

Appendix B


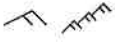

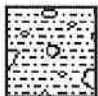





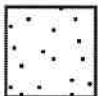
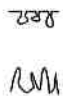

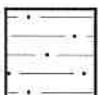



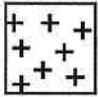



Stratigraphic Data

The following figures are a collection of stratigraphic logs that represent the surficial geology at the 24 field stations along the Quesnel and Cariboo Rivers. A map depicting the station locations is also provided. Each stratigraphic log is identified by an alphanumeric label whereby field stations conducted at a landslide contain the letter 'L' followed by a number whereas other exposures are denoted by an 'S'. In total, there are 10 stratigraphic logs from landslides and 14 from exposures. Some field stations have more than one profile, if two distinct sections were examined, and are denoted by the suffix 'P1' or 'P2'. Standard sedimentological characteristics such as grain-size, angularity, compaction, structure and contacts are described for each unit. A legend of symbols used is provided. The Unified system was used for describing grain-size and the angularity classification system described by Powers (1953). The interpreted depositional environment is provided at the end of each unit description in parenthesis and in bold. An additional sheet is included for field stations conducted at landslides that summarize the major characteristics of the landslide. Standard measurements and nomenclature suggested by UNESCO Working Party on World Landslide Inventory (1991; 1993a; 1993b) and IAEG Commission on Landslides (1990) were used. Landslide types were named using the system proposed by Cruden and Varnes (1996). In addition, an image from an orthophoto that shows the area affected by land sliding as it was in 1998 and a profile of the landslide is provided. Finally, ICP-MS results from till samples throughout the study area are given in a table.

Field Station Locations



Legend

Material Types	Structure Symbols	Contact Symbols
 Diamicton	 Ripples, Climbing Ripples	 Erosive or Undulating
 Colluvium	 Trough Cross-bedding	 Sharp
 Sand and Gravel	 Drape Structures	 Gradational
 Sand	 Soft Sediment Deformation (Ball and Pillow, Flame)	 Boulder Lag
 Silt	 Drop Stones	
 Clay	 Dipping Bed (Strike and Dip)	
 Bedrock	 Faulting	
	 Rythmites or Laminations	
	 Imbrication	

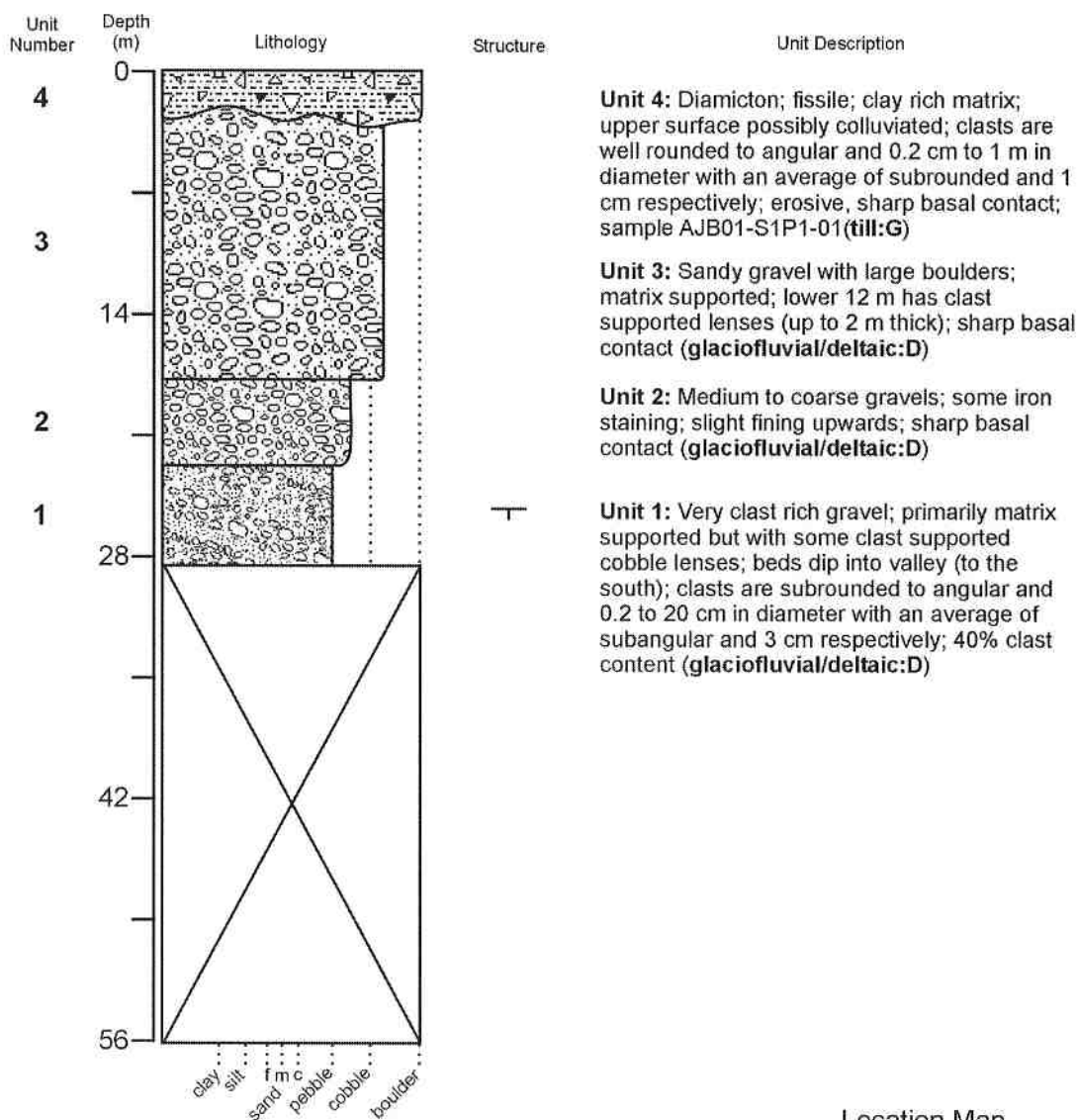
Section Number: AJB01-S1

Easting: 591975 m

Northing: 5836797 m

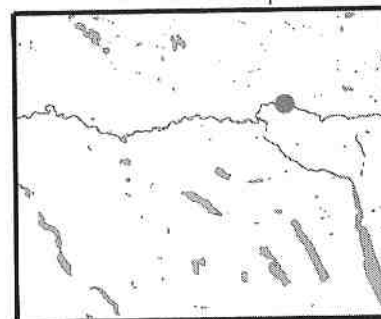
Base Elevation: 685 m

Orientation: Northeast-southwest



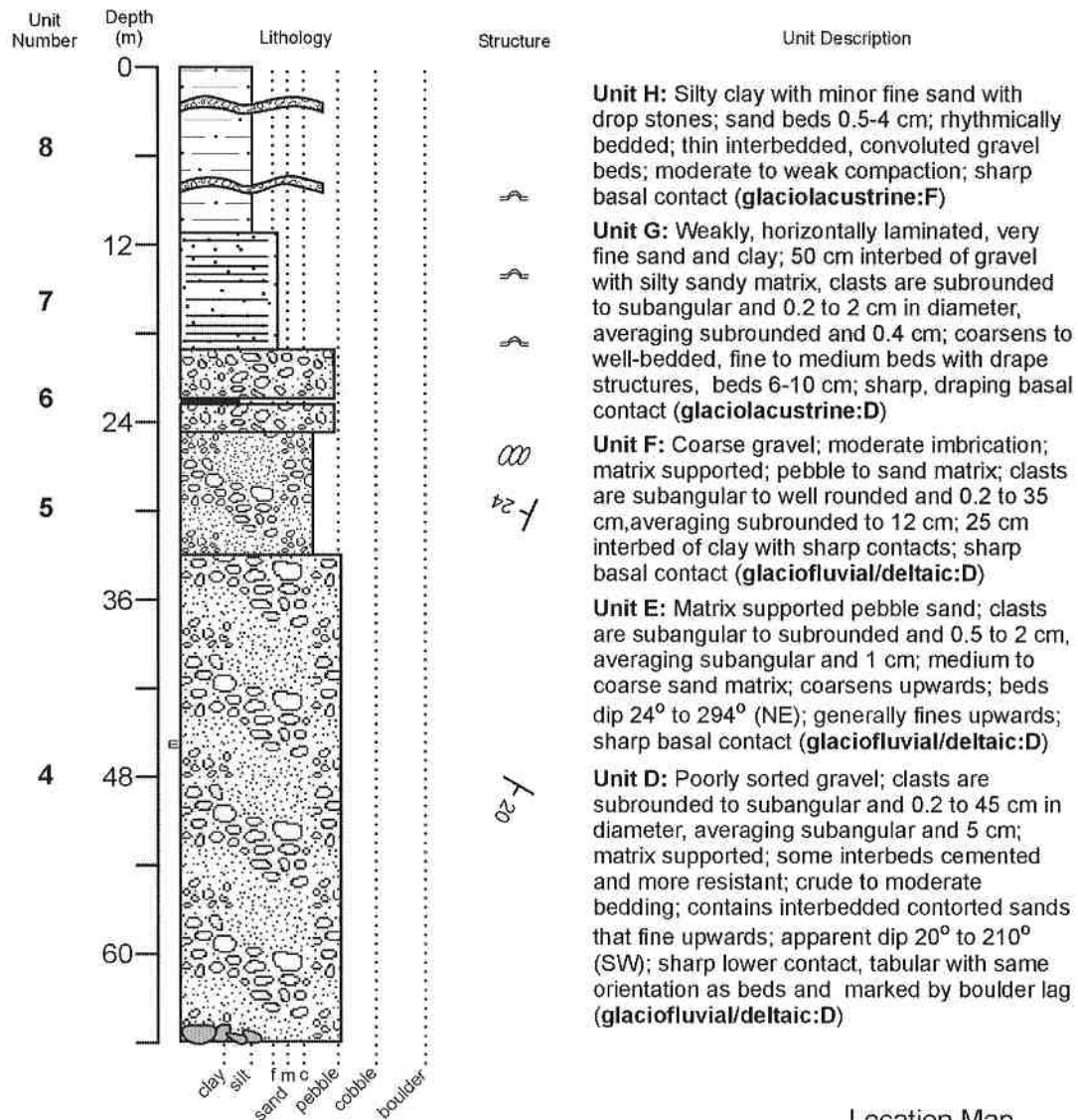
Site Description: Stratigraphy of 28 m vertical face approximately 56 m above river level. The section is approximately 330 m wide and is 3.5 km upstream from Quesnel Forks on the north side of the Cariboo River. Boat access only.

Location Map



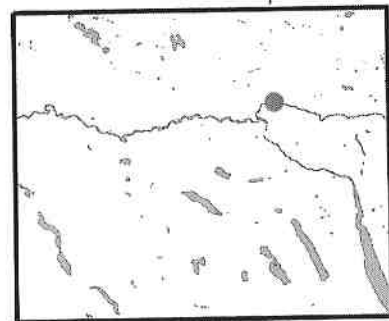
Section Number: AJB01-S2a
 Easting: 591047 m
 Northing: 5836908 m

Base Elevation: 680 m
 Orientation: Northeast-southwest



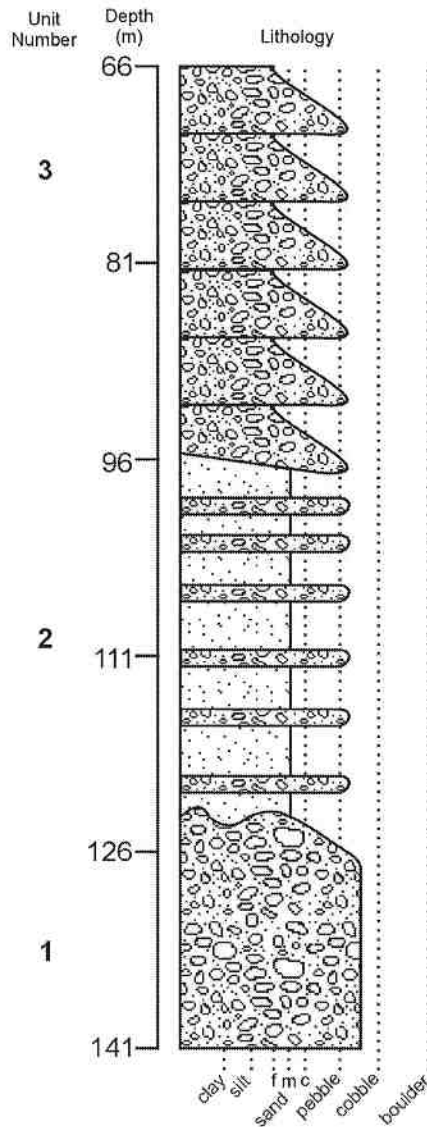
Site Description: Upper 66 m of stratigraphy of an approximately 140 m vertical face starting at river level. It is approximately 400 m wide. The section is 2.5 km upstream from Quesnel Forks on the north side of the Cariboo River. Boat access only. Stratigraphy continued in section S2b.

Location Map



Section Number: AJB01-S2b
 Easting: 591047 m
 Northing: 5836908 m

Base Elevation: 680 m
 Orientation: Northeast-southwest



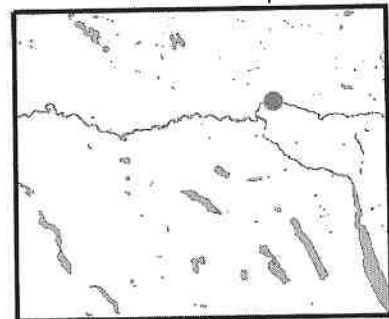
Unit 3: Fining upwards sequence of cobble gravel and gravelly sand; clasts are bimodal-large clasts are subrounded to angular and 10 cm to 1 m in diameter, averaging subangular and 12 cm while small clasts are subrounded to angular and 0.2 to 3 cm in diameter, averaging subangular and 1.5 cm; beds are marked by clast supported boulder cobble gravel horizon that grades upwards to sand; sharp, erosional contact between sequences; moderate to well bedded in west, becoming cruder to east; lower contact is sharp, erosional, and marked by clast supported gravel (dips 10° to 260°) (**glaciolacustrine:D**)

Unit 2: Rhythmically bedded coarse sand with sandy cobble pebble gravel; clasts are rounded to angular and 0.2 to 15 cm in diameter, averaging subangular and 4 cm; 5-10 cm thick beds; sand layers have minor silt; unit has a distinct blue-grey colour attributed to the high abundance of local phyllitic bedrock; lower contact sharp and undulating (**glaciolacustrine:D**)

Unit 1: Massive, poorly stratified boulder cobble gravel; coarse sand matrix; upper metre is fining upwards (fines to a moderately, sorted sand); lower contact indeterminate; clasts are rounded to subangular and 0.2 cm to 1 m in diameter, averaging subangular and 3 cm; (**glaciofluvial/deltaic:D**)

Site Description: Lower 75 m of stratigraphy of an approximately 140 m vertical face starting at river level. It is approximately 400 m wide. The section is 2.5 km upstream from Quesnel Forks on the north side of the Cariboo River. Boat access only.

Location Map



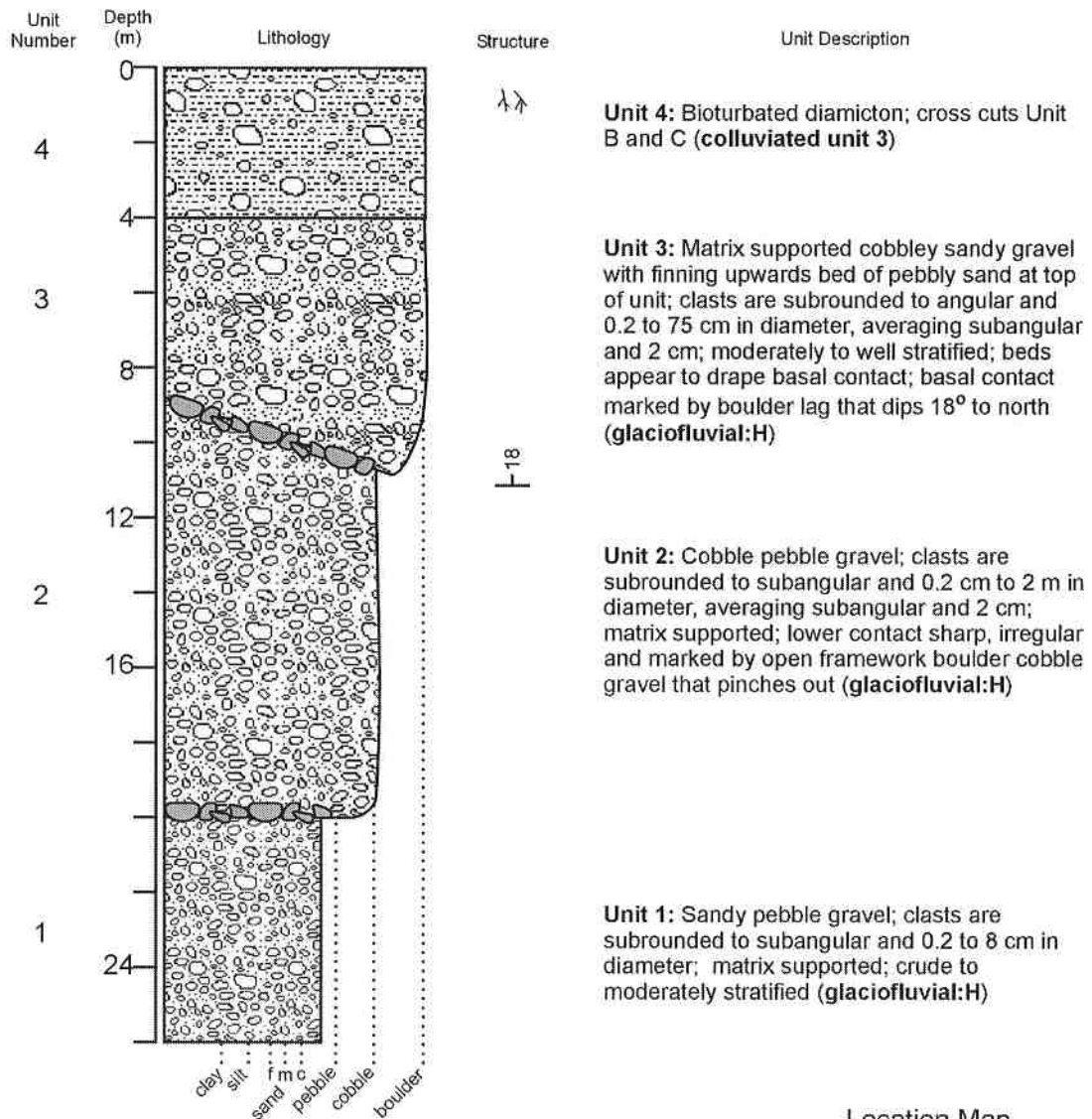
Section Number: AJB01-S3P1

Easting: 587115 m

Northing: 5835643 m

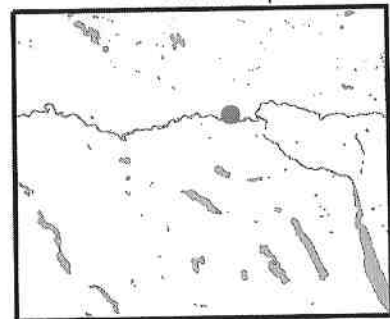
Base Elevation: 660 m

Orientation: Northeast-southwest



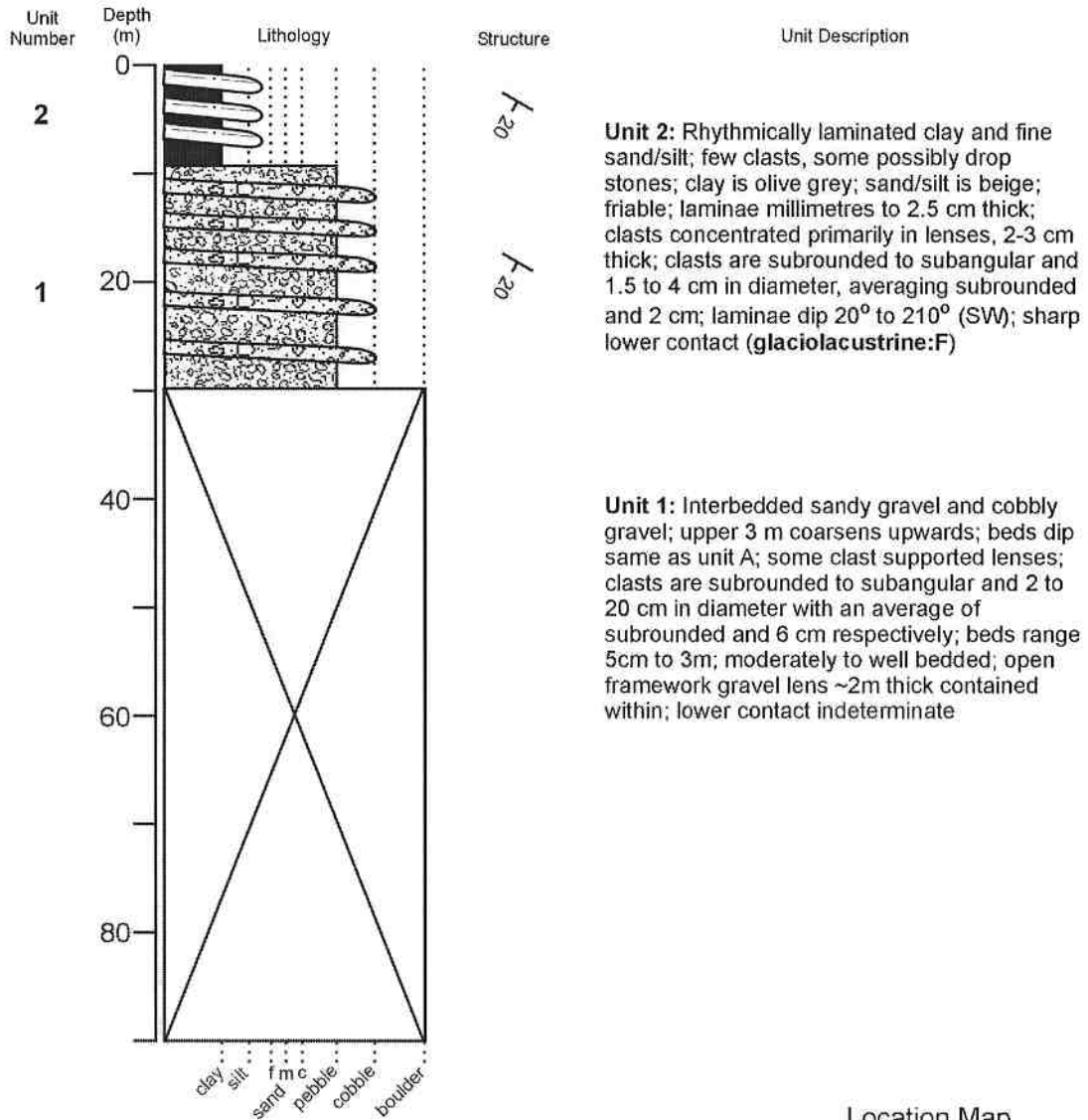
Site Description: A 26 m, near vertical face located approximately 3.25 km downstream of Quesnel Forks on the north side of the Quesnel River. It is approximately 200 m wide. Possibly part of a glaciofluvial fan. Boat access only.

Location Map



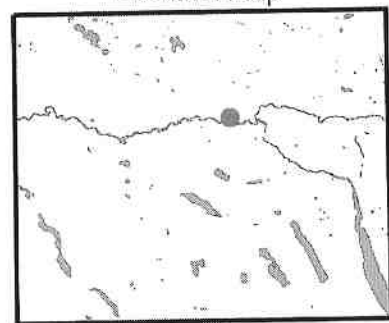
Section Number: AJB01-S3P2
 Easting: 587341 m
 Northing: 5835727 m

Base Elevation: 660 m
 Orientation: East-west



Site Description: A 30 m section approximately 60 m above the river level. Located 230 m to the east of S1 on the northern valley side. The section is approximately 180 m wide and is 3.25 km downstream of Quesnel Forks. Boat access only.

Location Map



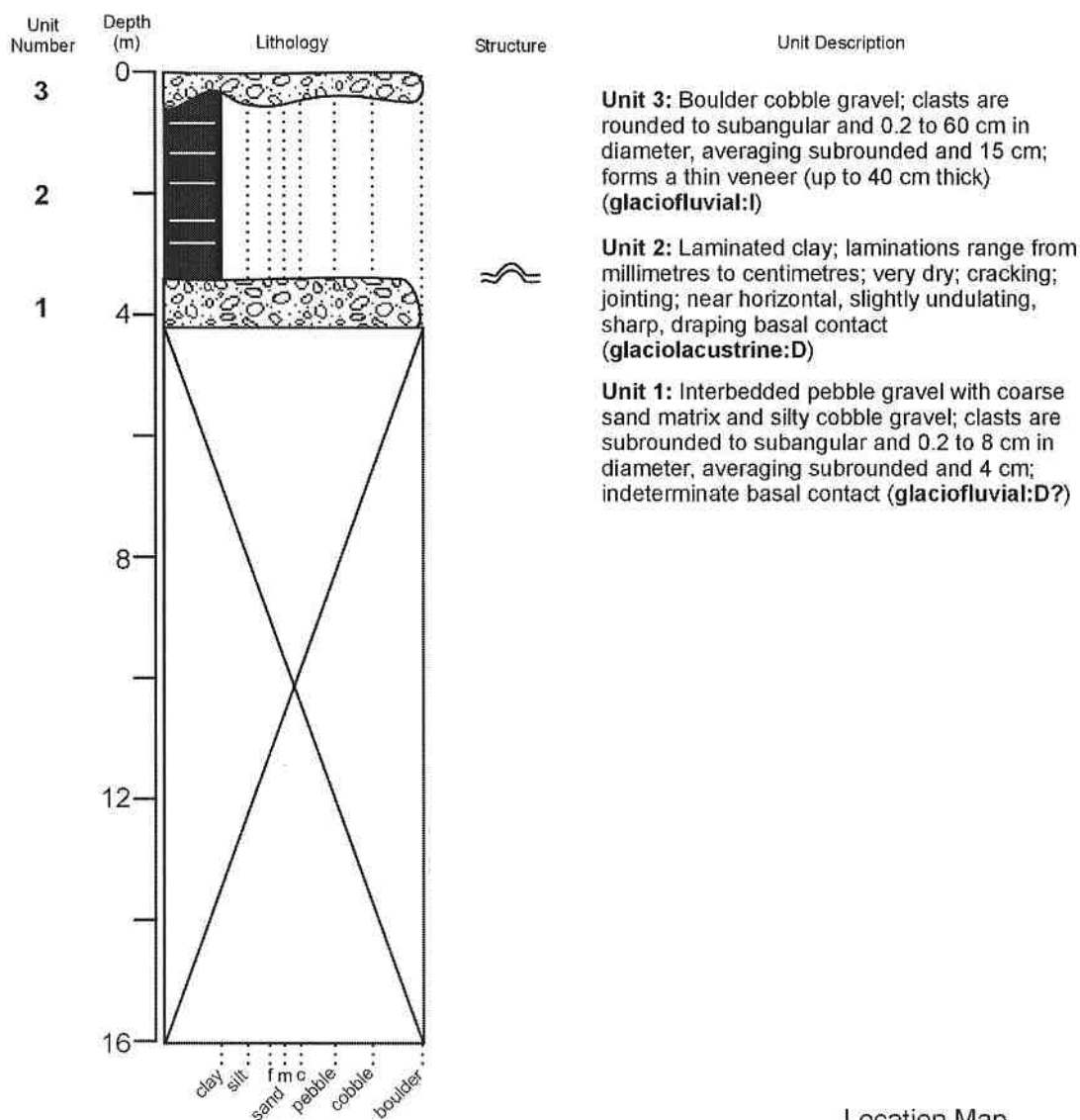
Section Number: AJB01-S4

Easting: 579854 m

Northing: 5834390 m

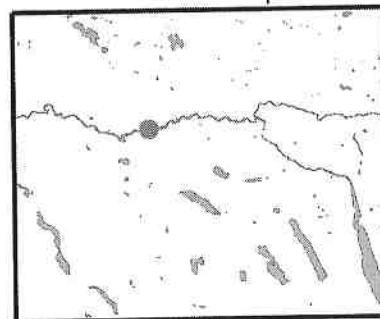
Base Elevation: 645 m

Orientation: East-west



Site Description: Sixteen metre section (4 m of stratigraphy and 12 m of scree) directly across river from L7 on the north side of the Quesnel River. The exposure is 220 m wide. From airphoto, it appears to be part of a glaciofluvial fan. The site is 12 km downstream of Quesnel Forks near Moorehead Creek. Boat access only.

Location Map



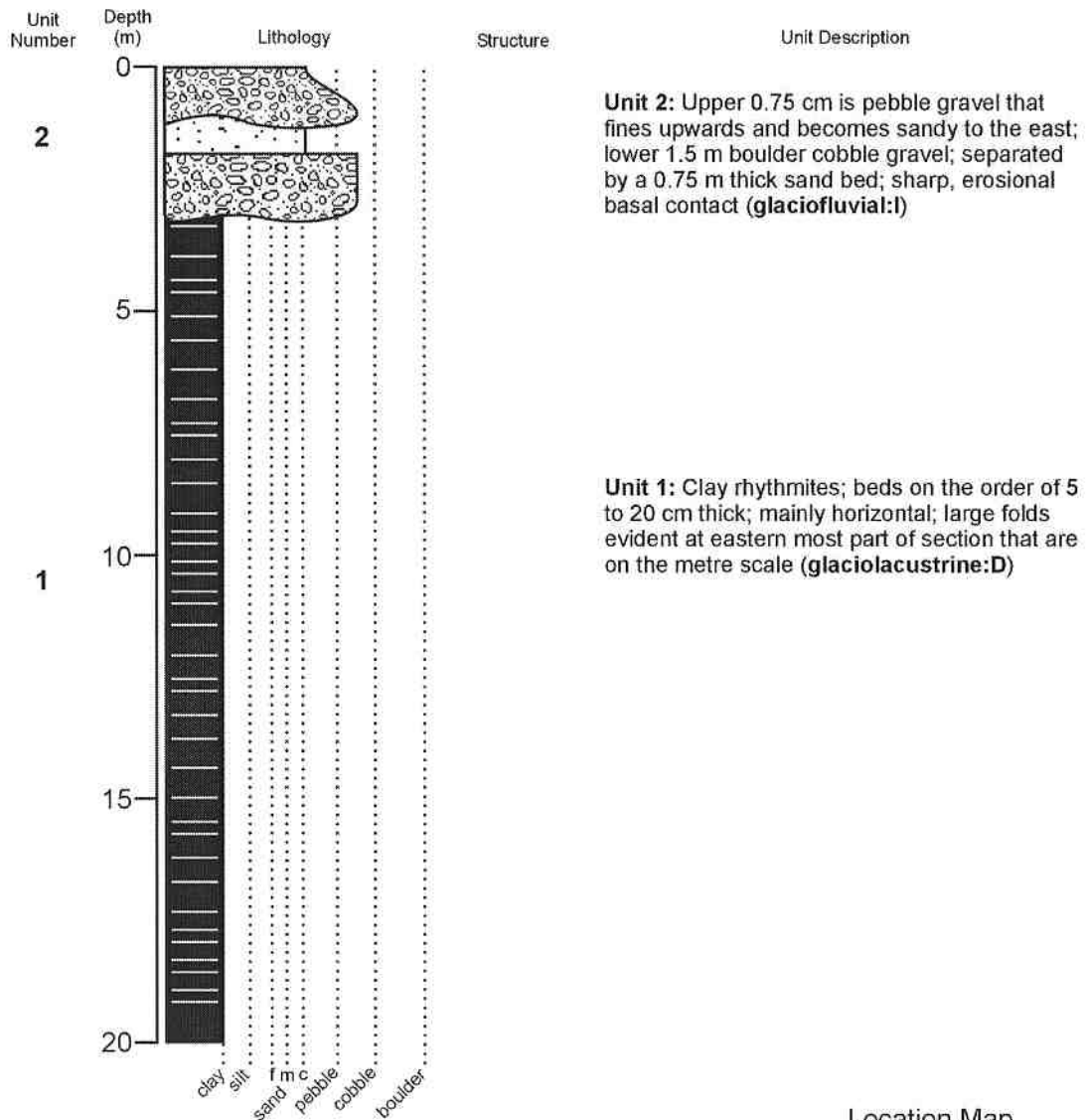
Section Number: AJB01-S5

Easting: 577548 m

Northing: 5834002 m

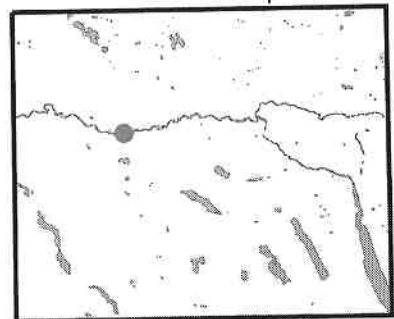
Base Elevation: 640 m

Orientation: Northeast-southwest



Site Description: A 20 m high section that is part of a glaciofluvial terrace located approximately 14 km downstream of Quesnel Forks on the north side of the Quesnel River. The exposure is approximately 600 m long and is separated from the main flow of the river by a lateral bar and back channel. Boat access only.

Location Map



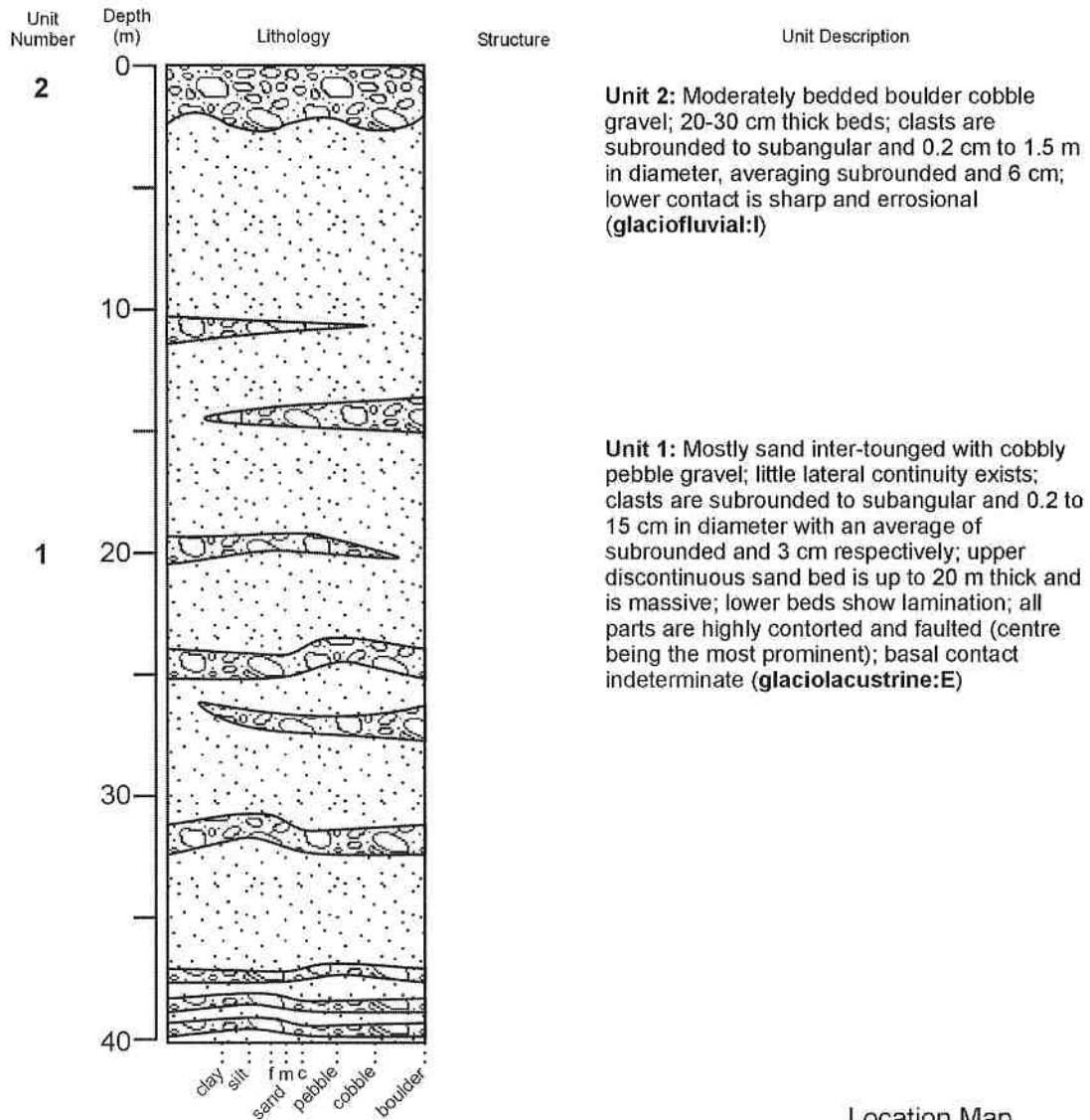
Section Number: AJB01-S6

Base Elevation: 605 m

Easting: 567647 m

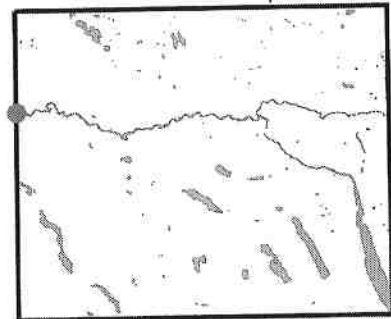
Orientation: Northwest-southeast

Northing: 5835712 m



Site Description: A 40 m, near vertical face located approximately 32 km downstream of Quesnel Forks on the north side of the Quesnel River and on the western boundary of the study area. The section is approximately 190 m wide. Boat access only.

Location Map



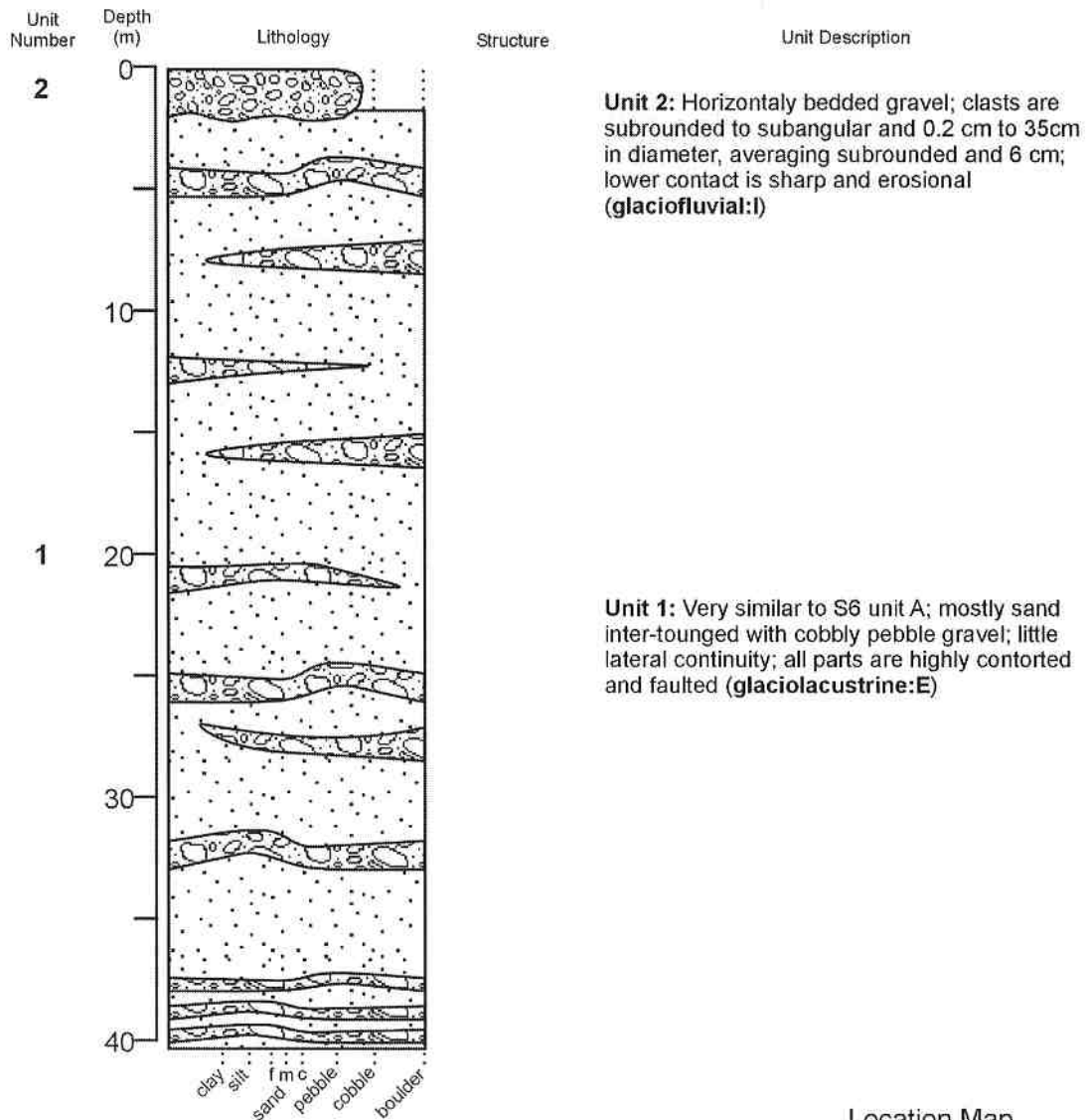
Section Number: AJB01-S7

Easting: 568038 m

Northing: 5835512 m

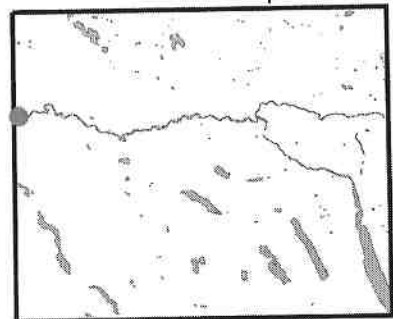
Base Elevation: 605 m

Orientation: Northeast-southwest



Site Description: A 40 m high, near vertical face located approximately 31.5 km downstream of Quesnel Forks on the south side of Quesnel River and near the western boundary of the study area. The section is approximately 80 m wide. Boat access only.

Location Map



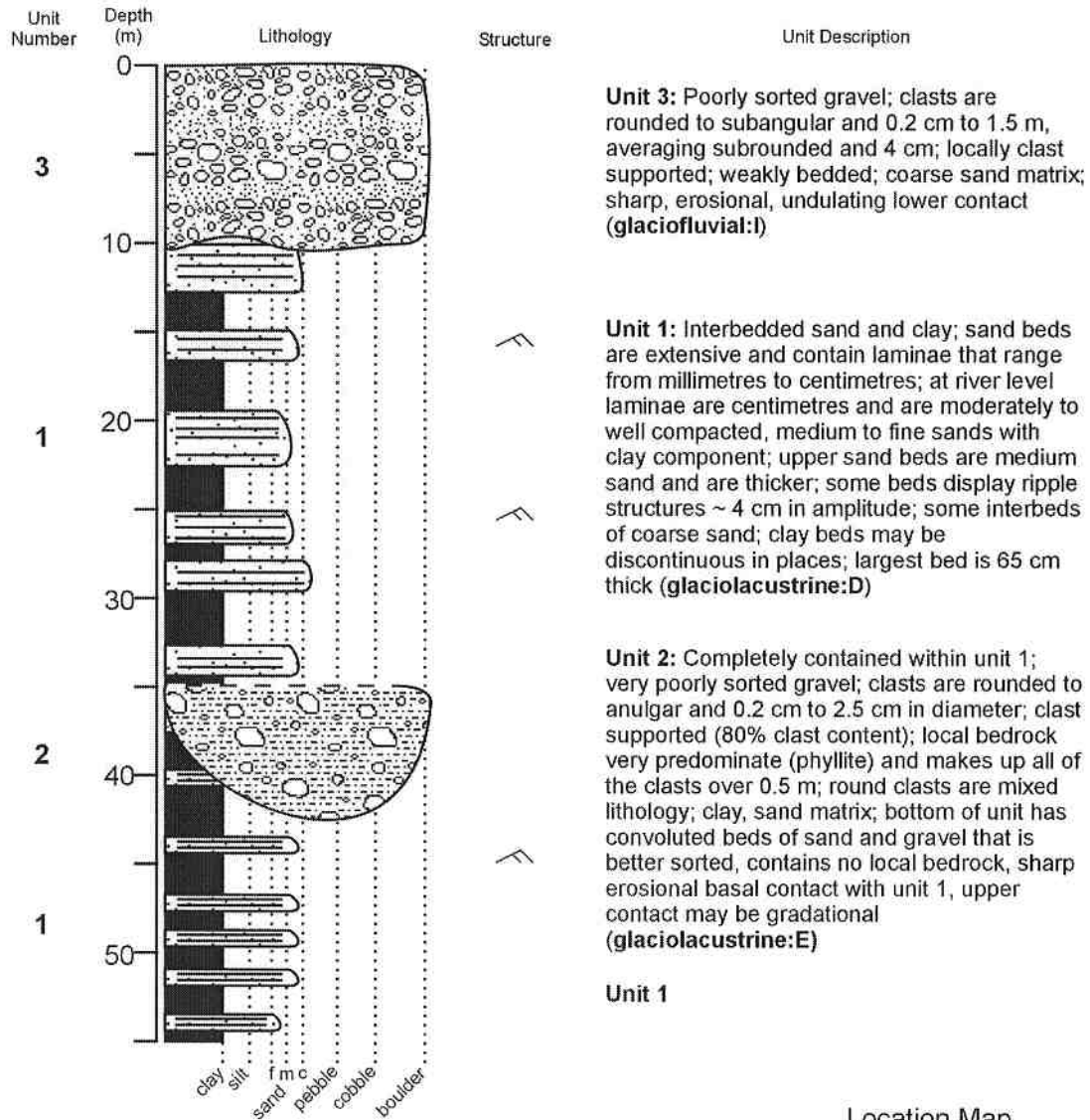
Section Number: AJB01-S8P1

Easting: 568566 m

Northing: 5835756 m

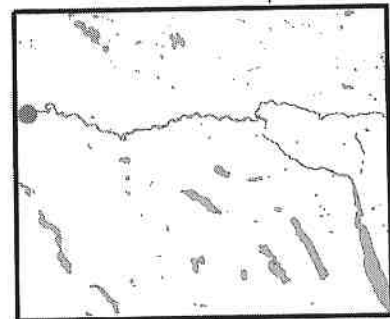
Base Elevation: 610 m

Orientation: East-west



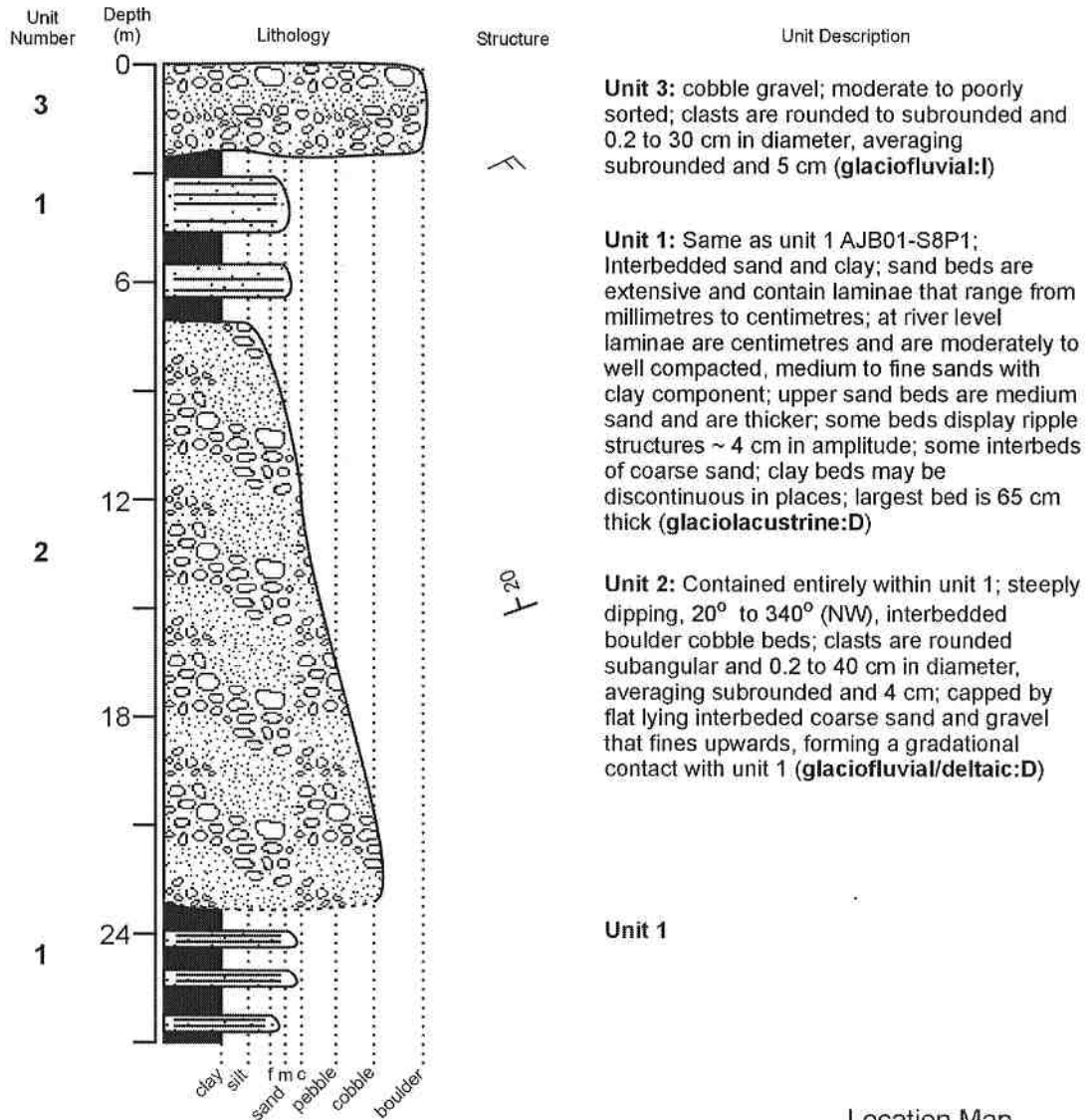
Site Description: A 55 m face located approximately 31 km downstream of Quesnel Forks on the north side of the Quesnel River. The exposure is approximately 300 m long. Boat access only.

Location Map



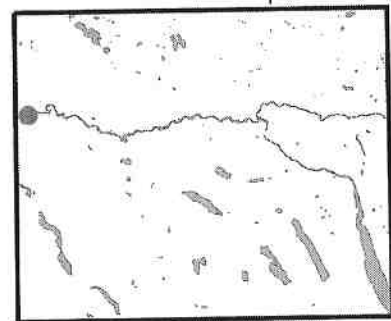
Section Number: AJB01-S8P2
 Easting: 568735 m
 Northing: 5835641 m

Base Elevation: 610 m
 Orientation: Northwest-southeast



Site Description: A 27 m face located approximately 31 km downstream of Quesnel Forks on the north side of the Quesnel River. It is immediately to the east of S8P1 in a terrace. The exposure is approximately 70 m long. Boat access only

Location Map



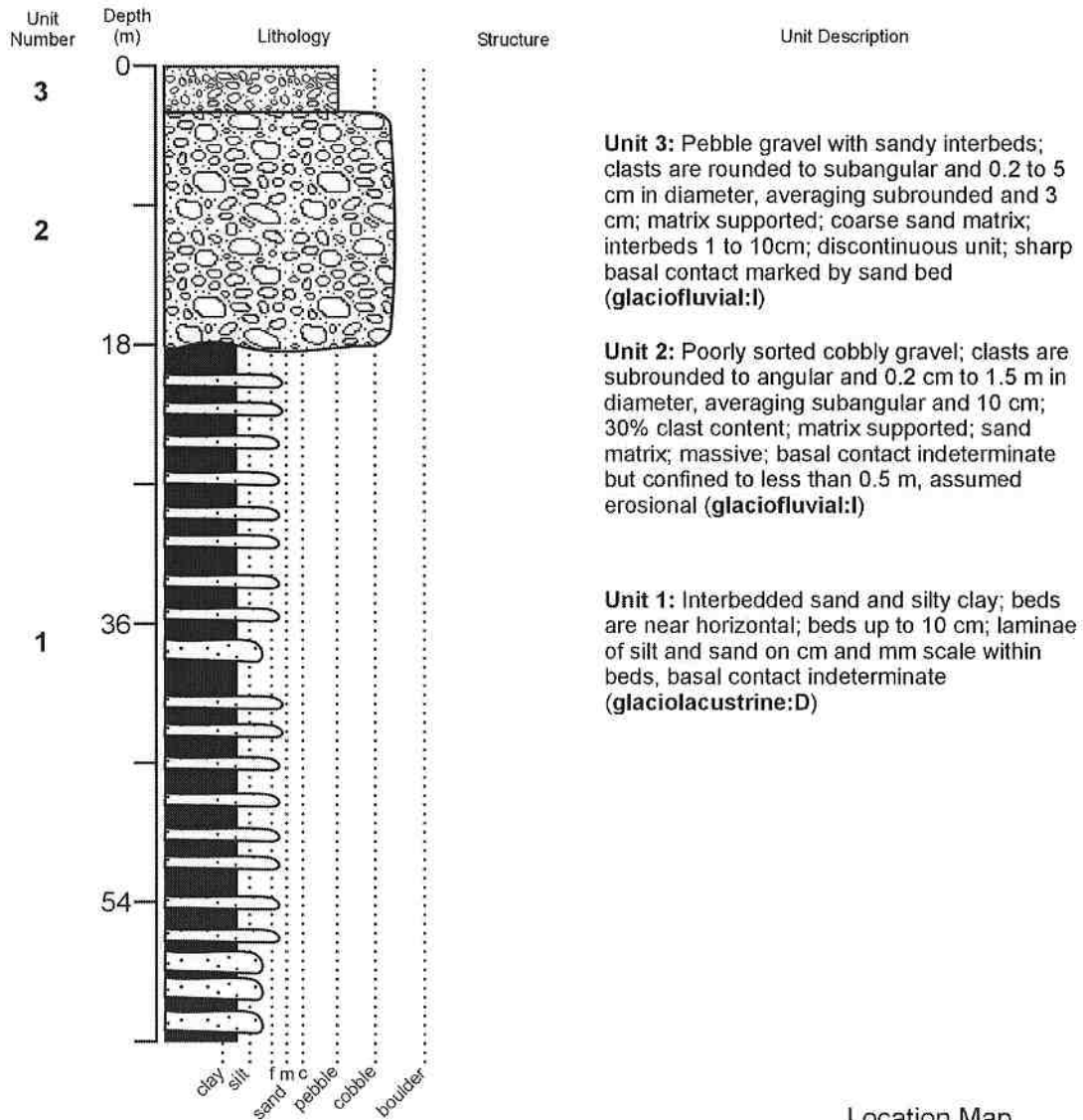
Section Number: AJB01-S9

Easting: 570642 m

Northing: 5835872 m

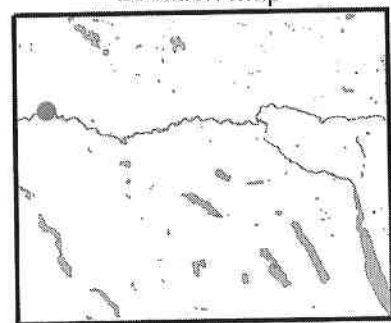
Base Elevation: 620 m

Orientation: East-west



Site Description: A 63 m face located approximately 28.5 km downstream of Quesnel Forks on the south side of the Quesnel River. The exposure is approximately 70 m wide. Boat access only.

Location Map



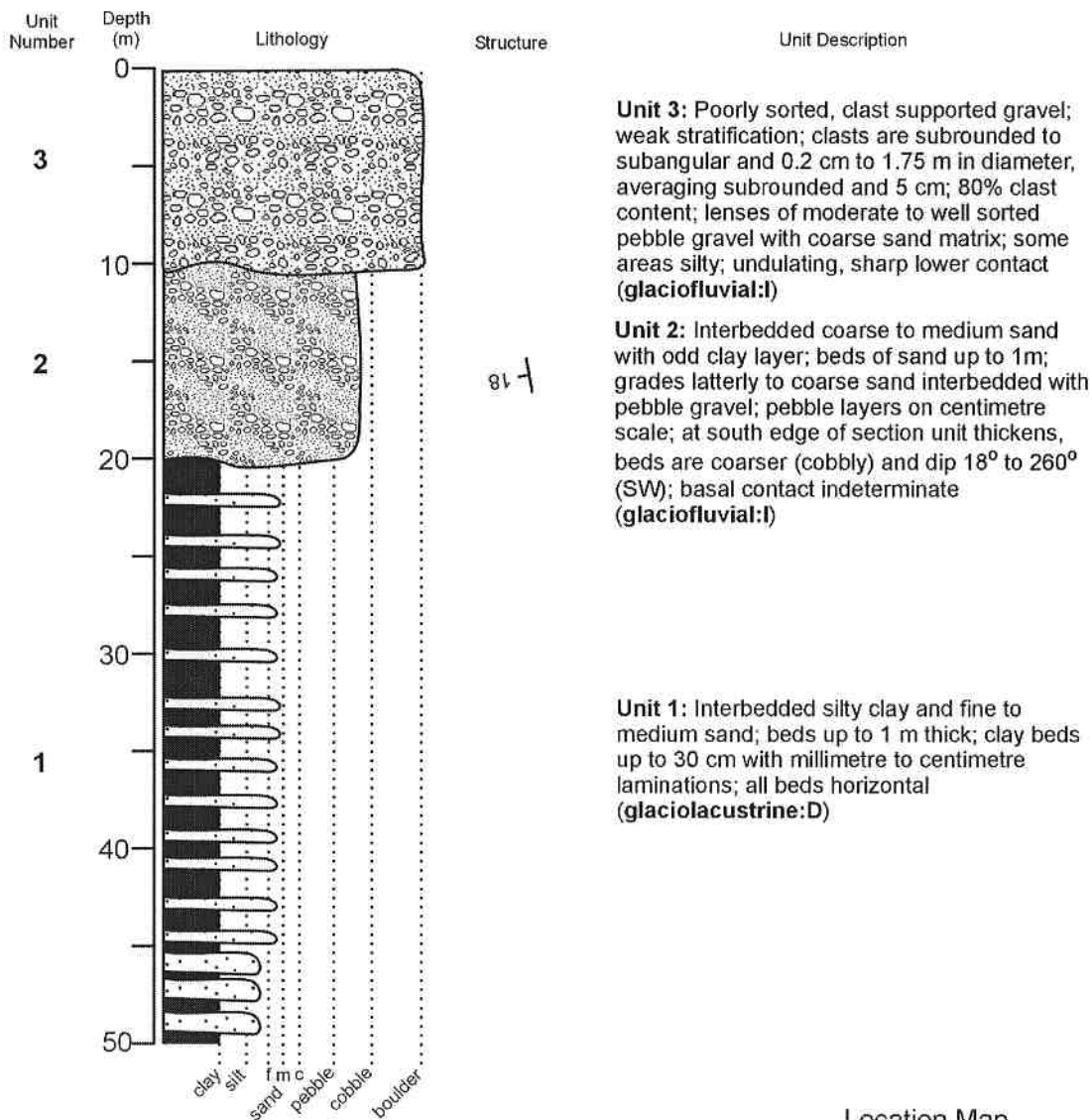
Section Number: AJB01-S10

Easting: 570403 m

Northing: 5836257 m

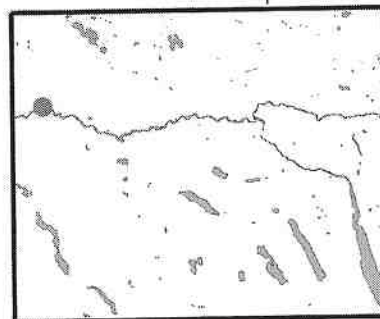
Base Elevation: 620 m

Orientation: Northwest-southeast



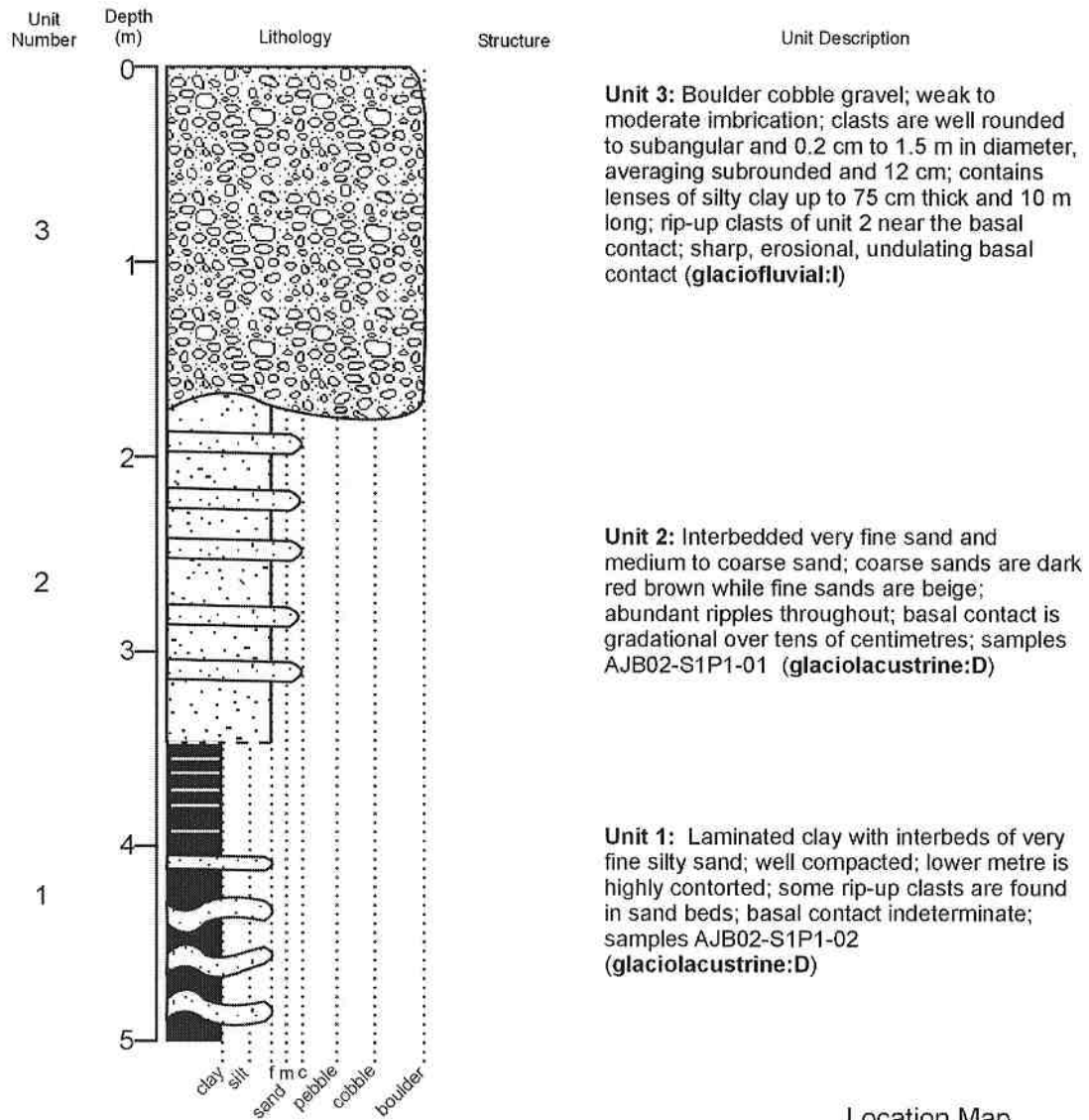
Site Description: Stratigraphy of a 50 m exposure located approximately 28 kilometres downstream of Quesnel Forks on the north side of the Quesnel River. It is immediately adjacent to landslide L9, downstream. Access is by boat only.

Location Map



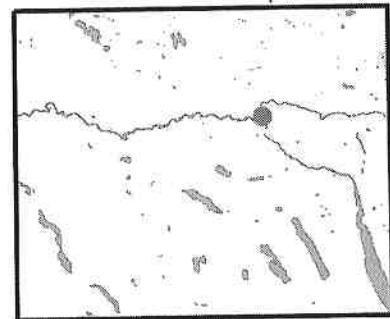
Section Number: AJB02-S11
 Easting: 589680 m
 Northing: 5835645 m

Base Elevation: 660 m
 Orientation: East-west



Site Description: A 5 m section located on the north side of the Quesnel river in the southern bank of Quesnel Forks town site, directly across from the Quesnel Forks Landslide.

Location Map



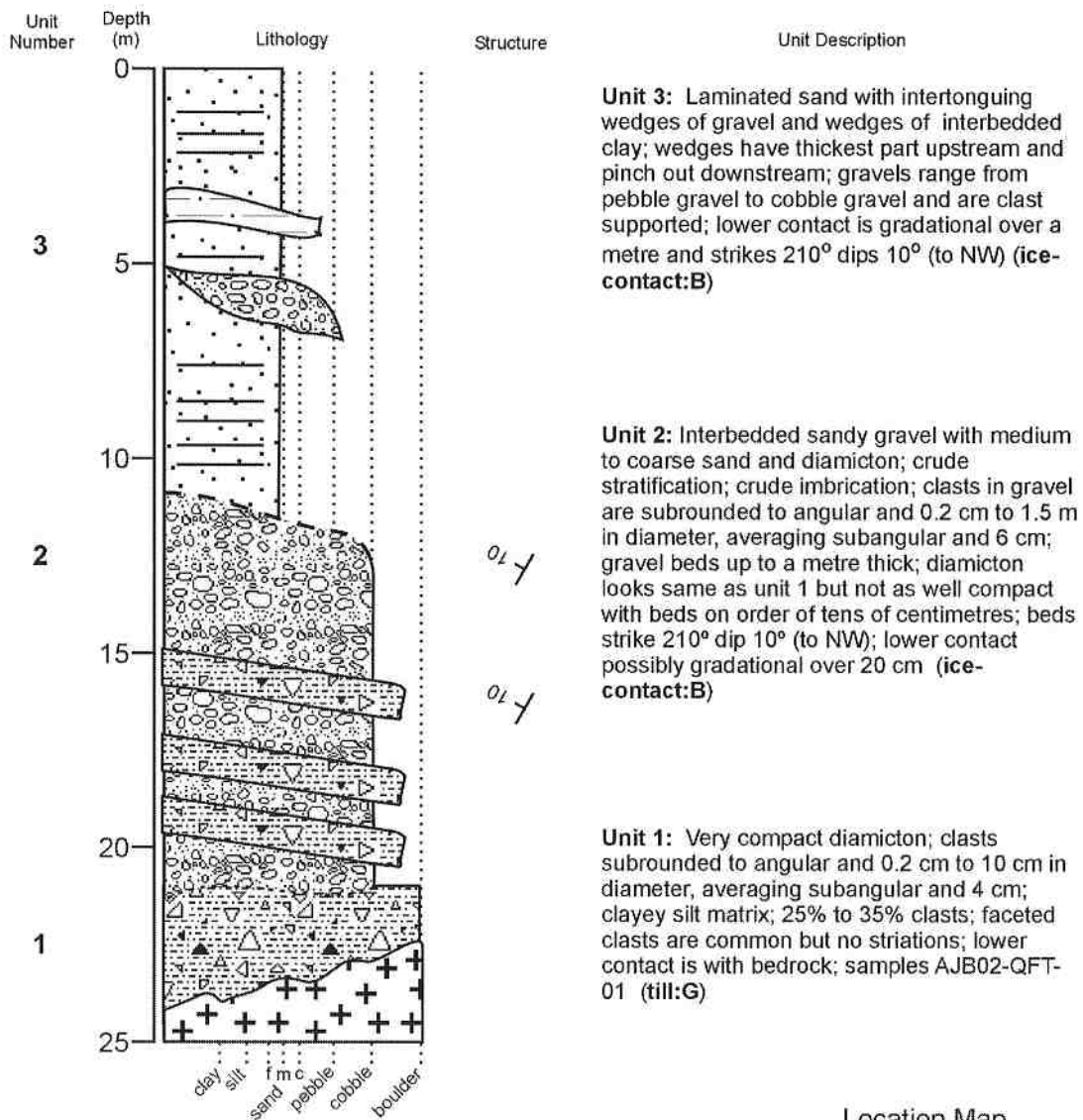
Section Number: AJB02-S12

Easting: 590035 m

Northing: 5835510 m

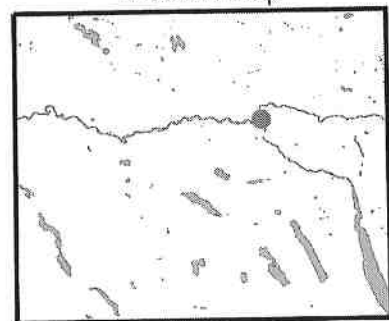
Base Elevation: 660 m

Orientation: Northwest-southeast



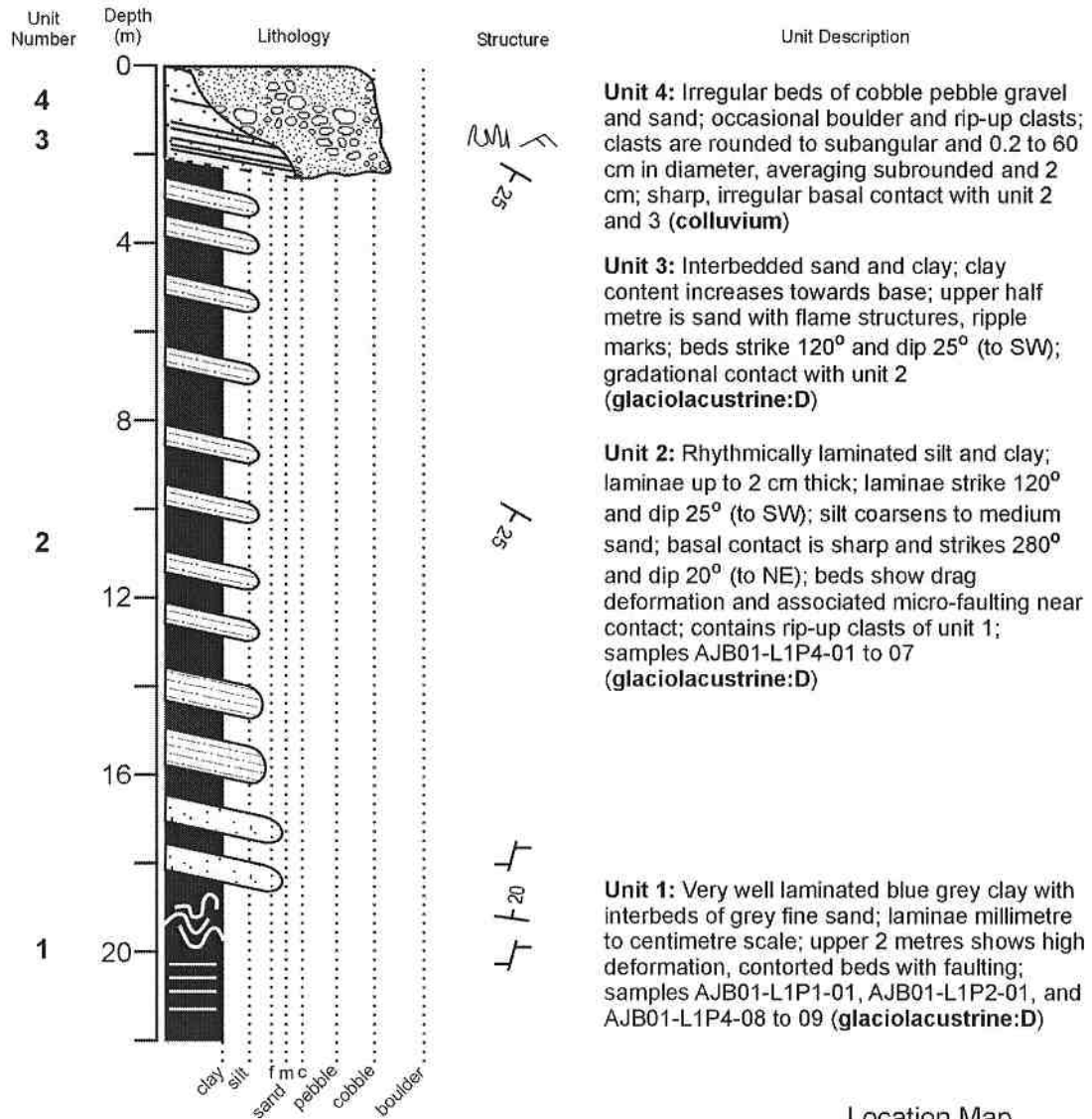
Site Description: A 25 metre section located on the north side of the Quesnel River directly across from the Quesnel Forks Landslide, just east of the Quesnel Forks town site.

Location Map



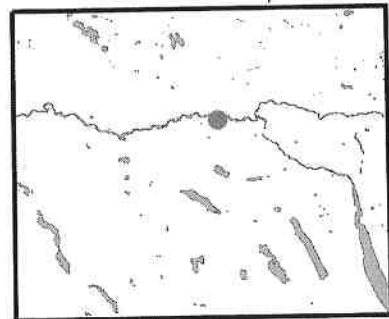
Section Number: AJB01-L1
 Easting: 586090 m
 Northing: 5835176 m

Base Elevation: 660 m
 Orientation: East-west



Site Description: Stratigraphy obtained along the scarp of a landslide to approximately 22 m above the river level. The site is 4 km downstream from Quesnel Forks on the south side of the Quesnel River. Road access from the west is possible from a rough road at the end of Little Lake Road.

Location Map



Approximate Date of Occurrence: 1978-1985 (active)

Type of Failure: Active, retrogressive, wet earth slide-earth flow

Elevation of Crown: 682 m asl

Elevation of Toe of Rupture Surface: 660 m asl

Elevation of Tip of Landslide: 660 m asl

Dimensions

Length of Rupture Surface (L_r): 110 m

Width of Rupture Surface (W_r): 235 m

Depth of Rupture Surface (D_r): 19 m

Length of Displaced Mass (L_d): 88 m

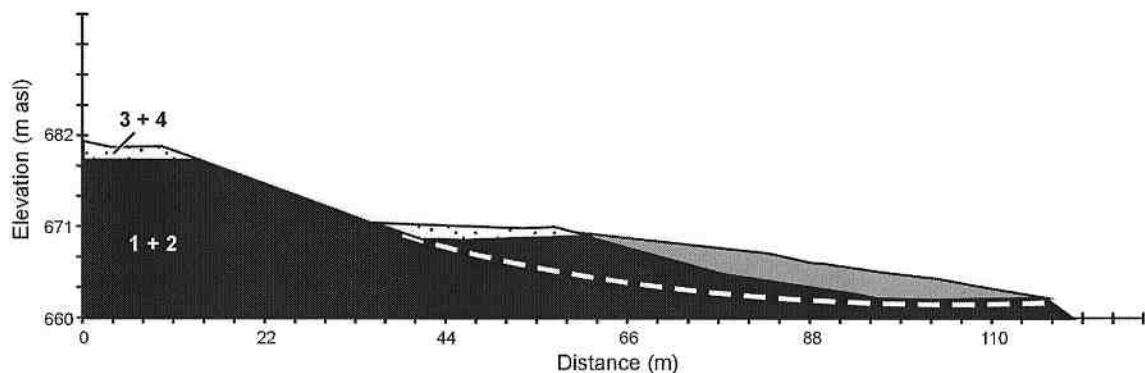
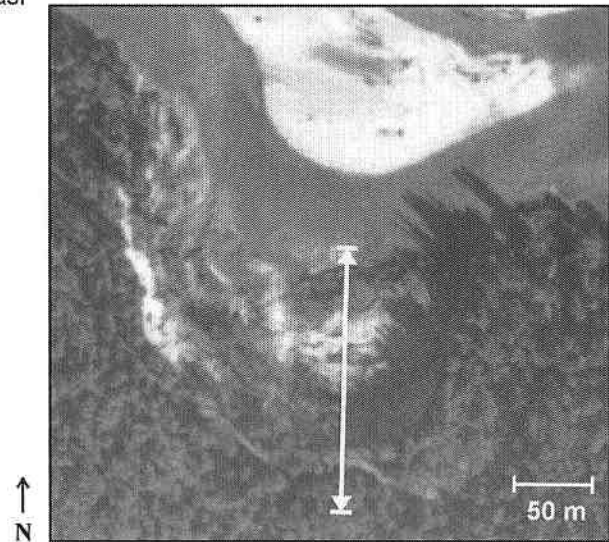
Width of Displaced Mass (W_d): 235 m

Depth of Displaced Mass (D_d): 10 m

Total Length (L): 120 m

Surface Area: $32 \text{ m}^2 \times 10^3$

Volume ($\rho L_d D_d W_d / 6$): $108 \text{ m}^3 \times 10^3$



Description:

The landslide is located on the south side of the Quesnel River on an outer, erosive bend. The crown of the headscarp is immediately adjacent to a road that follows the length of the scarp. Closest to the headscarp are intact blocks of soil that appear to have rotated from their undisturbed positions. Rotational movement appears to be dormant. At the edge of the main rotational blocks, transverse ridges are present made of small rotational slivers. Below this, the dominant mode of motion is by flow where the blocks have become disaggregated. Active flows are found adjacent to the river. The primary material making up the flow is silt and clay (unit 1 and 2) though in places the surface of the flow contains sand and gravel (units 3 and 4). Where active, the material is saturated. Pre-slide vegetation is primarily concentrated near the headscarp and consists of jack-strawed trees and ground-cover. Post-slide vegetation is found throughout the slide except where flows are still active. No surface water is present. The apparent failure plane of the rotational component of the slide, or of an older slide, is visible near the eastern edge of the landslide.

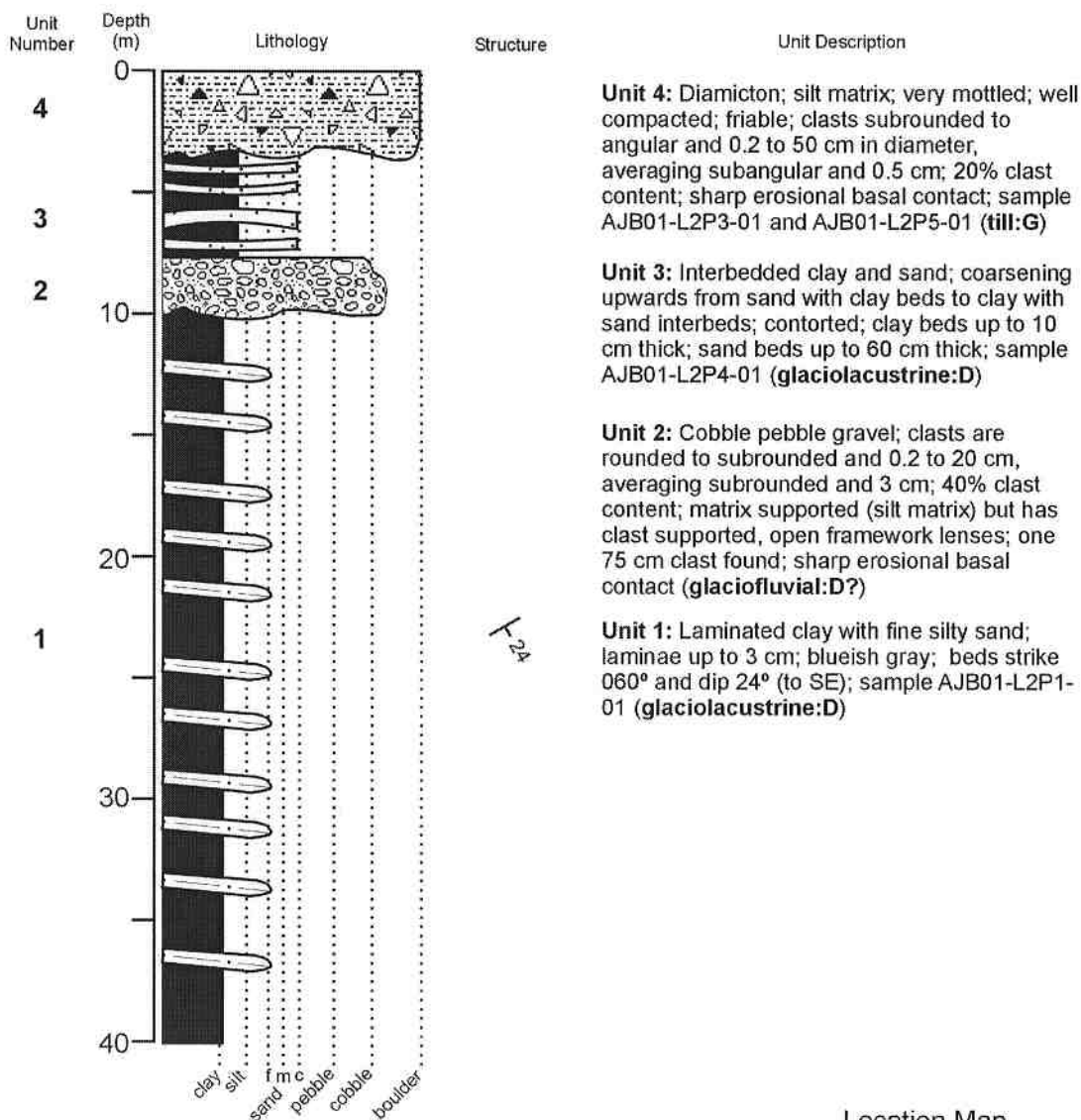
Section Number: AJB01-L2

Easting: 582092 m

Northing: 5835059 m

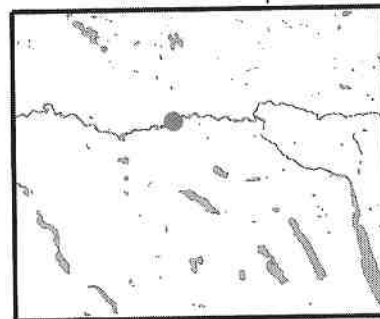
Base Elevation: 650 m

Orientation: East-west



Site Description: Stratigraphy obtained along scarp of landslide up to 40 m above river. Located 9.3 km downstream of Quesnel Forks on the south side of the Quesnel River. Road access via Little Lake Road.

Location Map



Approximate Date of Occurrence: <1955, 1996 - 1998 (active)

Type of Failure: Reactivated, diminishing, wet earth slide-earth flow

Elevation of Crown: 680 m asl

Elevation of Toe of Rupture Surface: 650 m asl

Elevation of Tip of Landslide: 650 m asl

Dimensions

Length of Rupture Surface (L_r): 275 m

Width of Rupture Surface (W_r): 165 m

Depth of Rupture Surface (D_r): 10 m

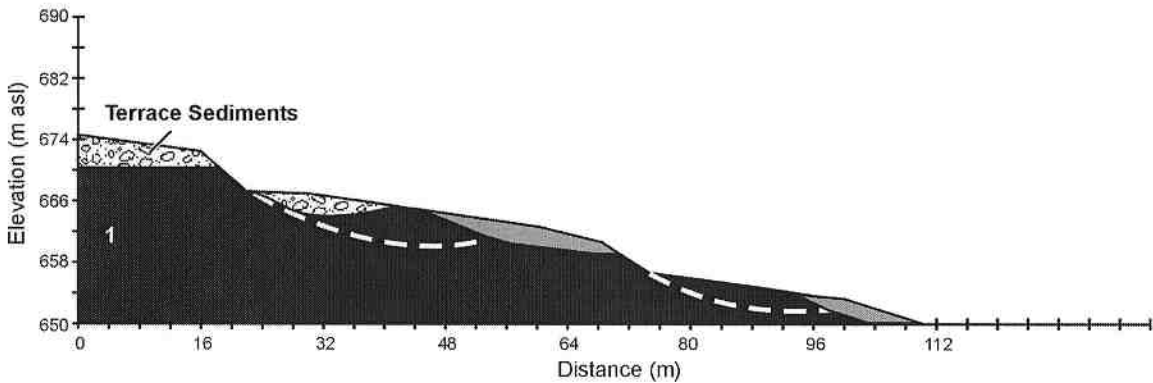
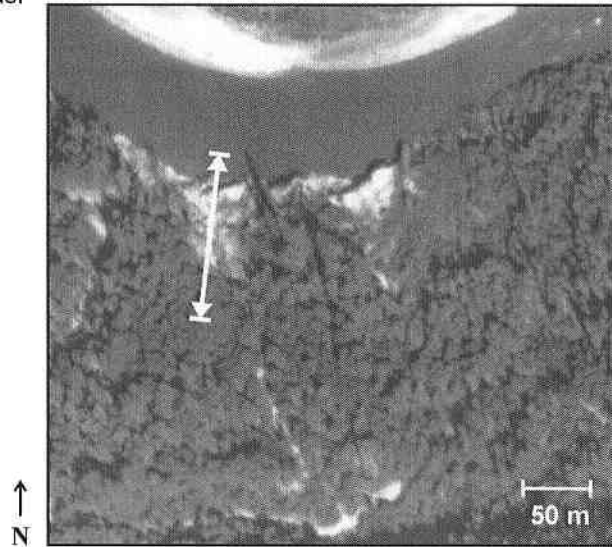
Length of Displaced Mass (L_d): 280 m

Width of Displaced Mass (W_d): 165 m

Depth of Displaced Mass (D_d): 10 m

Total Length (L): 295 m

Surface Area: $11 \text{ m}^2 \times 10^9$



Description:

The landslide is located on the south side of the Quesnel River on an outer, erosive bend. It appears to be a reactivation of an older slide that was much larger, extending approximately 300 m from the river. At the head of the older slide, a road now exists in an area of ponding water related to a spring. According to the local community, the road often washes out. Where the slide is active, it has retrogressed into an adjacent glaciofluvial terrace (profile depicted above). Here, the failure is in the form of several small slumps though flow processes dominate. The forest floor of the older slide remains intact though some trees are jack-strawed. Over the active portions of the landslide, little of the original forest floor remains and vegetation is primarily young, secondary growth. Debris from the original forest floor, as well as overturned trees, are evident.

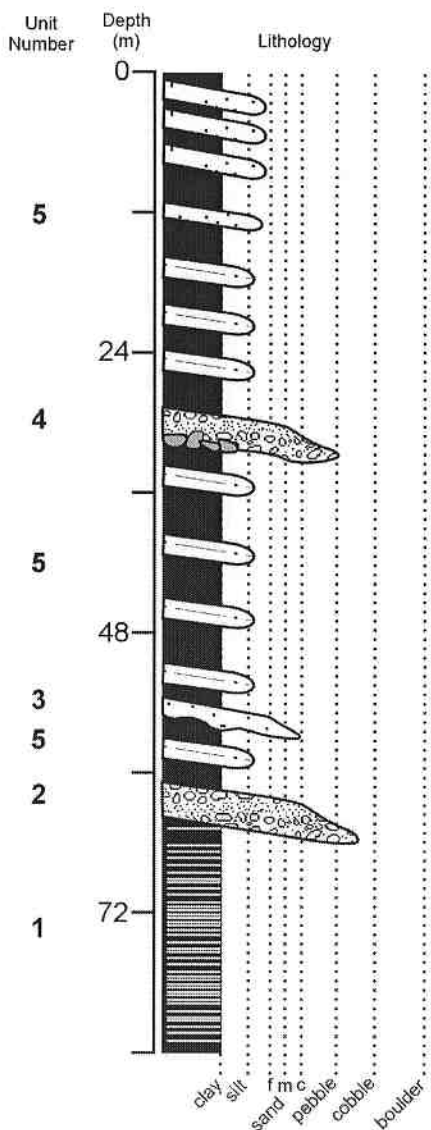
Section Number: AJB01-L3

Easting: 583486 m

Northing: 5835330 m

Base Elevation: 655 m

Orientation: East-west



Unit 5: Interbedded medium to fine sand with clay; clay beds 1 to 3 cm thick; sand beds 10 to 15 cm thick; sand dominant in upper unit; clay dominant in lower unit; bedding becomes thinner and sand becomes silty at base of unit with laminae on order of mm and cm; beds strike 353° and dip 9° (to E); moderate to well compacted; sharp contacts with other units contained within (glaciolacustrine:D)

Unit 4: Fining upwards sequence of pebbly gravel and coarse sand with medium sand; gravel beds 4 to 10 cm thick; clasts are rounded to subrounded and 0.2 to 10 cm in diameter, averaging subrounded and 2 cm; sharp basal contact marked by boulder lag (glaciofluvial:D?)

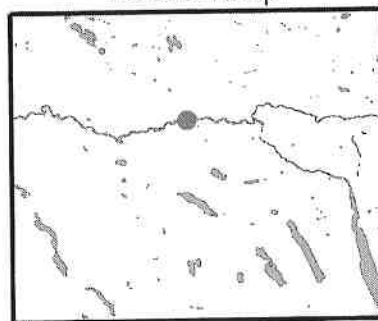
Unit 3: Sand bed; grades from coarse-medium at bottom to fine-medium sand at top; clay rip-ups present or clay blocks; some clasts near upper contact; lower contact is sharp and undulating (glaciofluvial:D?)

Unit 2: Interbedded gravel and sand; gravel up to 0.5m thick; clasts are subangular and are 0.2 to 15 cm in diameter averaging subrounded to 2 cm; sand is medium to coarse; sand beds up to 5cm; overall slightly fining upwards sequence; lower contact is sharp, erosional, slightly undulating (glaciofluvial:D?)

Unit 1: Laminated clay; laminae on millimetre to centimetre scale (glaciolacustrine:D)

Site Description: Stratigraphy taken along scarp of landslide to a height of approximately 84 m above the river level. The slide is 7.5 km downstream of Quesnel Forks on the south side of the Quesnel River. Access by boat only.

Location Map



Approximate Date of Occurrence: 1970 - 1978 (active)

Type of Failure: Reactivated, diminishing, wet earth slide-earth flow

Elevation of Crown: 740 m asl

Elevation of Toe of Rupture Surface: 655 m asl

Elevation of Tip of Landslide: 655 m asl

Dimensions

Length of Rupture Surface (L_r): 385 (220) m

Width of Rupture Surface (W_r): 715 (330) m

Depth of Rupture Surface (D_r): ? m

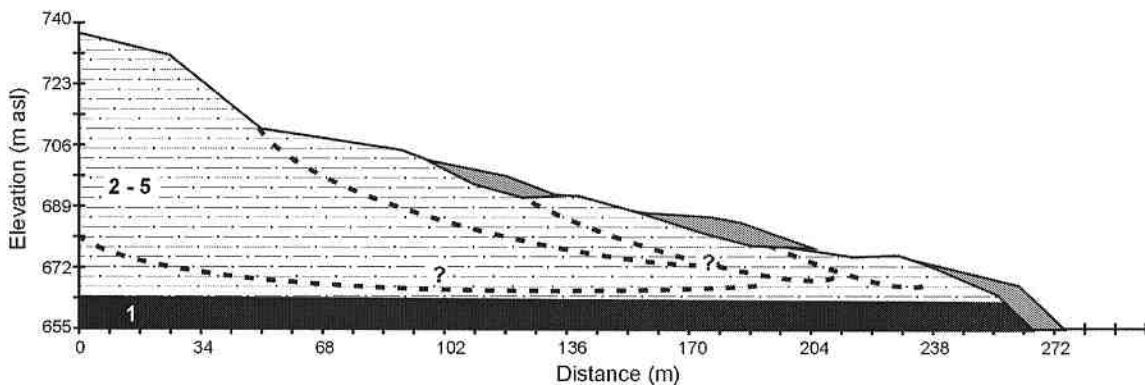
Length of Displaced Mass (L_d): 385 (210) m

Width of Displaced Mass (W_d): 715 (330) m

Depth of Displaced Mass (D_d): ? m

Total Length (L): 385 (220) m

Surface Area: $49 \text{ m}^2 \times 10^3$



Description:

The landslide is located on the south side of the Quesnel River on an outer, erosive bend. From airphoto, it appears to be a reactivation of a much larger landslide. In addition, found within the western side scarp is a thick unit of colluvium that contains large buried trees that all point into the valley's centre. All stratigraphic units, with the exception of unit 1, dip into the valley side, which may also support an earlier failure. The active landslide is composed of several smaller slumps that subsequently turn into flows. Similar to landslide L1, transverse ridges can be found adjacent to slumped blocks. Thick, pre-slide vegetation covers much of the upper, active slide where as little vegetation, pre- or post-slide, is found on the lower active portion of the slide. The western side of the slide is much more active and is made of highly saturated silt and clay.

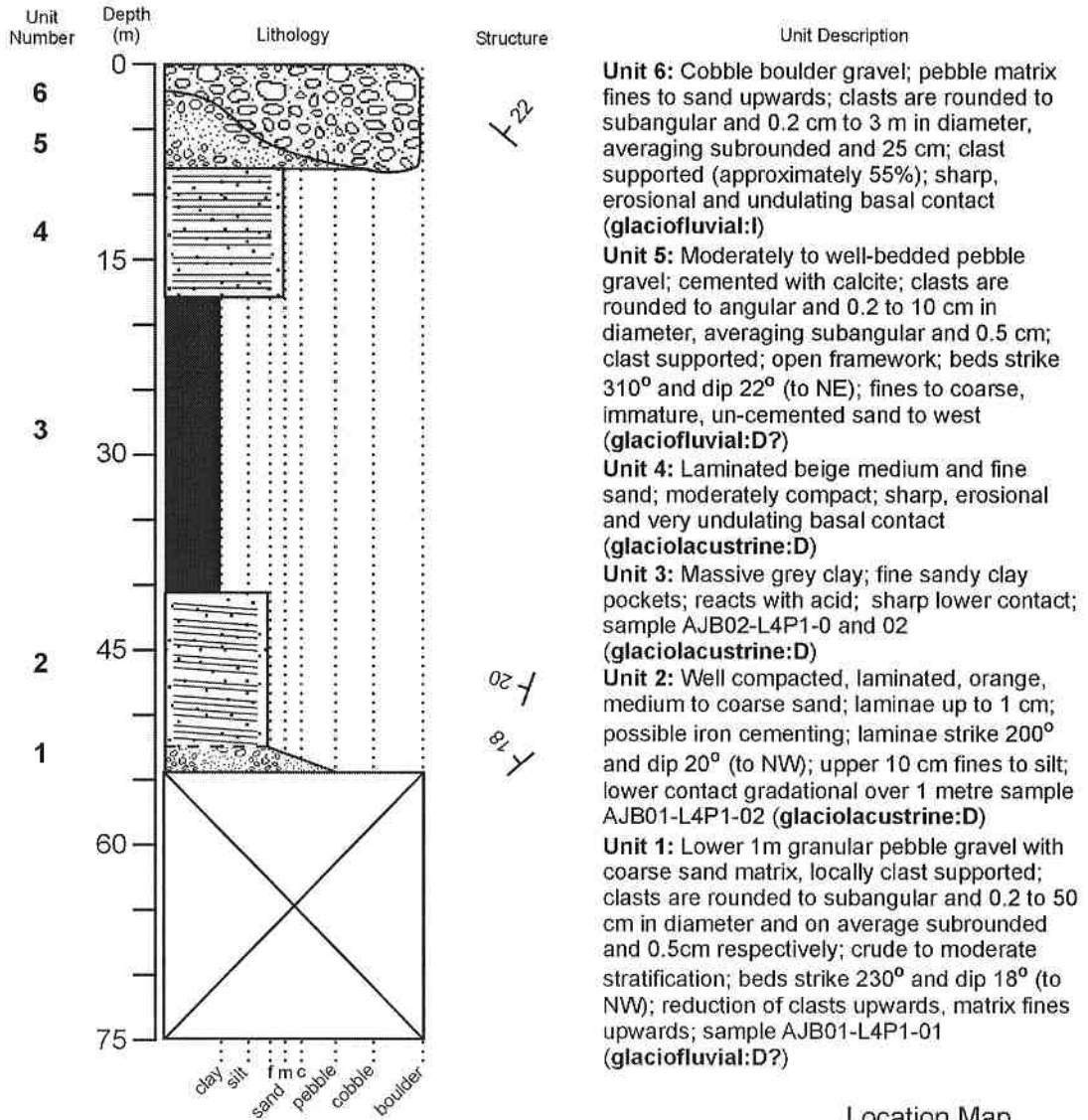
Section Number: AJB01-L4

Easting: 589941 m

Northing: 5835457 m

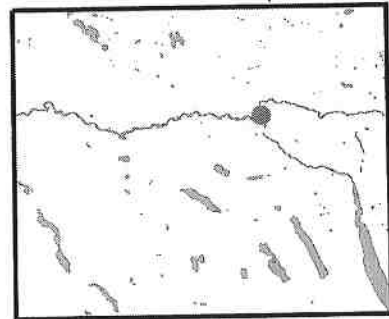
Base Elevation: 660 m

Orientation: Northwest-southeast



Site Description: Stratigraphy taken along scarp of landslide located at Quesnel Forks on the south side of the Quesnel River. Road access is from a logging road near the access for the Bullion Pit overlook.

Location Map



Approximate Date of Occurrence: April 28th, 1996 (inactive)

Type of Failure: Dormant, retrogressive, very rapid, dry earth slide-debris flow

Elevation of Crown: 732 m asl

Elevation of Toe of Rupture Surface: 660 m asl

Elevation of Tip of Landslide: 655 m asl

Dimensions

Length of Rupture Surface (L_r): 205 m

Width of Rupture Surface (W_r): 338 m

Depth of Rupture Surface (D_r): 34 m

Length of Displaced Mass (L_d): 390 m

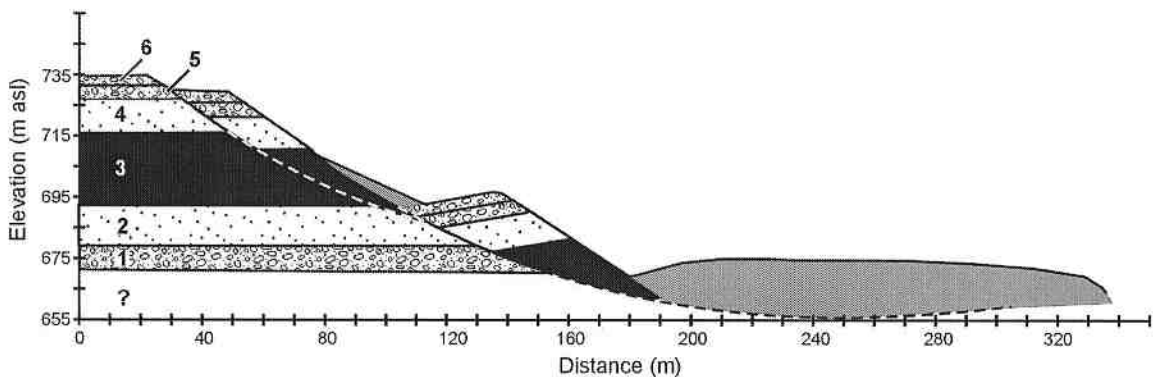
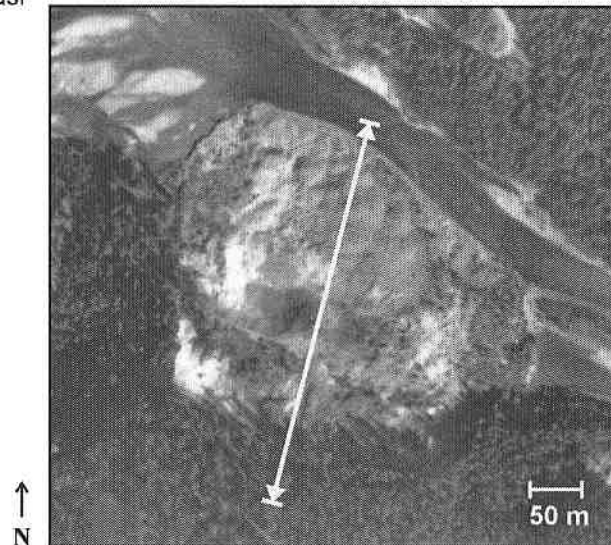
Width of Displaced Mass (W_d): 337 m

Depth of Displaced Mass (D_d): 12 m

Total Length (L): 398 m

Surface Area: $104 \text{ m}^2 \times 10^3$

Volume ($\rho L_d D_d W_d / 6$): $924 \text{ m}^3 \times 10^3$

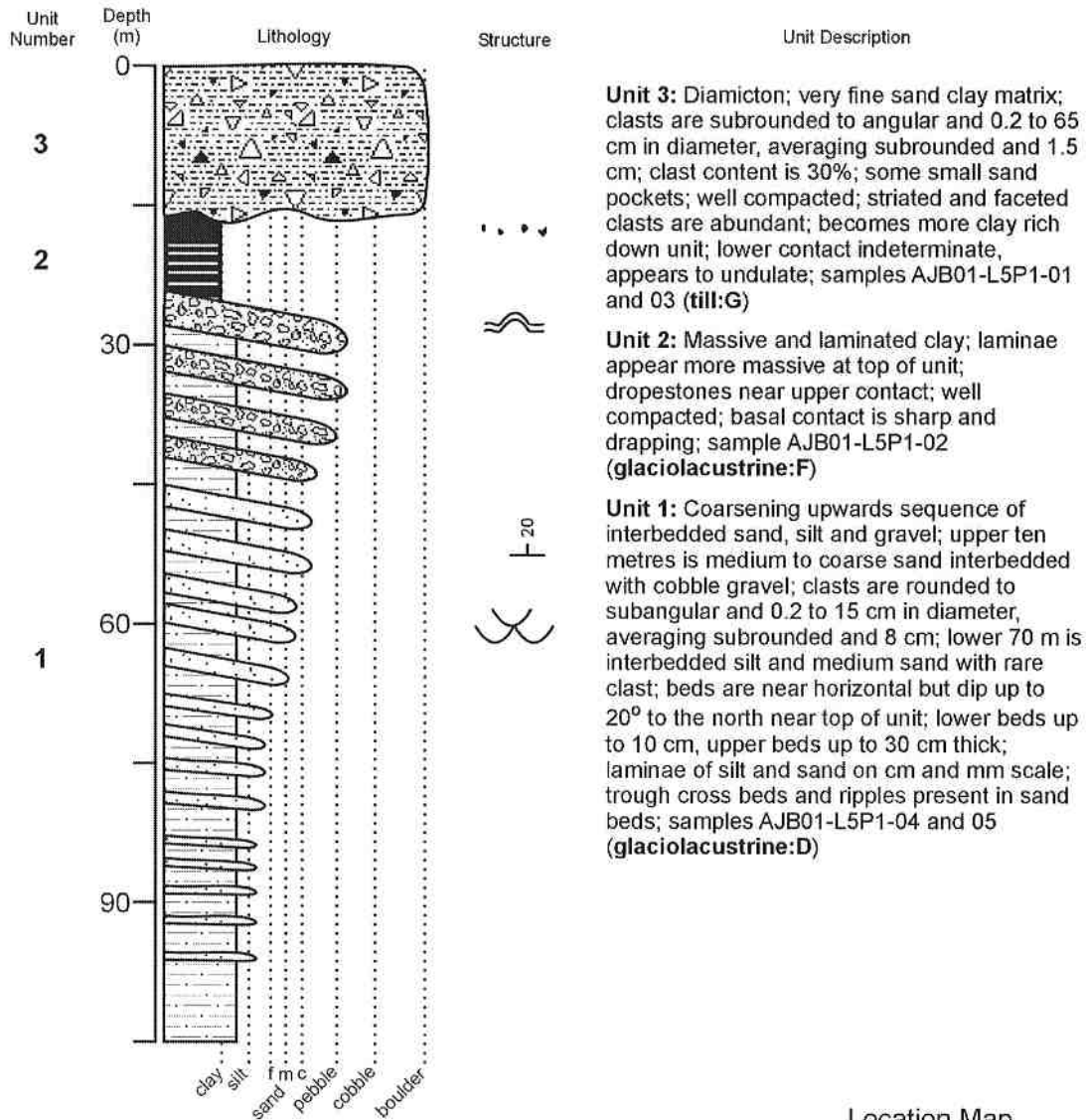


Description:

The landslide is on the south side of the Quesnel River in a glaciofluvial terrace, on what was a relatively short, straight reach immediately upstream from the Quesnel Forks. When the terrace failed, it blocked the river. It consists of two main rotated blocks as well as the run-out or toe of the slide which appears to be a flow. The upper rotational block remains heavily forested with several jack-strawed trees. On the lower rotational block, the forest floor remains partially intact, though most trees are overturned. Elsewhere, only limited vegetation exists. Virtually the entire slide remains dry, with the wettest area being near the eastern side scarp and at the centre of the slide, on the lower rotational block, where a small amount of surface water can be found. Stratigraphy within the rotational blocks is well preserved and shows little deformation. Material making up the toe of the slide is dominantly silty clay and sand, though clean, cobble gravel is found along the eastern edge of the toe. Where clay is dominant, cone type features, some more than 2 m high, are found.

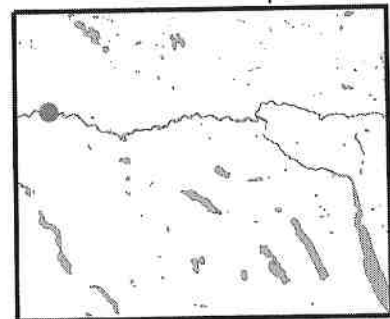
Section Number: AJB01-L5P1
 Easting: 571459 m
 Northing: 5835661 m

Base Elevation: 630 m
 Orientation: East-west



Site Description: Stratigraphy along scarp and gully to approximately 105 m above the river located 26 km downstream of Quesnel Forks on the south side of the Quesnel River. It is accessible by land via the 2600 Road logging road.

Location Map



Approximate Date of Occurrence: Spring 2001 (active)

Type of Failure: Reactivated, retrogressive, complex, wet earth slide-earth flow

Elevation of Crown: 720 m asl

Elevation of Toe of Rupture Surface: 670 m asl

Elevation of Tip of Landslide: 630 m asl

Dimensions

Length of Rupture Surface (L_r): 120 m

Width of Rupture Surface (W_r): 190 m

Depth of Rupture Surface (D_r): 15 m

Length of Displaced Mass (L_d): 230 m

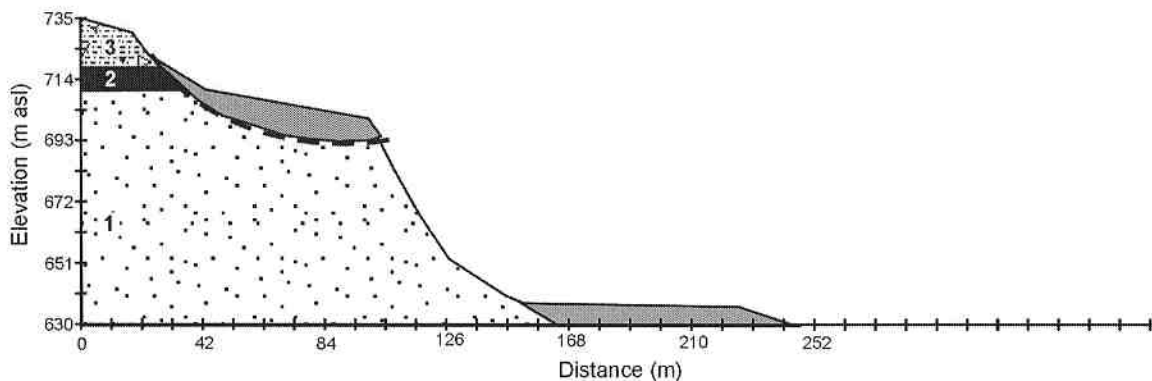
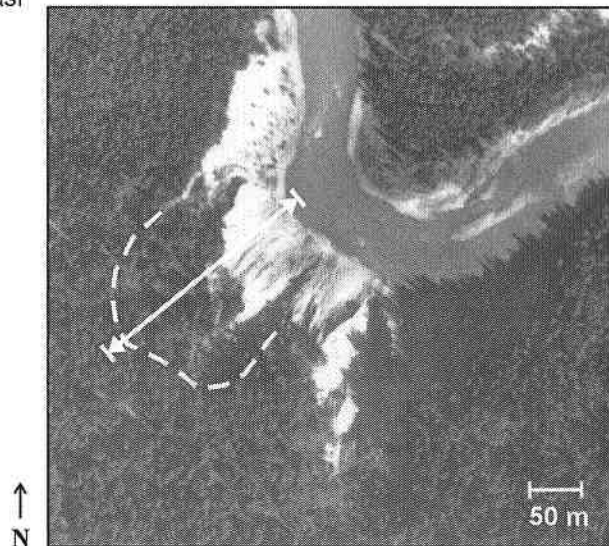
Width of Displaced Mass (W_d): 140 m

Depth of Displaced Mass (D_d): 10

Total Length (L): 237 m

Surface Area: $40 \text{ m}^2 \times 10^3$

Volume ($\rho L_d D_d W_d / 6$): $169 \text{ m}^3 \times 10^3$

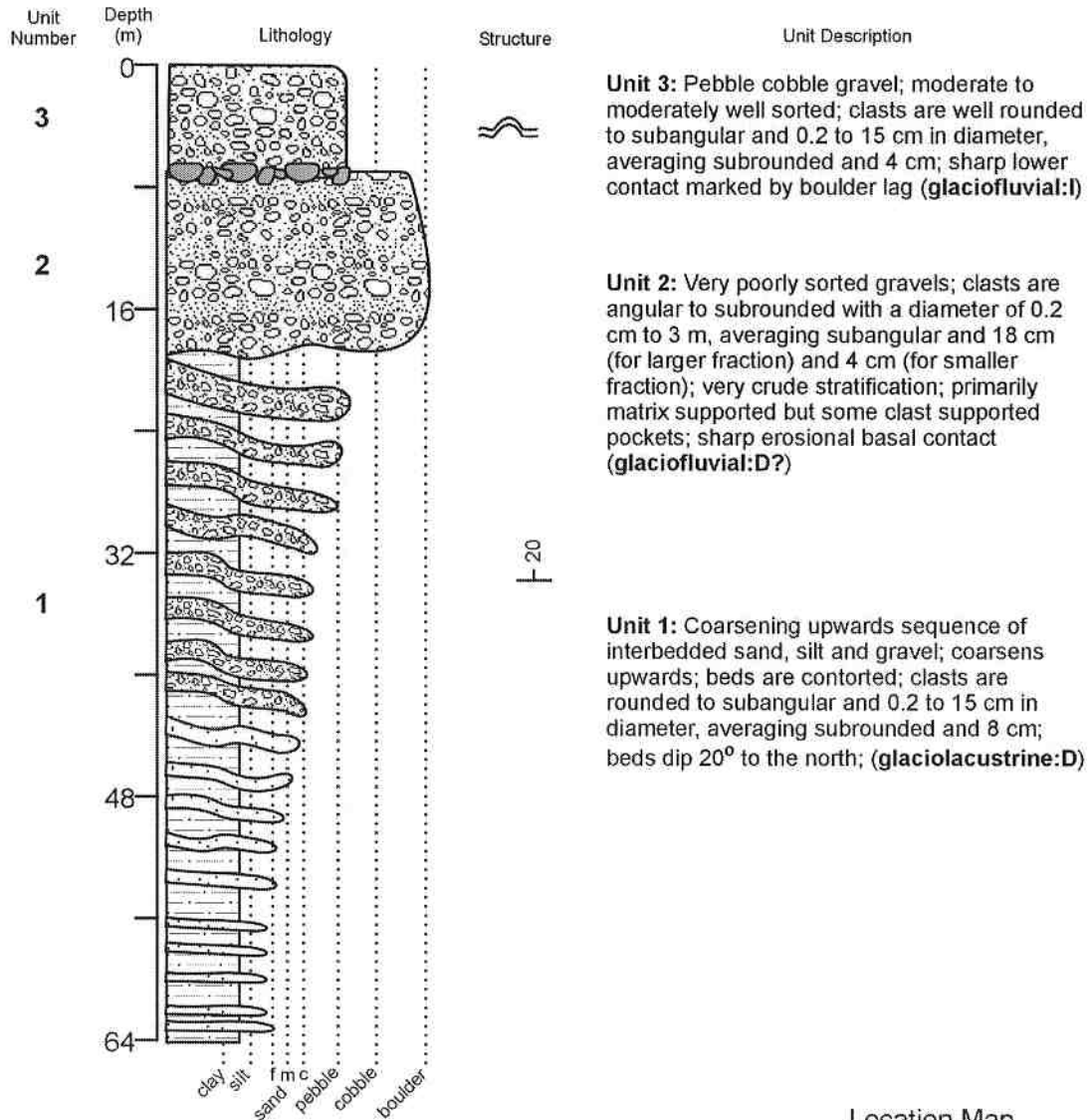


Description:

The landslide is located on the south side of the Quesnel River on an outer, erosive bend. During fieldwork in 2001, the south-western side of the headscarp of was located near a hairpin turn of a road. Upon returning to the site in 2002, the headscarp had moved another 20 metres past the road. The failure appears to be primarily a flow-type failure, though parts of the forest floor have remained intact and have translated or rotated to a lower position. The surface of rupture is likely concave, levelling out on a 'bench' approximately 60 m above the river. Material involved in the flow was then ejected over the side of the bench forming a toe at the river's level. In addition, immediately to the east of the landslide is a well defined debris torrent. Still further to the east are more, actively eroding slopes that has an older, dormant landslide above them. Vegetation on the active slide is limited to pre-slide trees and ground-cover, most being jack-strawed or overturned. No standing water was found though the upper units that have failed and make up the flow (2 and 3) are saturated.

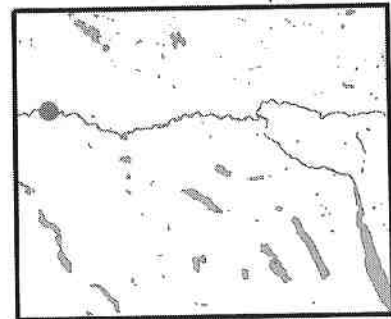
Section Number: AJB01-L5P2
 Easting: 571353 m
 Northing: 5835835 m

Base Elevation: 630 m
 Orientation: North-south



Site Description: Stratigraphy of terrace face to 64 m above the river, located approximately 26 km downstream of Quesnel Forks on the south side of Quesnel River. It is accessible by land via the 2600 Road logging road. This section is immediately adjacent section L5P1 to the northwest.

Location Map



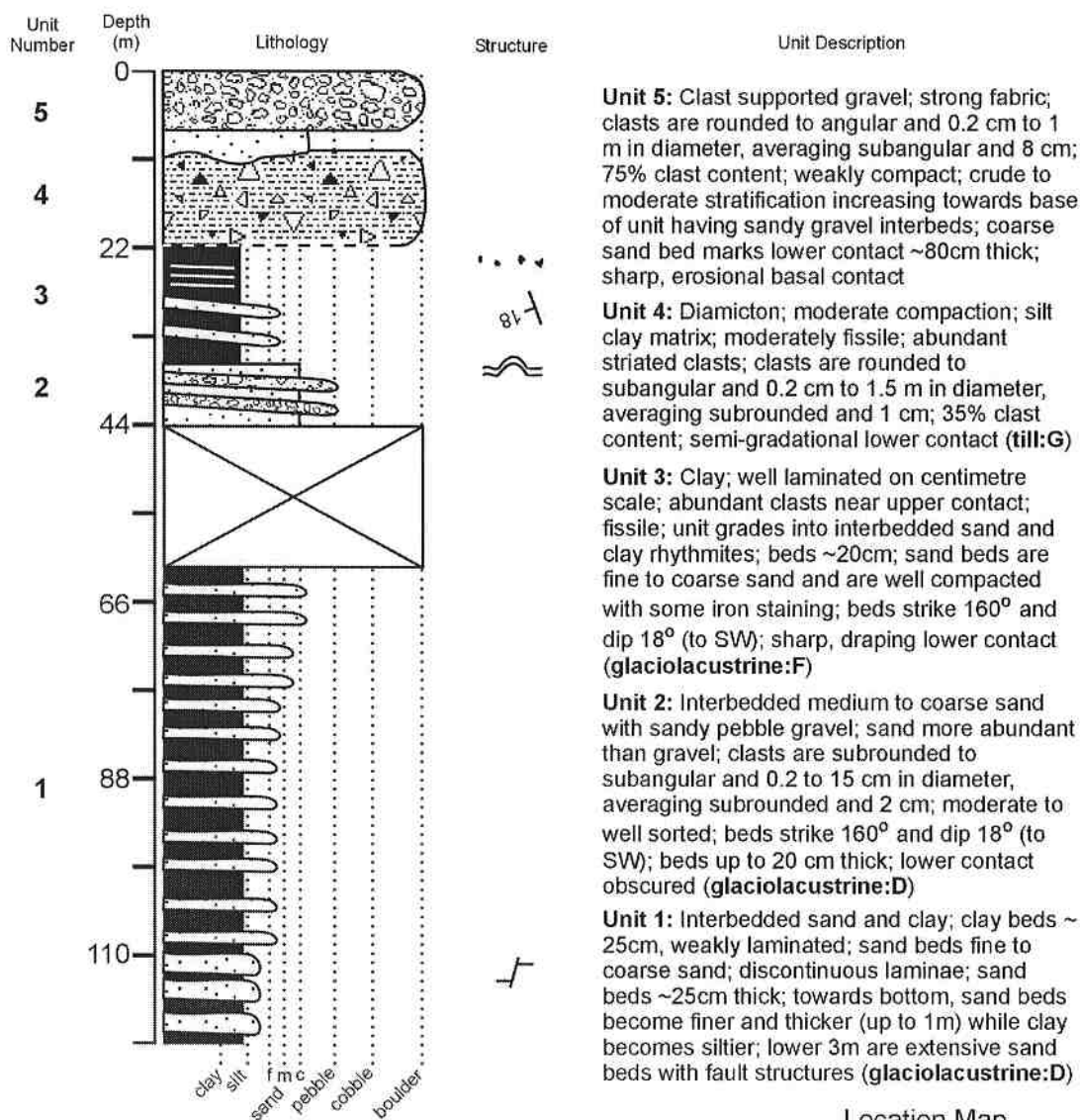
Section Number: AJB01-L6

Easting: 571945 m

Northing: 5835520 m

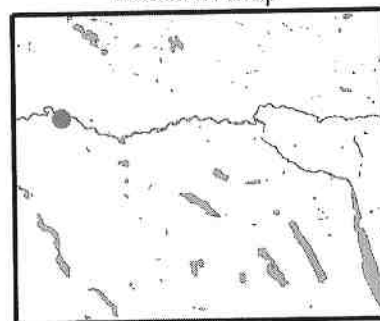
Base Elevation: 635 m

Orientation: Northwest-southeast



Site Description: Stratigraphy along scarp and gully to 121 m above the river level, located approximately 25 km downstream of Quesnel Forks on the south side of the Quesnel River. It is accessible by land via the 2600 Road logging road and is adjacent to L5P1, lying to the east.

Location Map



Approximate Date of Occurrence: pre-1998 (inactive)

Type of Failure: Reactivated, retrogressive, very wet earth flow

Elevation of Crown: 740 m asl

Elevation of Toe of Rupture Surface: 660 m asl

Elevation of Tip of Landslide: 635 m asl

Dimensions

Length of Rupture Surface (L_r): variable (120 m)

Width of Rupture Surface (W_r): 470 (165) m

Depth of Rupture Surface (D_r): variable (10 m)

Length of Displaced Mass (L_d): variable (280 m)

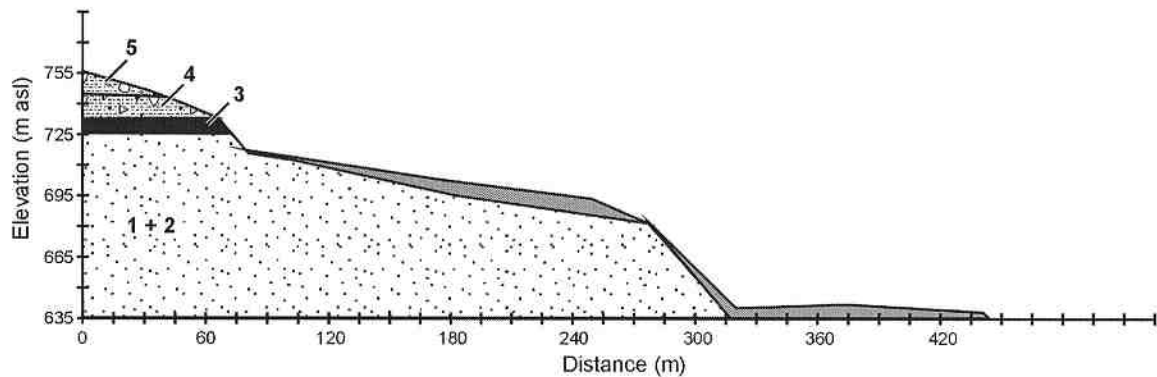
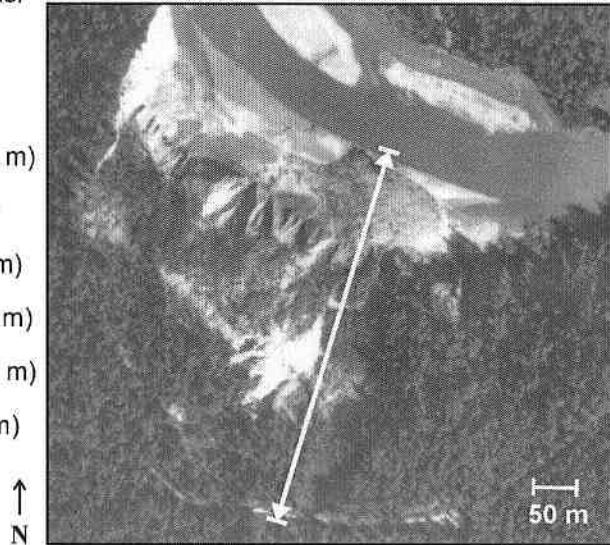
Width of Displaced Mass (W_d): variable (170 m)

Depth of Displaced Mass (D_d): variable (10 m)

Total Length (L): 430 (360) m

Surface Area: $32 \text{ m}^2 \times 10^3$

Volume ($\rho(W_d/2)^2 D_d/3$): variable ($75.7 \text{ m}^3 \times 10^3$)



Description:

The landslide is located on the south side of the Quesnel River on an outer, erosive bend. This slide has failed in a very similar manner to landslide L5. The upper fine-grained units (3 and 4) have flowed onto an upper 'bench' and then continued to flow over the edge. The bench has a fairly low angle and is almost fan like. The material making up the flow's surface is relatively dry though appears to become saturated during times of rainfall. This slide does not appear to be as active as landslide L5, with alders up to 3 metres growing on parts of the flow. The western half of the landslide is composed of an older failure that failed by the same method. Vegetation here is more well established.

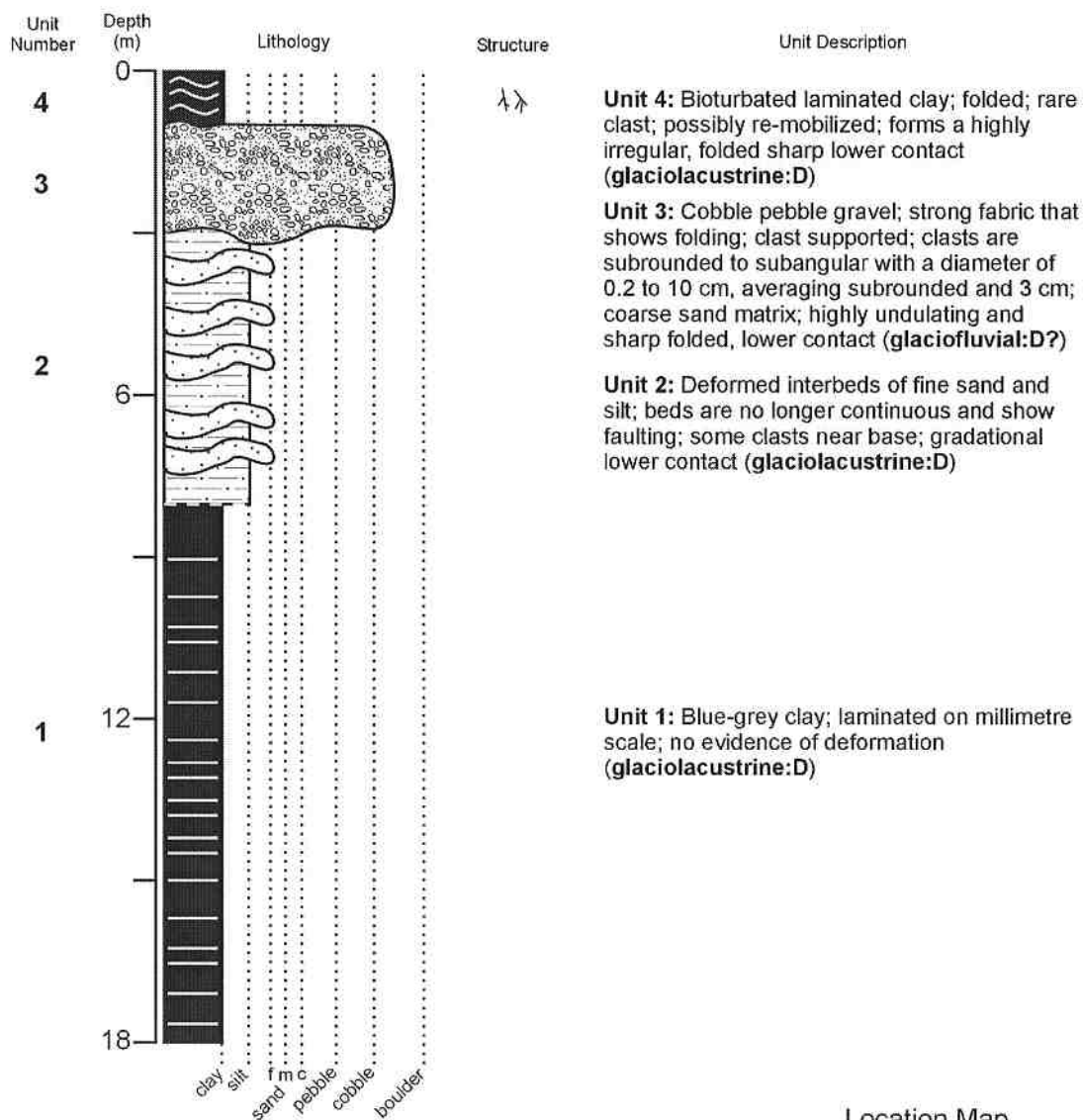
Section Number: AJB01-L7

Easting: 579912 m

Northing: 5834299 m

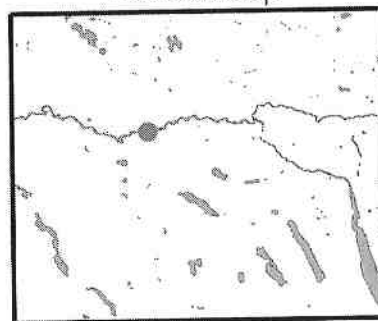
Base Elevation: 645 m

Orientation: East-west



Site Description: Stratigraphy taken at side scarp of landslide to approximately 18 m above the river. The site is 12 km downstream of Quesnel Forks on the south side of the Quesnel River near Moorehead Creek.

Location Map



Approximate Date of Occurrence: May 7, 1976, 1996 - 1998 (active)

Type of Failure: Reactivated, diminishing, complex, earth slide-earth topple

Elevation of Crown: 745(665) m asl

Elevation of Toe of Rupture Surface: 645 m asl

Elevation of Tip of Landslide: 645 m asl

Dimensions

Length of Rupture Surface (L_r): 760 (60) m

Width of Rupture Surface (W_r): 470 (275) m

Depth of Rupture Surface (D_r): ? (10) m

Length of Displaced Mass (L_d): 925(60) m

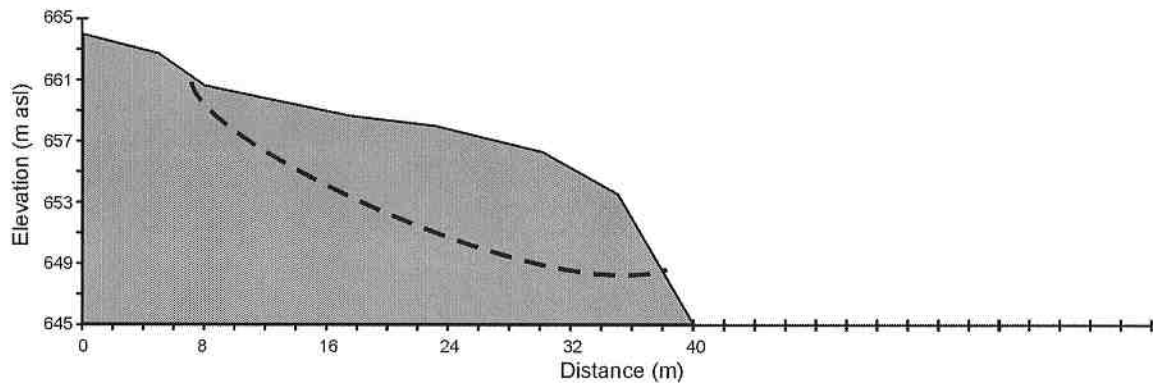
Width of Displaced Mass (W_d): 570 (275) m

Depth of Displaced Mass (D_d): ? (10) m

Total Length (L): 975 (60) m

Surface Area: 357 (16) $m^2 \times 10^3$

Volume ($pL_dD_dW_d/6$): > 1000 (58) $m^3 \times 10^3$



Description:

The landslide is located on the south side of the Quesnel River on an outer, erosive bend. At this location, a large landslide occurred in the spring of 1976 that blocked the river for several hours. Though the majority of the landslide appears to be stabilized, the toe continues to erode. The most recent activity is the reactivation of the toe where slumping and toppling of material from the earlier slide occurs.

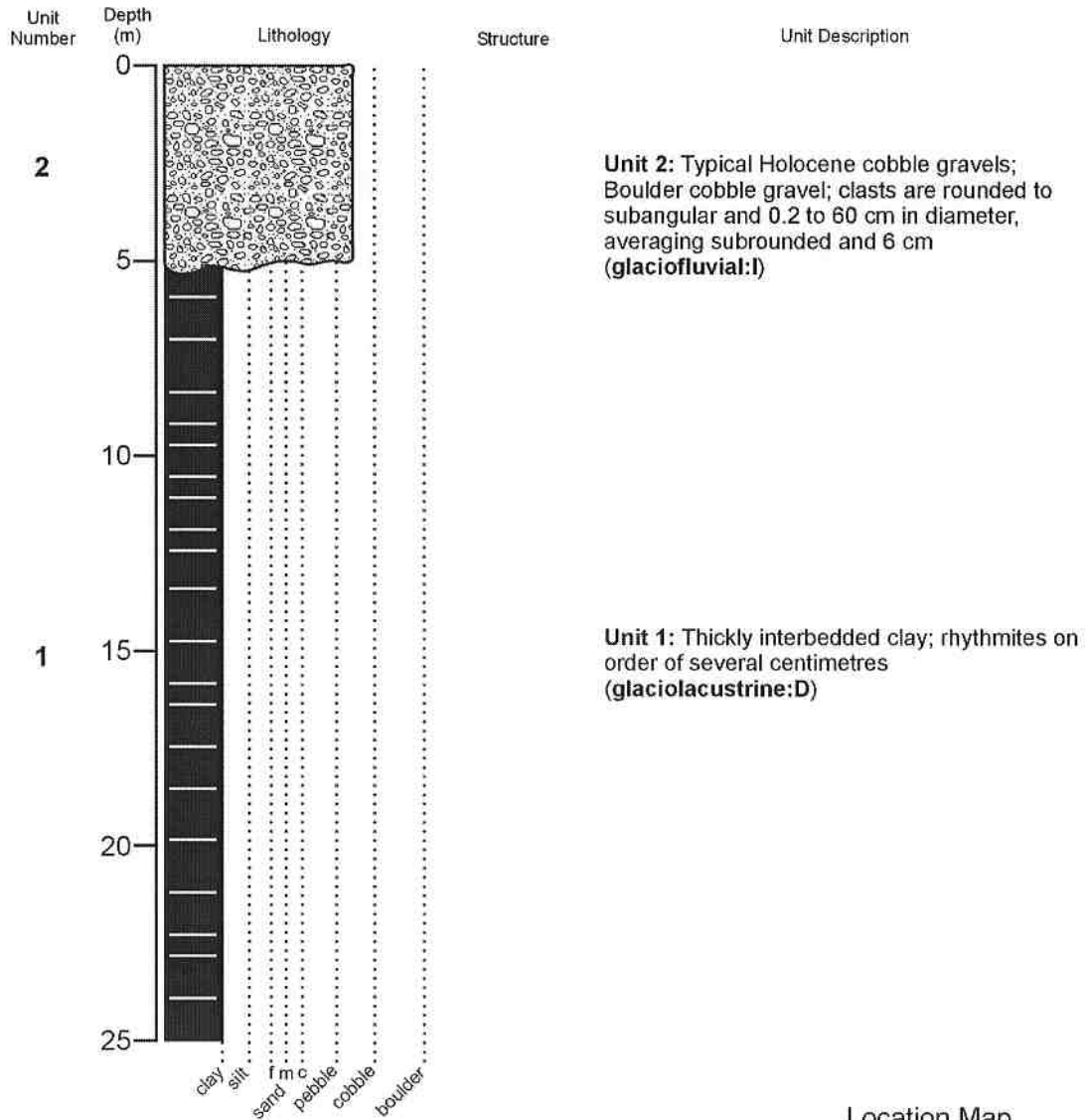
Section Number: AJB01-L8

Easting: 578375 m

Northing: 5834084 m

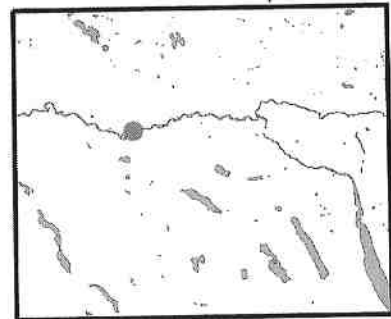
Base Elevation: 640 m

Orientation: Northeast-southwest



Site Description: A 25 m, near vertical face located approximately 13.5 km downstream of Quesnel Forks on the southside of the Quesnel River. Access by boat or from 2600 Road.

Location Map



Approximate Date of Occurrence: 1978 - 1986 (active)

Type of Failure: Active, complex, earth slide-earthtopple

Elevation of Crown: 665 m asl

Elevation of Toe of Rupture Surface: 640 m asl

Elevation of Tip of Landslide: 640 m asl

Dimensions

Length of Rupture Surface (L_r): 87 m

Width of Rupture Surface (W_r): 190 m

Depth of Rupture Surface (D_r): 15 m

Length of Displaced Mass (L_d): 85 m

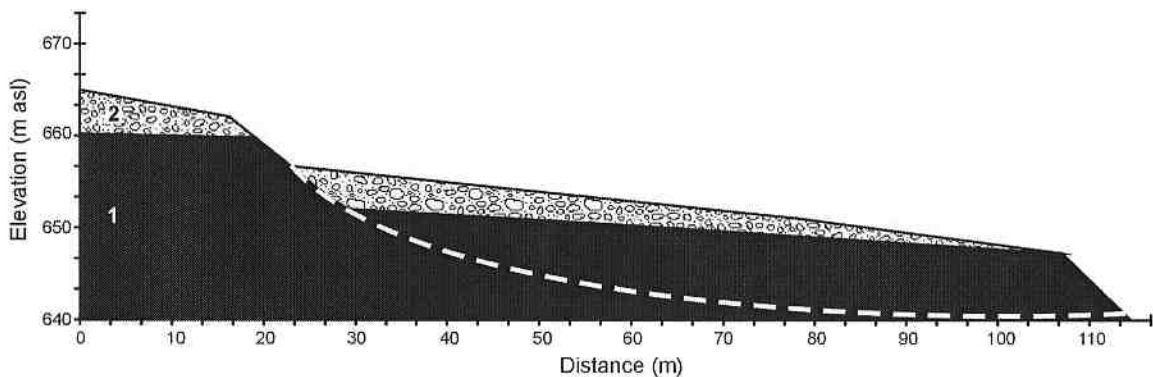
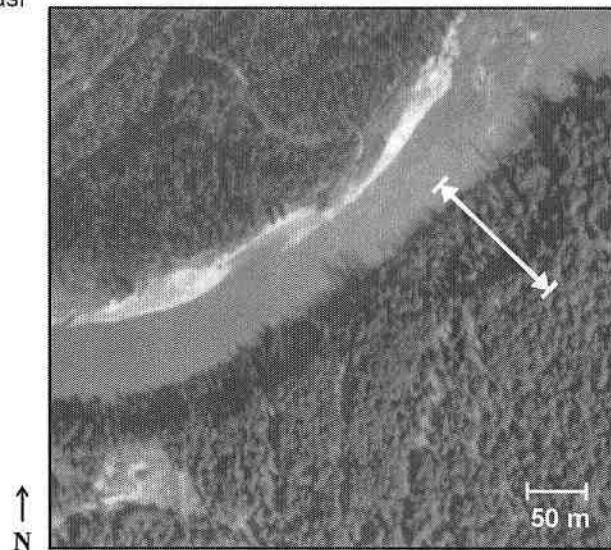
Width of Displaced Mass (W_d): 190 m

Depth of Displaced Mass (D_d): 5 m

Total Length (L): 87 m

Surface Area: $11 \text{ m}^2 \times 10^3$

Volume ($\rho L_d D_d W_d / 6$): $42.3 \text{ m}^3 \times 10^3$

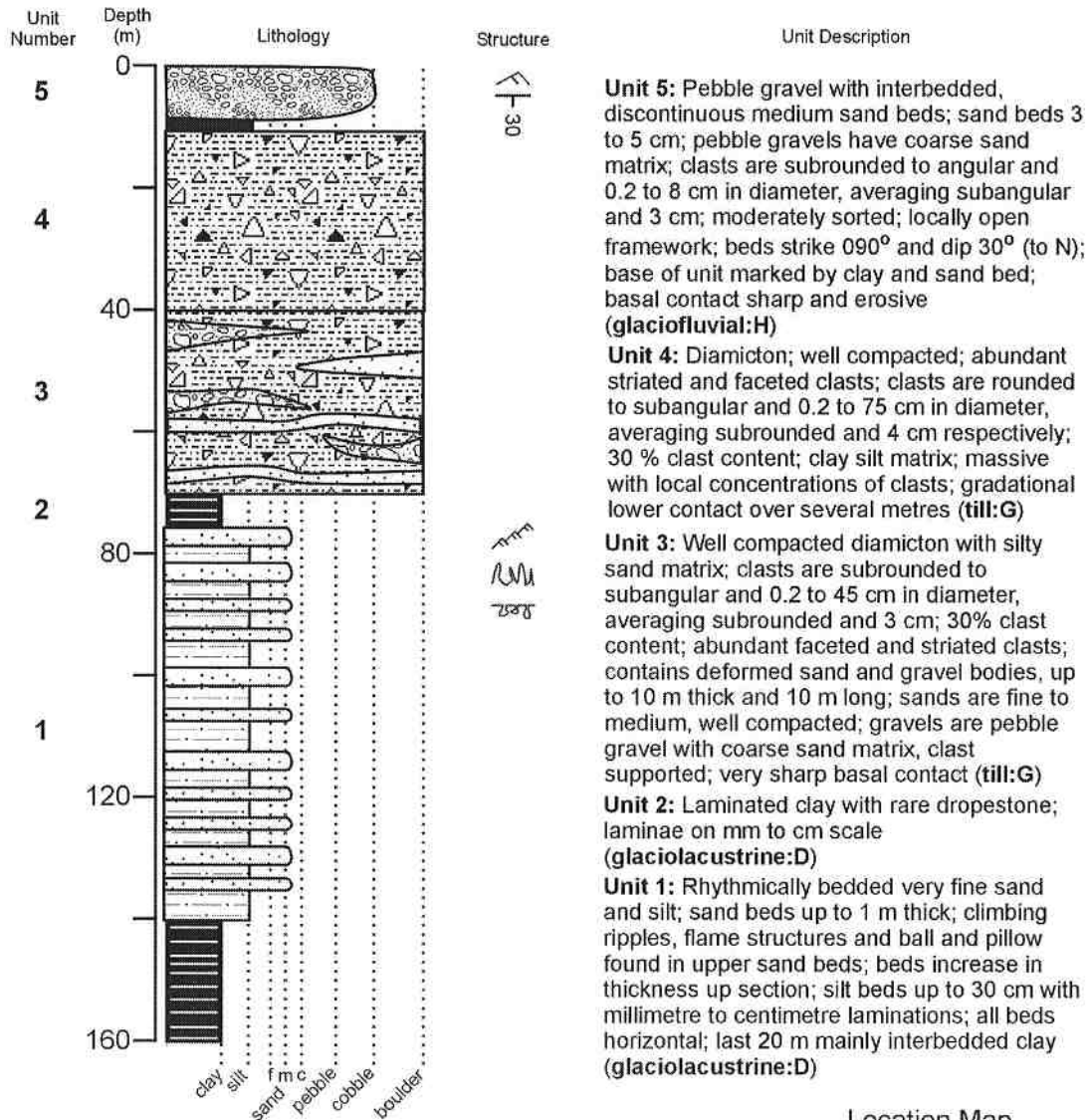


Description:

The landslide is located on the south side of the Quesnel River on a relatively straight reach, immediately upstream of a bend in the river. Directly upstream of the landslide, the river narrows, forcing the flow against the toe of the landslide. The failure appears to be primarily rotational with one, heavily forested block dropping several metres. The rotational component appears to be dormant for the moment. No toe is evident as material is removed by the flow of the river. Unit 1 is failing by topple where it is being eroded by the river.

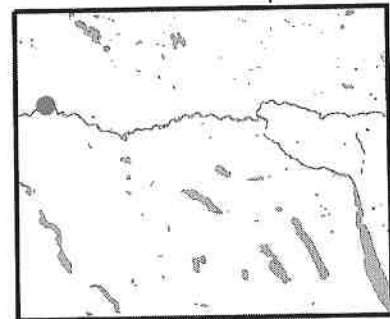
Section Number: AJB01-L9
 Easting: 570437 m
 Northing: 5836382 m

Base Elevation: 620 m
 Orientation: Northeast-southwest



Site Description: Stratigraphy to a height of approximately 160 m above the river obtained along scarps of landslide located approximately 28 km downstream of Quesnel Forks on the north side of the Quesnel River. Access is by boat only.

Location Map



Approximate Date of Occurrence: <1957, 1992 - 1996 (inactive)

Type of Failure: Dormant, retrogressive, wet, earth slide-debris flow

Elevation of Crown: 800 m asl

Elevation of Toe of Rupture Surface: 705 m asl

Elevation of Tip of Landslide: 620 m asl

Dimensions

Length of Rupture Surface (L_r): 388 m

Width of Rupture Surface (W_r): 243 m

Depth of Rupture Surface (D_r): 20 m

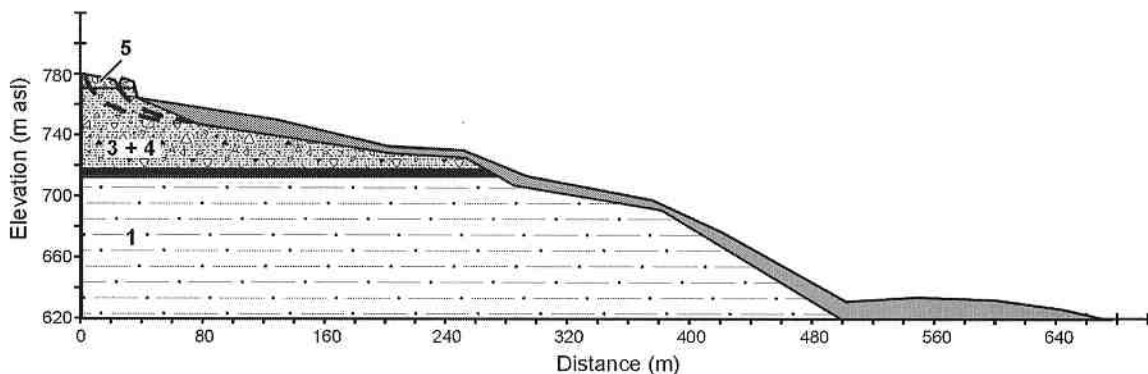
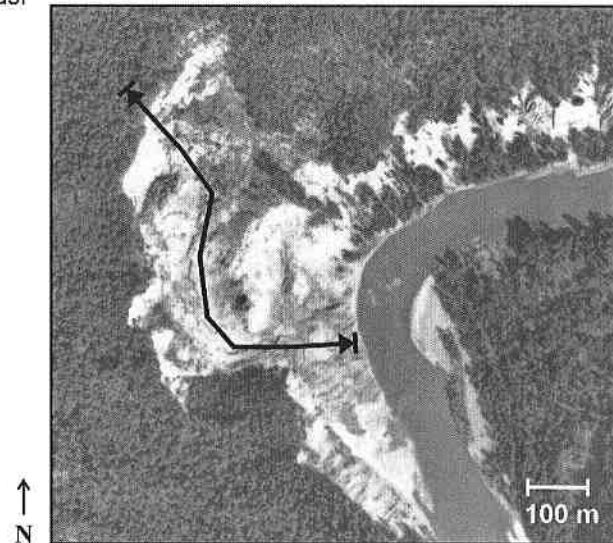
Length of Displaced Mass (L_d): 705 m

Width of Displaced Mass (W_d): 225 m

Depth of Displaced Mass (D_d): variable

Total Length (L): 716 m

Surface Area: $164 \text{ m}^2 \times 10^3$



Description:

The landslide is located on the north side of the Quesnel River on an outer, erosive bend. Failure near the crown is by translation or rotation. Discrete blocks consisting of unit 4 and 5 separate from the head scarp while remaining nearly upright. Beyond this, and making up the majority of the landslide, flow-type processes dominate with the diamicton and clay rich units (2, 3 and 4) flowing as a liquid from the crown all the way to the river. Where the material has flowed around stable bluffs, large levees are created (approximately 1.5 m high). Vegetation on the flow is relatively young and composes of ground cover with small alders. No surface water is evident though some local areas have saturated flow material. It is possible that this slide blocked the river and at the least severely restricted the flow of water.

Induced Plasma Mass Spectrometry (ICP-MS) Analytical Results for Diamicton Samples

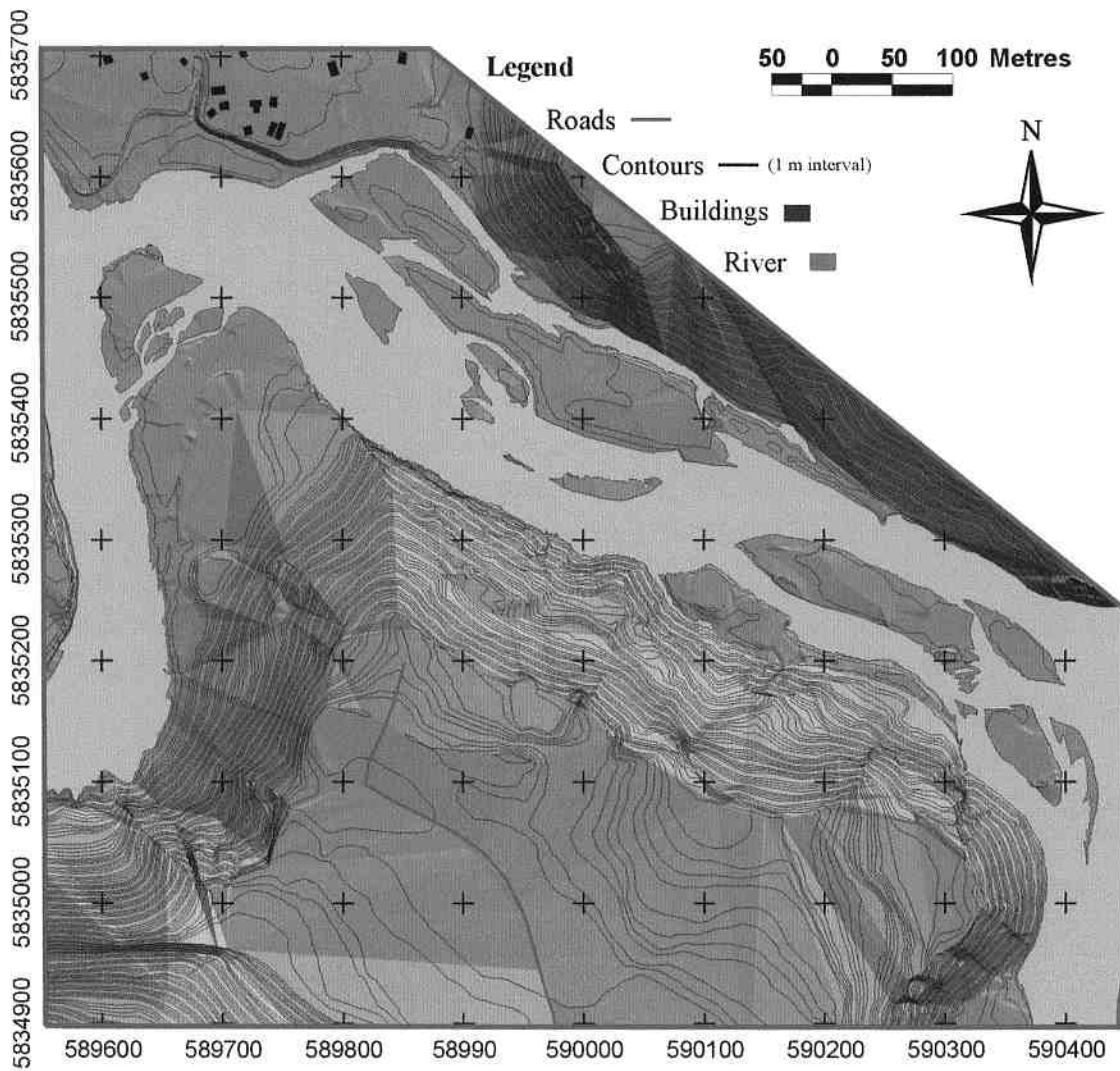
SAMPLES	Interpretation	ppb		ppm		%		ppm		%		ppm		%		ppm		%		ppm		%		ppm		%		ppm		%								
		Ag	As	Ba	Ba	Ca	Ca	Cd	Co	Co	Cu	Cu	Fe	Fe	Hg	Hg	La	La	Mg	Mg	Mn	Mn	Mo	Mo	Ni	Ni	Pb	Pb	S	S	Sb	Sb	Se	Se	Sr	Sr	V	V
AJB L2P3-01	Fraser Till	85	10.4	103.2	1.1	0.3	18.0	63.6	3.1	80	21.5	0.9	540	1.4	41.9	12.6	0.0	0.7	<.1	66.9	67	72.9																
AJB S10P1-01	Fraser Till	97	12.1	40.9	0.2	0.1	11.2	65.4	2.8	8	22.9	0.7	247	1.3	37.0	11.6	0.0	0.6	0.3	11.2	34	84.8																
AJB S1P1-01	Fraser Till	74	10.4	35.1	0.2	0.2	9.9	42.9	2.5	14	20.0	0.6	212	1.2	34.2	9.5	<.01	0.5	0.1	10.1	31	76.5																
AJB L5P1-01	Fraser Till	107	9.6	116.2	2.0	0.2	13.6	98.1	2.8	59	14.4	0.7	650	0.9	27.4	14.4	0.0	0.7	0.1	92.1	79	71.1																
AJB L9P1-01	Fraser Till	117	8.1	142.0	1.8	0.3	14.7	65.5	2.8	59	13.8	0.8	823	0.9	40.2	11.0	<.01	0.6	<.1	86.6	72	69.9																
AJB 27 Bull	Penultimate Till	215	32.4	74.4	3.0	0.5	18.2	102.9	3.1	130	9.3	0.9	699	1.8	33.1	9.0	0.2	1.1	1.6	122.7	83	68.9																
Bull 2	Penultimate Till	136	25.5	69.5	2.7	0.3	15.8	73.6	2.8	101	8.4	0.8	590	1.4	27.3	6.4	0.2	0.9	0.9	111.5	80	64.5																
AJB QFT	Penultimate Till	342	51.5	260.4	3.9	1.1	21.2	147.5	3.5	291	7.9	1.2	922	2.7	39.4	11.1	0.5	2.5	2.6	135.1	90	122.8																
QFT2	Penultimate Till	305	52.5	261.7	3.9	1.1	22.4	119.3	3.5	263	7.7	1.3	947	2.9	38.1	10.6	0.5	2.1	3.7	136.5	91	120.3																

Appendix C

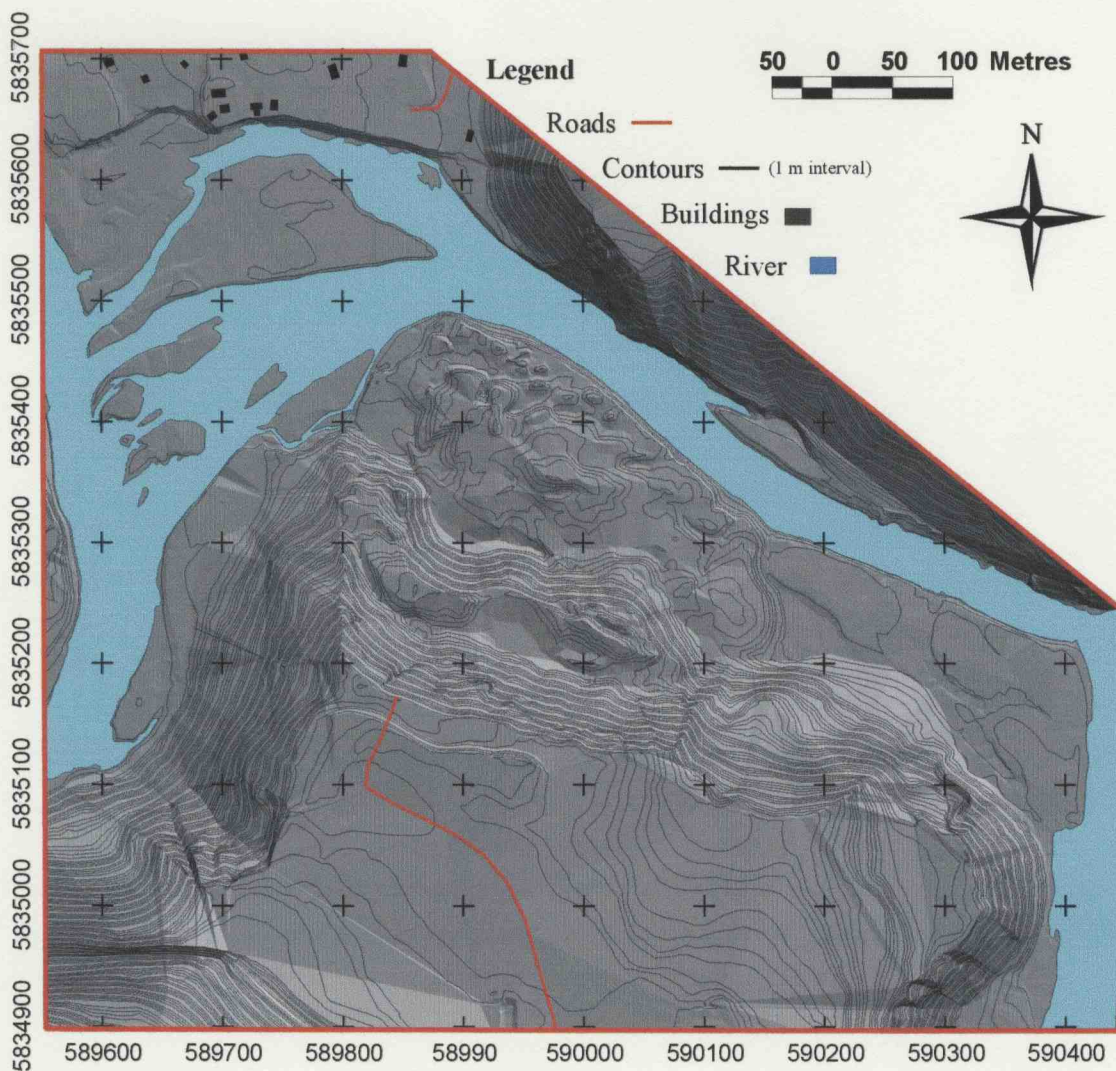
Digital Terrain Models

This appendix contains two topographic maps of the Quesnel Forks Landslide and surrounding area. Topographic data for both maps were supplied by McElhanney Consulting Services Ltd using pre-existing and newly acquired airphotos. The first map depicts the topography at Quesnel Forks prior to the landslide, in 1986. Photography was flown at a scale of 1:15 000 using colour and 305 mm film and camera (roll BCC478, frames # 215 and 216). The second map was constructed from airphotos taken in 2002. Photography was flown at a scale of 1:10 000 using black and white and 152 mm film and camera (roll IAS(02) 54490, frames 9475 and 9476).

1986 Topographic Map



2002 Topographic Map

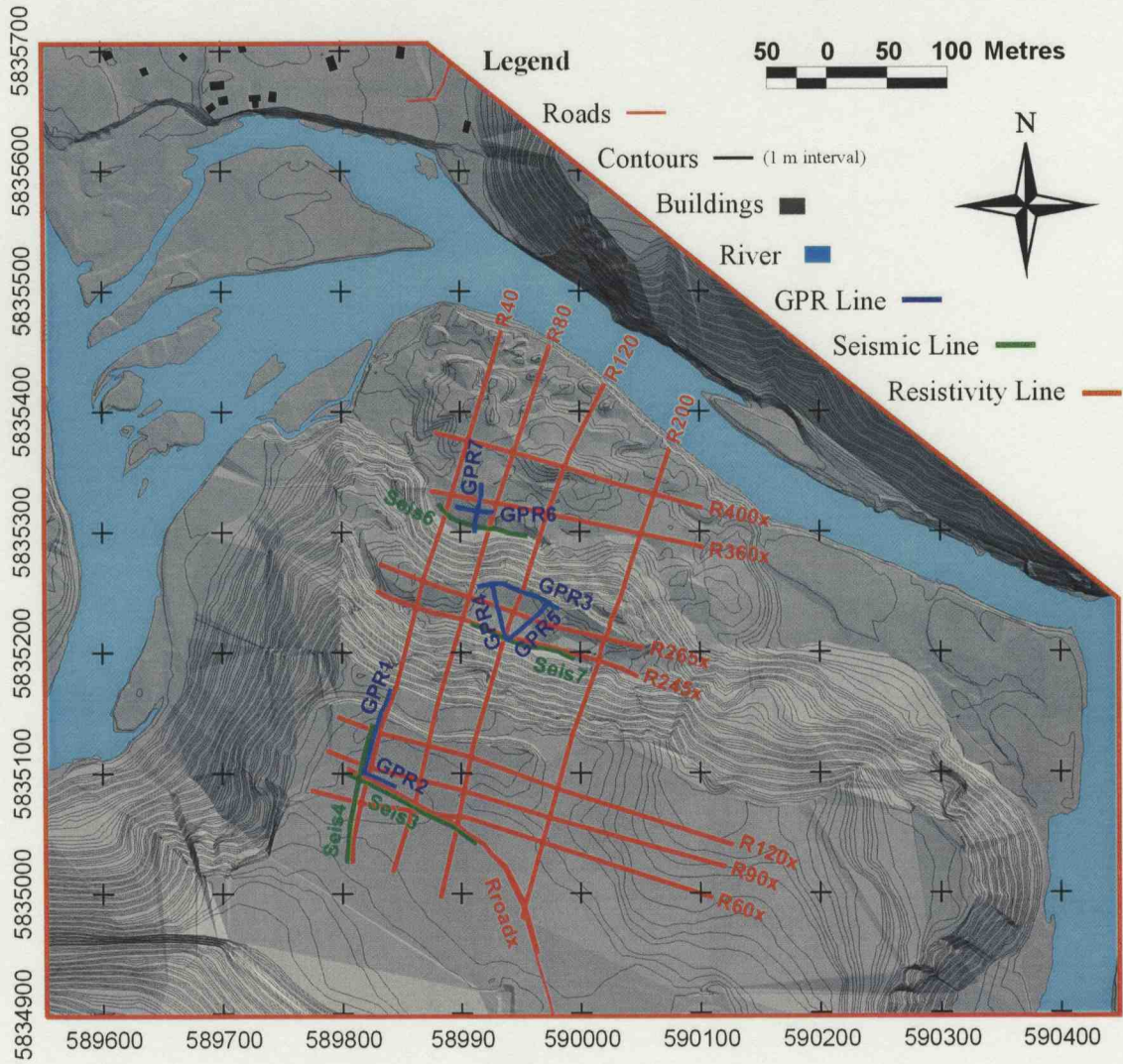


Appendix D

Geophysical Data

This appendix is divided into three sections according to the geophysical methods carried out on the Quesnel Forks Landslide: 1) ground penetrating radar, 2) dc resistivity and 3) seismic reflection and refraction. All survey lines are plotted on a common base map for ease of correlation. Each section begins with a brief description of the geophysical instrumentation used and the basic geometry and characteristics of the survey.

Geophysical Survey Lines



Appendix D (Section 1)

Ground Penetrating Radar Profiles

The following geophysical profiles were created using a PulseEkko IV ground penetrating radar system from Sensors and Software. The system was configured with a 50 Hz antenna and receiver, powered by a 12 V motorcycle battery, and controlled using a laptop personal computer. All surveys were run in reflection mode. Seven survey lines were conducted: two on the undisturbed terrace, three on the lower rotational block and two on the foot of the landslide. In total, approximately 340 m of data were collected. Each survey line used a receiver-antenna spacing of 2 m with a 0.5-metre spacing between sampling locations. Both the antenna and receiver were oriented perpendicular to the line. Profiles were obtained using the DOS-based module provided by Sensors and Software. Within this module, topographic corrections were applied. No other processing was conducted. For each survey line, a summary sheet containing the profile is provided, as well as a separate sheet containing the interpretation of reflective events.

The principles of ground penetrating radar (GPR) are similar to those of seismic reflection. A source of radio waves is emitted from the surface, into the ground and travels through the medium at a velocity described by:

$$v = c/(\sqrt{K})$$

where v is the velocity of the radar wave in the medium, c is the speed of light in a vacuum, and K is the dielectric constant (Davis and Annan 1989). When the wave intersects an inhomogeneity it is partially reflected, refracted and transmitted. The amplitude of the energy reflected is governed by the reflection coefficient, which is equal to:

$$R = (\sqrt{K_1} - \sqrt{K_2}) / (\sqrt{K_1} + \sqrt{K_2})$$

where R is the reflection coefficient and K_1 and K_2 are the dielectric constants for the two different mediums (Davis and Annan 1989). Reflected energy then returns to the surface where a receiver antenna records its arrival time. The reflected signals can then be interpreted and fit to geologic models.

The penetration of the signal within a medium is governed by the electrical properties of the material. The attenuation of the signal is defined by:

$$\alpha = 1.64\sigma/\sqrt{K}$$

where α is the attenuation and σ is the conductivity in ms/m and K is the dielectric constant in db/m.

Common midpoint profiles were conducted for velocity analysis. Velocities of approximately 0.105 m/ns were obtained and agree with assumed velocities used for calculating depth scales for the profile axis.

Ground Penetrating Radar Line: GPR1

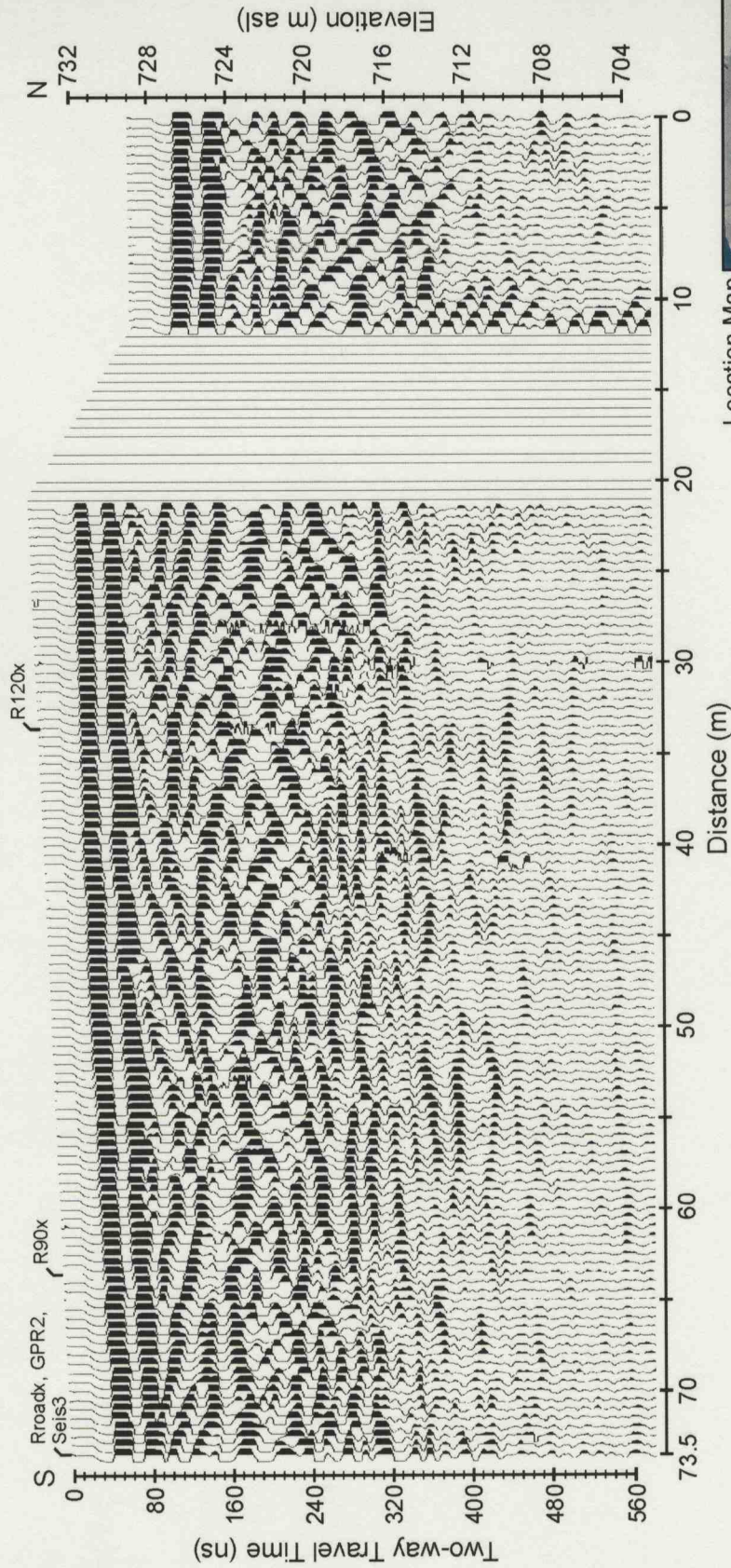
Total Line Length: 73.5 m

Orientation: NNE - SSW

Number of Traces: 148

Trace Interval: 0.5 m

Assumed Velocity: 0.100 m/ns



Line Description: The line begins on the undisturbed terrace and ends at the outer edge of the upper, rotational block. It runs approximately perpendicular to the head scarp. The entire length of the line was conducted on an old road base consisting of compacted overburden. The line crosses survey lines Roadx, GPR2, Seis3, R90x and R120x. It is also coincident with line R40 and Seis4.

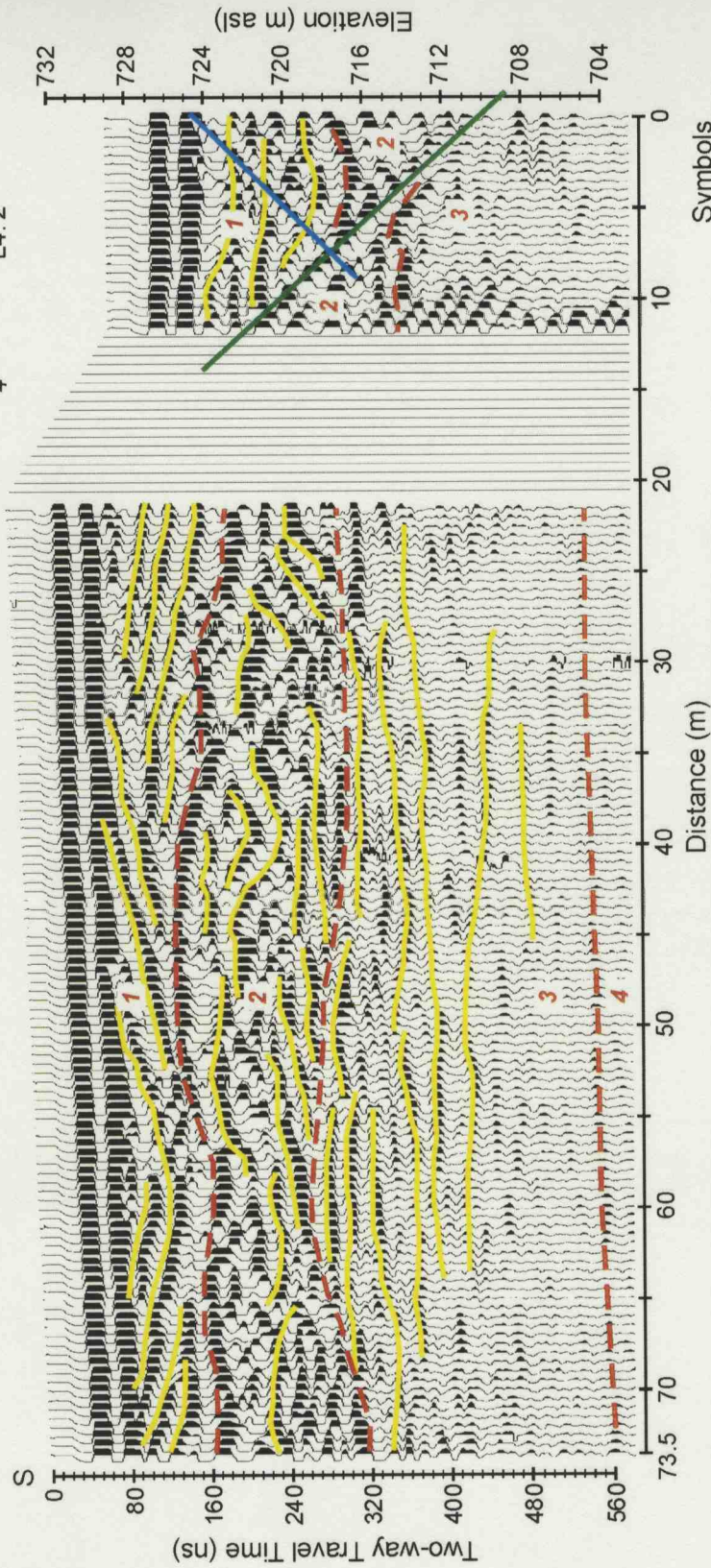
Location Map



Ground Penetrating Radar Line: GPR1

Interpretation
 GPR Facies Stratigraphic Unit
 (Section: Unit)

- 1 L4: 6
- 2 L4: 5
- 3 L4: 3
- 4 L4: 2



- Comments:
- The steeply dipping event at the outer edge upper rotational block (blue line) is an artifact related to a surface wave reflecting of the edge of the block.
 - Velocity analysis of the blue line yields a velocity of 0.105 m/ns.
 - The interpreted failure plane (green line) of the upper rotational block is approximately 40°.

Symbols

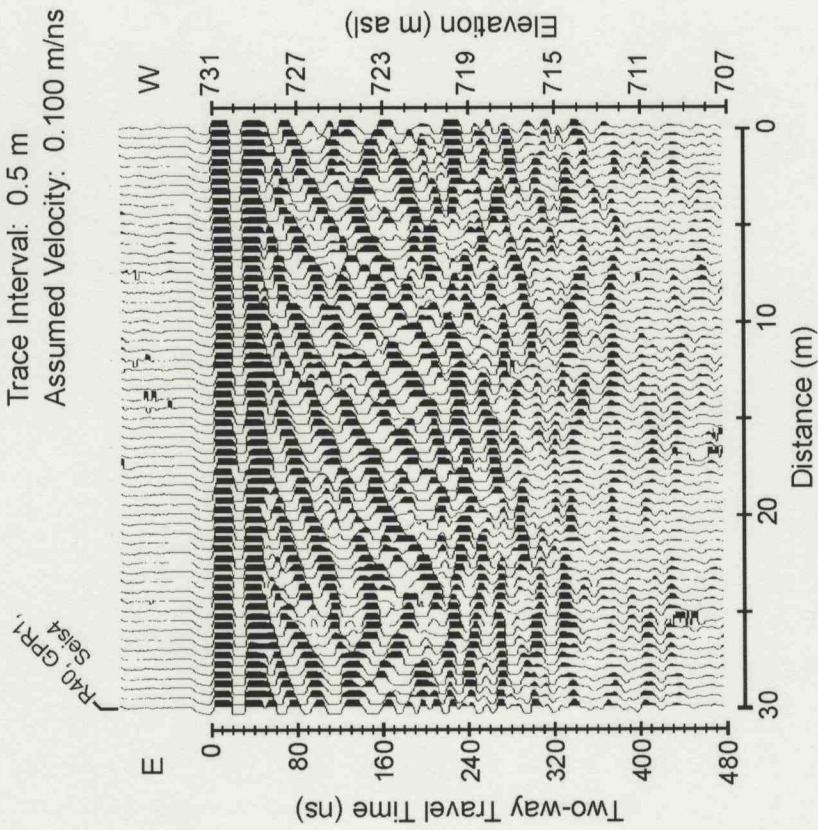
- 1 GPR Facies
- Facies Boundary
- Internal Structure
- Artifact
- Rupture Surface

Ground Penetrating Radar Line: GPR2

Total Line Length: 30 m

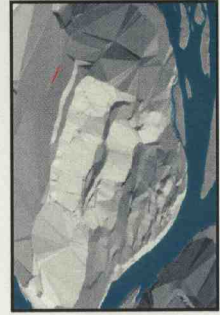
Orientation: WNW - ESE

Number of Traces: 61
Trace Interval: 0.5 m
Assumed Velocity: 0.100 m/ns



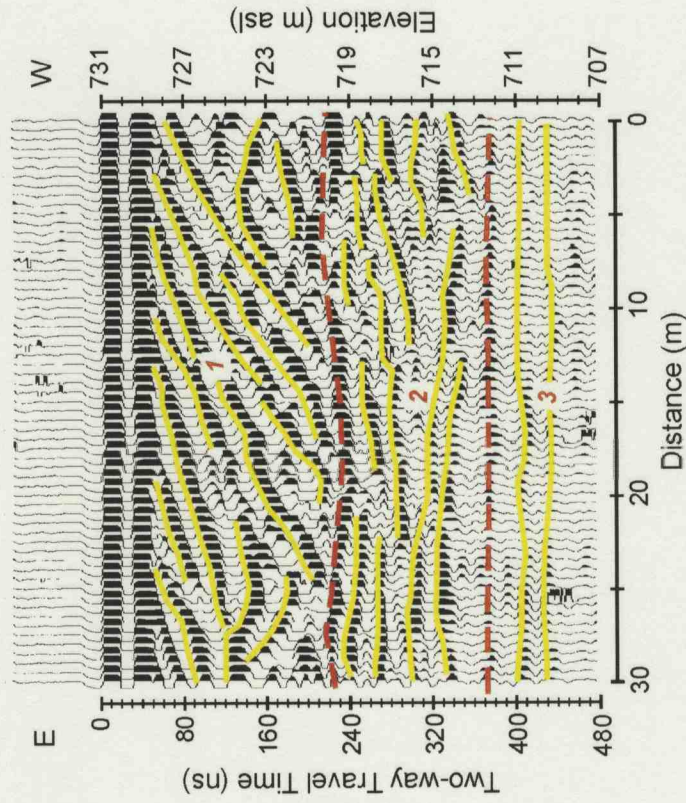
Line Description: The entire line is on the upper terrace, following the access road and roughly parallels the headscarp. Surficial material along the line consists of compacted overburden that forms the road. The line crosses survey lines R40, GPR1 and Seis3 at the approximate locations specified above.

Location Map



Ground Penetrating Radar Line: GPR2

Interpretation	GPR Facies	Stratigraphic Unit (Section: Unit)
1	L4: 6	
2	L4: 5	
3	L4: 3	



Comments: Facies 2 and 3 are more continuous and horizontal than when imaged in a perpendicular direction (i.e. line GPR1)

Ground Penetrating Radar Line: GPR3

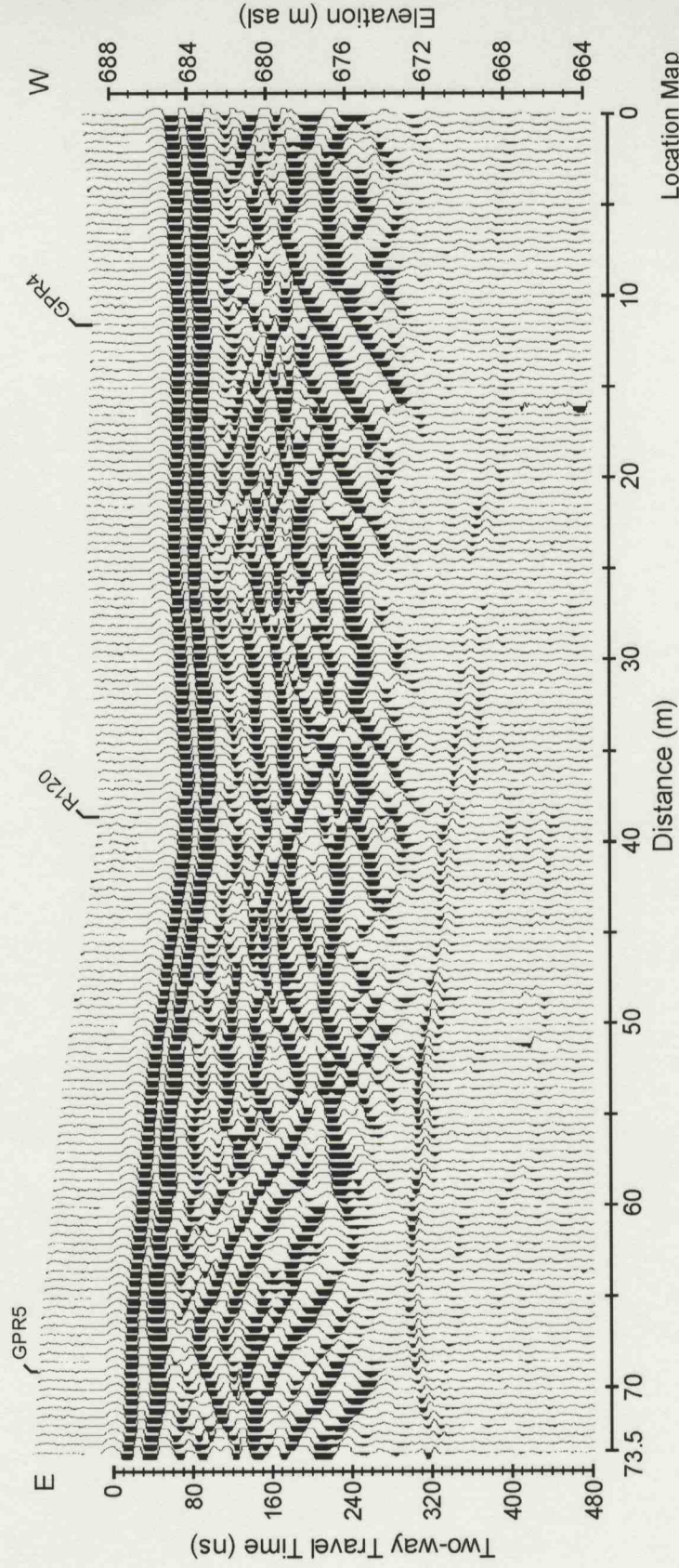
Total Line Length: 73.5 m

Orientation: WNW - ESE

Number of Traces: 148

Trace Interval: 0.5 m

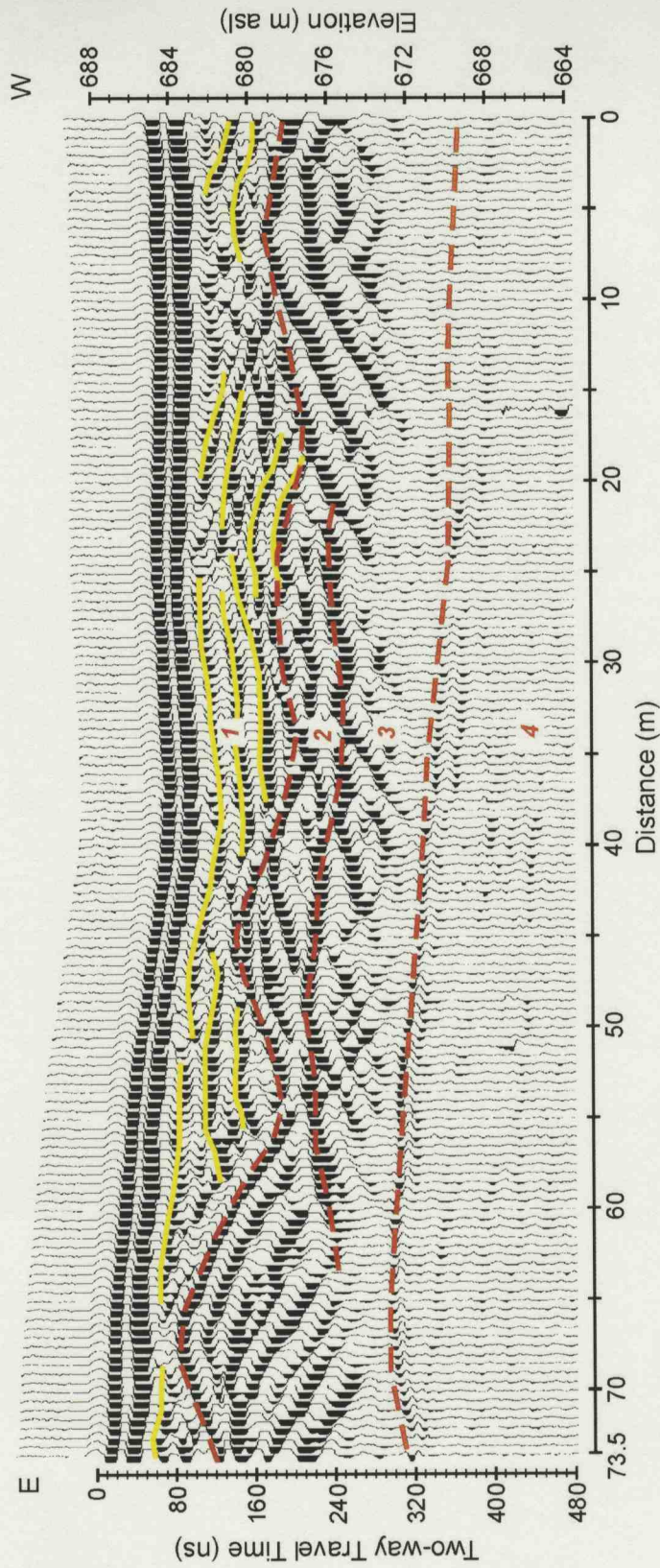
Assumed Velocity: 0.100 m/ns



Line Description: The line is located on the main rotational block and runs approximately parallel to the head scarp. It also parallels the edge of the rotational block, approximately 5 m from the outer edge. Surficial material along the line is dry gravel. The line crosses survey lines GPR5, R120 and GPR4 at the approximate locations specified above.

Ground Penetrating Radar Line: GPR3

Interpretation	
GPR Facies	Stratigraphic Unit (Section: Unit)
1	L4: 6
2	L4: 5
3	L4: 4
4	L4: 3



Symbols	
1	GPR Facies
- - -	Facies Boundary
—	Internal Structure

Comments:

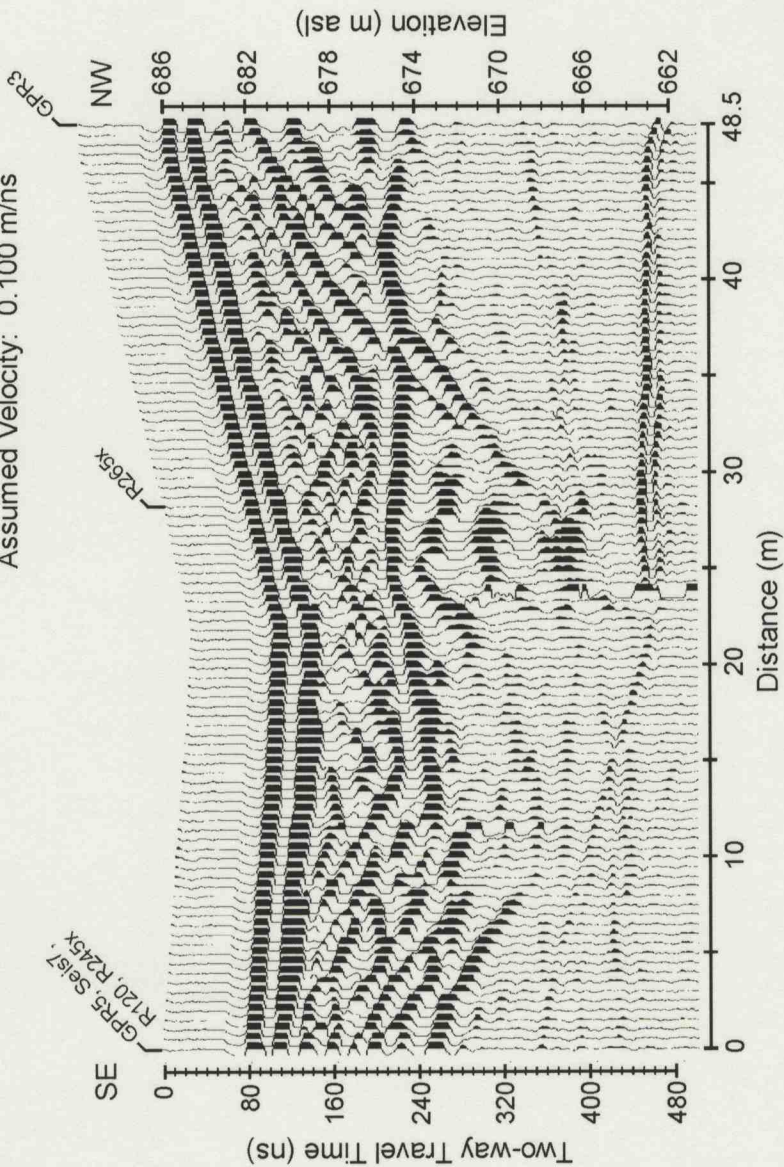
- The upper surface of facies 2 is possibly causing diffraction patterns that penetrate through the units boundaries
- If facies 2 is stratigraphic unit 5, it appears to have been deformed and reduced in thickness

Ground Penetrating Radar Line: GPR4

Total Line Length: 48.5 m

Orientation: NW - SE

Number of Traces: 98
Trace Interval: 0.5 m
Assumed Velocity: 0.100 m/ns



Location Map

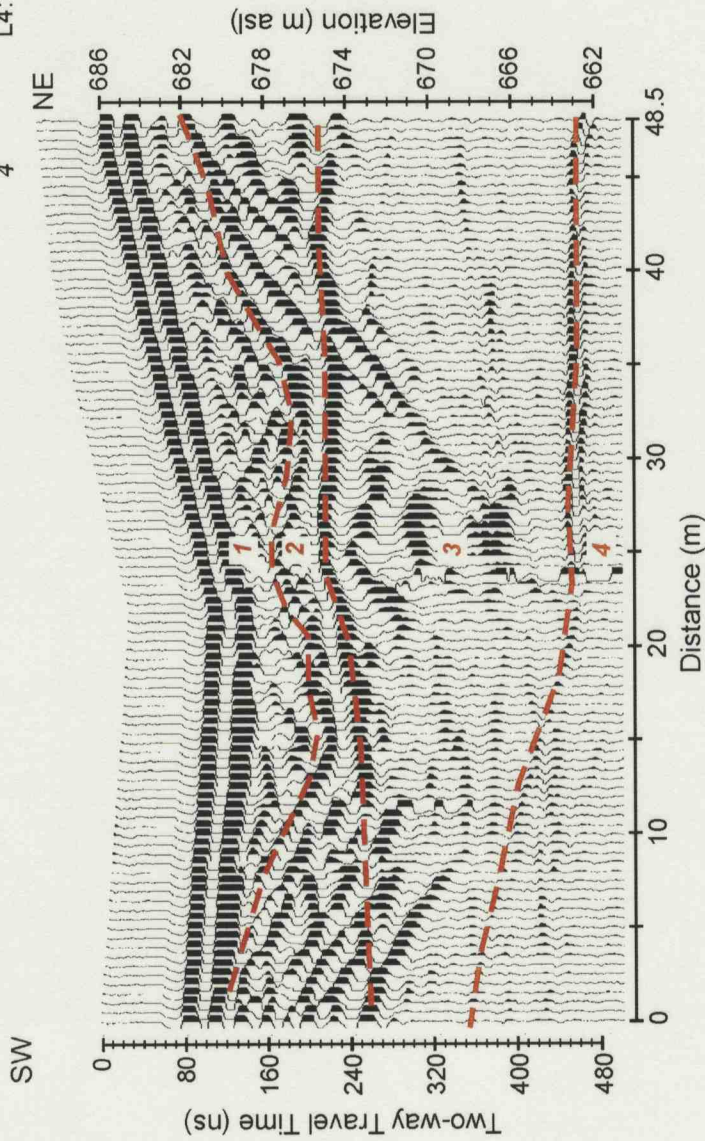


Line Description: The line is located on the main rotational block and runs approximately 35 degrees to the head scarp, from the inner edge to the outer edge of the rotational block. Surficial material along the line is damp sandy gravel for the first 23.5 m and dry gravel for the remaining 25 m. The line crosses survey lines GPR3, R265x, R245x, Seis7 and GPR5 at the approximate locations specified above.

Ground Penetrating Radar Line: GPR4

Interpretation
 GPR Facies Stratigraphic Unit
 (Section: Unit)

- 1 L4: 6
- 2 L4: 5
- 3 L4: 4
- 4 L4: 3



- Comments:
- The events centred about approximately 26 m are noise resulting from a generator used to power the computing system.
 - The upper surface of facies 2 is possibly causing diffraction patterns that penetrate through the units boundaries
 - If facies 2 is stratigraphic unit E, it appears to have been deformed and reduced in thickness

Symbols
 1 GPR Facies
 — Facies Boundary
 — Internal Structure

Ground Penetrating Radar Line: GPR5

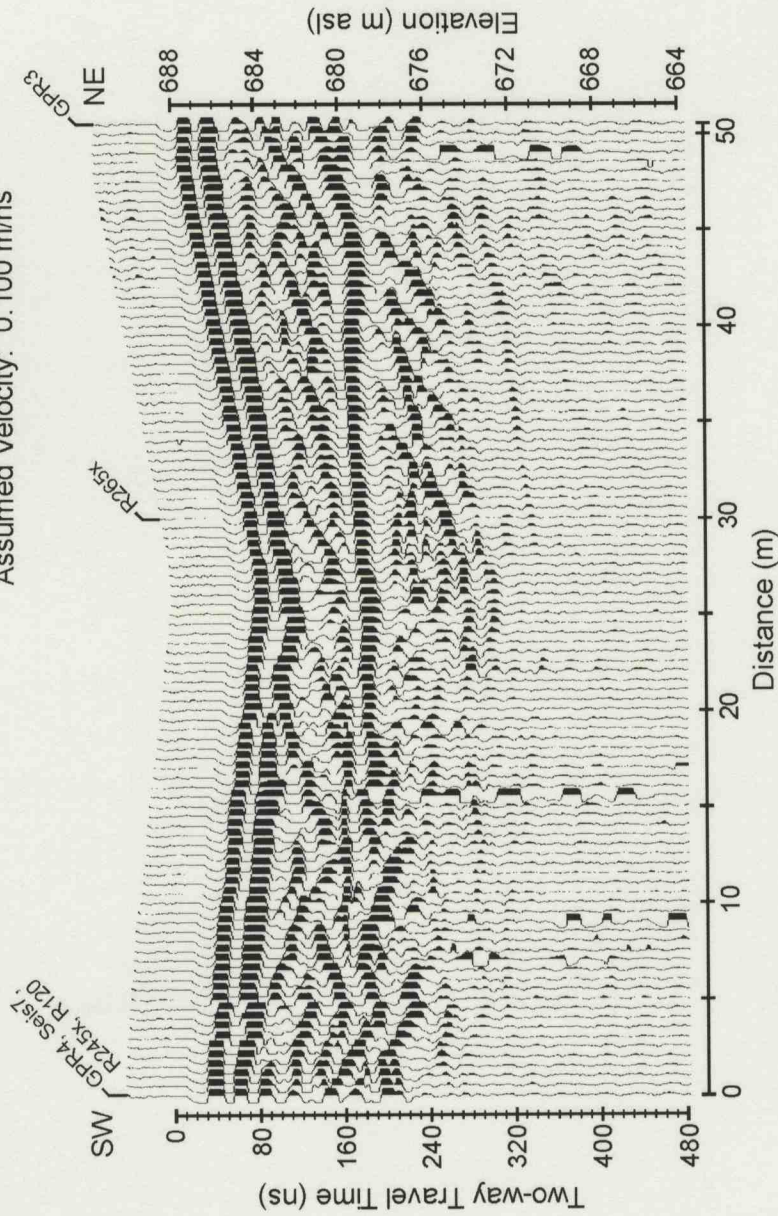
Total Line Length: 50.5 m

Orientation: NE - SW

Number of Traces: 102

Trace Interval: 0.5 m

Assumed Velocity: 0.100 m/ns

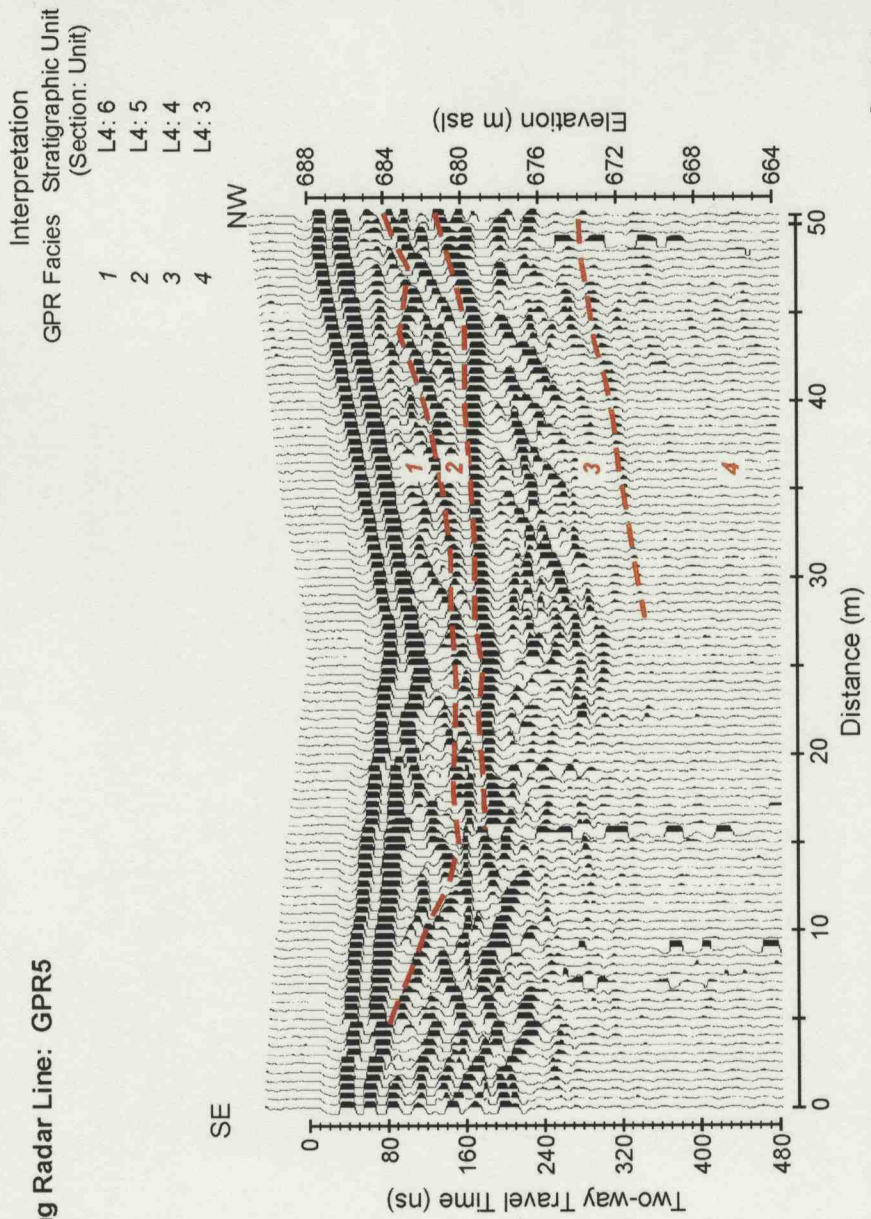


Location Map



Line Description: The line is located on the main rotational block and runs approximately 35 degrees to the head scarp, from the inner edge to the outer edge of the rotational block. Surficial material along the line is damp sandy gravel for the first 25.5 m and dry gravel for the remaining 25 m. The line crosses survey lines GPR3, R265x, R245x, Seis7 and GPR4 at the approximate locations specified above.

Ground Penetrating Radar Line: GPR5



- Comments:
- The events centred about approximately 26 m are noise resulting from a generator used to power the computing system
 - The upper surface of facies 2 is possibly causing diffraction patterns that penetrate through the units boundaries
 - If facies 2 is stratigraphic unit 5, it appears to have been deformed and reduced in thickness
 - Internal structure is mostly obscured by noise and artefacts related to facies 2

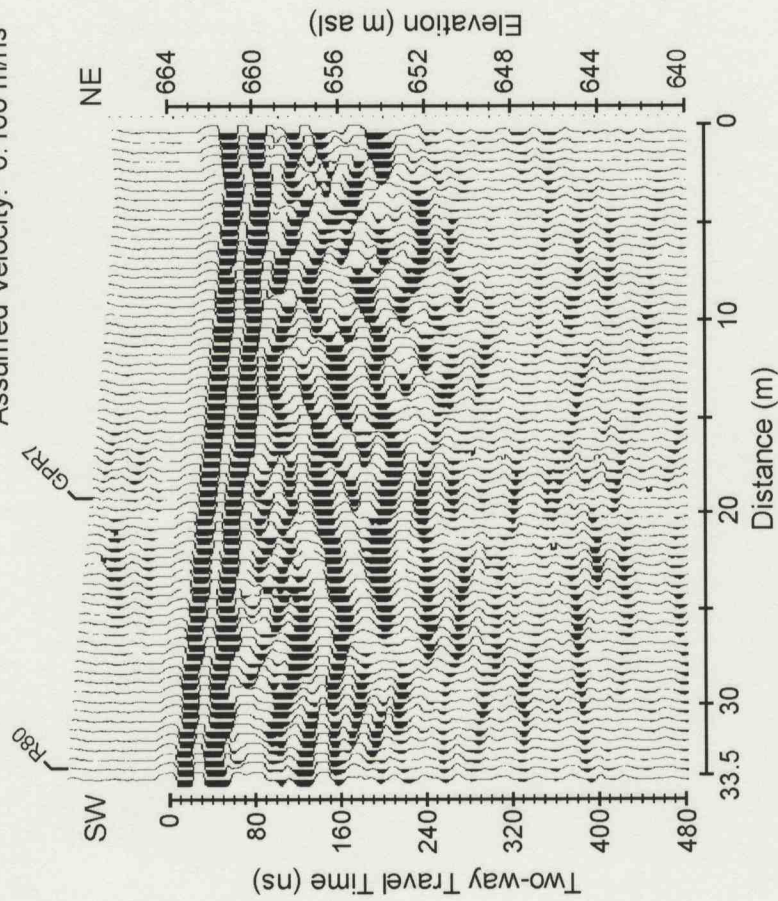
Symbols
 1 GPR Facies
 --- Facies Boundary

Ground Penetrating Radar Line: GPR6

Total Line Length: 33.5 m

Orientation: NE - SW

Number of Traces: 68
Trace Interval: 0.5 m
Assumed Velocity: 0.100 m/ns



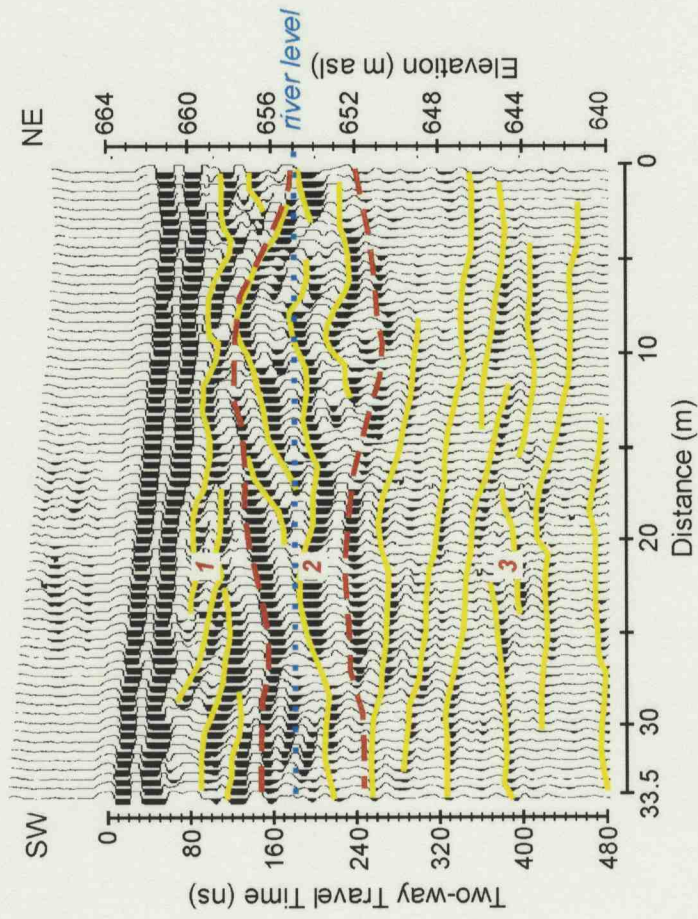
Line Description: The line is located on the toe of the landslide, near the edge of the main rotational block. It runs approximately parallel to the head scarp. Surficial material along the line is dry, unconsolidated sand and gravel. The line crosses survey lines GPR7 and R80 at the approximate locations specified above.

Location Map



Ground Penetrating Radar Line: GPR6

Interpretation	GPR Facies	Stratigraphic Unit (Section: Unit)
1	displaced material	
2	displaced material	
3	S11: 1 + 2	



Symbols	Interpretation
1	GPR Facies
---	Facies Boundary
—	Internal Structure

Comments:• The boundary between facies 2 and 3 may possibly represent the surface of separation.

Ground Penetrating Radar Line: GPR7

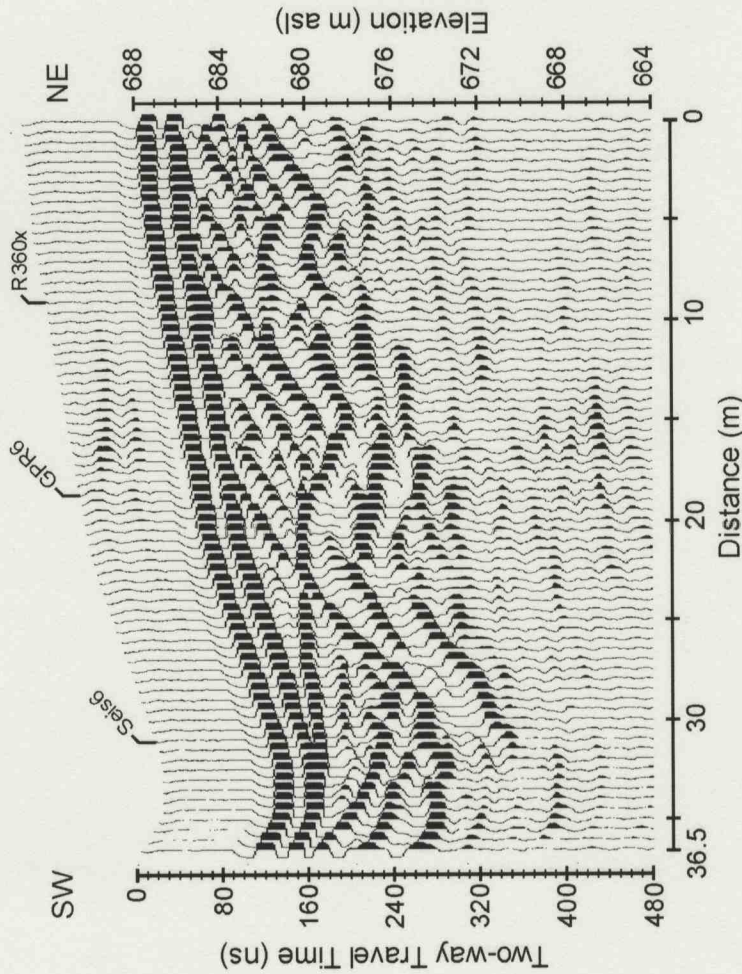
Total Line Length: 36.5 m

Orientation: NE - SW

Number of Traces: 74

Trace Interval: 0.5 m

Assumed Velocity: 0.100 m/ns



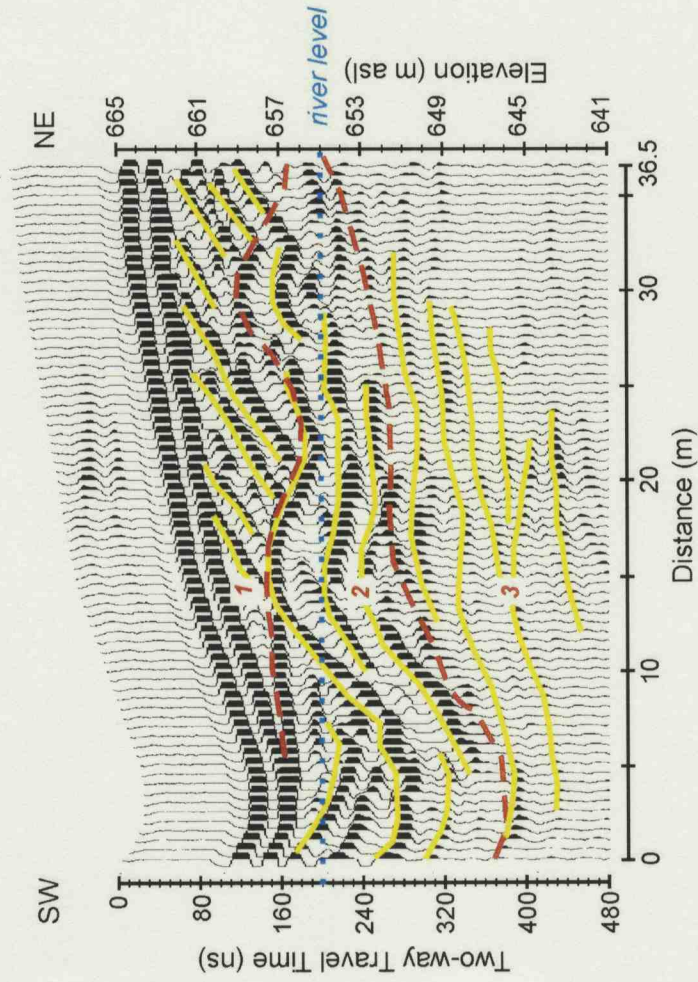
Line Description: The line is located on the toe of the landslide, near the edge of the main rotational block. It runs approximately perpendicular to the head scarp. Surficial material along the line is dry, unconsolidated sand and gravel. The line crosses survey lines Seis6, GPR6, and R360x at the approximate locations specified above.

Location Map



Ground Penetrating Radar Line: GPR7

Interpretation	
GPR Facies	Stratigraphic Unit (Section: Unit)
1	displaced material
2	displaced material
3	S11: 1 + 2



Symbols	
1	GPR Facies
---	Facies Boundary
---	Internal Structure

Comments:• The boundary between facies 2 and 3 may possibly represent the surface of separation.

Appendix D (Section 2)

Direct Current Resistivity Profiles

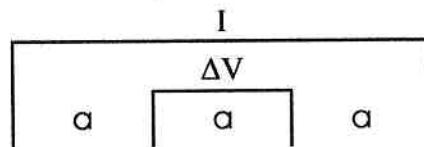
The following geophysical profiles were created using a Syscal IRIS DC resistivity instrument. The system has 48 channels with the option of multiple spreads. Electrodes were planted at a 5-metre spacing. Each survey line used a Wenner array configuration where the a -spacing was changed from 5, 10, 15, 25, 35, 45, 55, 65, and 75 m in a systematic process that allowed both profiling and sounding. Twelve survey lines were conducted: four on the undisturbed terrace, two on the lower rotational block, two on the foot of the landslide, and four that extend perpendicular to the head scarp and so crossed the terrace, rotational blocks, and foot. In total, 4100 m of data were collected.

Pseudosections (ρ_a vs a) were then obtained using the Res2Dinv v3.4 software package from GEOTOMO Software. The pseudosections were then used to invert the data into resistivity (model) sections with and without topographic corrections. An example of the models generated from the software is provided. For each survey line, a summary sheet containing the profile is provided, as well as a separate sheet containing the interpretation of resistivity data. A compilation of all survey lines in the form of a 3-dimensional fence diagram is also given.

A resistivity survey is carried out by applying an induced electric current (direct or alternating) to the ground and measuring the distribution of the electrical potentials at the surface between two electrodes according to the equation:

$$\rho_a = 2\pi a(V/I) \text{ (for Wenner array)}$$

where ρ_a is the apparent resistivity, V is the potential measured as a voltage, I is the current measured in amps, and a is the spacing between electrodes.

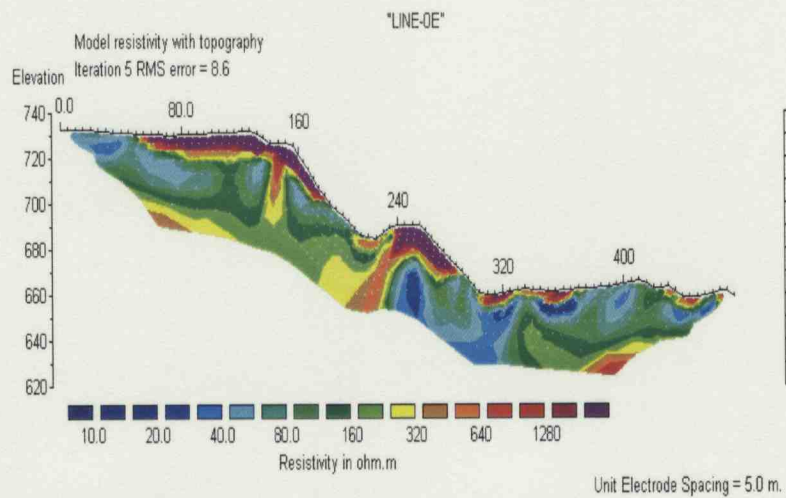
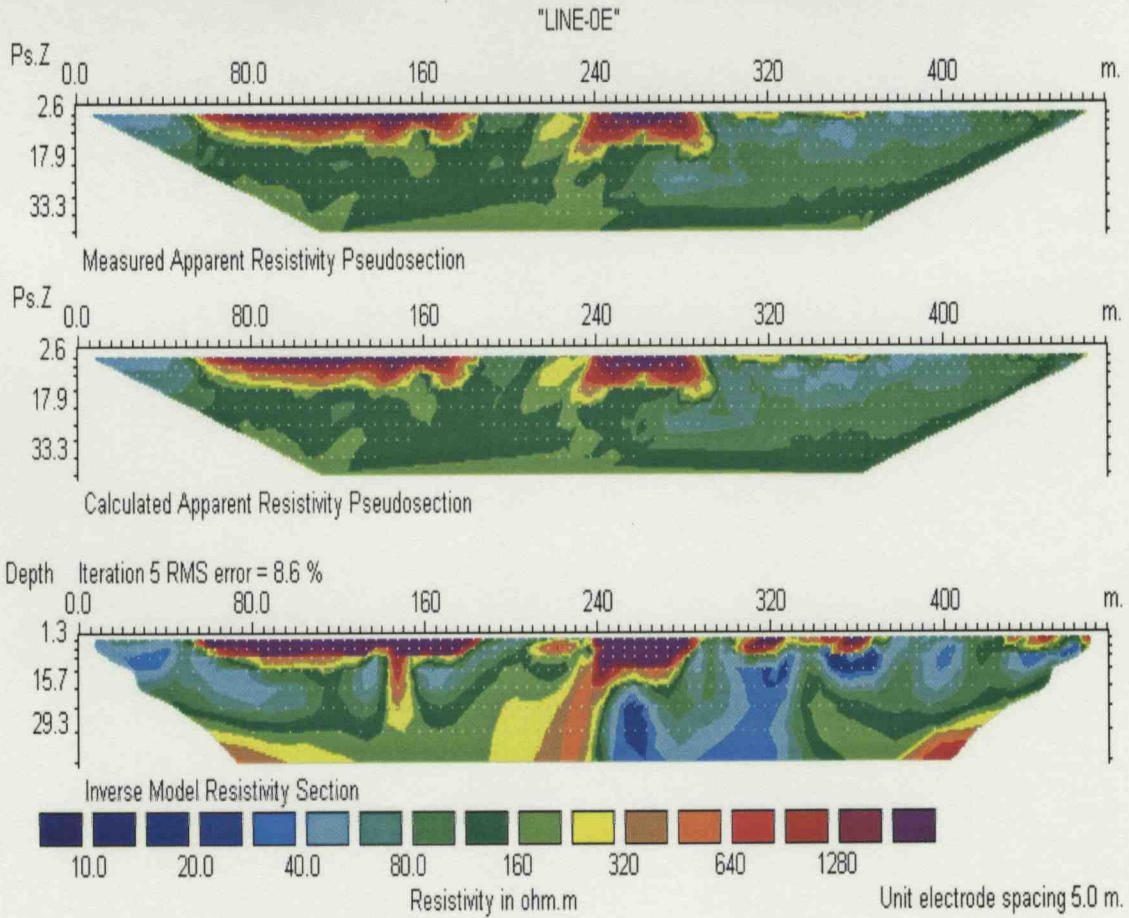


The variance of the potential at the surface, in comparison to a homogeneous earth, is determined by the size, shape, location and electrical resistivity of subsurface

inhomogeneities (Griffiths and King 1965). The interpretation of the deviance leads to models of subsurface geology (Ward 1990).

There are two methods of electrical resistivity surveys: vertical electrical sounding (VES) and profiling. During VES surveys, the separation between the transmitting electrodes is repeatedly enlarged about a centre point, in order to collect data of a layered earth at increasing depth. This is in contrast to profiling where both sets of electrodes are moved along the surface as to obtain lateral changes in resistivity at a fixed depth. Surveys that are a combination of both these methods tend to be the most useful in shallow subsurface exploration (Ward 1990) and were employed herein.

Model Example for Resistivity Line R40



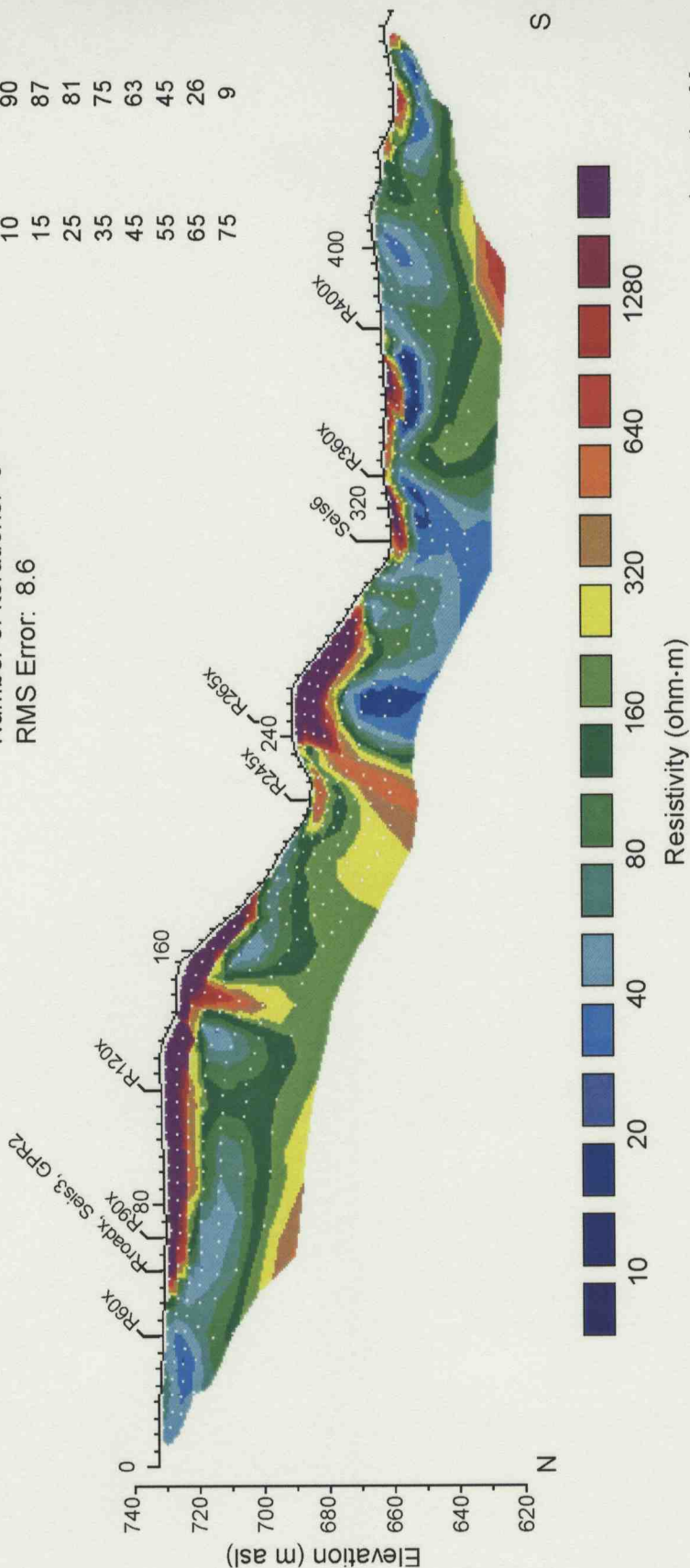
Horizontal scale is 7.50 pixels per unit spacing
 Vertical exaggeration in model section display = 1.00
 First electrode is located at 0.0 m.
 Last electrode is located at 475.0 m.

Resistivity Line: R40
 Total Line Length: 475 m
 Orientation: NNE - SSW

Wenner Array Configuration

'a' Spacing	Number of Data Point
5	90
10	90
15	87
25	81
35	75
45	63
55	45
65	26
75	9

Number of Electrodes: 96
 Total Number of Data Points: 566
 Number of Iterations: 5
 RMS Error: 8.6



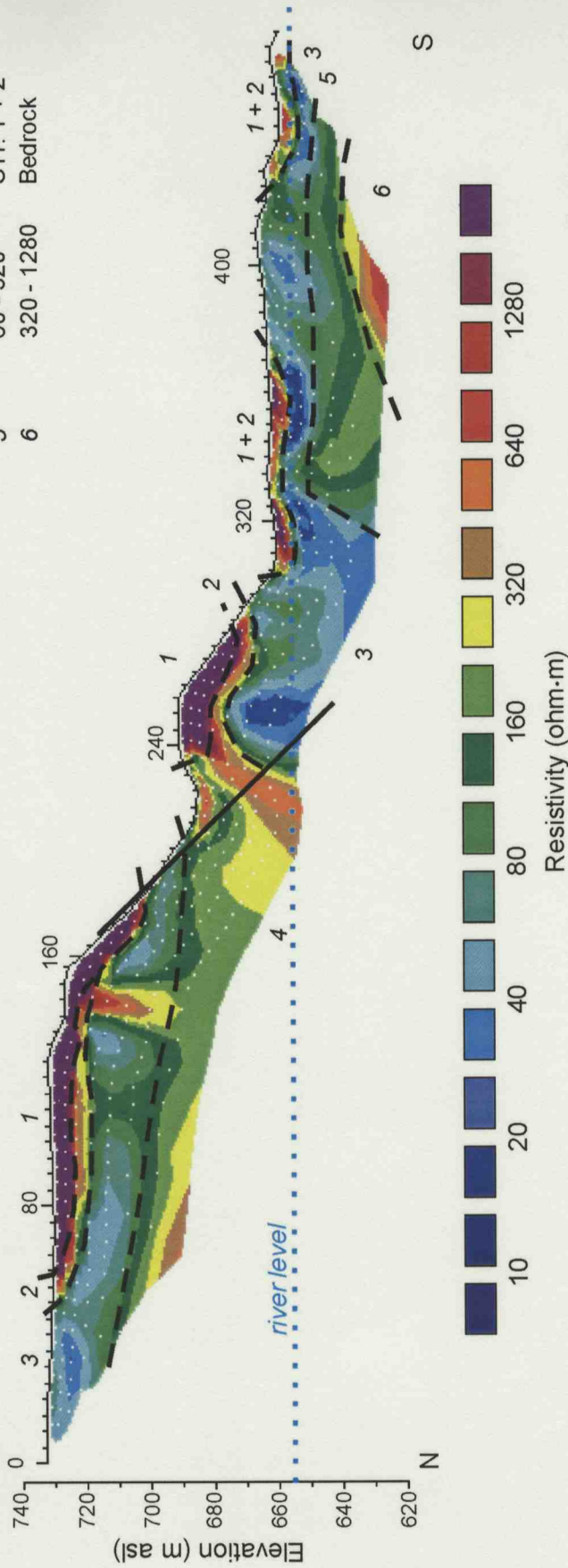
Line Description: The line begins on the upper terrace, running perpendicular to the headscarp and ending at the river. It is the western most perpendicular line. One full spread of electrodes (48) plus two roll-overs (24 each) were used during the survey. The line crosses survey lines R60x, Rroadx, Seis3, GPR2, R90x, R120x, R245x, R265x, Seis6, R360x and R400x at the approximate locations specified above. In addition, it overlies line Seis4 and GPR1.

Location Map



Resistivity Line: R40

Resistivity Unit	Resistivity Range	Stratigraphic Unit (Section: Unit)	Interpretation
1	> 960	L4: 5 + 6	
2	240 - 960	L4: 4	
3	< 120	L4: 3	
4	120 - 640	L4: 1 + 2	
5	60 - 320	S11: 1 + 2	
6	320 - 1280	Bedrock	



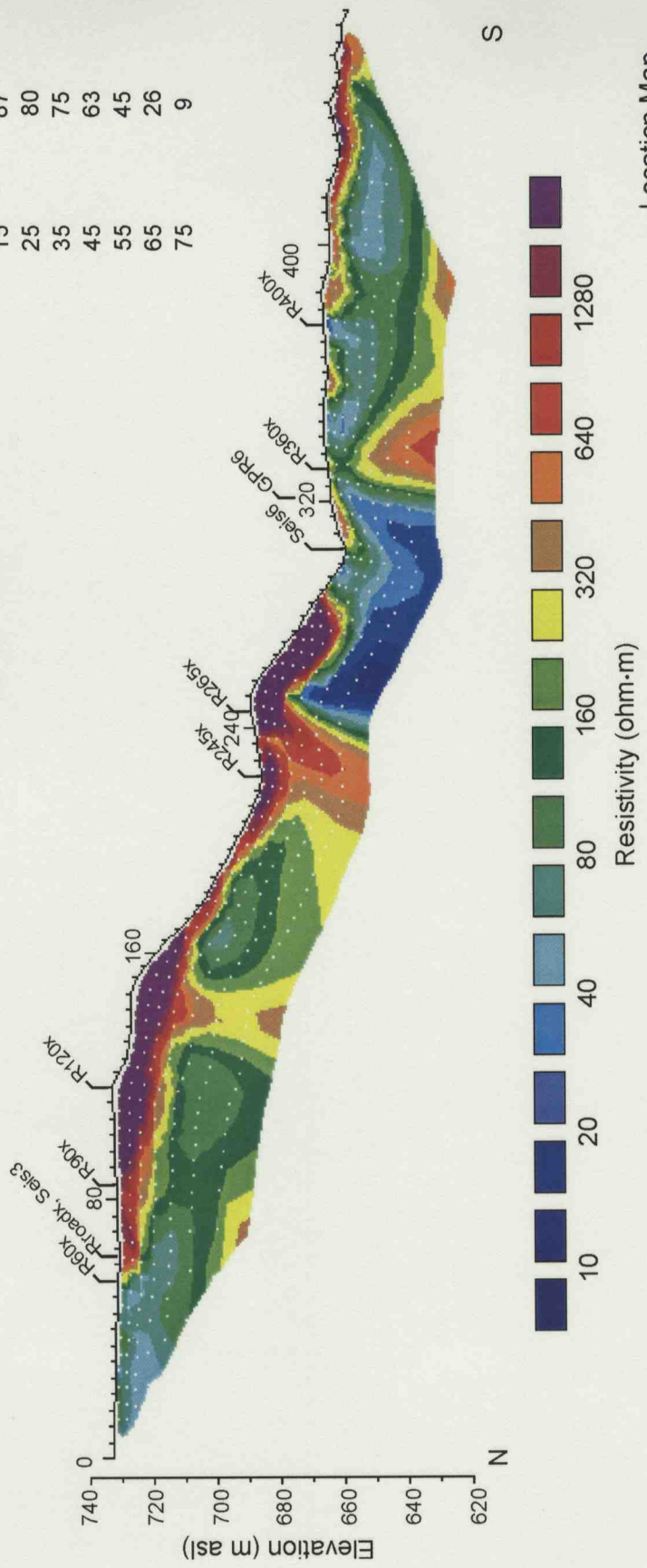
- Comments:
- The near vertical, highly resistive features at 140 m and 230 m are thought to be artificial.
 - The failure plane for the lower rotational block is not well defined in this profile but is estimated at approximately 45°.

Resistivity Line: R80
 Total Line Length: 475 m
 Orientation: NNE - SSW

Number of Electrodes: 96
 Total Number of Data Points: 567
 Number of Iterations: 5
 RMS Error: 8.3

Wenner Array Configuration

'a' Spacing	Number of Data Point
5	93
10	89
15	87
25	80
35	75
45	63
55	45
65	26
75	9



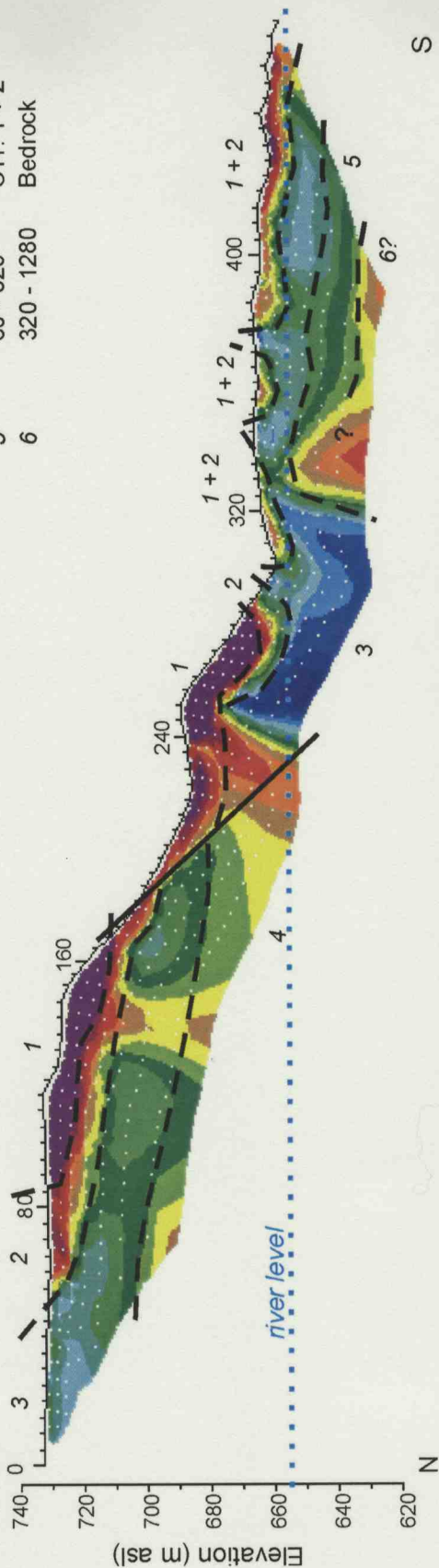
Line Description: The line begins on the upper terrace, running perpendicular to the headscarp and ending at the river. It is the second most western, perpendicular line. One full spread of electrodes (48) plus two roll-overs (24 each) were used during the survey. The line crosses survey lines R60x, Rroadx, Seis3, R90x, R120x, R245x, R265x, Seis6, GPR6, R360x and R400x at the approximate locations specified above.

Location Map



Resistivity Line: R80

Resistivity Unit	Interpretation Resistivity Range	Stratigraphic Unit (Section: Unit)
1	> 960	L4: 5 + 6
2	240 - 960	L4: 4
3	< 120	L4: 3
4	120 - 640	L4: 1 + 2
5	60 - 320	S11: 1 + 2
6	320 - 1280	Bedrock



Symbols

- 1 Resistivity Unit
- Resistivity Unit Boundary
- Failure Plane

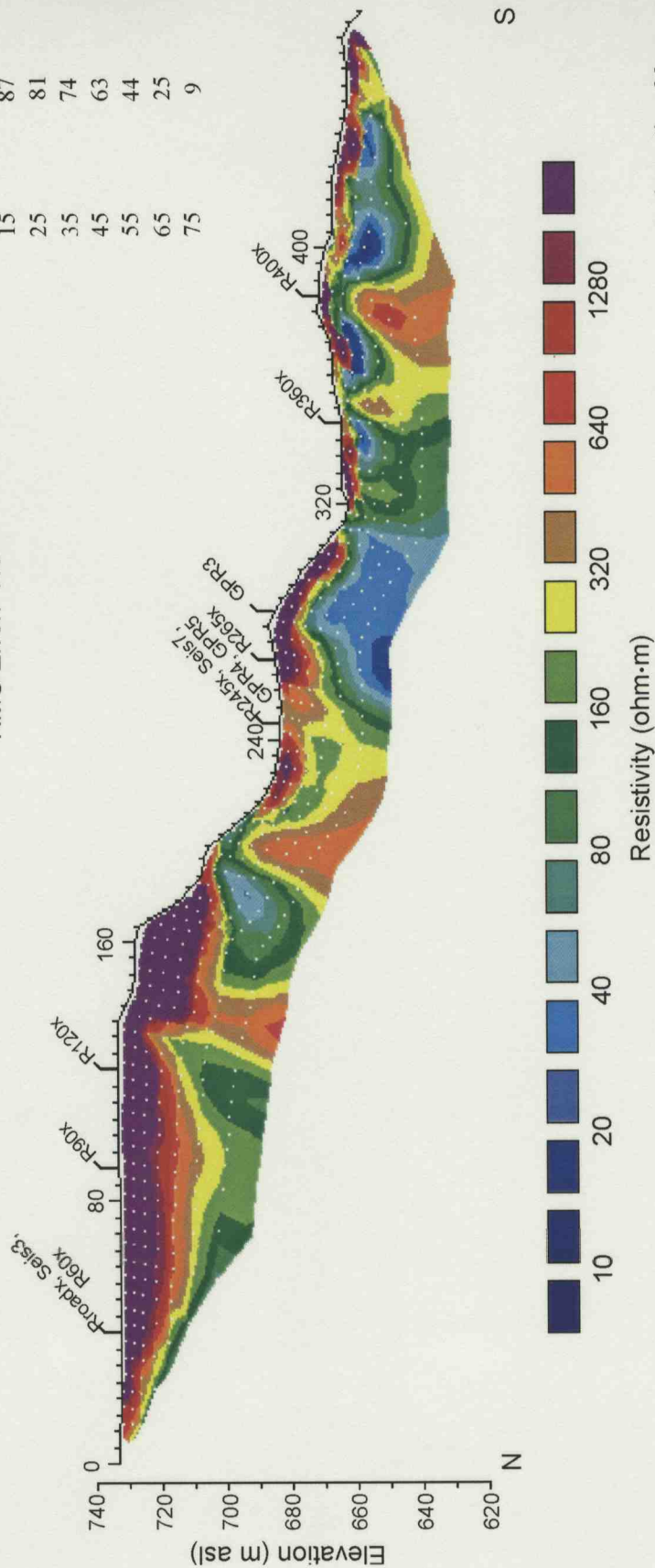
- Comments:
- The near vertical, highly resistive features at 140 m and 240 m are thought to be artificial.
 - The difference in resistivity values between unit 3 in the undisturbed terrace and the lower rotational block is likely the result of poor resolution at depth and a masking effect of the overlying, thick, highly resistive units on the terrace during the inversion process.
 - The highly resistive feature in the toe of the landslide is unexplained and could be an artifact.

Resistivity Line: R120
 Total Line Length: 475 m
 Orientation: NNE - SSW

Number of Electrodes: 96
 Total Number of Data Points: 566
 Number of Iterations: 5
 RMS Error: 7.0

Wenner Array Configuration

'a' Spacing	Number of Data Point
5	93
10	90
15	87
25	81
35	74
45	63
55	44
65	25
75	9



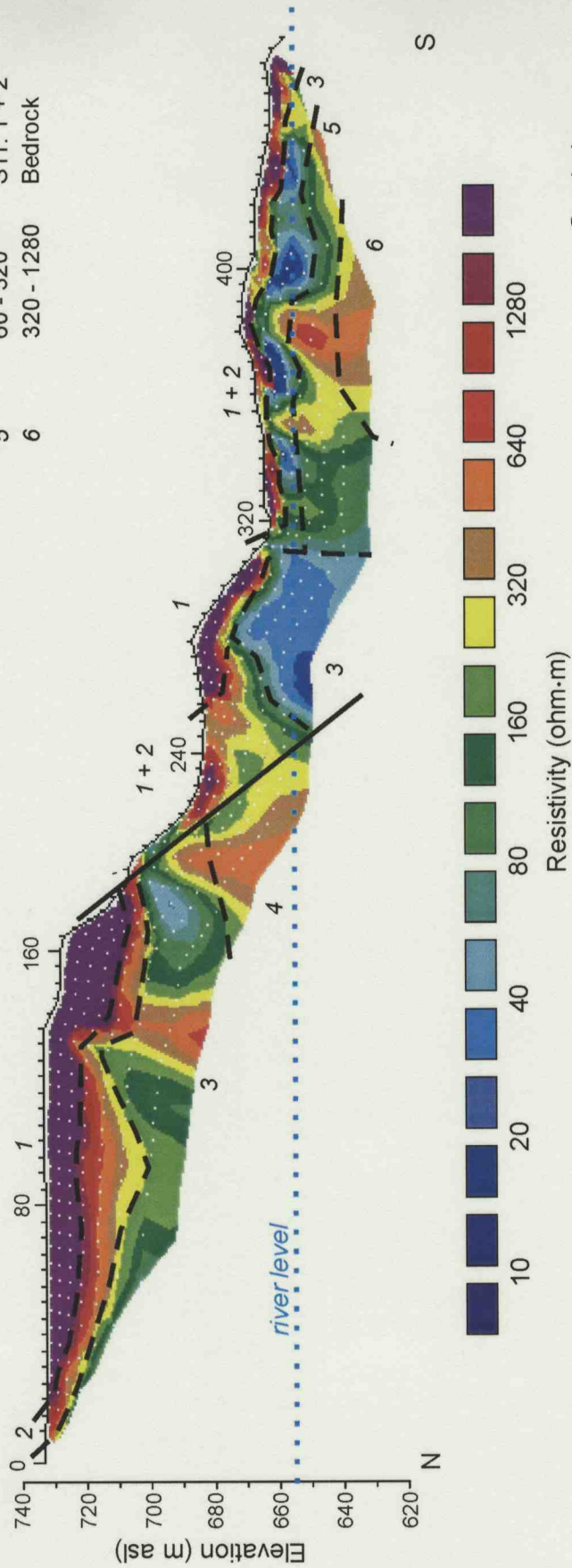
Line Description: The line begins on the upper terrace, running perpendicular to the headscarp through the centre of the landslide and ending at the river. One full spread of electrodes (48) plus two roll-overs (24 each) were used during the survey. The line crosses survey lines Rroadx, Seis3, R60x, R90x, R120x, R245x, Seis7, GPR4, R265x, GPR3, R360x and R400x at the approximate locations specified above.

Location Map



Resistivity Line: R120

Resistivity Unit	Resistivity Range	Stratigraphic Unit (Section: Unit)	Interpretation
1	> 960	L4: 5 + 6	
2	240 - 960	L4: 4	
3	< 120	L4: 3	
4	120 - 640	L4: 1 + 2	
5	60 - 320	S11: 1 + 2	
6	320 - 1280	Bedrock	



- Comments:
- The near vertical, highly resistive feature at 140 m is thought to be artificial.
 - The difference in resistivity values between unit 3 in the undisturbed terrace and the lower rotational block is likely the result of poor resolution at depth and a masking effect of the overlying, thick, highly resistive units on the terrace during the inversion process.
 - The low resistive features between 320 m and 460 m are thought to be discrete blocks of unit 3.

Symbols

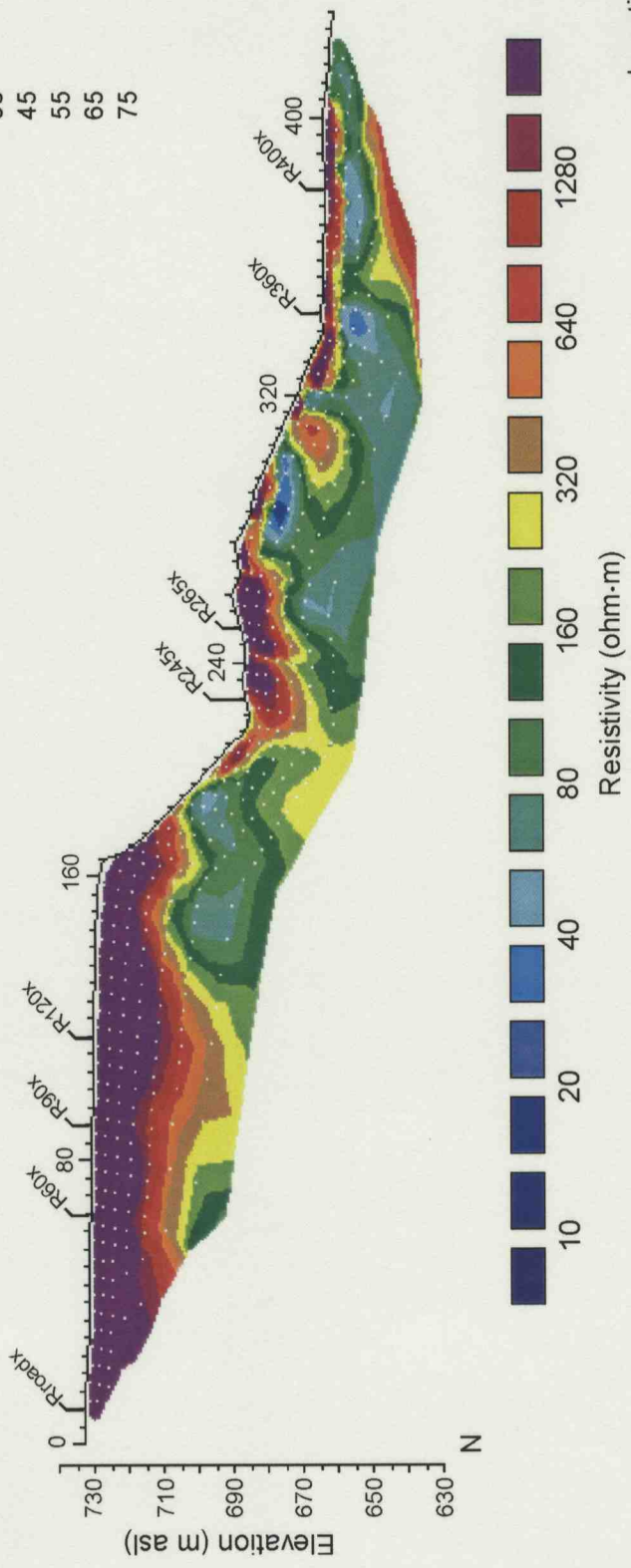
/	Resistivity Unit
- - -	Resistivity Unit Boundary
—	Failure Plane

Resistivity Line: R200
 Total Line Length: 430m
 Orientation: NNE - SSW

Number of Electrodes: 87
 Total Number of Data Points: 562
 Number of Iterations: 5
 RMS Error: 6.4

Wenner Array Configuration

'a' Spacing	Number of Data Point
5	92
10	90
15	86
25	80
35	73
45	63
55	45
65	25
75	8



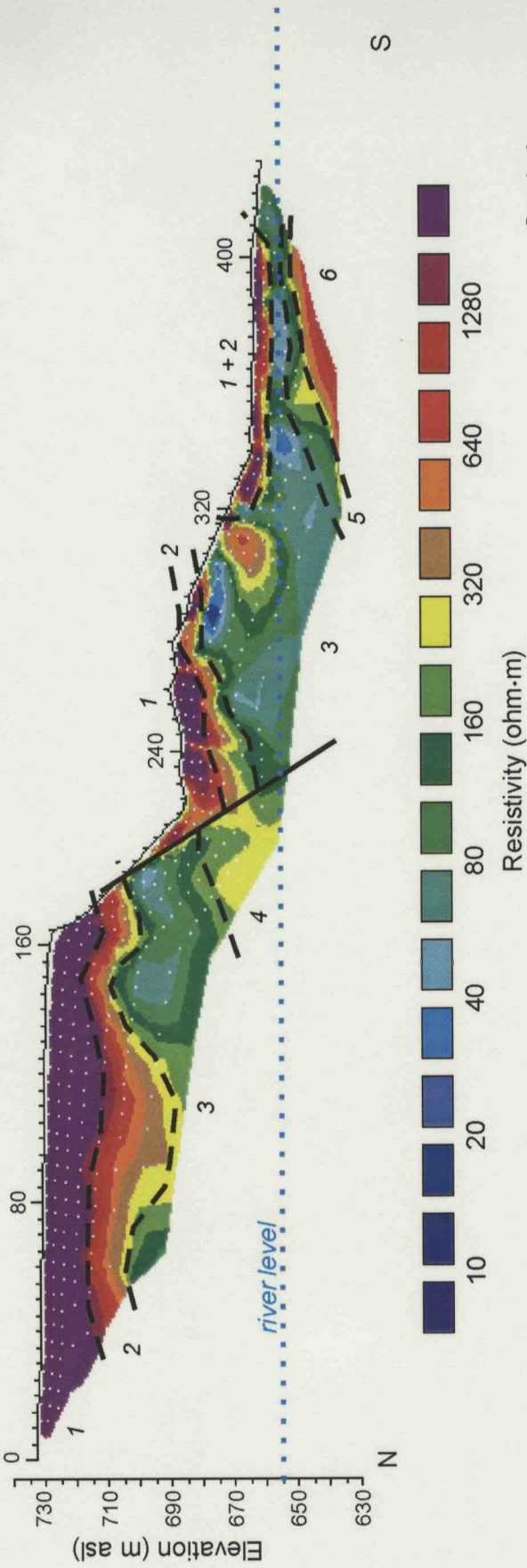
Location Map



Line Description: The line begins on the upper terrace, running perpendicular to the headscarp and ending at the river. It is the most eastern, perpendicular line. One full spread of electrodes (48) plus one full roll-over (24) and one partial roll-over (15) were used during the survey. The line crosses survey lines R60x, Roadx, R90x, R120x, R245x, R265x, R360x and R400x at the approximate locations specified above.

Resistivity Line: R200

Resistivity Unit	Resistivity Range	Stratigraphic Unit (Section: Unit)	Interpretation
1	> 960	L4: 5 + 6	
2	240 - 960	L4: 4	
3	< 120	L4: 3	
4	120 - 640	L4: 1 + 2	
5	60 - 320	S11: 1 + 2	
6	320 - 1280	Bedrock	



Symbols

- 1 Resistivity Unit
- Resistivity Unit Boundary
- Failure Plane

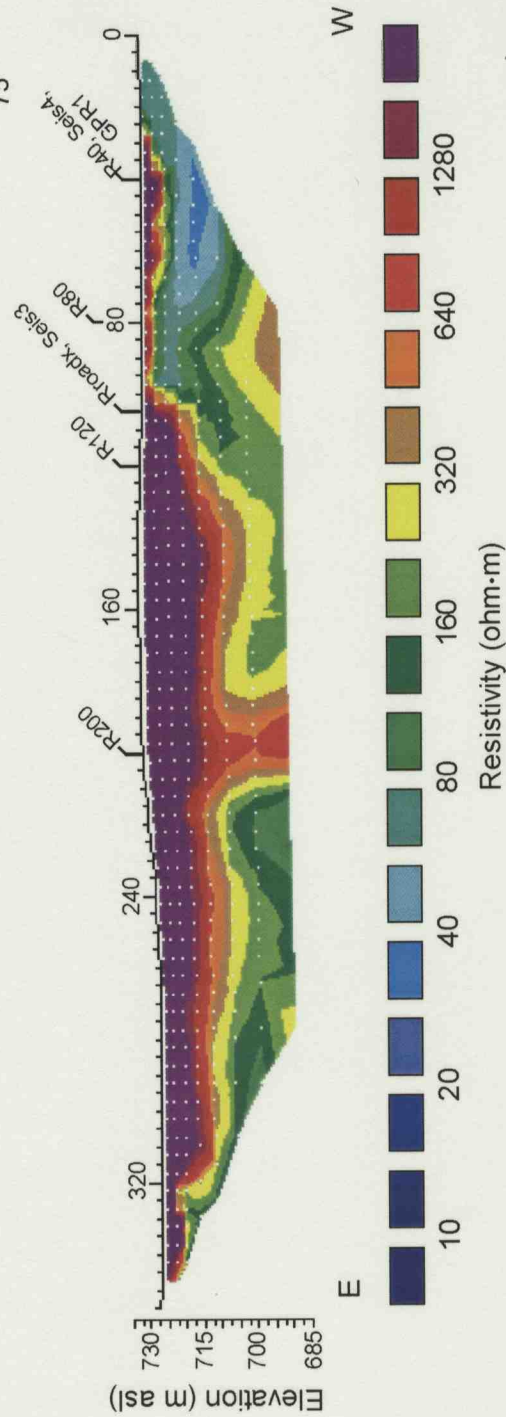
- Comments:
- The landslide toe is thinnest of all of the perpendicular lines.
 - Resistivity unit 6 is well defined and shows a high resistivity value range.
 - There is no upper rotational block encountered in this profile.
 - The interpreted failure plane of the lower rotational block is approximately 60°.

Resistivity Line: R60x
 Total Line Length: 355 m
 Orientation: VNW - ESE

Number of Electrodes: 72
 Total Number of Data Points: 401
 Number of Iterations: 5
 RMS Error: 4.6

Wenner Array Configuration

'a' Spacing	Number of Data Point
5	69
10	66
15	63
25	57
35	51
45	42
55	30
65	17
75	6



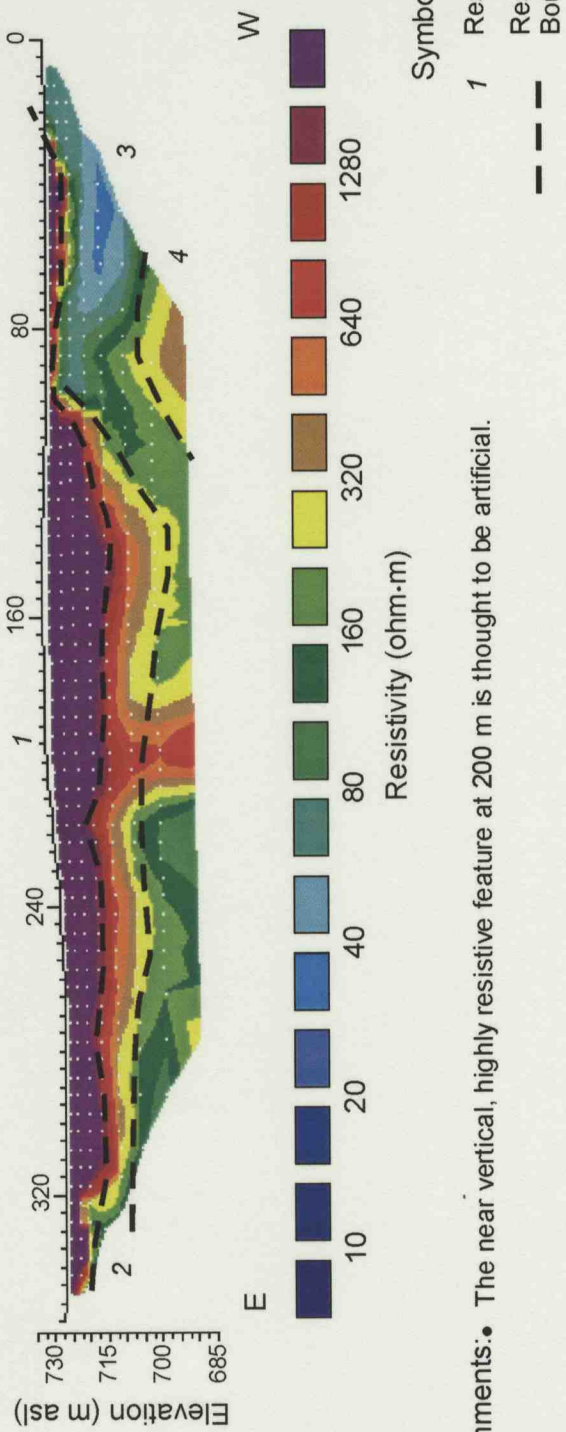
Location Map



Line Description: The entire line is on the upper terrace, running approximately parallel to the headscarp. It is the furthest cross line from the headscarp, on the terrace. One full spread of electrodes (48) plus one roll-over (24) were used during the survey. The line crosses survey lines R40, Seis4, GPR1, R80, Rroadx, Seis3, R120 and R200 at the approximate locations specified above.

Resistivity Line: R60x

Resistivity Unit	Resistivity Range	Stratigraphic Unit (Section: Unit)	Interpretation
1	> 960	L4: 5 + 6	
2	240 - 960	L4: 4	
3	< 120	L4: 3	
4	120 - 640	L4: 1 + 2	

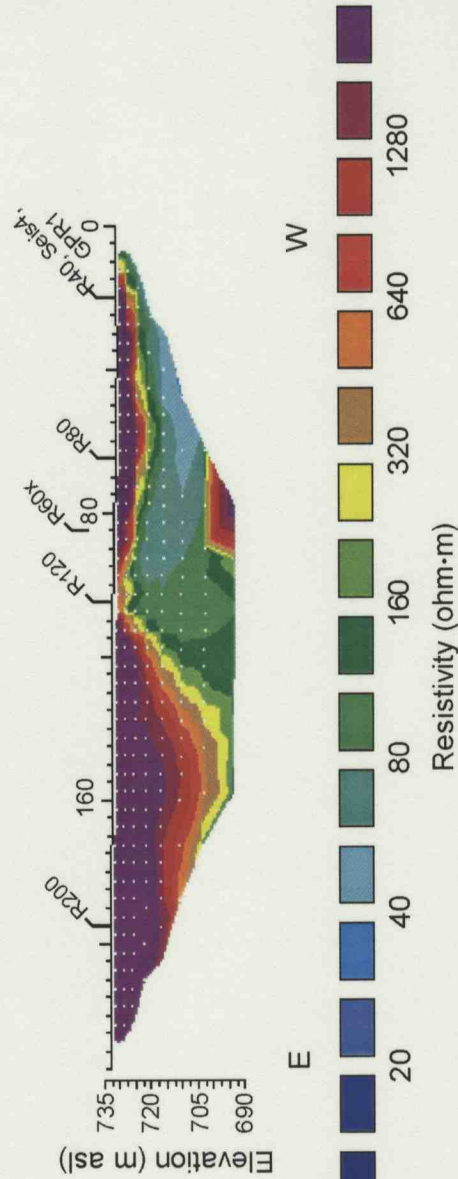


Resistivity Line: Roadx
 Total Line Length: 235 m
 Orientation: WNW - ESE

Number of Electrodes: 48
 Total Number of Data Points: 234
 Number of Iterations: 5
 RMS Error: 5.2

Wenner Array Configuration

'a' Spacing	Number of Data Point
5	45
10	42
15	39
25	33
35	27
45	21
55	15
65	9
75	3



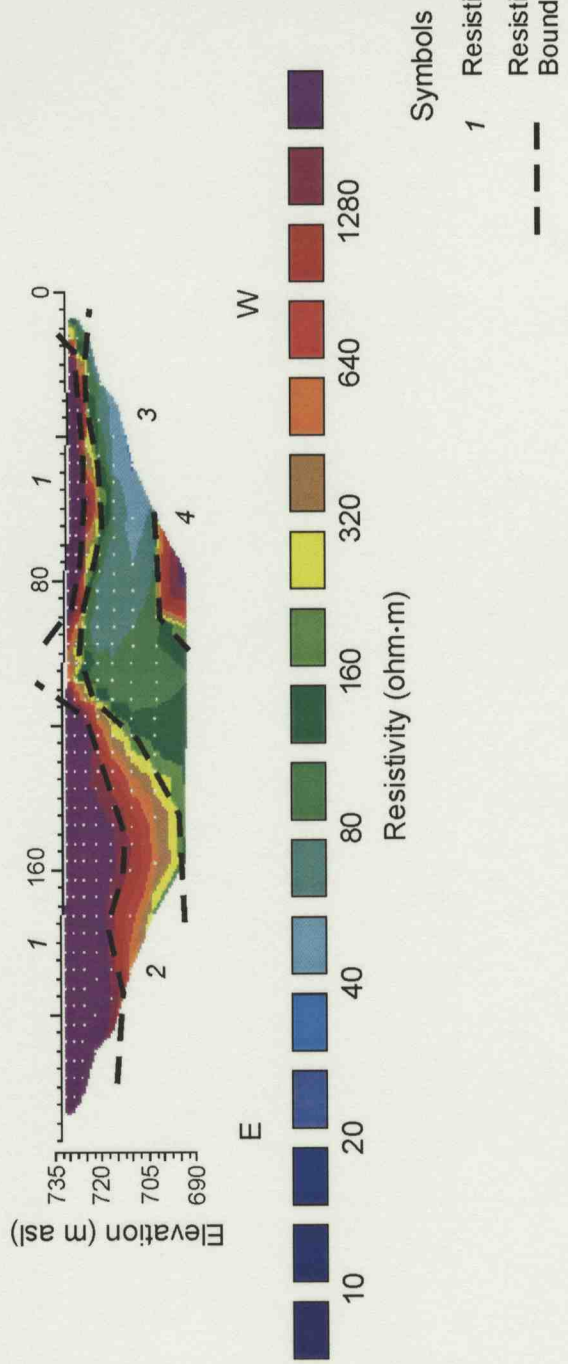
Location Map



Line Description: The entire line is on the upper terrace, following the access road. One full spread of electrodes (48) plus one roll-over (24) were used during the survey. The line crosses survey lines R40, Seis4, GPR1, R80, Roadx, Seis3, R120 and R200 at the approximate locations specified above. In addition, it was surveyed directly overtop of lines Seis3 and GPR2.

Resistivity Line: Rroadx

Resistivity Unit	Resistivity Range	Stratigraphic Unit (Section: Unit)	Interpretation
1	> 960	L4: 5 + 6	
2	240 - 960	L4: 4	
3	< 120	L4: 3	
4	120 - 640	L4: 1 + 2	

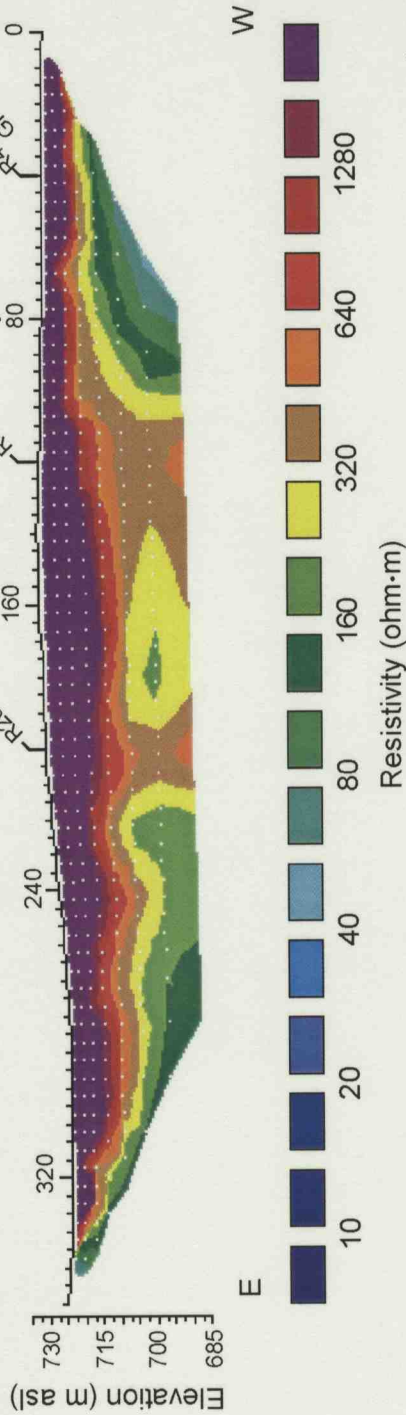


Resistivity Line: R90x
 Total Line Length: 355 m
 Orientation: WNW - ESE

Number of Electrodes: 72
 Total Number of Data Points: 402
 Number of Iterations: 5
 RMS Error: 3.6

Wenner Array Configuration

'a' Spacing	Number of Data Point
5	69
10	66
15	63
25	57
35	51
45	42
55	30
65	18
75	6



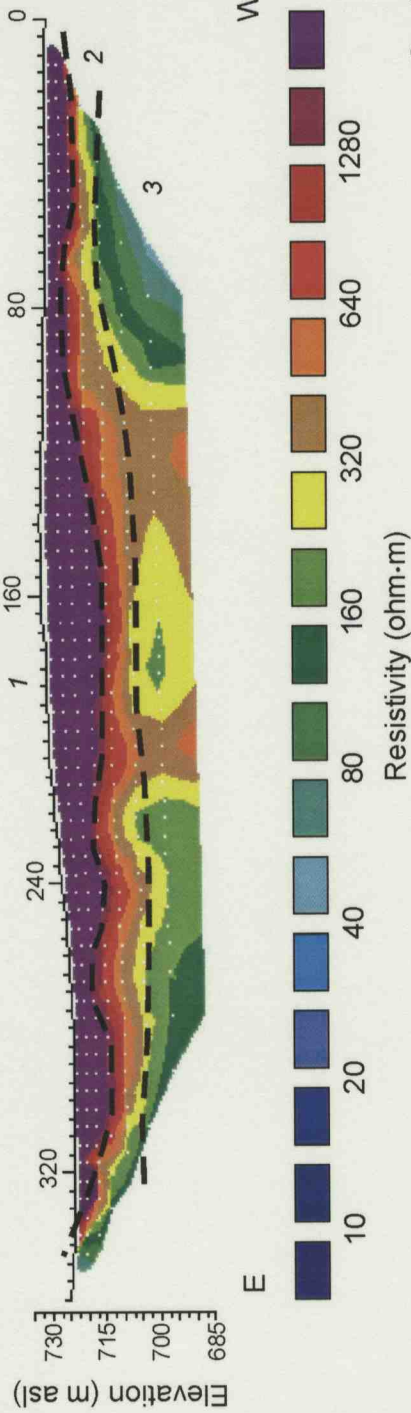
Location Map



Line Description: The entire line is on the upper terrace, running approximately parallel to the headscarp. It is the second closest line to the headscarp. One full spread of electrodes (48) plus one roll-over (24) were used during the survey. The line crosses survey lines R40, Seis4, GPR1, R80, R120 and R200 at the approximate locations specified above.

Resistivity Line: R90x

Interpretation	
Resistivity Unit	Stratigraphic Unit (Section: Unit)
1	L4: 5 + 6
2	L4: 4
3	L4: 3



Symbols

- 1 Resistivity Unit
- Resistivity Unit Boundary

Comments:

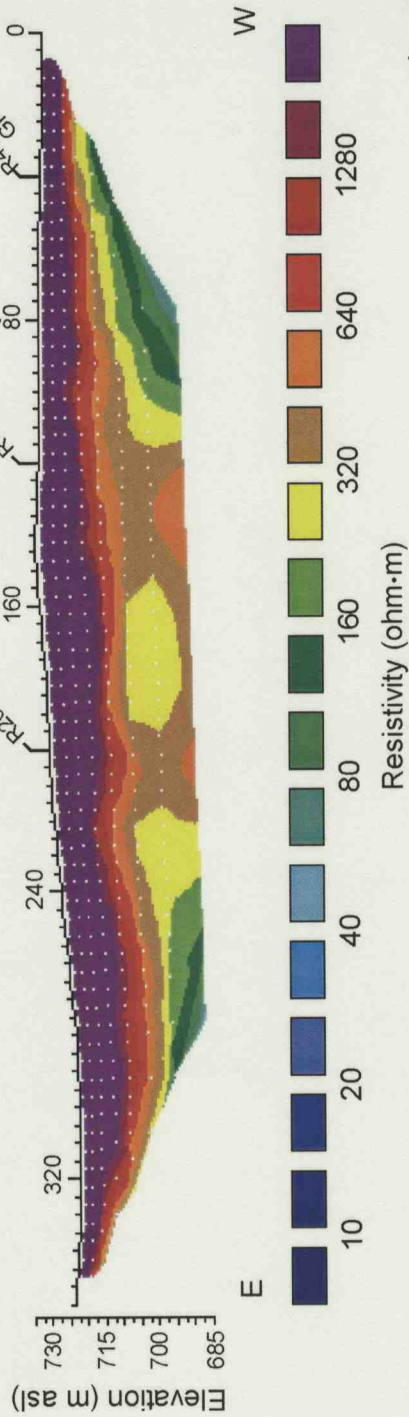
- The near vertical, highly resistive features at 120 m and 200 m are thought to be artificial.
- The difference in higher resistivity values of unit 3 is likely the result of poor resolution at depth and a masking effect of the overlying, thick, highly resistive units on the terrace during the inversion process.

Resistivity Line: R120x
 Total Line Length: 355 m
 Orientation: VNW - ESE

Number of Electrodes: 72
 Total Number of Data Points: 401
 Number of Iterations: 5
 RMS Error: 3.8

Wenner Array Configuration

'a' Spacing	Number of Data Point
5	69
10	66
15	63
25	57
35	51
45	42
55	30
65	17
75	6



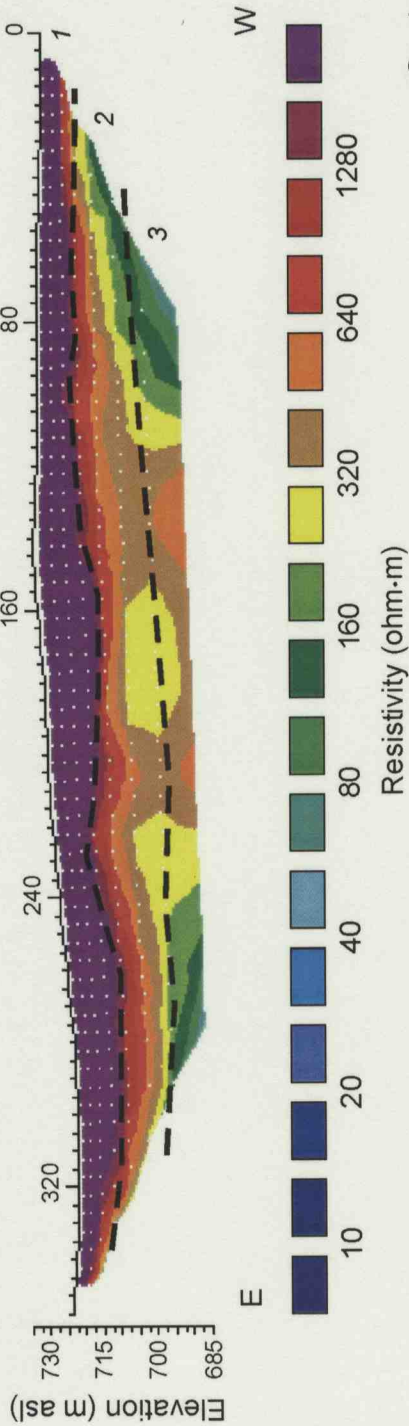
Location Map



Line Description: The entire line is on the upper terrace, running approximately parallel to the headscarp. It is the closest line to the head scarp. One full spread of electrodes (48) plus one roll-over (24) were used during the survey. The line crosses survey lines R40, Seis4, GPR1, R80, R120 and R200 at the approximate locations specified above.

Resistivity Line: R120x

Interpretation	
Resistivity Unit	Stratigraphic Unit (Section: Unit)
1	L4: 5 + 6
2	L4: 4
3	L4: 3



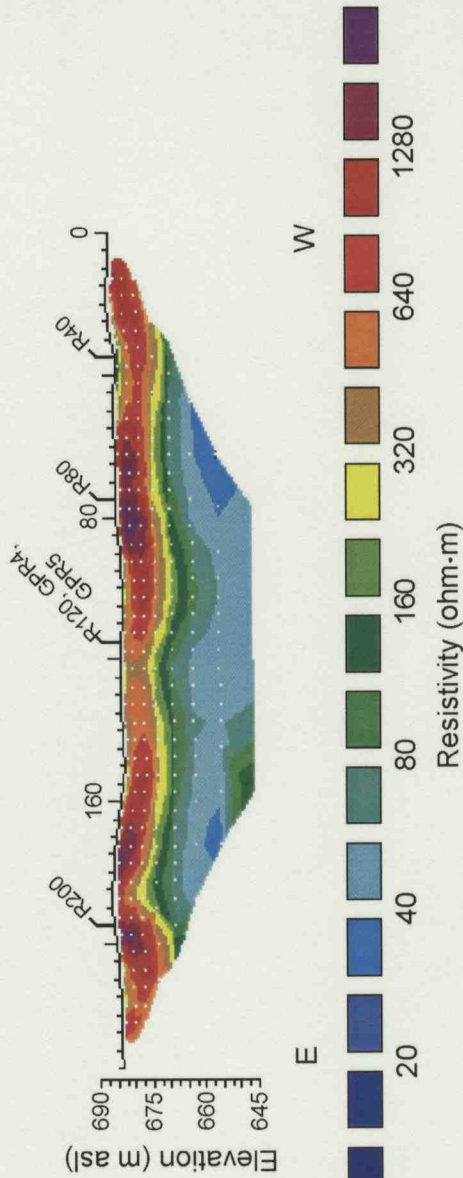
- Comments:
- The near vertical, highly resistive features at 140 m and 200 m are thought to be artificial.
 - The difference in higher resistivity values of unit 3 is likely the result of poor resolution at depth and a masking effect of the overlying, thick, highly resistive units on the terrace during the inversion process.

Resistivity Line: R245x
 Total Line Length: 235 m
 Orientation: WNW - ESE

Number of Electrodes: 48
 Total Number of Data Points: 234
 Number of Iterations: 5
 RMS Error: 7.0

Wenner Array Configuration

'a' Spacing	Number of Data Point
5	45
10	42
15	39
25	33
35	27
45	21
55	15
65	9
75	3



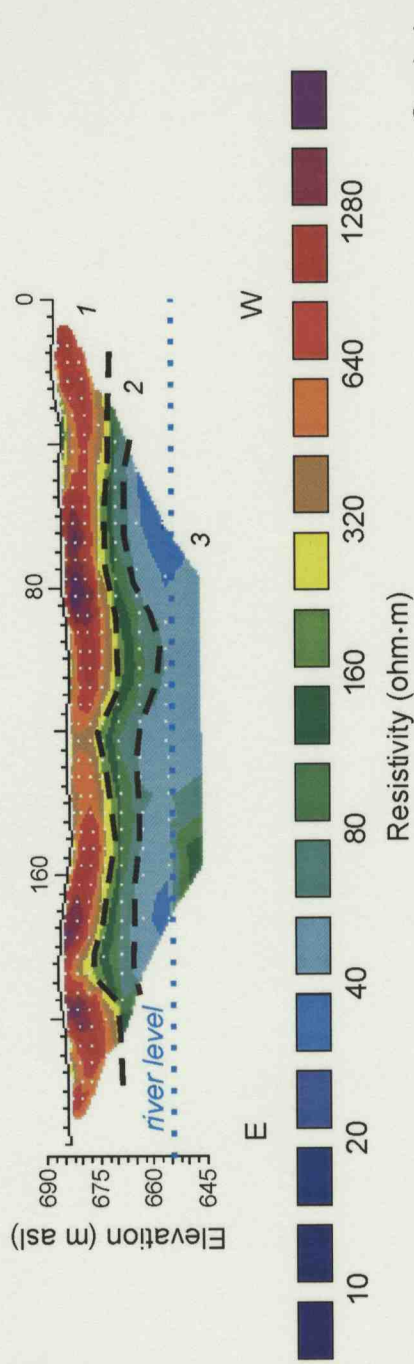
Location Map



Line Description: The entire line is on the main rotational block, roughly parallel to the headscarp. It is the closest cross line to the head scarp found on the main rotational block. One full spread of electrodes (48) plus one roll-over (24) were used during the survey. The line crosses survey lines R40, R80, R120, GPR4, GPR5 and R200 at the approximate locations specified above. In addition, it was surveyed directly overtop of line Seis7.

Resistivity Line: R245x

Resistivity Unit	Resistivity Range	Interpretation	Stratigraphic Unit (Section: Unit)
1	> 960		L4: 5 + 6
2	240 - 960		L4: 4
3	< 120		L4: 3



Comments:

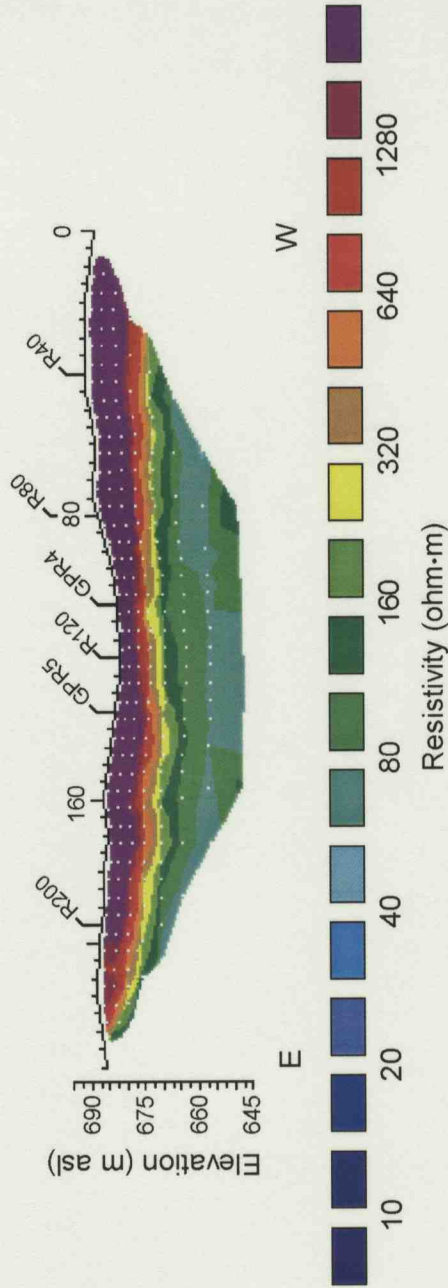
- Symbols
- 1 Resistivity Unit
 - Resistivity Unit Boundary

Resistivity Line: R265x
 Total Line Length: 235 m
 Orientation: WNW - ESE

Number of Electrodes: 48
 Total Number of Data Points: 234
 Number of Iterations: 5
 RMS Error: 6.5

Wenner Array Configuration

'a' Spacing	Number of Data Point
5	45
10	42
15	39
25	33
35	27
45	21
55	15
65	9
75	3



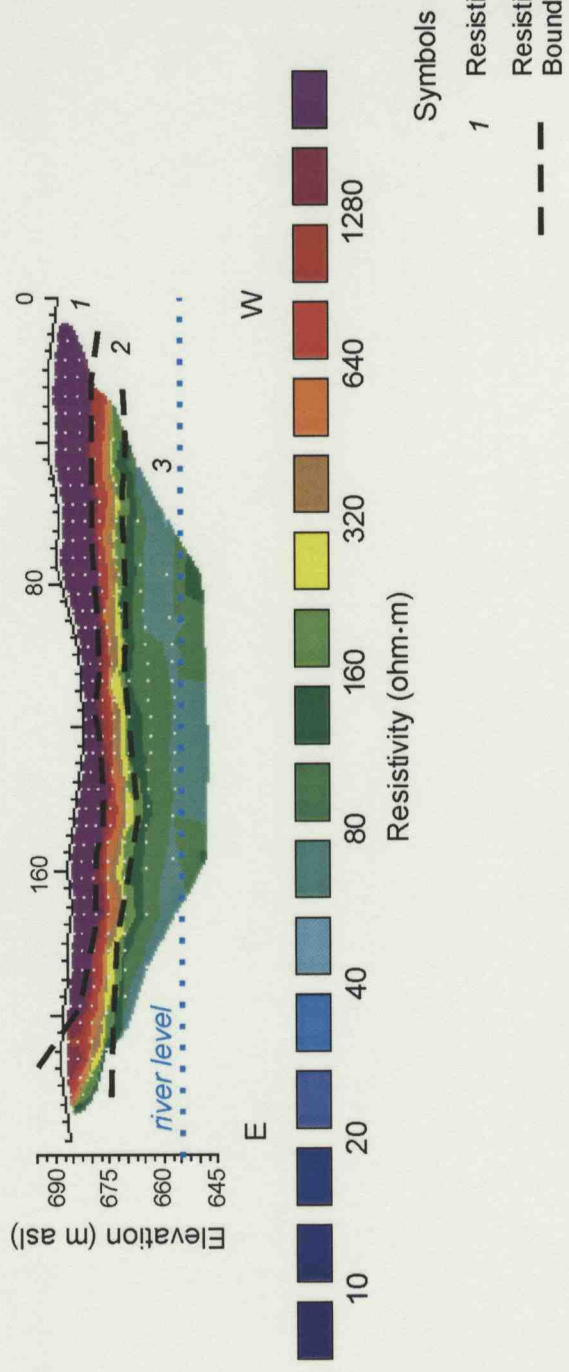
Line Description: The entire line is on the main rotational block, roughly parallel to the headscarp. It is the furthest cross line from the head scarp found on the main rotational block. One full spread of electrodes (48) plus one roll-over (24) were used during the survey. The line crosses survey lines R40, R80, GPR4, R120, GPR5 and R200 at the approximate locations specified above.

Location Map



Resistivity Line: R265x

Resistivity Unit	Resistivity Range	Interpretation	Stratigraphic Unit (Section: Unit)
1	> 960		L4: 5 + 6
2	240 - 960		L4: 4
3	< 120		L4: 3



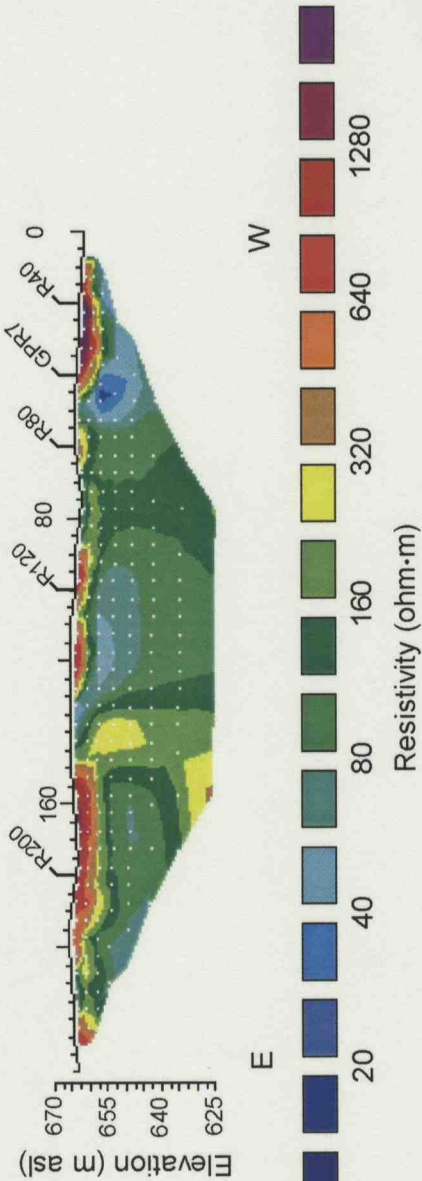
Comments:

Resistivity Line: R360x
 Total Line Length: 235 m
 Orientation: WNW - ESE

Number of Electrodes: 48
 Total Number of Data Points: 234
 Number of Iterations: 5
 RMS Error: 9.1

Wenner Array Configuration

'a' Spacing	Number of Data Point
5	45
10	42
15	39
25	33
35	27
45	21
55	15
65	9
75	3



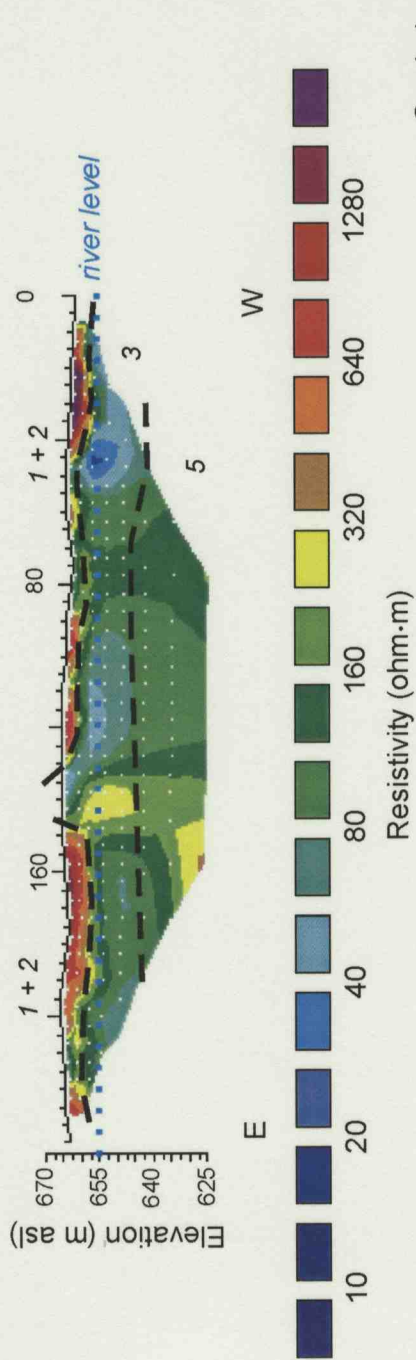
Line Description: The entire line is on the landslide toe, roughly parallel to the headscarp. It is the closest cross line to the headscarp found on the main landslide toe. One full spread of electrodes (48) plus one roll-over (24) were used during the survey. The line crosses survey lines R40, GPR7, R80, R120 and R200 at the approximate locations specified above.



Location Map

Resistivity Line: R360x

Interpretation		Stratigraphic Unit (Section: Unit)
Resistivity Unit	Range	
1	> 960	displaced material
2	240 - 960	displaced material
3	< 120	displaced material
5	60 - 320	S11: 1 + 2



Symbols

- 1 Resistivity Unit
- Resistivity Unit Boundary

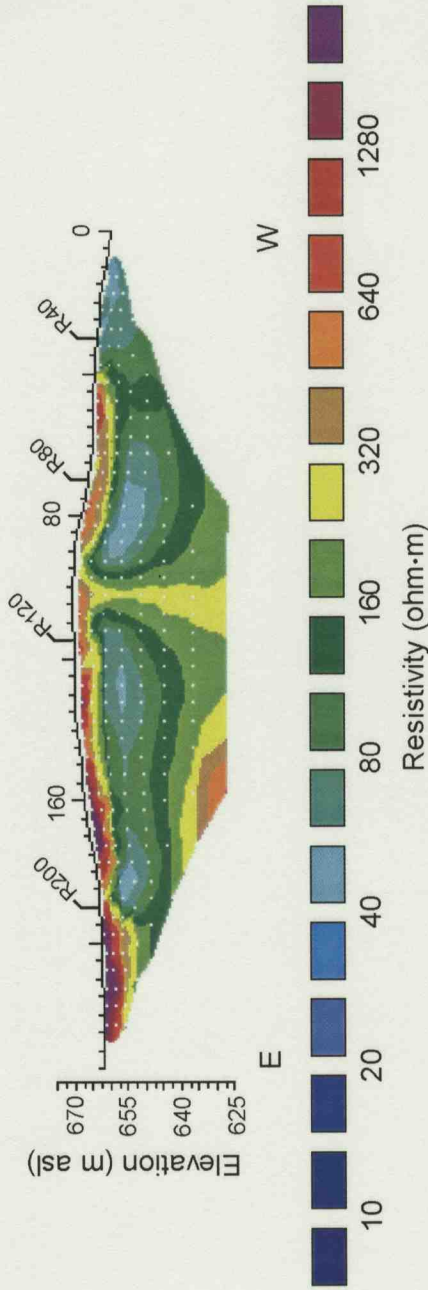
Comments:

Resistivity Line: R400x
 Total Line Length: 235 m
 Orientation: WNW - ESE

Number of Electrodes: 48
 Total Number of Data Points: 234
 Number of Iterations: 5
 RMS Error: 5.4

Wenner Array Configuration

'a' Spacing	Number of Data Point
5	45
10	42
15	39
25	33
35	27
45	21
55	15
65	9
75	3



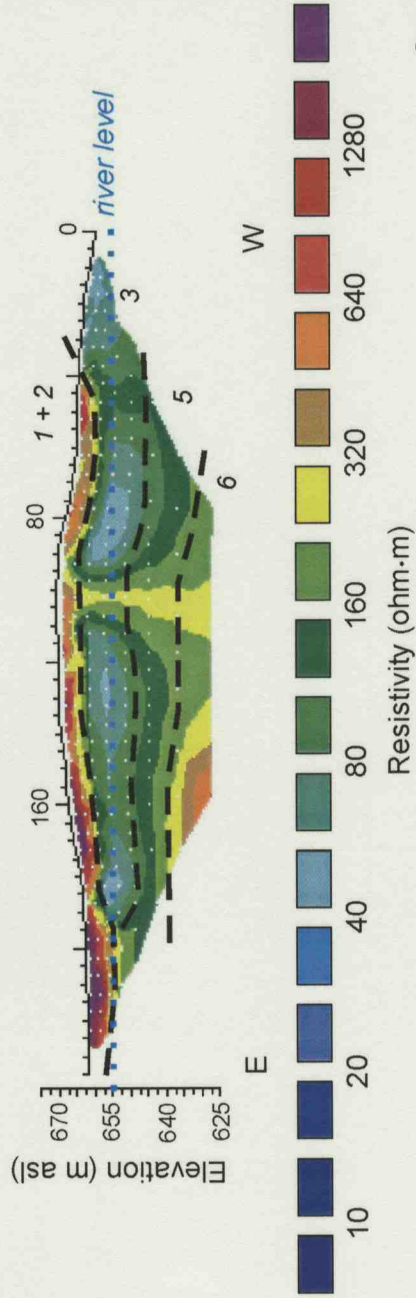
Line Description: The entire line is on the landslide toe, roughly parallel to the headscarp. It is the furthest cross line from the headscarp found on the toe. One full spread of electrodes (48) plus one roll-over (24) were used during the survey. The line crosses survey lines R40, R80, R120 and R200 at the approximate locations specified above.

Location Map



Resistivity Line: R400x

Interpretation		Stratigraphic Unit
Resistivity Unit	Resistivity Range	(Section: Unit)
1	> 960	displaced material
2	240 - 960	displaced material
3	< 120	displaced material
5	60 - 320	S11: 1 + 2
6	320 - 1280	Bedrock

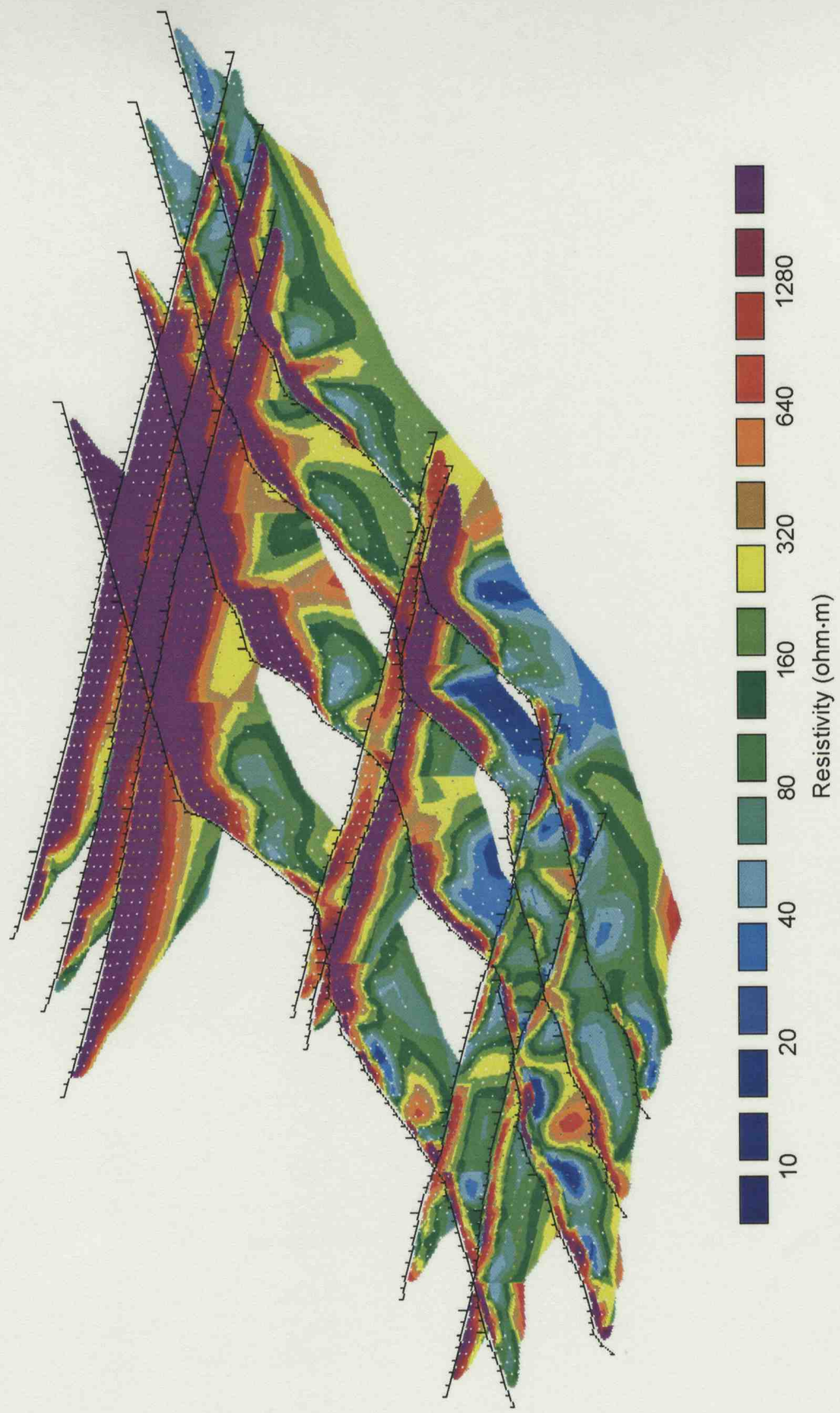


Symbols

- / Resistivity Unit
- Resistivity Unit Boundary

Comments:• The more resistive, near vertical feature at 100 m is thought to be an artifact

3D Compilation of Resistivity Data



Appendix D (Section 3)

Seismic Reflection and Refraction Profiles

The following geophysical profiles were created using a Geometrics SmartSeis seismograph. It is a 48-channel system, though only 36 channels were utilized. Both seismic reflection and refraction surveys were conducted. Nine surveys were carried out along four lines: 6 on the undisturbed terrace, 1 on the lower rotational block and 2 on the foot of the landslide. Of the 9 surveys, 2 were P-wave reflections, 4 were S-wave reflections, 1 was a P-wave refraction and 2 were S-wave refractions. In total, approximately 850 m of data were collected. The characteristics for each survey line are described on the profile sheets. Robert Burns and James Hunter of the Geological Survey of Canada carried out the processing of the seismic data. A summary of the processing history is provided. For each survey line, a summary sheet containing the profile is provided, as well as a separate sheet containing the interpretation of seismic events.

Seismic geophysical methods are based on changes in physico-mechanical properties (i.e. acoustic impedance, ρv) of subsurface materials (Goryainov *et al.* 1988). Elastic (seismic) waves are transmitted at different velocities, depending on the material's properties. In general, the velocity is equal to:

$$v = f\lambda$$

where v is the velocity of the seismic wave, f is the frequency, and λ is the wavelength.

When waves encounter an interface between mediums that differ in their physico-mechanical properties, energy is refracted, reflected, and transmitted by the discontinuity according to known physical laws. Waves refracted at the critical angle travel along the interface of the lower medium if its velocity is higher than the overlying unit. The amount of energy reflected across an interface is dependant on the differences in acoustic impedance, and is accommodated within the reflection coefficient as:

$$R = [(\rho_1 v_1)/(\rho_2 v_2) - 1] / [(\rho_1 v_1)/(\rho_2 v_2) + 1]$$

where R is the reflection coefficient, ρ is the density of the material, and v is the velocity of the seismic wave (Hack 2000). This holds true for both P and S-waves by interchanging appropriate velocities. Reflected and refracted energy then return to the surface where a geophone records its arrival time. The signals can then be interpreted and fit to geologic models.

Processing History

Line 3 – P Wave

Sort (assign geometry)
 Re-sort common offset
 Static correction
 Re-Sort common depth point
 Normal move-out correction

- Velocity 1450 m/s
- Stretch 0.6

 Stack
 Time Domain Filter

- Bandpass 150 – 800 Hz
- Window 31 points

 Static correction

Line 3 – S Wave

Sort (assign geometry)
 AGC Scaling

- Window length 100ms

 Time Domain Filter

- Bandpass 60 – 600 Hz
- Window 31 points

 Re-sort common offset
 Re-sort common depth point
 Normal move-out correction

- Velocity 540 m/s
- Stretch 0.6

 Stack

Line 4 – P Wave

Apply Mute
 Sort (assign geometry)
 Frequency Domain Filter

- Bandpass 50 – 150 – 600 - 1000 Hz

 AGC Scaling

- Window length 250ms

 Frequency Domain Filter

- Bandpass 100 – 150 – 500 - 550 Hz

 AGC Scaling

- Window length 250ms

 Kill Bad traces
 Frequency Domain Filter

- Bandpass 50 – 150 – 600 - 1000 Hz

 AGC Scaling

- Window length 250ms

Kill Bad traces
 Re-sort common depth point
 Static correction
 Normal move-out correction

- Velocity 1425 m/s
- Stretch 0.7

 Stack
 AGC Scaling

- Window length 250ms

 Static correction

Line 4 – S Wave

Kill Bad Traces
 Sort (assign geometry)
 Re-sort common offset
 Static correction
 Re-sort common depth point
 Normal move-out correction

- Velocity 330 m/s
- Stretch 0.7

 Frequency Domain Filter

- Bandpass 20 – 40 – 200 - 400 Hz

 Static correction
 Stack

Line 6 – S Wave

Sort (assign geometry)
 Re-sort common offset
 Static correction
 Re-sort common depth point
 Normal move-out correction

- Velocity 250 m/s
- Stretch 0.6

 Stack
 Time Domain Filter

- Bandpass 15 – 80 Hz
- Window 61 points

 Static correction

Line 7 – S Wave

Apply Mute
 Sort (assign geometry)
 Re-sort common depth point
 Time Domain Filter

- Bandpass 70 – 140 Hz
- Window 61 points

AGC Scaling

- Window length 1000ms

Normal move-out correction

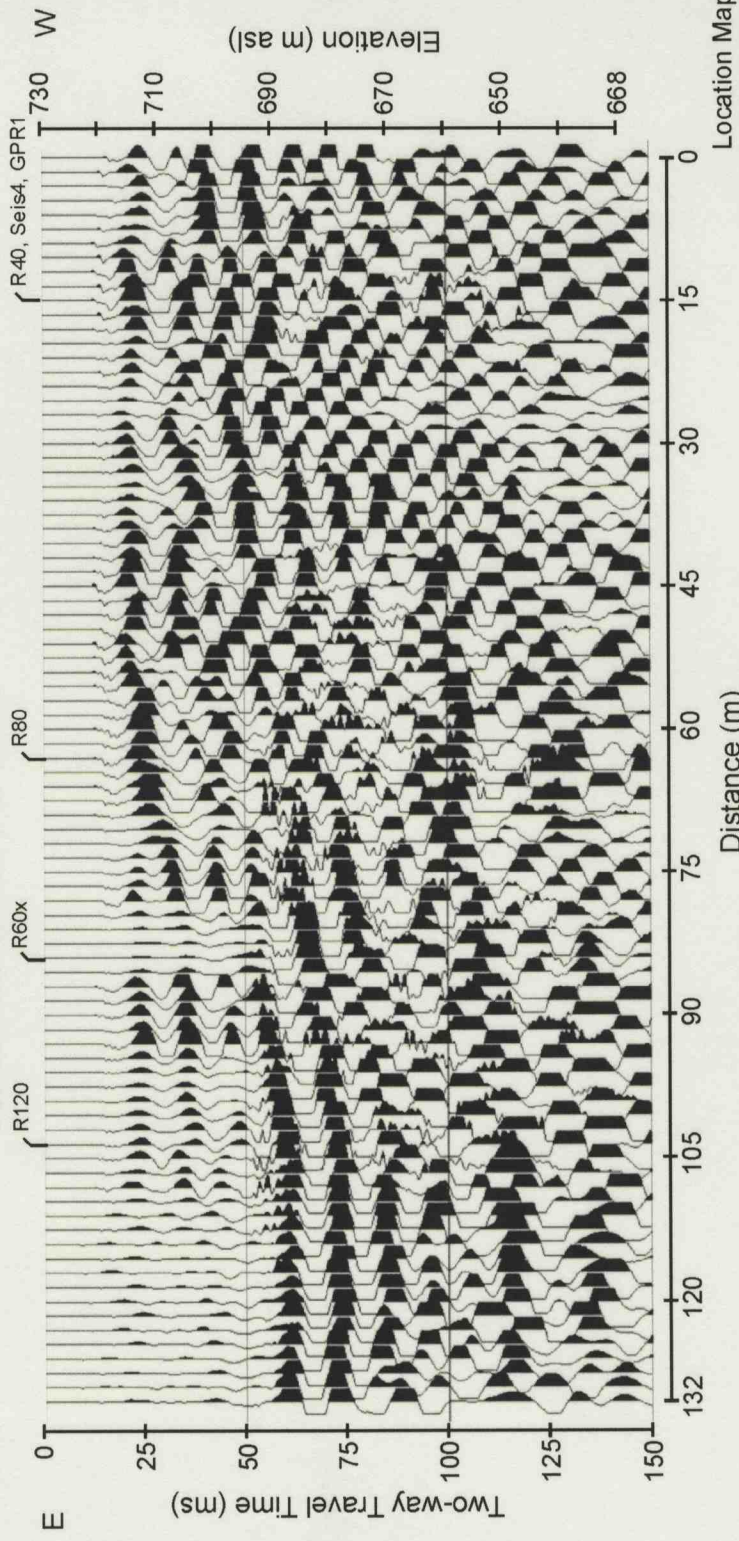
- 240 m/s @ 10 ms
- 260 m/s @ 100 ms
- 280 m/s @ 200 ms
- 300 m/s @ 400 ms
- 500 m/s @ 1000 ms
- Stretch 0.6

Stack

AGC Scaling

- Window length 1000ms

Seismic Reflection Line: Seis3 **Type: P-wave**
 Total Line Length: 132 m Channels: 36
 Orientation: WNW - ESE Geophones: 100 Hz Vertical
 Cable and shot spacing: 3 m
 Source: 16 lb hammer and l-beam
 Number of Traces: 88
 Trace Interval (CMP spacing): 1.5 m
 Normal Move-out Correction: 1450 m/s



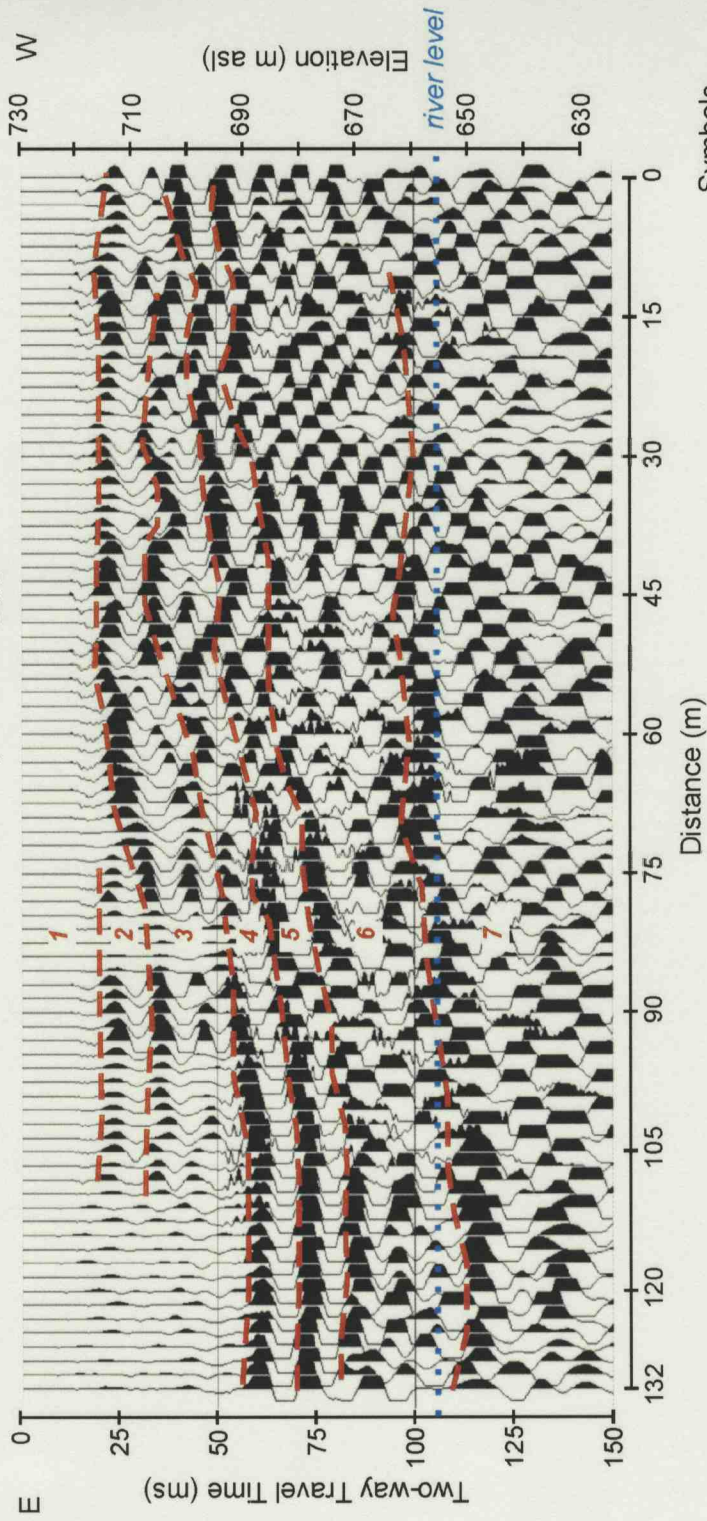
Line Description: The line is located on the upper terrace and runs approximately parallel to the headscarp for the first 100 metres, afterwards turning away from it. It follows the access road. Surficial material along the line is compacted overburden that forms the road. The line crosses survey lines R40, Seis4, GPR1, R80, R60x, and R120 at the approximate locations specified above. In addition, it partially coincides with lines Rroadx and GPR2.



Seismic Reflection Line: Seis3 Type: P-wave

Interpretation
Stratigraphic Unit (Section: Unit)
Seismic Facies

1	2	3	4	L4: 5 + 6	L4: 4	L4: 3	L4: 2	L4: 1	S11: 1 + 2	Bedrock
---	---	---	---	-----------	-------	-------	-------	-------	------------	---------



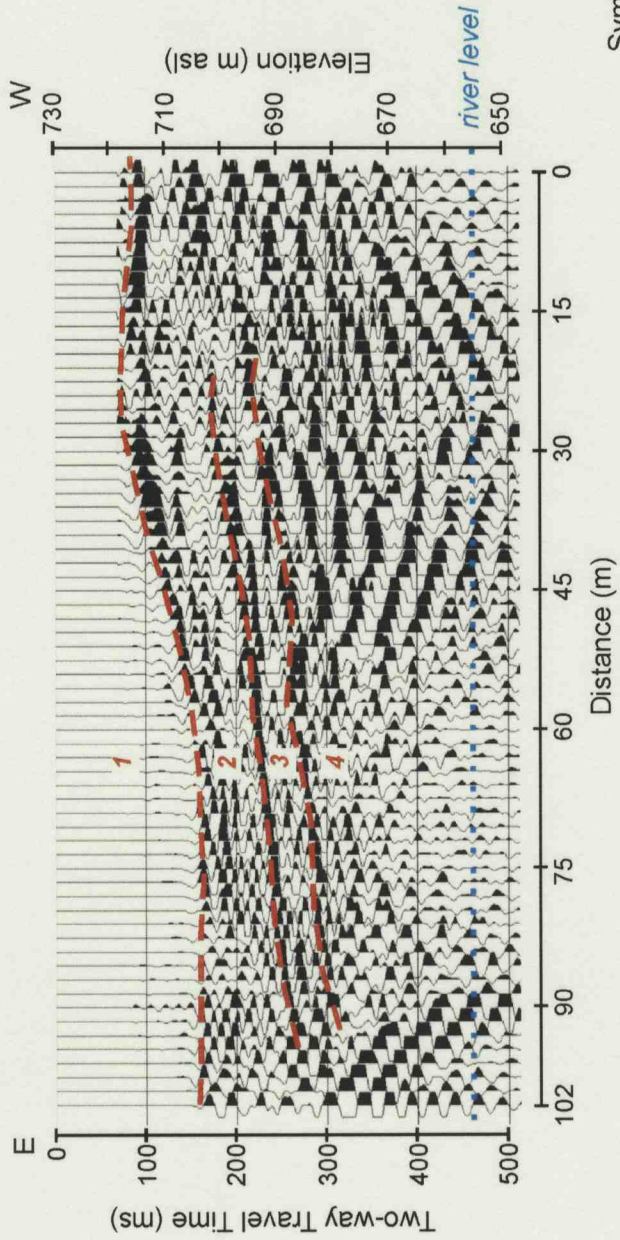
Symbols

- 1 Seismic Facies
- - - Facies Boundary

Comments:

Seismic Reflection Line: Seis3 Type: S-wave

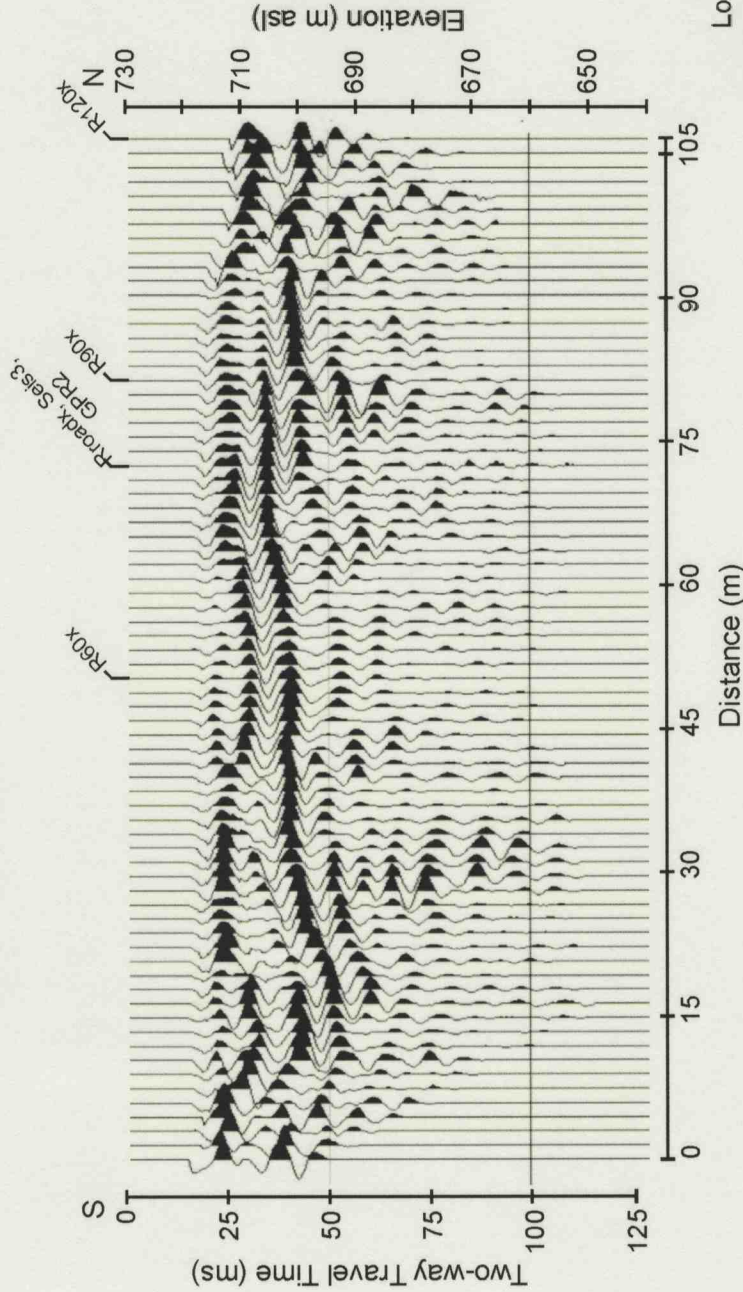
Seismic Facies	Interpretation Stratigraphic Unit (Section: Unit)
1	L4: 4 + 5 + 6
2	L4: 3
3	L4: 2
4	L4: 1



Comments: • No facies deeper than facies 4 are evident in this profile, likely due to attenuation of the signal.

Symbols
 1 Seismic Facies
 --- Facies Boundary

Seismic Reflection Line: Seis4 **Type: P-wave**
 Total Line Length: 108 m Channels: 36
 Orientation: NNE - SSW Geophones: 100 Hz Vertical
 Cable and shot spacing: 3 m Source: 16 lb hammer and l-beam
 Number of Traces: 72
 Trace Interval (CMP spacing): 1.5 m
 Normal Move-out Correction: 1425 m/s



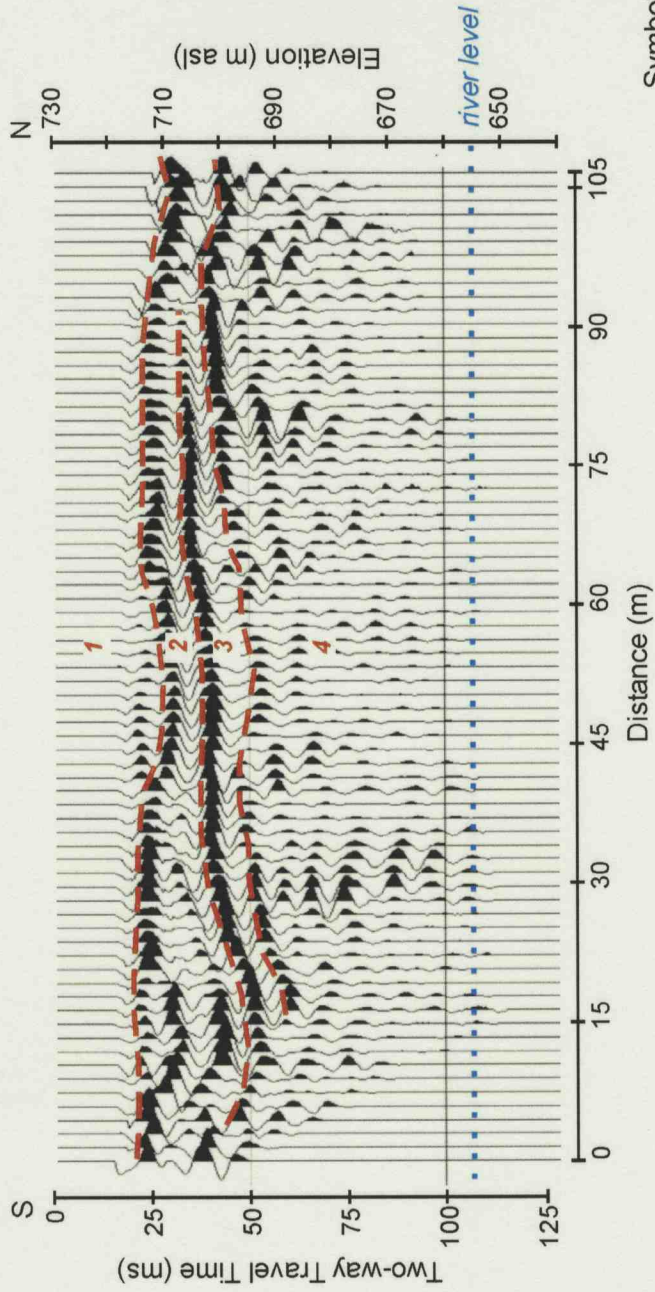
Location Map



Line Description: The line is located on the upper terrace and runs approximately perpendicular to the headscarp, following the access road. Surficial material along the line is compacted overburden that forms the road. The line crosses survey lines R60x, Rroadx, Seis3, GPR2, R90x and R120x at the approximate locations specified above. In addition, it partially coincides with lines R40 and GPR1.

Seismic Reflection Line: Seis4 Type: P-wave

Seismic Facies	Interpretation Stratigraphic Unit (Section: Unit)
1	L4: 4 + 5 + 6
2	L4: 3
3	L4: 1 + 2
4	S11: 1 + 2

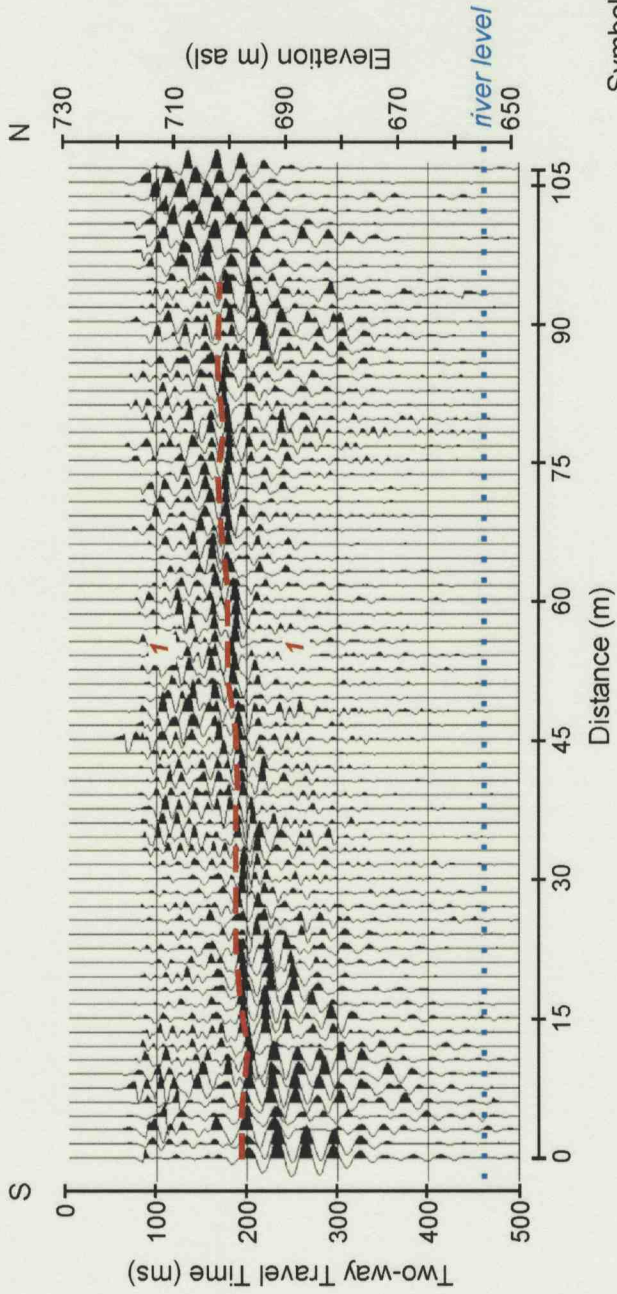


Symbols
 1 Seismic Facies
 --- Facies Boundary

- Comments:
- No facies deeper than facies 4 are evident in this profile, likely due to attenuation of the signal.
 - Depth values may be wrong, possibly 10 m too high.

Seismic Reflection Line: Seis4 Type: S-wave

Seismic Facies	Interpretation Stratigraphic Unit (Section: Unit)
1	L4: 4 + 5 + 6
2	L4: 3



Comments:

- No facies deeper than facies 2 are evident in this profile, likely due to attenuation of the signal.
- The boundary imaged is interpreted as the boundary between stratigraphic unit 3 and 4 from section L4.

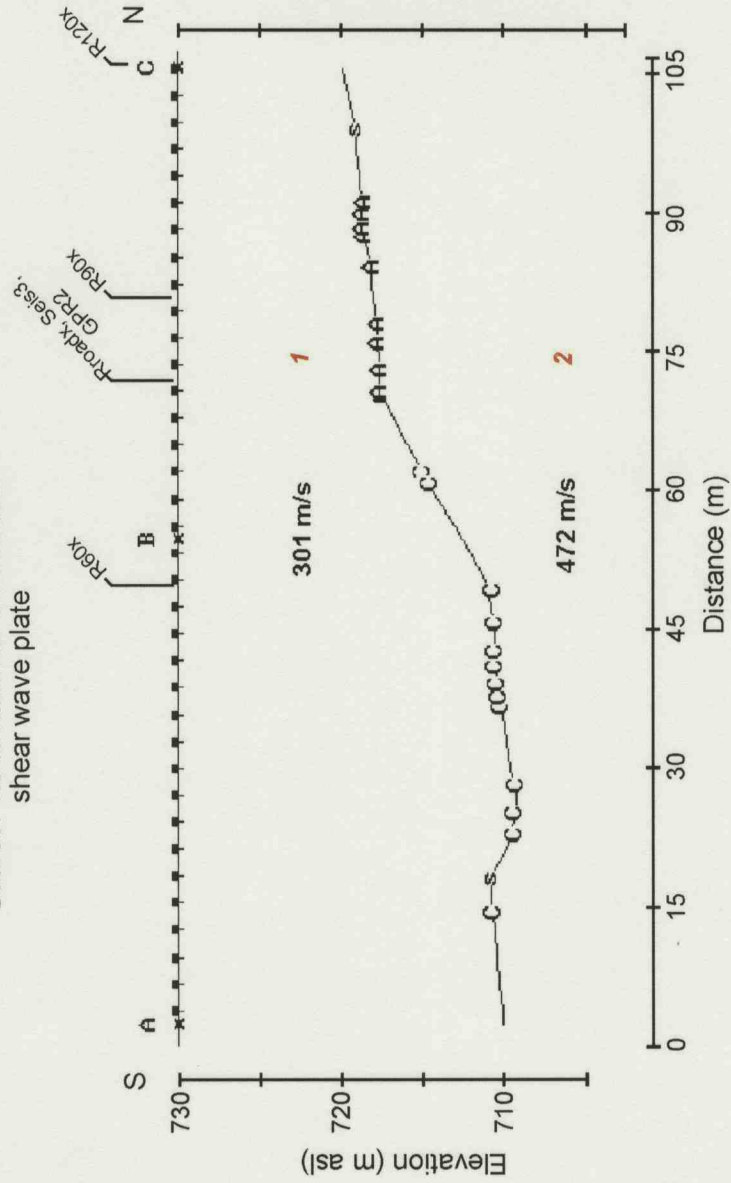
Symbols

- 1 Seismic Facies
- Facies Boundary

Seismic Refraction Line: Seis4
 Total Line Length: 108 m
 Orientation: NNE - SSW

Type: S-wave
 Channels: 36
 Geophones: 8 Hz Horizontal
 Cable and shot spacing: 3 m
 Source: 1.5 lb hammer on wooden shear wave plate

Interpretation
 Seismic Facies
 1
 2
 Stratigraphic Unit (Section: Unit)
 L4: ?
 L4: 3?



Symbols
 A Seismic Source
 1 Seismic Facies

Comments:

Seismic Reflection Line: Seis6

Total Line Length: 54 m

Orientation: WNW - ESE

Type: S-wave

Channels: 24

Geophones: 8 Hz Horizontal

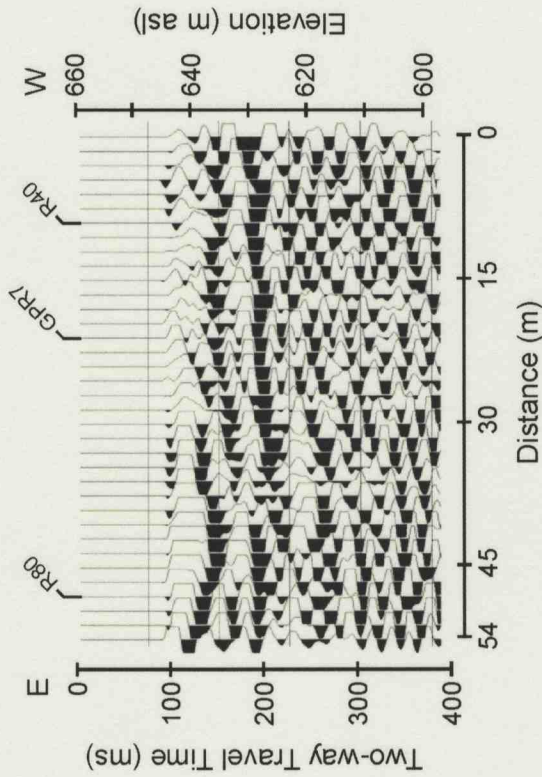
Cable and shot spacing: 3 m

Source: 1.5 lb hammer on wooden shear wave plate

Number of Traces: 36

Trace Interval (CMP spacing): 1.5 m

Normal Move-out Correction: 250 m/s



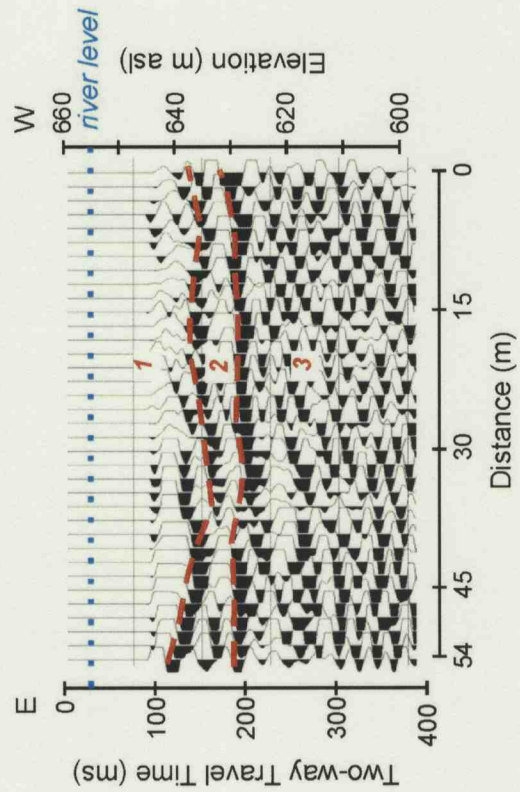
Line Description: The line is located on the toe of the landslide, near the edge of the main rotational block. It runs approximately parallel to the headscarp. Surficial material along the line is dry, unconsolidated sand and gravel. The line crosses survey lines R40, GPR7 and R80 at the approximate locations specified above.

Location Map



Interpretation
 Seismic Stratigraphic Unit
 Facies (Section: Unit)
 1 disturbed material
 2 S11: 1 + 2
 3 Bedrock

Seismic Reflection Line: Seis6 Type: S-wave



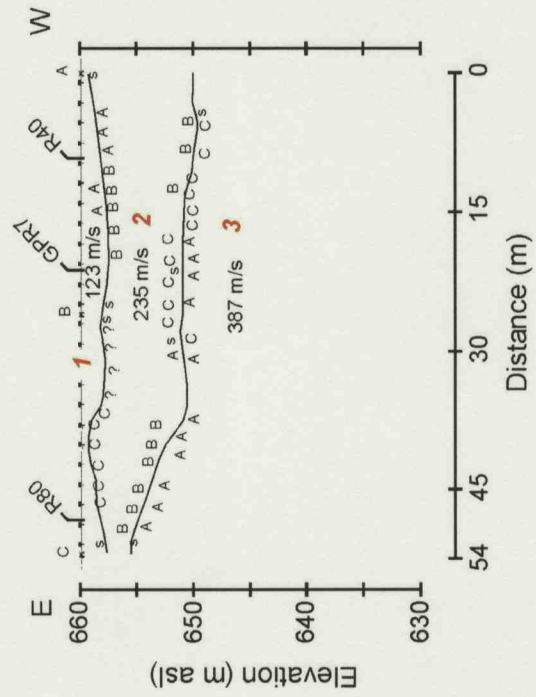
Symbols
 1 Seismic Facies
 --- Facies Boundary

Comments:

Seismic Reflection Line: Seis6
 Total Line Length: 54 m
 Orientation: WNW - ESE

Type: S-wave
 Channels: 24
 Geophones: 8 Hz Horizontal
 Cable and shot spacing: 3 m
 Source: 1.5 lb hammer on wooden shear wave plate

Interpretation
 Seismic Stratigraphic Unit
 Facies (Section: Unit)
 1 L4: 4 + 5 + 6
 2 L4: 3
 3 S11: 1 + 2

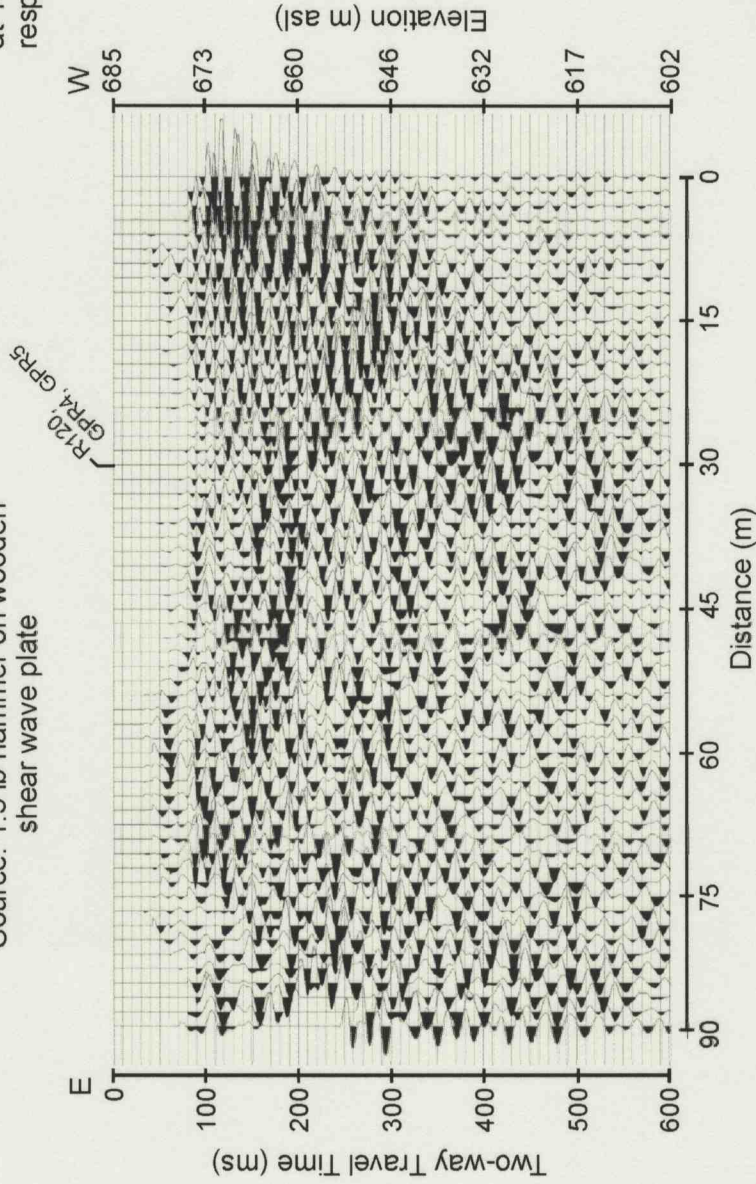


Symbols
 A Seismic Source
 1 Seismic Facies

Comments:
 • Seismic facies 1 makes up the dry sand and gravel at the surface of the landslide toe.
 • Seismic facies 2 makes up the clay rich portion of the landslide toe.
 • Seismic facies 3 is interpreted as undisturbed sediment underlying the landslide toe, i.e. the surface of separation.

Seismic Reflection Line: Seis7 **Type: S-wave**
 Total Line Length: 90 m Channels: 24
 Orientation: WNW - ESE Geophones: 8 Hz Horizontal
 Cable and shot spacing: 3 m
 Source: 1.5 lb hammer on wooden
 shear wave plate

Number of Traces: 60
 Trace Interval (CMP spacing): 1.5 m
 Normal Move-out Correction: 240, 260, 280 and 300 m/s
 at 10, 100, 200 and 400 ms
 respectively



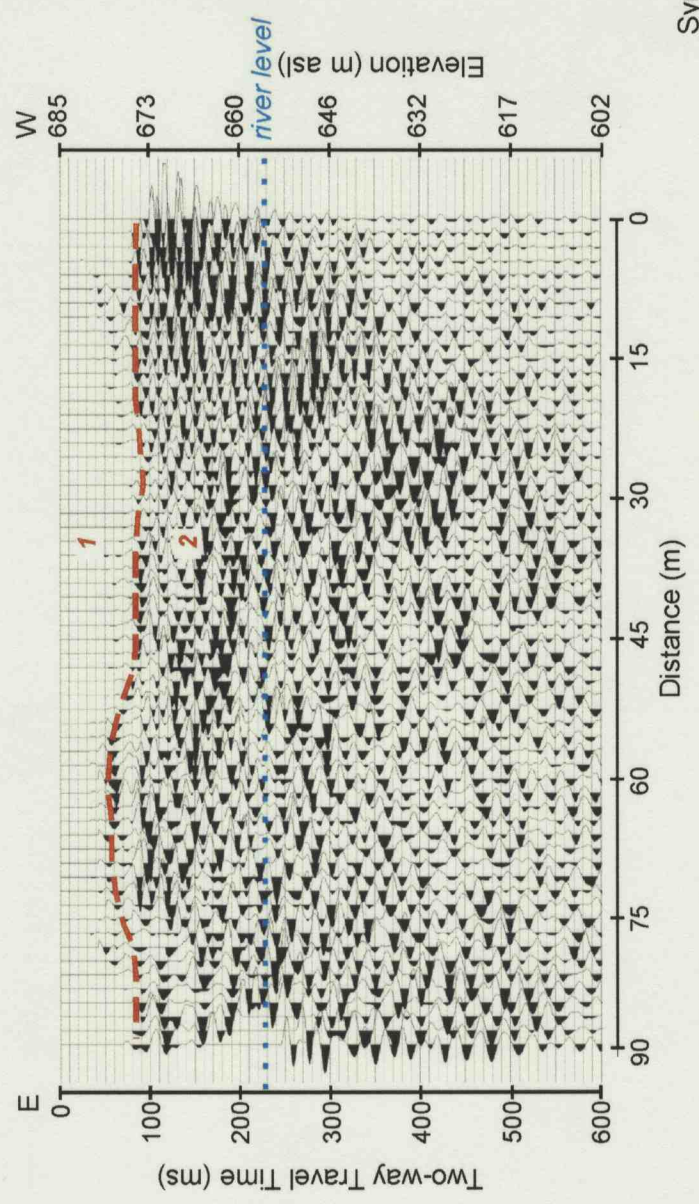
Location Map



Line Description: The line is located on the main rotational block and runs approximately parallel to the headscarp. It also parallels the inner edge of the rotational block. Surficial material along the line is moist sand and gravel. The line crosses survey line R120, GPR4 and GPR5 at the approximate locations specified above.

Interpretation
 Seismic Stratigraphic Unit
 Facies (Section: Unit)
 1 L4: 3 + 4 + 5 + 6?
 2 L4: 1 + 2?

Seismic Reflection Line: Seis7 Type: S-wave



Comments: • The boundary imaged in this profile is weak and due to lack of reference, is ambiguous.

Symbols
 1 Seismic Facies
 - - - Facies Boundary